UNIVERSITY OF CALIFORNIA, SAN DIEGO

Chaperone Function of the Botulinum Neurotoxin Protein Translocating Channel

A Dissertation submitted in partial satisfaction of the

Requirements for the degree Doctor of Philosophy

in

Biology

by

Audrey Fischer

Committee in Charge:

Professor Mauricio Montal, Committee Chair
Professor Randy Hampton
Professor Melvin Okamura
Professor Julian Schroeder
Professor John Young

2008

The Dissertation of Audrey Fischer is approved, and it is acceptable in quality and form of publication on microfilm:

_____

_____

_____

_____

_____
Chair

University of California, San Diego

2008

Table of Contents

List of Abbreviations

The abbreviations used are: 3D, three-dimensional; γ, single channel conductance; βME, β-mercaptoethanol; BoNT, botulinum neurotoxin; DTT, dithiothreitol; EM, electron microscopy; LC, light chain; HC, heavy chain; mAb, monoclonal antibody; RBD, receptor binding domain; SNAP-25, synaptosome-associated protein of 25 kDa; SDS-PAGE, SDS-polyacrylamide gel electrophoresis; TCEP, tris-(2-carboxyethyl) phosphine; $V_{1/2}$, the voltage at which P_o = 0.5; SNARE, soluble NSF attachment protein receptor; TD, translocation domain.

List of Figures

List of Tables

Acknowledgements

I would like to acknowledge Mauricio Montal for taking an enormous amount of time to mentor me in the ways of biophysical experimentation and analysis and in the current environment of science and the best ways to survive it all. Maurice has been a bottomless well of suggestions and encouragement. I would like to thank my committee for their careful inspection of my research; their suggestions always led to the next exciting experimental result. I would like to acknowledge my father, David Fischer, for the tireless editing of each and every manuscript in an effort to remove all superfluous and unnecessarily artistic phrasings present within the first renditions of my manuscripts. Without you, Dad, I would just be flowery. I would also like to acknowledge Jose Santos for his patience in training me, perceptive comments on my research, and invaluable friendship through a grueling five years as a graduate student. My husband Brad has spent the past five years learning about Botulinum neurotoxin with enthusiasm; thank you for your loving support of my dream to be a Mad Scientist.

Chapter 1, in full, is a reprint of the material as it appears in the Journal of Neurotoxicity Research. Fischer, Audrey and Montal, Maurice, FP Graham Publ. Co., 2006. The manuscript is reproduced with the permission of M. Montal. The dissertation author was the primary investigator and an author of this paper.

Chapter 2, in full, is a reprint of the material as it appears in the Proceedings of the National Academy of Sciences. Fischer, Audrey and Montal, Maurice, Proceedings of the National Academy of Sciences of the United States of America, 2007. The manuscript is reproduced with the permission of M.

Montal. The dissertation author was the primary investigator and an author of this paper.

Chapter 3, in full, is a reprint of the material as it appears in the Journal of Biological Chemistry. Fischer, Audrey and Montal, Maurice, American Society for Biochemistry and Molecular Biology, 2007. The manuscript is reproduced with the permission of M. Montal. The dissertation author was the primary investigator and an author of this paper.

Chapter 4, in full, is a reprint of the material as it appears in the Journal of Biological Chemistry. Fischer, Audrey; Garcia-Rodriguez, Consuelo; Geren, Isin; Lou, Jianlong; Marks, James D; Nakagawa, Terunaga and Montal, Maurice, American Society for Biochemistry and Molecular Biology , 2007. The manuscript is reproduced with the permission of all co-authors. The dissertation author was the primary investigator and an author of this paper.

Chapter 5, in full, is a reprint of the material as it appears in the Public Library of Science, Pathogens. Brunger, Axel T.; Breidenbach, Mark A; Jin, Rongsheng; Fischer, Audrey; Santos, Jose S. and Montal, Maurice, Public Library of Science, 2007. The manuscript is reproduced with the permission of all co-authors. The dissertation author was an investigator and author of this paper.

Chapter 6, in part, will be submitted for publication of the material as it may appear. I, Audrey Fischer, will be the primary author of this paper.

Chapter 7, in part, will be submitted for publication of the material as it may appear. I, Audrey Fischer, will be a contiributing author of this paper.

Vita

1999	Teaching Assistant for Dr. Vivek Sharma, University of California, San Diego
1999-2000	Research Assistant for Dr. Melvin Okamura, University of California, San Diego
2000	Bachelor in Science in Biophysics, University of California, San Diego
2000-2002	Research Associate for Aurora Biosciences / Vertex Pharmaceuticals
2002-2008	Research Assistant for Dr. Mauricio Montal, University of California, San Diego
2008	Doctor of Philosophy, University of California, San Diego

Publications

Fischer, A. & Montal, M. Characterization of Clostridial botulinum neurotoxin channels in neuroblastoma cells. *Neurotox Res* **9**, 93-100 (2006).

Fischer, A. & Montal, M. Single molecule detection of intermediates during botulinum neurotoxin translocation across membranes. *Proc Natl Acad Sci U S A* **104**, 10447-10452 (2007).

Fischer, A. & Montal, M. Crucial role of the disulfide bridge between botulinum neurotoxin light and heavy chains in protease translocation across membranes. *J Biol Chem* **282**, 29604-29611 (2007).

Brunger, A.T., Breidenbach, M.A., Jin, R., Fischer, A., Santos, J.S. & Montal, M. Botulinum neurotoxin heavy chain belt as an intramolecular chaperone for the light chain. *PLoS Pathog* **3**, 1191-1194 (2007).

Fischer, A., Garcia-Rodriguez, C., Geren, I., Lou, J., Marks, J.D., Nakagawa, T., and Montal, M.Molecular architecture of botulinum neurotoxin E revealed by single particle electron microscopy. *J Biol Chem* in press (2007).

Fields of Study

Biophysical study of Receptor Binding Complex with Light Harvesting Complex Professors Melvin Okamura and George Feher.

Development of cell based high throughput screening for ion channel drug targets at Aurora Biosciences/Vertex Pharmaceuticals.

Biophysical study of Botulinum neurotoxin
Professor Mauricio Montal.

ABSTRACT OF THE DISSERTATION

Chaperone Function of the Botulinum Neurotoxin Protein Translocating Channel

by

Audrey Fischer

Doctor of Philosophy in Biology

University of California, San Diego, 2008

Professor Mauricio Montal, Chair

Clostridial botulinum neurotoxins (BoNTs) induce neuroparalysis by arresting synaptic exocytosis. BoNT consists of three functional domains: protease, translocation and receptor binding, and is cleaved into two disulfide linked, polypeptide chains: Light chain (LC) protease and Heavy chain (HC) translocon and receptor binding. One of the most elusive and intriguing steps of the BoNT intoxication process is the translocation of the proteolytic LC through the BoNT protein-conducting channel of the HC, from the endosomal compartment to the cytosol. In this dissertation, we utilize single-particle electron microscopy to resolve the discrepancies in multi-domain arrangement between

different isoforms of BoNT in an effort to visualize rearrangement of domains and conformational changes associated with the translocation process. We investigate the dynamics of protein-translocation focusing on the interactions between the HC channel/chaperone and its LC cargo. Single molecule translocation was monitored in real time using excised patches of neuronal cells. LC translocation requires translocation domain (TD) insertion in a receptor binding domain (RBD) dependent manner, coupled with LC unfolding and protein conduction through the TD channel. Translocation occurs as a series of progressive steps in an N- to C-terminus orientation; productive completion requires reduction of the disulfide bridge and proteolytic cleavage of the LC from the HC concurrent with LC refolding in the cytosol. The progressive, tight interplay between the individual domains inherent in the mechanism of BoNT intoxication resolve it as an elegant modular nanomachine.

Introduction

What is clostridium botulinum?

Clostridium botulinum is a spore forming, anaerobic, gram positive bacterium[1]. The bacterium is often found in the soil and in marine and freshwater sediments as well as the intestinal tracts of numerous mammalian species including humans, horses and chickens. Clostridium botulinum causes the neuroparalytic disease botulism, first discovered in the late 1700s Germany[2]. The disease is characterized by descending limb paralysis, dysarthria, facial muscle weakness, dyspnea, constipation, urinary retention and opthalmoplegia and can result in death by respiratory failure [3, 4]. An outbreak of botulism in 1895 in Belgium led Emile van Ermengem to determine the bacterial agent associated with botulism to be an extracellular toxin isolated from contaminated meat or vegetables[5].

The causative agent of botulism, botulinum neurotoxin (BoNT), can be acquired in one of four ways. Botulism from the ingestion of foods contaminated with BoNT is the oldest documented method of contraction; however, infant botulism is considered the most common[6]. In infant botulism, BoNT is produced when *C. botulinum* spores infect the intestinal tract and secrete the toxin to be circulated through the host infant, usually between 3 to 26 weeks old[7]. Wound botulism is similarly caused by toxin production *in vivo*; in this case the toxin is formed in a wound. Inhalational botulism could occur from the adsorption of aerosolized BoNT, making BoNT a dangerous bioweapon[8].

C. botulinum secretes 7 antigenically distinct isoforms of BoNT, designated A-G. The vast majority (~98.5% of cases where a specific serotype

was determined) of human botulism is caused by BoNT/A , B and E[9-11]. Botulism caused by BoNT/C, D, and F have been reported in rare cases in humans, although intoxication of animals is more common[12-15]. BoNT/G has been implicated in the sudden death of 5 humans, but otherwise has yet to be confirmed as capable of intoxicating humans or animals[16]. Initially considered a neuroparalytic illness of the central nervous system, botulism was later determined to act on the peripheral cholinergic nervous system[17]. BoNT attacks the presynaptic terminal, inhibiting exocytosis of the neurotransmitter, acetylcholine[18].

Botulinum neurotoxin complex

BoNT is secreted as a noncovalent multimeric complex of ~900 KDa, composed of the holotoxin responsible for inhibition of synaptic transmission and nontoxic projenitor proteins[7, 19, 20]. While most of the holotoxin-associated proteins are hemagglutinins; a large nontoxic nonhemagglutinating activity protein is always present as well[17]. The BoNT complex is more stable and resistant to denaturants and proteolysis than isolated BoNT holotoxin, however serve no role in the toxin induced arrest of synaptic transmission. Rather, the associated proteins serve to chaperone the holotoxin molecule in the traverse to the target neuron, protecting it from low pH and proteolytic enzymes within the gut[21-23].

BoNT holotoxin is synthesized as an inactive, single polypeptide chain of ~150 kDa; the active form, generated by clostridial or host cell proteolysis, is a

disulfide linked di-chain protein whose individual polypeptide chain lengths vary between serotypes, depending upon the proteolytic sites cleaved on the surface exposed loop region. The mature holotoxin is a disulfide linked di-chain molecule consisting of a 50 kDa light chain (LC) protease and a 100 KDa heavy chain (HC) chaperone[4, 24-27]. The LC is a sequence specific Zn2+ metalloprotease whose active site region shares structural similarity to thermolysin[28-34]. The HC encompasses two functional domains of ~50 kDa each, the translocation domain (TD), composed of a bundle of elongated α helices, and the double lobed receptor binding domain (RBD), made up of a β-barrel and β-trefoil motifs[33-36]. Individually the HC and LC are harmless; the tight interplay and precisely timed sequential function of each domain transform BoNT holotoxin into the most potent toxin known[8].

Mechanism of BoNT intoxication

Oral contraction of botulism requires the BoNT holotoxin to escape the gastrointestinal system, enter general circulation and find the peripheral cholinergic nervous system[22, 37]. In order to do this BoNT holotoxin RBD binds receptors on the mucosal surface of gut epithelial cells; this process occurs independent of associated BoNT complex proteins. The holotoxin then undergoes receptor mediated endocytosis and transcytosis with subsequent delivery to the basolateral side of the epithelial cell[38-40]. Once released to the

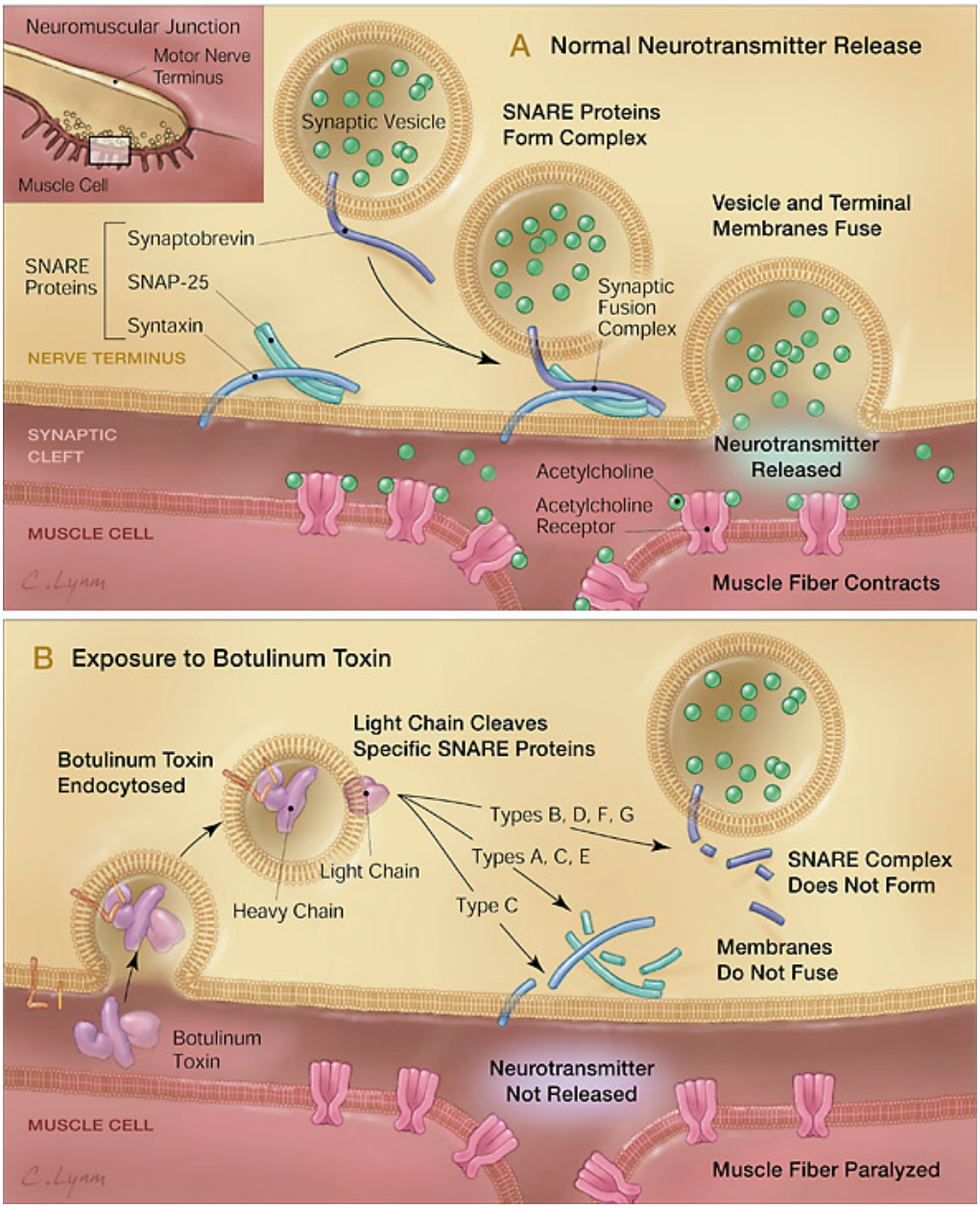

Fig. 1. Excerpt from Arnon et al, 2001. Mechanism of Action of Botulinum Toxin A, Release of acetylcholine at the neuromuscular junction is mediated by the assembly of a synaptic fusion complex that allows the membrane of the synaptic vesicle containing acetylcholine to fuse with the neuronal cell membrane. The synaptic fusion complex is a set of SNARE proteins, which include synaptobrevin, SNAP-25, and syntaxin. After membrane fusion, acetylcholine is released into the synaptic cleft and then bound by receptors on the muscle cell. B, Botulinum toxin binds to the neuronal cell membrane at the nerve terminus and enters the neuron by endocytosis. The light chain of botulinum toxin cleaves specific sites on the SNARE proteins, preventing complete assembly of the synaptic fusion complex and thereby blocking acetylcholine release. Botulinum toxins types B, D, F, and G cleave synaptobrevin; types A, C, and E cleave SNAP-25; and type C cleaves syntaxin. Without acetylcholine release, the muscle is unable to contract. SNARE indicates soluble NSF-attachment protein receptor; NSF, N-ethylmaleimide-sensitive fusion protein; and SNAP-25, synaptosomal-associated protein of 25 kd.[8]

circulation BoNT holotoxin reaches cholinergic nerve cells and a second round of cell entry occurs. BoNTs enter sensitive neurons *via* receptor-mediated endocytosis (Fig. 1) [17, 41, 42]. The BoNT receptor-binding domain establishes the cellular specificity mediated by its high affinity interaction with a surface protein receptor and a ganglioside (GT_{1B}) co-receptor[43-46]. The protein receptors are the synaptic vesicle protein SV2 for BoNT/A, and synaptotagmins I and II for BoNT/B and BoNT/G. Intracellular processing involves residence of the BoNT-receptor complex in the acidic environment of endosomes, resulting in a major conformational change and the consequent synchronized partial unfolding of the LC and insertion of the HC into the endosomal bilayer membrane[47, 48]. The HC forms a protein conducting channel that translocates the LC from the acidic, oxidized endosome to the reduced, neutral pH cytosol[48-50].

The LC cleaves SNARE (soluble NSF attachment protein receptor) proteins within the cytosol, inhibiting formation of the SNARE core complex (Fig. 1)[17, 51-57]. Synaptic neurotransmitter release is mediated by the assembly of a synaptic fusion complex that allows the membrane of the synaptic vesicle to fuse with the neuronal cell membrane; assembly of the SNARE core complex is considered a key step preceding fusion of synaptic vesicles [17, 52, 58]. The SNARE complex is formed by the specific interaction between segments of three proteins[54]: synaptobrevin-2/VAMP-2, a vesicle-associated membrane protein, and syntaxin 1A and SNAP-25 (synaptosomal-associated protein of 25 kDa), two distinct proteins associated with the plasma membrane (Fig. 2). SNAP-25, a palmitoylated membrane associated protein, binds with high affinity to the plasma

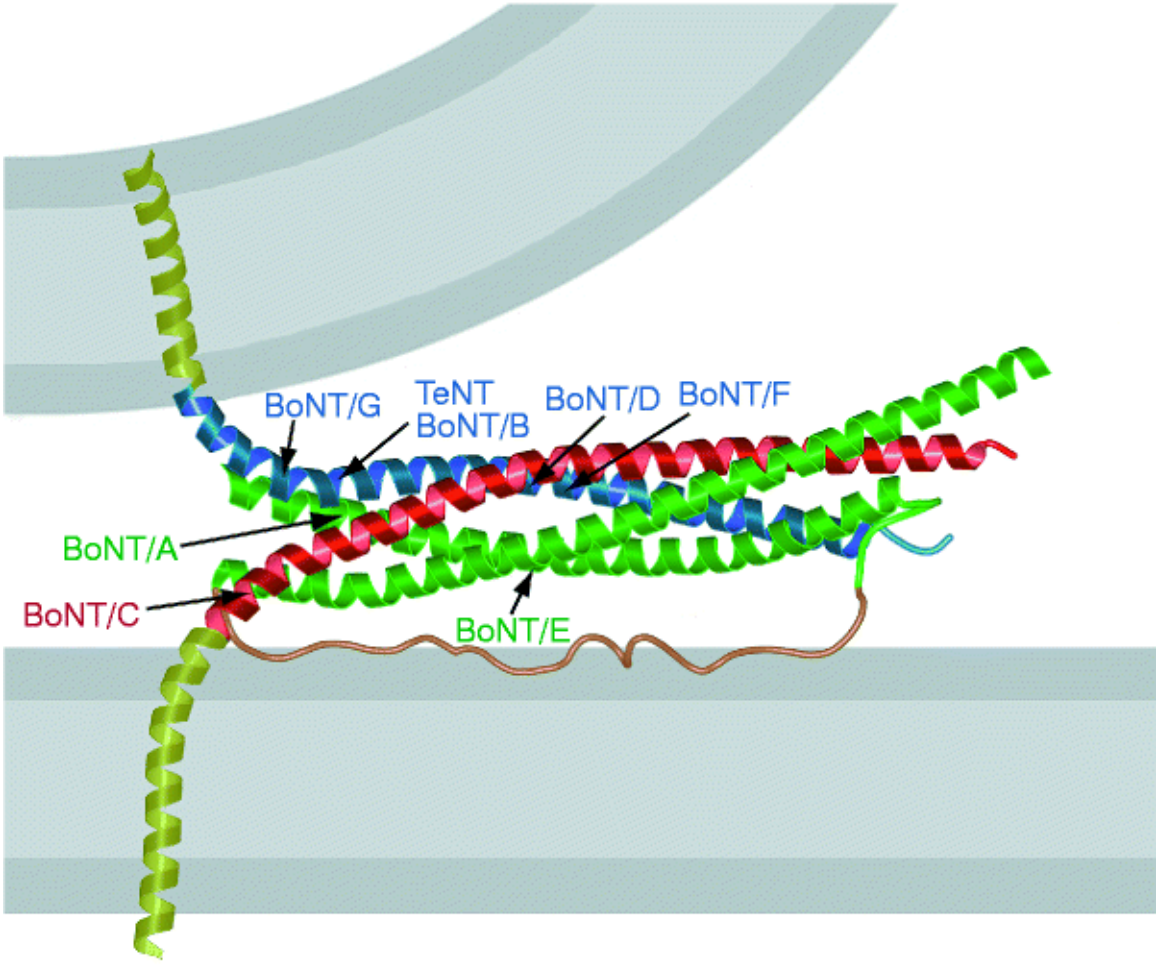

Fig. 2. Excerpt from Sutton et al, 1998. We extended the synaptic fusion complex crystal structure to include the transmembrane domains (yellow) of syntaxin-1A (red) and synaptobrevin-II (blue), and the loop connecting the Sn1 and Sn2 fragments (green). The transmembrane domains and the linker to the Sx fragment are represented as α-helices. Hypothetical bends of the syntaxin and synaptobrevin α-helices were modelled close to the lipid bilayers. The loop between the Sn1 and Sn2 fragments was modelled as an unstructured polypeptide chain. The conformation of this loop is speculative. The loop between the Sn1 and Sn2 domains is shown in orange. We assumed that the lipid bilayers (grey) have a thickness of roughly 30 Å. The synaptobrevin-II neurotoxin-mediated cleavage site for tetanus toxin (TeNT) and botulinum toxin (BoNT) type B (BoNT/B) is between Gln 76 and Phe 77; for BoNT/F, between Gln 58 and Lys 59; for BoNT/G, between Ala 81 and Ala 82; and for BoNT/D, between Lys 59 and Leu 60. The syntaxin-1A BoNT/C cleavage site is between Lys 253 and Ala 254. Cleavage sites in SNAP-25B are between Asp 193 and Glu 194 for BoNT/E, and between Arg 176 and Gln 177 for BoNT/A. [54]

membrane protein syntaxin [59-62]. Synaptobrevin is localized to synaptic vesicles; when these vesicles move close to the plasma membrane, synaptobrevin binds to syntaxin–SNAP-25 and forms a coiled-coil α-helical bundle that drives vesicle fusion with the plasma membrane [54]. Synaptotagmin binds Ca^{2+} and proteins within the SNARE complex coupling Ca^{2+} release with vesicle fusion[63, 64]; recently synaptobrevin has been shown to exert force on membranes to initiate fusion at the moment of the intracellular Ca^{2+} increase[65]. Fusion of synaptic vesicles containing acetylcholine at the neuromuscular junction releases acetylcholine into the synaptic cleft where it binds to receptors on the muscle cell thereby triggering muscle contraction.

BoNT/ A, C and E cleave SNAP-25, whereas BoNT/B, D, F, and G cleave synaptobrevin, and BoNT/C also cleaves syntaxin, all at unique sites (Fig. 2) [51, 66-74]. SNARE cleavage by BoNT LC requires an extended enzyme-substrate interface for optimal catalytic efficiency, illustrated by the X-ray structure of BoNT/A-LC in complex with the C-terminal residues 141–204 of BoNT/A substrate SNAP-25[32]. An extensive array of substrate binding sites distant from the active site (exosites) orientate the substrate onto the vicinity of the active site and determine the target specificity[32, 75].

The mechanism of LC translocation has remained elusive, and as such is the focus of this dissertation. The dynamic interactions between the HC channel/chaperone and the LC cargo and the minimal requirements for completion of productive LC translocation from the endosome to the cytosol have yet to be determined. Understanding of this process could lead to the

development of a more effective therapy for botulism. The LC has been a popular drug target, although high specificity, low cross-reactivity lead compounds have yet to be generated. The BoNT channel is an ideal target to arresting botulism prophylactically. In addition, this study aims to give insight to the mechanisms of more complex protein translocating channels like the mitochondrial and chloroplast protein translocases, and the translocons in eukarya, bacteria and archae.

Correlation between BoNT and Cellular Chaperones

The interplay between an unfolded LC embedded within the HC is reminiscent of the maintenance of an unfolded or partially folded state of polypeptides by chaperones. It is therefore fitting to further consider plausible similarities. The translocon, the universally conserved protein-conducting channel responsible for the translocation of nascent proteins across membranes or for the insertion of integral membrane proteins into targeted membranes, has been the subject of intense inquiry[76, 77]. The translocon is a membrane protein complex composed of three different protein subunits: $\alpha\beta\gamma$ in the ER Sec61 complex of eukaryotes, and the corresponding SecYEG in eubacteria, and SecYEβ in archae. This tightly regulated channel allows the nascent polypeptide to percolate through the membrane and controls the concerted folding of the emergent protein at the membrane-water interface. The structure of the *Escherichia coli* SecYEG protein-conducting channel bound to a translating ribosome was recently obtained by cryo-EM reconstruction to a resolution of ~15

Å[78]. And the crystal structure of the protein-conducting channel from the archaeon *Methanococcus jannaschii* SecYEβ was determined at 3.2 Å resolution[79]. These two structures are instructive as they provide detailed information on protein-conducting channels pertaining to both cotranslational and postranslational translocation systems, and define blueprints for protein-conducting channels for which the underlying protein fold is a compact transmembrane α-helical bundle. Both of these structures evoke a tantalizing resemblance to the occluded BoNT channel. The cryo-EM reconstruction of the *E. coli* SecYEG led to the view that the nascent polypeptide chain is tightly accommodated within the channel hindering conductance and, given a channel constriction of ~15 Å, it is permissive to accommodate α-helices[78, 80]. The crystal structure of the archaeal SecYEβ shows that the protein-conducting channel is occluded by a short helix, ~10 residues long. The channel lumen is lined by hydrophobic residues around the major constriction of only 3 Å; however, the channel translocates α-helices (12 -14 Å). It is conceivable that the solved structure corresponds to the closed, occluded channel. Indeed, disulfide bridge formation between SecY (the α-subunit of the SecYEβ heterotrimer) and the translocating polypeptide indicates that the cargo travels through the center of the channel[81]. And, molecular dynamics simulations of the archaeal SecYEβ protein-conducting channel are consistent with the view that the occluding short helix is transiently displaced unoccluding the channel while the translocating peptide partially unfolds at the narrowest constriction of the channel lumen[82]. .

The SecYEβ protein-conducting channel, therefore, changes conformation during translocation. Even at this level of resolution it is unclear if the functionally active entity is monomeric or, at least, a minimum dimeric oligomer[78, 79, 82]. It appears, however, that a monomer is sufficient[82]. These two structures outline the intricacies of the initial stages of protein translocation and are consistent with the occurrence of discrete transient intermediates involving extensive interactions between the chaperone and the cargo in a dynamic succession which dictates the progress and directionality of translocation and, ulitmately, determine the fate of cargo either as a folded secreted protein or as an integral membrane polypeptide. The analogy that emerges from the findings reported here for BoNT, a modular nanomachine in which one of its modules – the HC channel – operates as a specific protein translocating transmembrane chaperone for another of its component modules – the LC protease – is probably more than coincidental and points to a fundamental common principle of molecular design.

Protein import in mitochondria and chloroplasts occurs postranslationally and involves unfolded proteins[83-85]. A number of protein translocase complexes have been identified. A case in point is the inner mitochondrial membrane TIM23 translocase with pore diameter of ~13 Å[86] which uses the membrane potential across the inner membrane to drive preprotein translocation across and insertion into the inner membrane. For chloroplasts, the peptide translocating channels of the outer (Toc75)[87] and inner (Tic110)[88] membranes display pore diameters of ~14 Å and 15 Å. The secondary structure of the precursor polypeptide cargos are therefore

necessarily constrained to be either extended or α-helical segments in order to fit into a channel of ~15 Å in diameter. An analogous requirement for unfolded cargo is required by protein translocases for which the underlying protein fold is a transmembrane hollow β-barrel. A case in point is the protective antigen (PA) PA_{63} pore of anthrax toxin, a 14-stranded β-barrel formed at the center of the homoheptameric assembly which exhibits a central pore with a cross-section of ~15 Å[89]. An aromatic ring of seven phenylalanine residues contributed by each of the subunits is exposed at the entry into the pore lumen and is considered to act as a chaperone by providing a compatible hydrophobic surface for the unfolding lethal factor (LF) cargo[90-92]. Similar schemes have emerged from single channel measurements on the interactions between helical cargo peptides and the transmembrane β-barrel of the α-hemolysin protein pore[93]. Compared to the molecular complexity of the mitochondrial and chloroplast protein translocases, and the translocons in eukarya, bacteria and archae the BoNT protein highlights the simplicity of its modular design to achieve its exquisite activity.

Dissertation focus

The first chapter focuses on characterizing the channel properties of BoNT/A holotoxin on excised patches of neuronal cells. Previous studies have utilized either PC12 rat chromofin cells which are notoriously noisy and unstable for electrophysiology experiments or lipid bilayers which do not contain the same lipid composition or the BoNT cellular receptors. This study uses a mouse

neuroblastoma cell line, Neuro 2A and discovered that under these conditions the channels are voltage dependent, channel activity occurs in random bursts between random periods of quiescence, and display a subconductance state in addition to the previously understood closed and open states. This study serves as a baseline for BoNT channel analysis for all subsequent experiments performed.

The work presented in Chapter 2 moves beyond the steady state unoccluded HC channels presented in Chapter 1, uncovering a series of previously unsuspected intermediate stages in the process of BoNT/A LC translocation through the HC channel. Careful observation of the excised patch electrophysiology assay visualized progressive occluded stages in the HC channel occurring at the onset of channel activity. We proposed a model for the set of protein–protein interactions between translocase and cargo that correspond to an entry event where the HC channel has inserted into the membrane concomitant with the LC partially unfolding and entering the HC channel. This step is followed by a sequence of transfer steps in which the LC and HC transition through permissible intermediate conformations before the last step, corresponding to an exit event. The LC exits the HC channel, refolds and is released. This model is supported by experiments in which the LC is perturbed at the entry event by a bound, stable protein of equivalent size, and experiments in which the LC is peptidically anchored to the HC and unable to be released.

Chapter 3 explores the role of the disulfide and peptide linkages between the BoNT LC and HC. The disulfide bridge was determined to be necessary for

the duration of LC translocation, premature reduction resulting in arrest and irreversibly incomplete translocation. Peptidic linkages between the LC and HC were discovered to be insufficient replacements for the disulfide linkage. This allowed us to refine our previously presented model to include the disulfide as a driving force for LC translocation.

The aim of Chapter 4 was to determine the intermediate resolution structure of BoNT/E holotoxin by single particle electron microscopy. The structure of BoNT/A was compared with that of BoNT/E revealing a novel molecular architecture of the three modular domains. The three dimensional reconstruction of BoNT/E was supported by specific binding to the LC and TD by Fab fragments.

Chapter 5 explores the hypothesis that the unstructured belt of the HC functions as a chaperone for the LC. The sequence and structure of the belt regions of multiple BoNT serotypes were compared to those of the SNARE substrate resulting in interesting inferences. The belt region may function as a pseudo substrate, protecting the LC from cleaving non specific substrates and as a chaperone ensuring a translocation competent conformation of the LC during its transit from the acidic endosome to the neutral cytosol.

The experiments performed in Chapter 6 aimed to discern the role of the belt region and the RBD of BoNT/A in HC channel activity and LC translocation. The TD without the belt region does exhibit channel activity over a range of pH gradient values, however the belt may be required for LC translocation. The RBD induces pH dependent insertion of the TD into the membrane, insuring

synchronized formation of the protein-conducting channel with partial unfolding of LC to a translocation competent conformation.

The BoNT channel may represent a potential target for intervention to attenuate BoNT neurotoxicity. A search for channel blockers and their eventual identification may provide proof-of-principle thereby paving the way towards the development of BoNT selective antidotes. The neuronal cell electrophysiology assay allowed us to study blockers of the BoNT channel activity as well as inhibition of LC translocation. The experiments performed in Chapter 7 demonstrate the arrest of LC translocation by the small molecule Toosendanin. This derivative found in Chinese herbal medicine does not function as a channel blocker albeit inhibits LC translocation with nM sensitivity through a more complex mechanism involving the tight interactions between the LC cargo and HC channel/chaperone.

References

1. Schantz, E.J. and E.A. Johnson, *Botulinum toxin: the story of its development for the treatment of human disease.* Perspect Biol Med, 1997. **40**(3): p. 317-27.

2. Dunbar, E.M., *Botulism.* J Infect, 1990. **20**(1): p. 1-3.

3. Mahajan, S.T. and L. Brubaker, *Botulinum toxin: from life-threatening disease to novel medical therapy.* Am J Obstet Gynecol, 2007. **196**(1): p. 7-15.

4. DasGupta, B.R., *Structures of botulinum neurotoxin, its functional domains, and perspectives on the cristalline type A toxin*. Therapy with botulinum toxin, ed. M.H. Jankovic. 1994, New York: Marcel Dekker, Inc. 15-39.

5. Erbguth, F.J., *Botulinum toxin, a historical note.* Lancet, 1998. **351**(9118): p. 1820.

6. Goonetilleke, A. and J.B. Harris, *Clostridial neurotoxins.* J Neurol Neurosurg Psychiatry, 2004. **75 Suppl 3**: p. iii35-9.
7. Sugiyama, H., *Clostridium botulinum neurotoxin.* Microbiol Rev, 1980. **44**(3): p. 419-48.

8. Arnon, S.S., R. Schechter, T.V. Inglesby, D.A. Henderson, J.G. Bartlett, M.S. Ascher, E. Eitzen, A.D. Fine, J. Hauer, M. Layton, S. Lillibridge, M.T. Osterholm, T. O'Toole, G. Parker, T.M. Perl, P.K. Russell, D.L. Swerdlow, and K. Tonat, *Botulinum toxin as a biological weapon: medical and public health management.* Jama, 2001. **285**(8): p. 1059-70.

9. Popoff, M.R., *Ecology of neurotoxigenic strains of clostridia.* Curr Top Microbiol Immunol, 1995. **195**: p. 1-29.

10. Whittaker, R.L., Gilbertson, R. B., Garrett, A. S. Jr., *BOTULISM, TYPE E; REPORT OF EIGHT SIMULTANEOUS CASES.* Ann Intern Med, 1964. **61**: p. 448-454.

11. Dolman, C.E., Iida, H., *Type E botulism: its epidemiology, prevention and specific treatment.* Can J Public Health, 1963. **54**: p. 293-308.

12. Prevot, A.R., R. Sillioc, and J. Proute, *[Study of the center of bovine botulism caused by Clostridium botulinum C.].* Ann Inst Pasteur (Paris), 1955. **88**(4): p. 513-5.

13. Demarchi, J.M., C., Orio, J. Prevot, A. R., *Existence du botulisme humain de Type D.* Bull Acad Natl Med Paris, 1958. **142**: p. 580-582.

14. Green, J., Spear, H., Brinson, R. R., *Human botulism (type F)--a rare type.* Am J Med, 1983. **75**: p. 893-895.

15. Midura, T.F., Nygaard, G. S., Wood, R. M., Bodily, H. L., *Clostridium botulinum type F: isolation from venison jerky.* Appl Microbiol, 1972. **24**: p. 165-167.

16. Sonnabend, O., W. Sonnabend, R. Heinzle, T. Sigrist, R. Dirnhofer, and U. Krech, *Isolation of Clostridium botulinum type G and identification of type G botulinal toxin in humans: report of five sudden unexpected deaths.* J Infect Dis, 1981. **143**(1): p. 22-7.

17. Schiavo, G., M. Matteoli, and C. Montecucco, *Neurotoxins affecting neuroexocytosis.* Physiol Rev, 2000. **80**(2): p. 717-66.

18. Burgen, A.S., F. Dickens, and L.J. Zatman, *The action of botulinum toxin on the neuro-muscular junction.* J Physiol, 1949. **109**(1-2): p. 10-24.

19. McMahon, H.T., Y.A. Ushkaryov, L. Edelmann, E. Link, T. Binz, H. Niemann, R. Jahn, and T.C. Sudhof, *Cellubrevin is a ubiquitous tetanus-toxin substrate homologous to a putative synaptic vesicle fusion protein.* Nature, 1993. **364**(6435): p. 346-9.

20. Mironov, S.L., V. Sokolov Yu, A.N. Chanturiya, and V.K. Lishko, *Channels produced by spider venoms in bilayer lipid membrane: mechanisms of ion transport and toxic action.* Biochim Biophys Acta, 1986. **862**(1): p. 185-98.

21. Chen, F., G.M. Kuziemko, and R.C. Stevens, *Biophysical characterization of the stability of the 150-kilodalton botulinum toxin, the nontoxic component, and the 900-kilodalton botulinum toxin complex species.* Infect Immun, 1998. **66**(6): p. 2420-5.

22. Sakaguchi, G., *Clostridium botulinum toxins.* Pharmacol Ther, 1982. **19**(2): p. 165-94.

23. Kukreja, R.V. and B.R. Singh, *Comparative Role of Neurotoxin-Associated Proteins in the Structural Stability and Endopeptidase Activity of Botulinum Neurotoxin Complex Types A and E.* Biochemistry, 2007.

24. DasGupta, B.R., *The structure of botulinum neurotoxin. In: Botulinum Neurotoxin and Tetanus Toxin*. Therapy with botulinum toxin, ed. L.L. Simpson. 1994, New York: Marcel Dekker, Inc.

25. Krieglstein, K.G., A.H. Henschen, U. Weller, and E. Habermann, *Limited proteolysis of tetanus toxin. Relation to activity and identification of cleavage sites.* Eur J Biochem, 1991. **202**(1): p. 41-51.

26. Weller, U., M.E. Dauzenroth, D. Meyer zu Heringdorf, and E. Habermann, *Chains and fragments of tetanus toxin. Separation, reassociation and pharmacological properties.* Eur J Biochem, 1989. **182**(3): p. 649-56.

27. Sathyamoorthy, V. and B.R. DasGupta, *Separation, purification, partial characterization and comparison of the heavy and light chains of botulinum neurotoxin types A, B, and E.* J Biol Chem, 1985. **260**(19): p. 10461-6.

28. Agarwal, R., T. Binz, and S. Swaminathan, *Structural analysis of botulinum neurotoxin serotype F light chain: implications on substrate binding and inhibitor design.* Biochemistry, 2005. **44**(35): p. 11758-65.

29. Agarwal, R., S. Eswaramoorthy, D. Kumaran, T. Binz, and S. Swaminathan, *Structural analysis of botulinum neurotoxin type E catalytic domain and its mutant Glu212-->Gln reveals the pivotal role of the Glu212 carboxylate in the catalytic pathway.* Biochemistry, 2004. **43**(21): p. 6637-44.

30. Arndt, J.W., W. Yu, F. Bi, and R.C. Stevens, *Crystal structure of botulinum neurotoxin type G light chain: serotype divergence in substrate recognition.* Biochemistry, 2005. **44**(28): p. 9574-80.

31. Arndt, J.W., Q. Chai, T. Christian, and R.C. Stevens, *Structure of botulinum neurotoxin type D light chain at 1.65 A resolution: repercussions for VAMP-2 substrate specificity.* Biochemistry, 2006. **45**(10): p. 3255-62.

32. Breidenbach, M.A. and A.T. Brunger, *Substrate recognition strategy for botulinum neurotoxin serotype A.* Nature, 2004. **432**(7019): p. 925-9.

33. Lacy, D.B., W. Tepp, A.C. Cohen, B.R. DasGupta, and R.C. Stevens, *Crystal structure of botulinum neurotoxin type A and implications for toxicity.* Nat Struct Biol, 1998. **5**(10): p. 898-902.

34. Swaminathan, S., and Eswaramoorthy, S., *Structural analysis of the catalytic and binding sites of Clostridium botulinum neurotoxin B.* Nat Struct Biol, 2000. **7**: p. 693-699.

35. Jin, R., A. Rummel, T. Binz, and A.T. Brunger, *Botulinum neurotoxin B recognizes its protein receptor with high affinity and specificity.* Nature, 2006. **444**(7122): p. 1092-5.

36. Chai, Q., J.W. Arndt, M. Dong, W.H. Tepp, E.A. Johnson, E.R. Chapman, and R.C. Stevens, *Structural basis of cell surface receptor recognition by botulinum neurotoxin B.* Nature, 2006. **444**(7122): p. 1096-100.

37. Bonventre, P.F., *Absorption of botulinal toxin from the gastrointestinal tract.* Rev Infect Dis, 1979. **1**(4): p. 663-7.

38. Maksymowych, A.B., M. Reinhard, C.J. Malizio, M.C. Goodnough, E.A. Johnson, and L.L. Simpson, *Pure botulinum neurotoxin is absorbed from the stomach and small intestine and produces peripheral neuromuscular blockade.* Infect Immun, 1999. **67**(9): p. 4708-12.

39. Maksymowych, A.B. and L.L. Simpson, *Binding and transcytosis of botulinum neurotoxin by polarized human colon carcinoma cells.* J Biol Chem, 1998. **273**(34): p. 21950-7.

40. Maksymowych, A.B. and L.L. Simpson, *Structural features of the botulinum neurotoxin molecule that govern binding and transcytosis across polarized human intestinal epithelial cells.* J Pharmacol Exp Ther, 2004. **310**(2): p. 633-41.

41. Simpson, L.L., *Ammonium chloride and methylamine hydrochloride antagonize clostridial neurotoxins.* J Pharmacol Exp Ther, 1983. **225**: p. 546-552.

42. Simpson, L.L., *Identification of the major steps in botulinum toxin action.* Annu Rev Pharmacol Toxicol, 2004. **44**: p. 167-193.

43. Dong, M., F. Yeh, W.H. Tepp, C. Dean, E.A. Johnson, R. Janz, and E.R. Chapman, *SV2 is the protein receptor for botulinum neurotoxin A.* Science, 2006. **312**(5773): p. 592-6.

44. Mahrhold, S., A. Rummel, H. Bigalke, B. Davletov, and T. Binz, *The synaptic vesicle protein 2C mediates the uptake of botulinum neurotoxin A into phrenic nerves.* FEBS Lett, 2006. **580**(8): p. 2011-4.

45. Rummel, A., T. Karnath, T. Henke, H. Bigalke, and T. Binz, *Synaptotagmins I and II act as nerve cell receptors for botulinum neurotoxin G.* J Biol Chem, 2004. **279**(29): p. 30865-70.

46. Nishiki, T., Y. Tokuyama, Y. Kamata, Y. Nemoto, A. Yoshida, K. Sato, M. Sekiguchi, M. Takahashi, and S. Kozaki, *The high-affinity binding of Clostridium botulinum type B neurotoxin to synaptotagmin II associated with gangliosides GT1b/GD1a.* FEBS Lett, 1996. **378**(3): p. 253-7.

47. Cai, S., R. Kukreja, S. Shoesmith, T.W. Chang, and B.R. Singh, *Botulinum neurotoxin light chain refolds at endosomal pH for its translocation.* Protein J, 2006. **25**(7-8): p. 455-62.

48. Koriazova, L.K. and M. Montal, *Translocation of botulinum neurotoxin light chain protease through the heavy chain channel.* Nat Struct Biol, 2003. **10**(1): p. 13-8.

49. Sheridan, R.E., *Gating and permeability of ion channels produced by botulinum toxin types A and E in PC12 cell membranes.* Toxicon, 1998. **36**(5): p. 703-17.

50. Hoch, D.H., M. Romero-Mira, B.E. Ehrlich, A. Finkelstein, B.R. DasGupta, and L.L. Simpson, *Channels formed by botulinum, tetanus, and diphtheria toxins in planar lipid bilayers: relevance to translocation of proteins across membranes.* Proc Natl Acad Sci U S A, 1985. **82**(6): p. 1692-6.

51. Blasi, J., E.R. Chapman, E. Link, T. Binz, S. Yamasaki, P. De Camilli, T.C. Sudhof, H. Niemann, and R. Jahn, *Botulinum neurotoxin A selectively cleaves the synaptic protein SNAP-25.* Nature, 1993. **365**(6442): p. 160-3.

52. Jahn, R., T. Lang, and T.C. Sudhof, *Membrane fusion.* Cell, 2003. **112**(4): p. 519-33.

53. Schiavo, G., O. Rossetto, A. Santucci, B.R. DasGupta, and C. Montecucco, *Botulinum neurotoxins are zinc proteins.* J Biol Chem, 1992. **267**(33): p. 23479-83.

54. Sutton, R.B., Fasshauer, D., Jahn, R., and Brunger, A. T., *Crystal structure of a SNARE complex involved in synaptic exocytosis at 2.4 A resolution.* Nature, 1998. **395**: p. 347-353.

55. Weber, T., Zemelman, B. V., McNew, J. A., Westermann, B., Gmachl, M., Parlati, F., Söllner, T. H., and Rothman, J. E., *SNAREpins: minimal machinery for membrane fusion.* Cell, 1998. **92**(759-772).

56. Ferrer-Montiel, A.V., L.M. Gutierrez, J.P. Apland, J.M. Canaves, A. Gil, S. Viniegra, J.A. Biser, M. Adler, and M. Montal, *The 26-mer peptide released from SNAP-25 cleavage by botulinum neurotoxin E inhibits vesicle docking.* FEBS Lett, 1998. **435**(1): p. 84-8.

57. Apland, J.P., J.A. Biser, M. Adler, A.V. Ferrer-Montiel, M. Montal, J.M. Canaves, and M.G. Filbert, *Peptides that mimic the carboxy-terminal domain of SNAP-25 block acetylcholine release at an Aplysia synapse.* J Appl Toxicol, 1999. **19 Suppl 1**: p. S23-6.

58. Jackson, M.B. and E.R. Chapman, *Fusion pores and fusion machines in Ca2+-triggered exocytosis.* Annu Rev Biophys Biomol Struct, 2006. **35**: p. 135-60.

59. Oyler, G.A., J.W. Polli, M.C. Wilson, and M.L. Billingsley, *Developmental expression of the 25-kDa synaptosomal-associated protein (SNAP-25) in rat brain.* Proc Natl Acad Sci U S A, 1991. **88**(12): p. 5247-51.

60. Rickman, C., F.A. Meunier, T. Binz, and B. Davletov, *High affinity interaction of syntaxin and SNAP-25 on the plasma membrane is abolished by botulinum toxin E.* J Biol Chem, 2004. **279**(1): p. 644-51.

61. Vogel, K., J.P. Cabaniols, and P.A. Roche, *Targeting of SNAP-25 to membranes is mediated by its association with the target SNARE syntaxin.* J Biol Chem, 2000. **275**(4): p. 2959-65.

62. Davletov, B., M. Bajohrs, and T. Binz, *Beyond BOTOX: advantages and limitations of individual botulinum neurotoxins.* Trends Neurosci, 2005. **28**(8): p. 446-52.

63. Schiavo, G., G. Stenbeck, J.E. Rothman, and T.H. Sollner, *Binding of the synaptic vesicle v-SNARE, synaptotagmin, to the plasma membrane t-SNARE, SNAP-25, can explain docked vesicles at neurotoxin-treated synapses.* Proc Natl Acad Sci U S A, 1997. **94**(3): p. 997-1001.

64. Lynch, K.L., R.R. Gerona, E.C. Larsen, R.F. Marcia, J.C. Mitchell, and T.F. Martin, *Synaptotagmin C2A Loop 2 Mediates Ca2+-dependent SNARE Interactions Essential for Ca2+-triggered Vesicle Exocytosis.* Mol Biol Cell, 2007. **18**(12): p. 4957-68.

65. Kesavan, J., M. Borisovska, and D. Bruns, *v-SNARE actions during Ca(2+)-triggered exocytosis.* Cell, 2007. **131**(2): p. 351-63.

66. Blasi, J., E.R. Chapman, S. Yamasaki, T. Binz, H. Niemann, and R. Jahn, *Botulinum neurotoxin C1 blocks neurotransmitter release by means of cleaving HPC-1/syntaxin.* Embo J, 1993. **12**(12): p. 4821-8.

67. Foran, P., G.W. Lawrence, C.C. Shone, K.A. Foster, and J.O. Dolly, *Botulinum neurotoxin C1 cleaves both syntaxin and SNAP-25 in intact and permeabilized chromaffin cells: correlation with its blockade of catecholamine release.* Biochemistry, 1996. **35**(8): p. 2630-6.

68. Schiavo, G., A. Santucci, B.R. Dasgupta, P.P. Mehta, J. Jontes, F. Benfenati, M.C. Wilson, and C. Montecucco, *Botulinum neurotoxins serotypes A and E cleave SNAP-25 at distinct COOH-terminal peptide bonds.* FEBS Lett, 1993. **335**(1): p. 99-103.

69. Schiavo, G., C.C. Shone, M.K. Bennett, R.H. Scheller, and C. Montecucco, *Botulinum neurotoxin type C cleaves a single Lys-Ala bond within the carboxyl-terminal region of syntaxins.* J Biol Chem, 1995. **270**(18): p. 10566-70.

70. Schiavo, G., C.C. Shone, O. Rossetto, F.C. Alexander, and C. Montecucco, *Botulinum neurotoxin serotype F is a zinc endopeptidase specific for VAMP/synaptobrevin.* J Biol Chem, 1993. **268**(16): p. 11516-9.

71. Schiavo, G., C. Malizio, W.S. Trimble, P. Polverino de Laureto, G. Milan, H. Sugiyama, E.A. Johnson, and C. Montecucco, *Botulinum G neurotoxin cleaves VAMP/synaptobrevin at a single Ala-Ala peptide bond.* J Biol Chem, 1994. **269**(32): p. 20213-6.

72. Schiavo, G., F. Benfenati, B. Poulain, O. Rossetto, P. Polverino de Laureto, B.R. DasGupta, and C. Montecucco, *Tetanus and botulinum-B neurotoxins block neurotransmitter release by proteolytic cleavage of synaptobrevin.* Nature, 1992. **359**(6398): p. 832-5.
73. Yamasaki, S., T. Binz, T. Hayashi, E. Szabo, N. Yamasaki, M. Eklund, R. Jahn, and H. Niemann, *Botulinum neurotoxin type G proteolyses the Ala81-Ala82 bond of rat synaptobrevin 2.* Biochem Biophys Res Commun, 1994. **200**(2): p. 829-35.

74. Yamasaki, S., A. Baumeister, T. Binz, J. Blasi, E. Link, F. Cornille, B. Roques, E.M. Fykse, T.C. Sudhof, R. Jahn, and et al., *Cleavage of members of the synaptobrevin/VAMP family by types D and F botulinal neurotoxins and tetanus toxin.* J Biol Chem, 1994. **269**(17): p. 12764-72.

75. Breidenbach, M.A. and A.T. Brunger, *New insights into clostridial neurotoxin-SNARE interactions.* Trends Mol Med, 2005. **11**(8): p. 377-81.

76. Blobel, G., *Intracellular protein topogenesis.* Proc Natl Acad Sci U S A, 1980. **77**(3): p. 1496-500.

77. Blobel, G., P. Walter, C.N. Chang, B.M. Goldman, A.H. Erickson, and V.R. Lingappa, *Translocation of proteins across membranes: the signal hypothesis and beyond.* Symp Soc Exp Biol, 1979. **33**: p. 9-36.

78. Mitra, K., C. Schaffitzel, T. Shaikh, F. Tama, S. Jenni, C.L. Brooks, 3rd, N. Ban, and J. Frank, *Structure of the E. coli protein-conducting channel bound to a translating ribosome.* Nature, 2005. **438**(7066): p. 318-24.

79. Van den Berg, B., Clemons, W. M., Jr., Collinson, I., Modis, Y., Hartmann, E., Harrison, S. C., and Rapoport, T. A., *X-ray structure of a protein-conducting channel.* Nature, 2004. **427**: p. 36-44.

80. Beckmann, R., C.M. Spahn, N. Eswar, J. Helmers, P.A. Penczek, A. Sali, J. Frank, and G. Blobel, *Architecture of the protein-conducting channel associated with the translating 80S ribosome.* Cell, 2001. **107**(3): p. 361-72.

81. Cannon, K.S., E. Or, W.M. Clemons, Jr., Y. Shibata, and T.A. Rapoport, *Disulfide bridge formation between SecY and a translocating polypeptide localizes the translocation pore to the center of SecY.* J Cell Biol, 2005. **169**(2): p. 219-25.

82. Gumbart, J. and K. Schulten, *Molecular dynamics studies of the archaeal translocon.* Biophys J, 2006. **90**(7): p. 2356-67.

83. Mokranjac, D. and W. Neupert, *Protein import into mitochondria.* Biochem Soc Trans, 2005. **33**(Pt 5): p. 1019-23.

84. Schnell, D.J. and D.N. Hebert, *Protein translocons: multifunctional mediators of protein translocation across membranes.* Cell, 2003. **112**(4): p. 491-505.

85. Rehling, P., K. Brandner, and N. Pfanner, *Mitochondrial import and the twin-pore translocase.* Nat Rev Mol Cell Biol, 2004. **5**(7): p. 519-30.

86. Truscott, K.N., Kovermann, P., Geissler, A., Merlin, A., Meijer, M., Driessen, A. J., Rassow, J., Pfanner, N., and Wagner, R., *A presequence- and voltage-sensitive channel of the mitochondrial preprotein translocase formed by Tim23.* Nat Struct Biol, 2001. **8**: p. 1074-1082.

87. Hinnah, S.C., R. Wagner, N. Sveshnikova, R. Harrer, and J. Soll, *The chloroplast protein import channel Toc75: pore properties and interaction with transit peptides.* Biophys J, 2002. **83**(2): p. 899-911.

88. Heins, L., A. Mehrle, R. Hemmler, R. Wagner, M. Kuchler, F. Hormann, D. Sveshnikov, and J. Soll, *The preprotein conducting channel at the inner envelope membrane of plastids.* Embo J, 2002. **21**(11): p. 2616-25.

89. Zhang, S., E. Udho, Z. Wu, R.J. Collier, and A. Finkelstein, *Protein translocation through anthrax toxin channels formed in planar lipid bilayers.* Biophys J, 2004. **87**(6): p. 3842-9.

90. Krantz, B.A., R.A. Melnyk, S. Zhang, S.J. Juris, D.B. Lacy, Z. Wu, A. Finkelstein, and R.J. Collier, *A phenylalanine clamp catalyzes protein translocation through the anthrax toxin pore.* Science, 2005. **309**(5735): p. 777-81.

91. Krantz, B.A., A.D. Trivedi, K. Cunningham, K.A. Christensen, and R.J. Collier, *Acid-induced unfolding of the amino-terminal domains of the lethal and edema factors of anthrax toxin.* J Mol Biol, 2004. **344**(3): p. 739-56.

92. Krantz, B.A., A. Finkelstein, and R.J. Collier, *Protein translocation through the anthrax toxin transmembrane pore is driven by a proton gradient.* J Mol Biol, 2006. **355**(5): p. 968-79.

93. Movileanu, L., J.P. Schmittschmitt, J.M. Scholtz, and H. Bayley, *Interactions of peptides with a protein pore.* Biophys J, 2005. **89**(2): p. 1030-45.

Chapter 1

Characterization of Clostridium Botulinum Neurotoxin Channels in Neuroblastoma Cells

F.P. Graham Publishing Co.

Characterization of *Clostridial botulinum* Neurotoxin Channels in Neuroblastoma Cells

AUDREY FISCHER and MAURICIO MONTAL*

Section of Neurobiology, Division of Biological Sciences, University of California San Diego, La Jolla, CA 92093-0366, USA. mmontal@ucsd.edu

(Received 21 September 2005; Revised 20 December 2005; In final form 20 December 2005)

The channel and chaperone activities of *Clostridial botulinum* neurotoxin (BoNT) A were investigated in Neuro 2a neuroblastoma cells under conditions that closely emulate those prevalent at the endosome. Channel activity occurs in bursts interspersed between periods of little or no activity. The channels are voltage dependent, opening only at negative voltages. Within bursts, the channel resides preferentially in the open state. The channels open to a main conductance of 105 ± 5 pS or 65 ± 4 pS in 200 mM CsCl or NaCl, respectively. The BoNT channels display a conspicuous subconductance of 10 ± 2 pS. The neuroblastoma cell line appears, therefore, to be a suitable system to characterize the BoNT channel and to pursue evaluation of plausible strategies for targeted drug delivery thereby minimizing the requirement for *in vivo* animal testing.

Keywords: Botulinum neurotoxin; Channels; Chaperones; Targeted drug screen; Protein translocation

INTRODUCTION

Chemoprophylaxis and therapeutic intervention of the deadly intoxication by botulinum neurotoxins requires understanding the mechanisms by which it abrogates neurotransmitter release. Biochemically, BoNTs have two disulfide linked chains: a light chain of ~50 kD and a heavy chain of ~100 kD; structurally, BoNT consists of three domains (Lacy *et al.*, 1998; Lacy and Stevens, 1999; Schiavo *et al.*, 2000; Swaminathan and Eswaramoorthy, 2000): The N-terminal light chain is the catalytic domain whereas the heavy chain encompasses the translocation domain (the N-terminal half) and the receptor-binding domain (the C-terminal half). Our aim is to elucidate the fundamental molecular mechanisms that confer to BoNT its exquisite ability to move efficiently and selectively within neurons exploiting such tri-modular organization. An immediate objective is to understand the intricacies of intracellular trafficking of BoNT that may disclose novel pathways to escort, target, and insert it into membranes. This information may prove diagnostic in identifying unsuspected sites for intervention and plausible strategies for targeted drug delivery.

BoNTs enter sensitive cells *via* receptor-mediated endocytosis (Hoch *et al.*, 1985, Schiavo *et al.*, 2000). The BoNT receptor-binding module establishes the cellular specificity mediated by its high affinity interaction with a surface protein receptor and a ganglioside co-receptor (Nishiki *et al.*, 1996; Dong *et al.*, 2003; Rummel *et al.*, 2004). Given that the BoNT heavy chain forms channels in lipid bilayers (Hoch *et al.*, 1985; Donovan and Middlebrook, 1986; Blaustein *et al.*, 1987) and PC12 cells (Sheridan, 1998), predominantly under acidic conditions and only after chemical reduction, it has been surmised that the BoNT translocation module mediates the passage of the enzymatic module from the interior of the endosome into the cytosol (Hoch *et al.*, 1985; Schiavo *et al.*, 2000). Recently, we discovered that the heavy chain of BoNT acts as both a channel and a transmembrane chaperone for the light chain to ensure a translocation competent conformation during its transit from the acidic endosome into the cytosol - its site of action (Koriazova and Montal, 2003). The light chain is a Zn^{2+}-metalloprotease that cleaves the protein components involved in synaptic vesicle fusion with the neuronal membrane, thereby abrogating synaptic transmission (Schiavo *et al.*, 2000). To accomplish this task, the heavy chain operates as a transmembrane protein-conducting channel: the channel is occluded by the light chain during transit, and open after completion of translocation and release of cargo, acting intriguingly similar to the protein-conducting/translocating channels of the endoplasmic reticulum (ER), mitochondria, and chlo-

*Corresponding author. Tel.: 1 858-534-0931; FAX: 1 858-822-3763; E-mail: mmontal@ucsd.edu
ISSN 1029 8428 print/ ISSN 1476-3524 online.

roplasts (Koriazova and Montal, 2003). This finding has outlined a novel way of thinking about BoNT neurotoxicity, shifting the focus of attention on its translocation within cells rather than on the protease activity of the light chain, which is known not to be toxic unless it is internalized. And, it has suggested that the BoNT channel represents a potential target for intervention based on the identification of open channel blockers as a single class of drugs that would be effective against all seven *Clostridial butulinum* neurotoxin isoforms. To investigate this option we have developed a neuronal system to characterize the channel and chaperone activities of BoNT under conditions which closely emulate those prevalent at the endosome, and which are relevant to the neurotropism and neuroparalytic effects of BoNTs. Here we show that Neuro 2a neuroblastoma cells appear to be such a system.

MATERIALS AND METHODS

Unless otherwise specified, all chemicals were purchased from Sigma-Aldrich (St. Louis, MO). Purified native BoNT isoform A was from Metabiologics (Madison, WI).

Cell Culture

Neuro 2a neuroblastoma cells, derived from a spontaneous tumor of a Strain A albino mouse, were obtained from the American Type Culture Collection and passaged in DMEM (BioWhittaker, Rockland, ME) supplemented with penicillin 10mM/streptomycin 10 µg/mL/glutamine 2mM (Invitrogen, Carlsbad, CA), and 5% newborn bovine serum (Invitrogen). Neuro 2a cells were plated onto Matrigel (BD Biosciences, San Jose, CA) coated glass coverslips at 500 cells/coverslip, and cultured at 37°C, 5% CO_2 for 1-3 days prior to patch clamp recordings.

Patch Clamp Recordings

Capillaries of borosilicate glass from Hilgenberg (Germany) were polished and used at 3.5-7.0 MΩ resistance when immersed in recording solution. Excised patches in the inside-out configuration were used (Hamill *et al.*, 1981). After gigaohm (GΩ) seal formation, the patch is excised from the cell and current recordings are obtained under voltage clamp conditions. Records were acquired and analyzed using the patch clamp amplifier system (List EPC-9, HEKA Electronik, Germany) fitted with an ITC-16 interface (Instrutech, Port Washington, NY) and the Pulse/PulseFit acquisition and analysis software (HEKA, Germany). Data were acquired at a sampling frequency > 5 kHz and filtered online to 3 kHz with a 3-pole Bessel filter. Data were analyzed using Clampfit v.9.2 software (Axon Instruments, Sunnyvale, CA), Microsoft Excel and IGOR Pro (Wavemetrics, Portland, OR). All statistical values represent means ± SEM, unless otherwise indicated. *n* and *N* denote number of experiments and number of events, respectively. All experiments were conducted at 23 ± 1°C.

Solutions

To emulate endosomal conditions the external (bath) solution contains (in mM) CsCl or NaCl 200, NaMOPS [3-(N-morpholino) propanesulfonic acid] 5, (pH 7.0 with HCl), DTT (dithiothreitol) 1, and the internal (pipet) solution contains (in mM) CsCl or NaCl 200, NaMES [2-(N-morpholino) ethanesulfonic acid] 5, (pH 5.3 with HCl), DTT 1. The osmolarity of both solutions is adjusted to ~370 mOsm. To improve seal stability in the recordings using NaCl, the reductant DTT was removed from the pipette solution and the bath solution was supplemented with 0.25mM Tris(2-carboxy-ethyl)phosphine hydrochloride (TCEP). Channel insertion is achieved by supplementing 5 µg/ml BoNT A holotoxin to the internal (pipet) solution, which is set to an endosomal pH of 5.3.

RESULTS

Neuro 2a cells constitute a good neuronal model for neurosecretion and electrophysiology. Neuro 2a cells are highly sensitive to BoNTs (Yowler *et al.*, 2002) and are readily accessible for patch clamp recordings (Hamill *et al.*, 1981). To attenuate or eliminate endogenous channel activity while selectively augmenting the detection of BoNT channel currents, the external and internal solutions contain CsCl: Cs^+ acts as the current carrier for the BoNT channel (Sheridan, 1998) and it does not permeate through endogenous K^+ or Na^+ channels (Hille, 2001). In addition, the solutions are supplemented with 1 mM $ZnCl_2$ (bath) or 1 mM 4,4-diisothiocyanostilbene-2,2'-disulfonic acid (DIDS) (pipet) to eliminate currents arising from endogenous Cl^- channels known to be present in these cells (Lascola *et al.*, 1998; Carpaneto *et al.*, 1999). Under these conditions, the endogenous channel activity of Neuro 2a cells is practically abolished (*n* = 361 control experiments).

Toxin insertion and channel formation are pH and redox dependent; no channels are detected when the internal solution is held at pH 7 rather than pH 5.3 or when the bath solution does not contain reductant. The current flowing through individual BoNT channels at the indicated voltages is shown in figure 1. The channels are voltage dependent, opening only at negative voltages. Single-channel currents were determined

at each voltage from amplitude histograms (Keller *et al.*, 1986). The single-channel current (I)-voltage (V) curves for BoNT channels are displayed in figures 2a and 2b. BoNT channels open to a main conductance of 105 ± 5 pS and display a conspicuous subconductance of ~10 pS ($6 \leq n \leq 22$; $N = 2{,}820$ per data point) (FIG. 2a). Inspection of figure 1 clearly shows that the BoNT channel activity occurs in bursts interspersed between periods of little or no activity; the frequency of burst occurrence is also voltage dependent, increasing with negative voltages up to ~ -80 mV. The quiescent periods between bursts are prolonged at voltages more negative than this threshold even though the channel fast gating to the open state continues to increase up to -110mV.

Within the bursts, the channel resides preferentially in the open state (O) making frequent and fast transitions to the closed state (C). The open channel probability

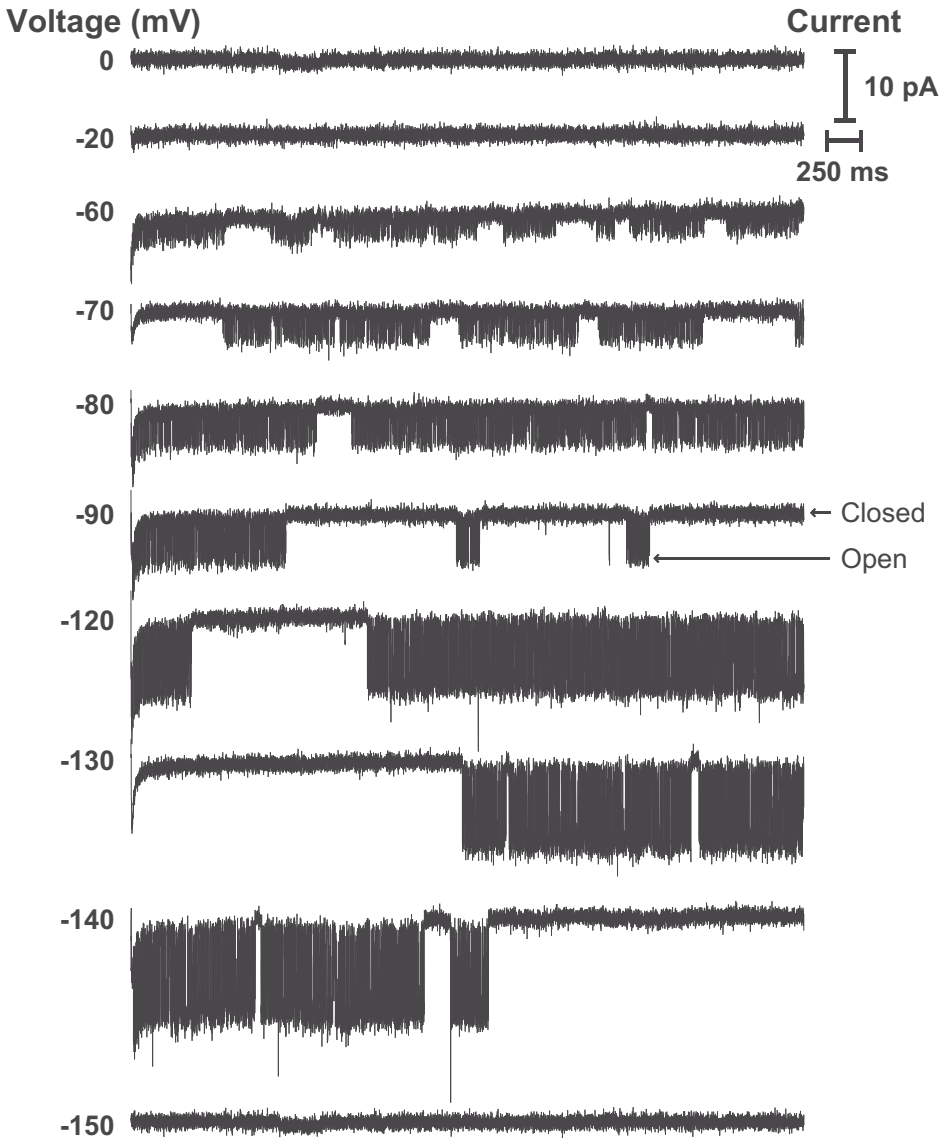

FIGURE 1 Botulinum neurotoxin A channels in excised patches of Neuro 2a cells. Representative single-channel currents at the indicated voltages; consecutive voltage pulses applied to the same patch. Channel opening is indicated by a downward deflection. BoNT A channels occur in bursts; the burst frequency and duration are voltage-dependent. Recordings were obtained in 200 mM CsCl solutions. BoNT A channels open to a main conductance of ~105 pS.

(P_o) within bursts sharply increases with negative voltages: the voltage at which $P_o = 0.5$ is 45 ± 7 mV ($6 \leq n \leq 22$; $N = 2{,}820$ per data point) (FIG. 2d).

At the onset of a burst, the channel enters the ~10 pS subconductance state (S) and then undergoes quick transitions between this intermediate state and the open state (FIG. 2b). This is clearly shown in figure 3. The open state shows very fast transitions to the substate and to the closed state giving the appearance of flickering between the open state and the substate, the predominant activity within a burst. A section delimited by the arrows is displayed at higher time resolution in the lower panel, in which transitions between the three indicated states are clearly discerned. Channel opening (O) is indicated as a downward deflection and the approximate value of the subconductance state (S) is marked. The characteristic opening and closing transitions are resolved, showing the occurrence of fast transitions to the substate. Figure 2c illustrates the transitions between a closed (C), open substate (S) and the fully open state (O). The magnitude of the arrows connecting the states is proportional to the frequency of occurrence of transitions between the three states. Within a burst, the channel rarely returns to the closed state from the open state, exhibiting a high propensity to fluctuate between the subconductance and open states or the subconductance and closed states. Thus, the subconductance state and the transitions into and out of this state are clearly recognized in the single-channel recordings. This pattern of channel activity was previously identified in single-channel recordings from tetanus toxin, another clostridial neurotoxin reconstituted in lipid bilayers (Gambale and Montal, 1988), suggesting similarities of the assembled and functional clostridial channels in membranes.

To investigate the BoNT channel properties under ionic conditions that approximate more closely those prevalent in endosomes, the BoNT channel was characterized in 200 mM NaCl and compared with the properties hitherto described in 200 mM CsCl. Representative

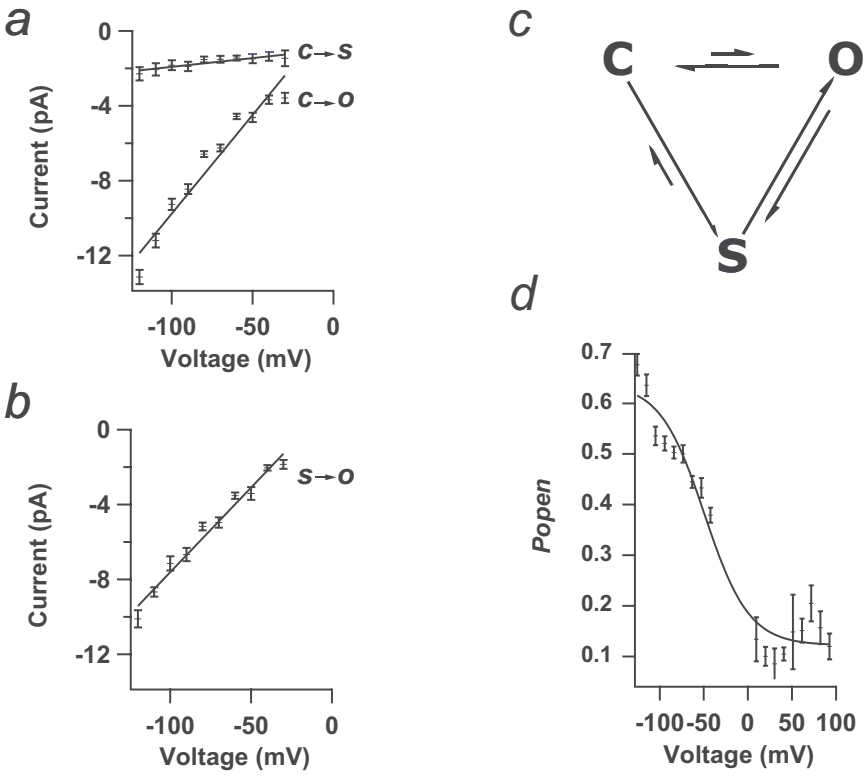

FIGURE 2 Analysis of BoNT A channels in Neuro 2a cells. (**a**) Single channel current-voltage characteristics for transitions from the closed state (C) to substate (S) with a conductance of 10 ± 2 pS and from closed state to open state with a conductance of 105 ± 5 pS (O). (**b**) Single channel current-voltage characteristics for transitions from the substate to the open state with a conductance of 95 ± 2 pS. (**c**) Transitions between closed (C), substate (S) and fully open (O) state of BoNT A channels. Arrow magnitude is proportional to probability of transition. (**d**) Probability of channel residence in the open state (P_o) as a function of voltage; the voltage at which $P_o = 0.5$ is -45 ± 7 mV. Analysis is based on single bursts of channel activity within a record; ($6 \leq n \leq 22$ per data point; the average N per data point = 2,820 events). Other conditions as in figure 1.

records obtained under these experimental conditions are shown in figure 4a. The patch was exposed to BoNT and voltage ramps from -100 mV to 100 mV with a cycle duration of 10 s were applied. In the absence of BoNT in the pipet (-) no channel activity is recorded. In contrast, when the BoNT is present inside the pipet (+), the occurrence of discrete transitions between the closed and open state of the channel are distinctly resolved. The pattern of activity is similar both in Cs^+ (middle panel) or Na^+ (lower panel). A major difference is the single channel conductance: For Cs^+, the single channel conductance is 105 ± 5 pS ($6 \leq n \leq 22$; $N = 2{,}820$ per data point) (FIG. 2) and for Na^+, 65 ± 4 pS ($n = 6$, $N = 12{,}000$). A segment of a current record obtained at -90 mV in Na^+ is displayed in figure 4b at higher resolution. The occurrence of the subconductance state (S) of 10 ± 2 pS is clearly discerned in the single channel recording. The signal to noise ratio of these recordings is very high, therefore validating the strategy and providing a sensitive assay to characterize the properties of the BoNT channel, and modifications introduced by channel blocker candidates. The transmembrane voltage may be readily modified and a variety of pulse stimulation protocols may be applied to examine alterations ensued by these modifiers on the conduction pathway or the lifetime of the channel in open or closed states, namely the gating kinetics.

CONCLUSIONS

Remarkably, the pattern of channel activity displayed by BoNT A in Neuro 2a cells is similar to that previously characterized in lipid bilayers composed of phosphatidylcholine, phosphatidylethanolamine, phosphatidylserine and the ganglioside GT1b (Koriazova and Montal, 2003). No other cellular components are required in order to retrieve BoNT A channel activity in lipid membranes. BoNT A holotoxin single channel conductance (γ) in planar lipid bilayers bathed in 0.2 M KCl is 74 ± 12 pS (L. Koriazova and M. Montal, unpublished results). This value is in good agreement with a γ = 65 ± 4 pS recorded in Neuro 2a cells bathed in 0.2 M NaCl, given the equivalent ionic conductance in aqueous solution for KCl = 1.18 NaCl (Hille, 2001).

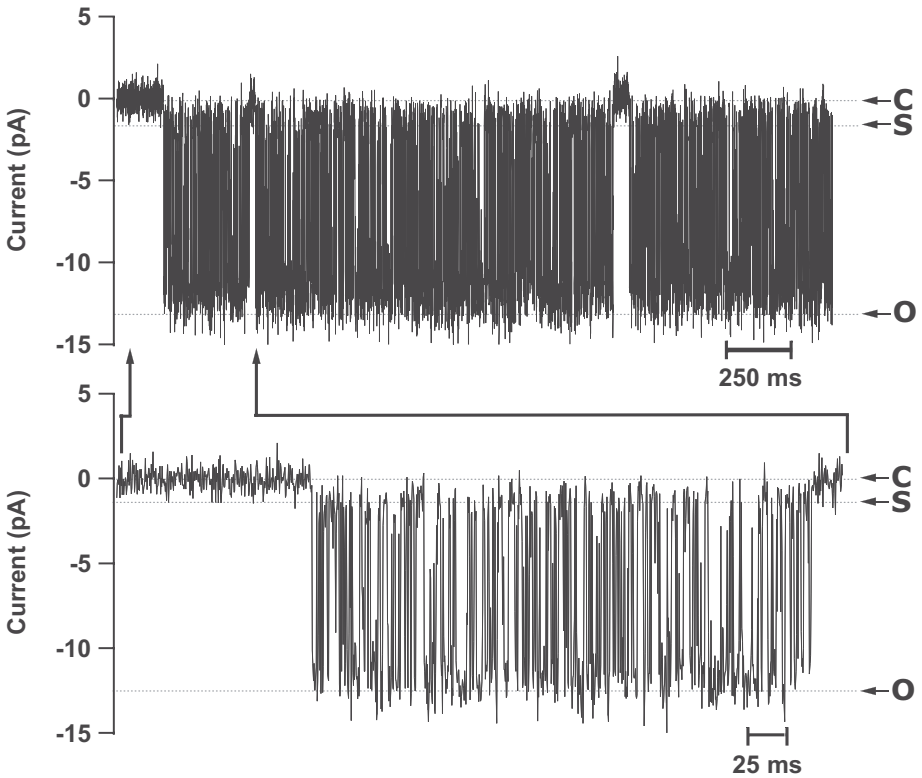

FIGURE 3 BoNT A bursting channel activity in excised patches of Neuro 2a cells. At -130 mV transitions from the closed (C) to the open (O) state and from the substate (S) to the open state are clearly resolved. The BoNT A channels open to a main conductance of ~105 pS and a subconductance of ~10 pS. The approximate current value for the subconductance state (S) is marked. The lower panel shows the section of the record delimited by the arrows at higher time resolution. Other conditions as in figure 1.

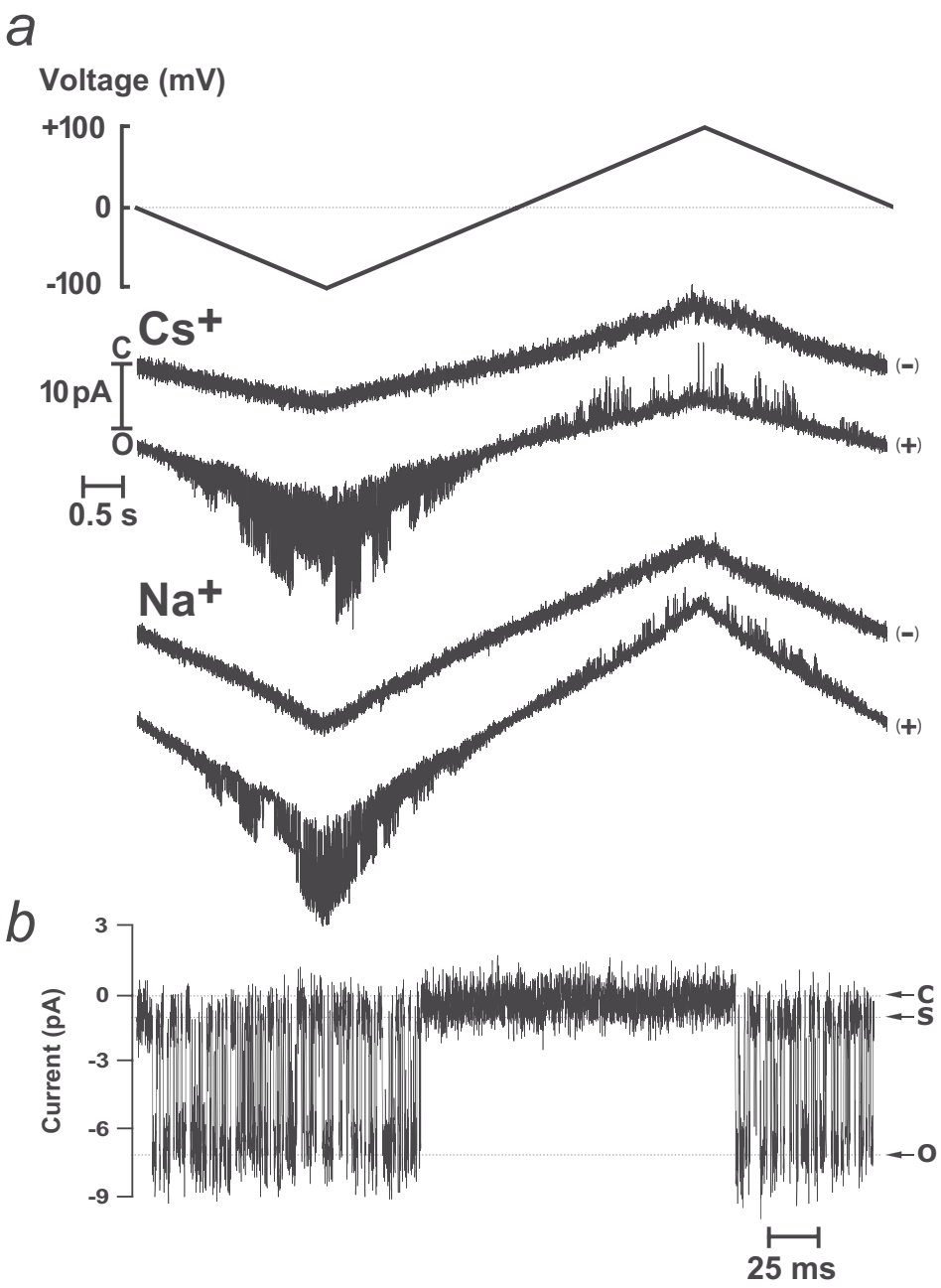

FIGURE 4a Current-voltage characteristics of BoNT A channels in Neuro 2a cells. Current records in response to a continuously cycled voltage of -100 mV to +100 mV (top panel) in symmetric 200 mM CsCl (middle panel) or NaCl (lower panel). Recordings obtained in the absence (-) or presence (+) of BoNT are indicated. Note the occurrence of two discrete channels with a single channel conductance of 105 pS in Cs^+ and 65 pS in Na^+; downward deflections indicate channel opening.

FIGURE 4b Single channel recording obtained in 200 mM NaCl at -90 mV. Transitions from the closed to the open state and from the substate to the open state are clearly resolved. The BoNT A channels open to a main conductance of ~65 pS and exhibit a subconductance of ~10 pS. Other conditons as in figure 1.

In addition, it is clear that the kinetics of the BoNT A single channel activity are modulated by the lipid composition of the bilayer; in Neuro 2a cells the mean lifetime of the channel in both closed and open states is ≤ 1 ms, whereas in lipid bilayers it is ≥ 5 ms. Membrane lipid composition is, therefore, an important regulator of channel activity as previously shown for tetanus toxin (Gambale and Montal, 1988; Rauch *et al.*, 1990).

A salient feature of the BoNT channel is that it is closed at positive voltages under conditions in which the orientation and the magnitude of the pH gradient, as well as the polarity and magnitude of the membrane potential, compare fairly well with those prevailing across endosomes: pH 5.3 and positive potential on the compartment containing the BoNT and pH 7.0 and negative potential on the opposite compartment. This suggests that the BoNT heavy chain channel would be closed in the endosome until it is gated by the BoNT light chain to initiate its translocation across the membrane into the cytosol.

The neuroblastoma cell line appears, therefore, to be a suitable system to characterize the BoNT channel and to pursue evaluation of plausible strategies for targeted drug delivery thereby minimizing the requirement for *in vivo* animal testing. In addition, the availability of sensitive assays for the light chain catalytic activity and for the heavy chain channel and chaperone activities in neuronal cells has opened new dimensions to investigate the conformational transitions of both chains linked to translocation across endosomes, the pivotal role of pH gradients, redox gradients, and electrical potentials across endosomes as driving forces underlying membrane insertion and translocation, and the requirements for light chain refolding and release at the endosome surface after translocation. These insights collectively with new findings obtained with similar modular toxins such as anthrax (Zhang *et al.*, 2004; Krantz *et al.*, 2005a,b) and diphtheria (Oh *et al.*, 1999; Ren *et al.*, 1999; Finkelstein *et al.*, 2000; Senzel *et al.*, 2000) are likely to be of fundamental significance to understanding the mechanism of protein translocation across membranes (Wickner and Schekman, 2005).

Acknowledgements

We thank Dr. Lilia Koriazova for single BoNT channel results in lipid bilayers and perceptive comments, and Dr. Mike Goodnough for his invaluable ongoing help. This work was supported by the U.S. Army Medical Research and Materiel Command under Grant DAMD17-02-C-0106. A. Fischer was supported in part by the Molecular Biophysics Training Grant T32 GM08326 from the National Institute of General Medical Sciences.

References

Blaustein RO, WJ Germann, A Finkelstein and BR DasGupta (1987) The N-terminal half of the heavy chain of botulinum type A neurotoxin forms channels in planar phospholipid bilayers. *FEBS Lett.* **226**, 115-120.

Carpaneto A, A Accardi, M Pisciotta and F Gambale (1999) Chloride channels activated by hypotonicity in N2A neuroblastoma cell line. *Exp. Brain Res.* **124**, 193-199.

Dong M, DA Richards, MC Goodnough, WH Tepp, EA Johnson and ER Chapman (2003) Synaptotagmins I and II mediate entry of botulinum neurotoxin B into cells. *J. Cell. Biol.* **162**, 1293-1303.

Donovan JJ and JL Middlebrook (1986) Ion-conducting channels produced by botulinum toxin in planar lipid membranes. *Biochemistry* **25**, 2872-2876.

Finkelstein A, KJ Oh, L Senzel, M Gordon, RO Blaustein and RJ Collier (2000) The diphtheria toxin channel-forming T-domain translocates its own NH_2-terminal region and the catalytic domain across planar phospholipid bilayers. *Int. J. Med. Microbiol.* **290**, 435-440.

Gambale F and M Montal (1988) Characterization of the channel properties of tetanus toxin in planar lipid bilayers. *Biophys. J.* **53**, 771-783.

Hamill OP, A Marty, E Neher, B Sakmann and FJ Sigworth (1981) Improved patch-clamp techniques for high-resolution current recording from cells and cell-free membrane patches. *Pflugers Arch.* **391**, 85-100.

Hille B (2001) *Ion Channels of Excitable Cells, 3rd Edition* (Sinauer: Sunderland, MA).

Hoch DH, M Romero-Mira, BE Ehrlich, A Finkelstein, BR DasGupta and LL Simpson (1985) Channels formed by botulinum, tetanus, and diphtheria toxins in planar lipid bilayers: relevance to translocation of proteins across membranes. *Proc. Natl. Acad. Sci. USA* **82**, 1692-1696.

Keller BU, RP Hartshorne, JA Talvenheimo, WA Catterall and M Montal (1986) Sodium channels in planar lipid bilayers. Channel gating kinetics of purified sodium channels modified by batrachotoxin. *J. Gen. Physiol.* **88**, 1-23.

Koriazova LK and M Montal (2003) Translocation of botulinum neurotoxin light chain protease through the heavy chain channel. *Nat. Struct. Biol.* **10**, 13-18.

Krantz BA, A Finkelstein and RJ Collier (2005a) Protein Translocation through the anthrax toxin transmembrane pore is driven by a proton gradient. *J. Mol. Biol.* 2005 Dec 1; [Epub ahead of print].

Krantz BA, RA Melnyk, S Zhang, SJ Juris, DB Lacy, Z Wu, A Finkelstein and RJ Collier (2005b) A phenylalanine clamp catalyzes protein translocation through the anthrax toxin pore. *Science* **309**, 777-781.

Lacy DB and RC Stevens (1999) Sequence homology and structural analysis of the clostridial neurotoxins. *J. Mol. Biol.* **291**, 1091-1104.

Lacy DB, W Tepp, AC Cohen, BR DasGupta and RC Stevens (1998) Crystal structure of botulinum neurotoxin type A and implications for toxicity. *Nat. Struct. Biol.* **5**, 898-902.

Lascola CD, DJ Nelson and RP Kraig (1998) Cytoskeletal actin gates a Cl^- channel in neocortical astrocytes. *J. Neurosci.* **18**, 1679-1692.

Nishiki T, Y Tokuyama, Y Kamata, Y Nemoto, A Yoshida, M Sekiguchi, M Takahashi and S Kozaki (1996) Binding of botulinum type B neurotoxin to Chinese hamster ovary cells transfected with rat synaptotagmin II cDNA. *Neurosci. Lett.* **208**, 105-108.

Oh KJ, L Senzel, RJ Collier and A Finkelstein (1999) Translocation of the catalytic domain of diphtheria toxin across planar phospho-

lipid bilayers by its own T domain. *Proc. Natl. Acad. Sci. USA* **96**, 8467-8470.

Rauch G, F Gambale and M Montal (1990) Tetanus toxin channel in phosphatidylserine planar bilayers: conductance states and pH dependence. *Eur. Biophys. J.* **18**, 79-83.

Ren J, K Kachel, H Kim, SE Malenbaum, RJ Collier and E London (1999) Interaction of diphtheria toxin T domain with molten globule-like proteins and its implications for translocation. *Science* **284**, 955-957.

Rummel A, T Karnath, T Henke, H Bigalke and T Binz (2004) Synaptotagmins I and II act as nerve cell receptors for botulinum neurotoxin G. *J. Biol. Chem.* **279**, 30865-30870.

Schiavo G, M Matteoli and C Montecucco (2000) Neurotoxins affecting neuroexocytosis. *Physiol. Rev.* **80**, 717-766.

Senzel L, M Gordon, RO Blaustein, KJ Oh, RJ Collier and A Finkelstein (2000) Topography of diphtheria toxin's T domain in the open channel state. *J. Gen. Physiol.* **115**, 421-434.

Sheridan RE (1998) Gating and permeability of ion channels produced by botulinum toxin types A and E in PC12 cell membranes. *Toxicon*. **36**, 703-717.

Swaminathan S and S Eswaramoorthy (2000) Structural analysis of the catalytic and binding sites of clostridium botulinum neurotoxin B. *Nat. Struct. Biol.* **7**, 693-699.

Wickner W and R Schekman (2005) Protein translocation across biological membranes. *Science* **310**, 1452-1456.

Yowler BC, RD Kensinger and CL Schengrund (2002) Botulinum neurotoxin A activity is dependent upon the presence of specific gangliosides in neuroblastoma cells expressing synaptotagmin I. *J. Biol. Chem.* **277**, 32815-32819.

Zhang S, E Udho, Z Wu, RJ Collier and A Finkelstein (2004) Protein translocation through anthrax toxin channels formed in planar lipid bilayers. *Biophys. J.* **87**, 3842-3849.

Acknowledgements

Chapter 1, in full, is a reprint of the material as it appears in the Journal of Neurotoxicity Research. Fischer, Audrey and Montal, Maurice, FP Graham Publ. Co., 2006. The dissertation author was the primary investigator and an author of this paper.

Chapter 2

Single molecule detection of intermediates during botulinum neurotoxin translocation across membranes

Single molecule detection of intermediates during botulinum neurotoxin translocation across membranes

Audrey Fischer and Mauricio Montal*

Section of Neurobiology, Division of Biological Sciences, University of California at San Diego, La Jolla, CA 92093-0366

Edited by Tom A. Rapoport, Harvard Medical School, Boston, MA, and approved March 30, 2007 (received for review January 3, 2007)

The dynamics of *Clostridium botulinum* neurotoxins (BoNTs) protein-translocation across membranes was investigated by using a single molecule assay with millisecond resolution on excised patches of neuronal cells. Translocation of BoNT/A light chain (LC) by heavy chain (HC) was observed in real time as an increase of channel conductance: the HC channel is occluded by the LC during transit, then unoccluded after completion of translocation and release of LC-cargo. We identified an entirely unknown succession of intermediate conductance stages during LC translocation. For the single-chain BoNT/E, by contrast to the di-chain BoNT/A, we demonstrate that productive translocation requires proteolysis of the LC cargo from the HC chaperone. We propose a model for the set of protein–protein interactions between translocase and cargo at each step of translocation that supports the notion of an interdependent, tight interplay between the HC chaperone and the LC cargo preventing LC aggregation and dictating the outcome of translocation: productive passage of cargo or abortive channel occlusion by cargo.

channels | chaperones | protein translocation | synaptic exocytosis

Botulinum neurotoxin (BoNT) is considered the most potent toxin known; it is the causative agent of botulism, a neuroparalytic illness (1), and a major bioweapon (2). *Clostridium botulinum*, a spore-forming, obligate anaerobic bacterium, secretes seven BoNT isoforms designated A to G. All isoforms, together with the related tetanus neurotoxin (TeNT) secreted by *Clostridium tetani*, are Zn^{2+}-endoproteases that block synaptic exocytosis by cleaving SNARE (soluble NSF attachment protein receptor) proteins (3–8). Assembly of the SNARE core complex is a key step preceding fusion of synaptic vesicles with the neuronal plasma membrane (5, 6, 9).

How do the proteases reach their cytosolic substrates? BoNTs have two chains linked by a disulfide bond: an N-terminal light chain (LC) of ≈50 kDa and a heavy chain (HC) of ≈100 kDa; structurally, BoNT consists of three domains (6, 10–12): the catalytic LC and the HC encompassing the translocation domain (the N-terminal half) and the receptor-binding domain (the C-terminal half). BoNTs enter sensitive cells by means of receptor-mediated endocytosis (6, 13, 14). The BoNT receptor-binding module establishes the cellular specificity mediated by its high affinity interaction with a surface protein receptor, SV2 for BoNT/A (15, 16) and synaptotagmins I and II for BoNT/B and BoNT/G (17), and a ganglioside (GT_{1B}) coreceptor (15–18). Exposure of the BoNT–receptor complex to the acidic milieu of endosomes (13, 14, 19, 20) results in a major conformational change and the insertion of the HC into the endosomal bilayer membrane.

Early studies have shown that BoNT HC forms channels in lipid bilayers (21–23) and PC12 cells (24), predominantly under acidic conditions and only after chemical reduction. These results were the cornerstone to view the BoNT translocation domain as the conduit for the passage of the enzymatic module from the interior of the endosome into the cytosol allowing contact between the protease and the SNARE substrates (6, 13, 23). Previously, we discovered that the HC of BoNT/A acts as both a channel and a transmembrane chaperone for the LC to ensure a translocation competent conformation during its transit from the acidic endosome into the cytosol (25). These findings provided compelling evidence of retrieval of endopeptidase activity of BoNT LC in the trans-compartment only after productive translocation across bilayers (25). The beginning and the end of the translocation step are known; however the intricacies of the translocation process remain unknown.

Here, the dynamics of protein translocation focusing on the interactions between the HC channel/chaperone and its LC cargo were probed under conditions that closely emulate those prevalent at the endosome. We developed an assay in neuronal cells to monitor interactions between the HC and the LC during translocation with single molecule sensitivity. The system allows us to selectively probe the accessibility of the LC by its interaction with a specific monoclonal antibody or with proteases at different stages during translocation from the acid to the neutral compartment. We characterized in real time the BoNT channel and chaperone activities to determine the constraints for LC unfolding and refolding at the entry and exit interfaces of the chaperone. This analysis led us to uncover an unknown succession of clear intermediate states in the course of LC translocation and to dissect a single translocation event into its component parts namely, entry, a series of transfer steps, and exit. These findings indicate that BoNT translocation involves an acid pH-induced membrane insertion step coupled to LC unfolding and entry into the HC chaperone/channel, LC protein conduction through the HC channel, and subsequent release of the LC cargo from chaperone by reduction of the disulfide bridge concomitant with LC refolding at the cytosol.

Results

Holotoxin Channels Display a Time-Dependent Conductance Increase. We developed a translocation assay at the single channel level in excised patches of BoNT/A-sensitive Neuro 2A cells to investigate the dynamics of protein translocation focusing on the interactions between the HC channel/chaperone and its LC cargo. This highly sensitive assay can monitor the activity of BoNT at the single molecule level, and it is specific because no channel activity is detected in these cells in the absence of toxin. Channel activity was recorded on excised patches of Neuro 2A cells exposed to purified BoNT/A holotoxin [supporting information (SI) Fig. 6] only under conditions that emulate the pH and redox gradient across endosomes, i.e., pH 5.3 on the cis-compartment containing BoNT and pH 7.0 on the trans-

Author contributions: A.F. and M.M. designed research; A.F. and M.M. performed research; M.M. contributed new reagents/analytic tools; A.F. and M.M. analyzed data; and A.F. and M.M. wrote the paper.

The authors declare no conflict of interest.

This article is a PNAS Direct Submission.

Abbreviations: γ, single channel conductance; BoNT, botulinum neurotoxin; LC, light chain; HC, heavy chain; P_o, channel open probability; TCEP, tris-(2-carboxyethyl) phosphine; $V_{½}$, the voltage at which $P_o = 0.5$; SNARE, soluble NSF attachment protein receptor.

*To whom correspondence should be addressed. E-mail: mmontal@ucsd.edu.

This article contains supporting information online at www.pnas.org/cgi/content/full/0700046104/DC1.

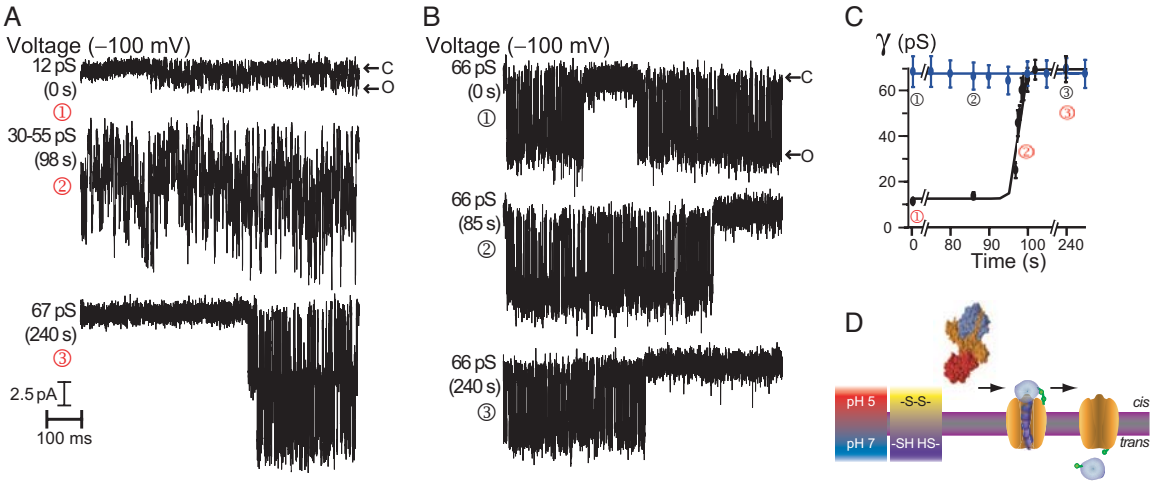

Fig. 1. BoNT/A holotoxin and HC channels in excised patches of Neuro 2A cells. Single-channel currents for holotoxin (*A*) and HC (*B*) at −100 mV and the indicated times. Holotoxin (*A*) and HC (*B*) channel activity begins 20 min and 21 min after GΩ seal formation. The letters C and O denote the closed and open states. (*C*) Time course of γ change of holotoxin (black circle) and HC (blue circle) for the representative experiments (average *N* per data point = 570). γ values associated with raw data (colored numbers) from *A* and *B* are indicated. (*D*) Structure of BoNT/A holotoxin (10). Shown are LC (purple), translocation domain (orange), and receptor binding domain (red) before insertion in the membrane (gray bar with magenta boundaries); then is shown a schematic of the membrane inserted BoNT/A during translocation of the LC (purple) through the HC channel (orange) with intact disulfide bridge (green) while located in the cis-compartment. Conventions hold for all figures.

compartment supplemented with the membrane nonpermeable reductant Tris-(2-carboxyethyl) phosphine (TCEP). Without these pH and redox gradients across the membrane, no channel activity is recorded (25). Under these conditions, the toxin changes from a water soluble di-chain protein to a membrane inserted channel which can be assayed by monitoring the sodium conductance of the channel (Fig. 1*A* and SI Fig. 7*A*). The time course of change of the single channel conductance (γ) after insertion of holotoxin into the membrane displays discrete transient intermediate conductances before achieving a γ of 67.1 ± 2.0 pS, corresponding to transitions from the closed to the open state. Once plateaued, γ remains constant throughout the typically 1 h experiment, as calculated from the current amplitude histograms (SI Fig. 7*B* and SI Table 1). In this experiment, two holotoxin channels were inserted into the membrane, as shown in the second and third traces. BoNT channel activity occurs in bursts and only opens at negative voltages (26). Trace displays holotoxin channels undergoing a continuous increase in γ and reaching a stable value by trace . In contrast, the isolated HC exhibits a constant γ = 66.4 ± 2.4 pS over the entire experiment regardless of the applied voltage (Fig. 1*B* and SI Fig. 7 *B* and *C*). This invariant γ is a signature of the HC channel, and is characteristic of holotoxin channels after completion of a single increasing conductance event. The half-time for completion of such event, estimated from the abrupt transition from low to high conductance is ≈10 s (Fig. 1*C*) with an initial γ ≅ 13 pS and a final, constant γ ≅ 67 pS characteristic of the unoccluded HC after event completion. We interpret the progressive, stepwise increase in channel conductance with time as the progress of LC translocation during which the HC channel initially conducts Na^+ and partially unfolded LC, detected as channel block. After translocation is complete the channel is unoccluded (Fig. 1*D*).

Holotoxin Channels Exhibit Discrete Intermediate Conductances Which Reflect Permissive Stages During Translocation. To rigorously characterize the translocation process, the time course of γ change for six separate experiments was analyzed. The average time course of γ change after insertion of holotoxin into membranes reaches a plateau after ≅ 260 s (Fig. 2*A*). A succession of discrete transient intermediate conductances, each defined as a minimum of 500 events, is discerned at γ ≅ 13 pS,

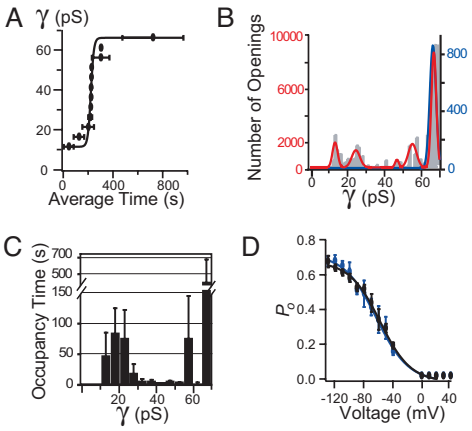

Fig. 2. Analysis of BoNT/A holotoxin and HC channels in Neuro 2A cells. (*A*) Average time course of channel γ change for holotoxin (*n* = 6, average *N* per data point = 4,650). (*B*) γ amplitude histogram (gray) and Gaussian fit calculated from the combined data set of six separate BoNT/A holotoxin experiments (red) and one representative BoNT/A HC experiment (blue). BoNT/A HC has a γ = 66.4 ± 2.4 pS (*N* = 10,200); holotoxin has γ values = 12.6 ± 2.0 pS, 24.1 ± 3.4 pS, 46.8 ± 1.6 pS, 55.3 ± 3.4 pS (*N* = 55,890). The endpoint γ = 67.1 ± 2.0 pS is equivalent to that of HC. (*C*) Average occupancy time of conductance states of BoNT/A holotoxin (*n* = 6, average *N* per data point = 4,650). (*D*) P_o as a function of voltage for holotoxin (black circle) ($V_{½}$ = −58.3 ± 1.7 mV) and for HC (blue circle) ($V_{½}$ = −63.4 ± 2.4 mV) (3 ≤ *n* ≤ 11 per data point; average *N* per data point = 2,630).

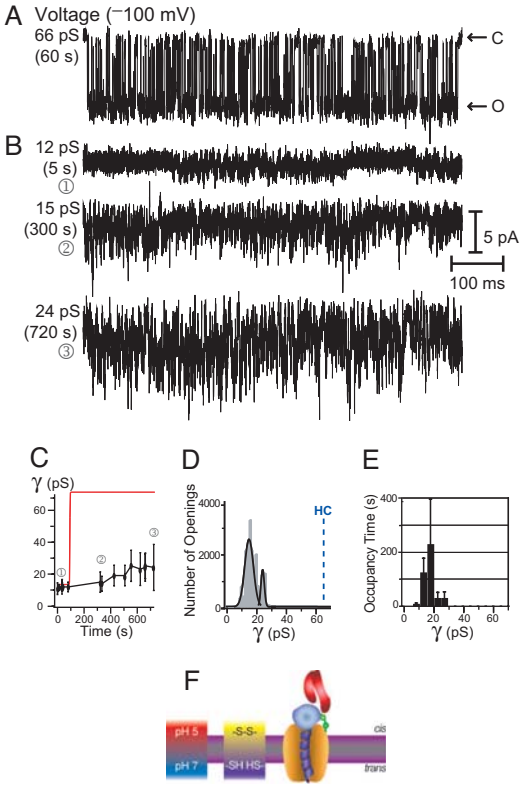

Fig. 3. LC/A translocation arrest by a LC/A specific Fab. Shown are single-channel currents for HC (*A*) and holotoxin (*B*) at −100 mV and the indicated times. HC (*A*) and holotoxin (*B*) channel activity begins 5 min after GΩ seal formation. (*B*) Trace- displays the pattern of activity at the beginning of the record. Multiple channel insertions occur with time (traces and). (*C*) Time course of holotoxin channel γ change (average *N* per data point = 600). Thin red line represents results for unmodified holotoxin/A. (*D*) γ amplitude histogram (gray) and Gaussian fit (black) with γ = 14.8 ± 4.1 pS and 24.0 ± 1.6 pS (*N* = 22,113). HC indicates the unoccluded HC conductance. (*E*) Average occupancy time of conductance states (*n* = 5, average *N* per data point = 5,170). (*F*) Schematic representation of BoNT/A holotoxin translocation arrested by Fab (red).

24 pS, 47 pS, and 55 pS before entering the stable γ of 67 pS (Fig. 2 *B* and *C*). This pattern of channel activity characteristic of holotoxin (Fig. 1*A*) allows us to operationally define three states of the BoNT channel. First, a closed state, and second, an "occluded state" with the partially unfolded LC trapped within the channel during the translocation process. This occluded state is identified as a set of intermediate conductances corresponding to transitions between the closed state and several blocked open states. Third, an "unoccluded state" visible upon completion of translocation and release of the LC associated to transitions between the closed state and the fully open state.

The endpoint γ for holotoxin (67 pS) and HC (66 pS) channels exhibit similar characteristics: both molecular entities display an indistinguishable voltage dependence, opening only at negative voltages; $V_{½}$, the voltage at which $P_o = 0.5$, is ≈ −60 mV (Fig. 2*D*). This analysis substantiates the view of the HC channel as an endpoint achieved after completion of LC translocation through the HC channel, as observed in holotoxin channels (Fig. 1).

A LC Specific Antibody Arrests Translocation After Initiation of LC Entry into the HC Channel. Is translocation affected by a LC which is tightly bound to a folded protein? To discern the underlying protein–protein interactions between BoNT/A LC and HC during translocation, we exploited the specificity of a monoclonal antibody generated against the BoNT/A LC. To test this model, Fab fragments were preincubated with BoNT/A holotoxin or HC (5:1 mole/mole) for 1 h at pH 7 before the translocation assay. This condition does not affect HC channel activity (Fig. 3*A*), however it transforms that of the holotoxin (Fig. 3*B*). Holotoxin channels are detected within a few minutes after patch excision albeit of lower conductance (≈15 pS and ≈24 pS), a feature which remains constant for the duration of the recording (Fig. 3*B*). The initial γs are comparable with those characteristic of the early intermediate γ states in unmodified holotoxin; however, instead of proceeding through the sequence of intermediates and ending with γ at 67 pS, the channels remain in the low γ states throughout the experiment (Fig. 3*C*). The second and third traces in Fig. 3*B* show multiple channels of low γ; in addition, the current transitions are faster and short-lived, giving the appearance of flickering between low and high γ states. This striking feature is characteristic of channel block (25).

Analysis of five experiments indicates that under such conditions the channel preferentially resides in the 15 pS and 24 pS states (Fig. 3 *D* and *E*). These γ values approximate the two lowest conductance intermediate states observed for the early intermediates of the Fab-free holotoxin during translocation (Fig. 2*B*). We interpret these intermediates as early steps in translocation in which the HC has formed a channel that is partially occluded by the LC (Fig. 3*F*). Fab binding to the LC does allow channel formation and early translocation, stabilizing intermediate protein–protein interactions. However, by binding to the LC and inhibiting its unfolding, the Fab locks the channel and the LC in a translocating conformation that is irreversibly incomplete.

Productive Translocation Requires Proteolytic Cleavage of LC Cargo from HC Channel. Our model predicts that a covalently linked, single-chain holotoxin should remain in a blocked state with the LC locked within the HC channel and not complete translocation. Channel formation and early intermediate steps would ensue; however, an arrested rather than a productive translocation event would be predicted to occur. An endogenous clostridial protease is known to "nick" BoNT/A between the LC and the HC producing the di-chain mature toxin. In contrast, BoNT/E is not cleaved before secretion and, therefore, a full length, single-chain protein is produced. Fig. 4*A* illustrates that BoNT/E holotoxin indeed forms channels; however, the channel persists in the low γ states similar to those seen during early steps of translocation in holotoxin BoNT/A (Fig. 2*B*). BoNT/E channel activity does not exhibit BoNT/A HC channel features, never reaching the γ ≅ 66 pS. This property provides a built-in assay to probe whether proteolytic cleavage of the LC anchor to the HC would allow for the completion of translocation. Trypsin is commonly used to "activate" BoNT/E in enzymatic assays of cleavage of its substrate, SNAP-25; this treatment proteolytically nicks the LC from the HC and enhances the intrinsically marginal protease activity of holotoxin/E (SI Fig. 6) (27, 28). As a control, we established that exposure of Neuro 2A cells to trypsin, in the absence of toxin, does not elicit channel activity. Next, we asked whether trypsin addition to Neuro 2A cells after detection of BoNT/E channel activity would alter the low γ pattern shown in Fig. 4*A*. Trypsin was added 300 s (Trace-) after the onset of channel activity (Trace-) (Fig. 4*B*). The channel remained in the low γ states displaying discrete intermediate conductances for ≈400 s, and then abruptly entered into the unoccluded state ≅ 65 pS, constant value for the remainder of the experiment (Trace-). The time course of conductance

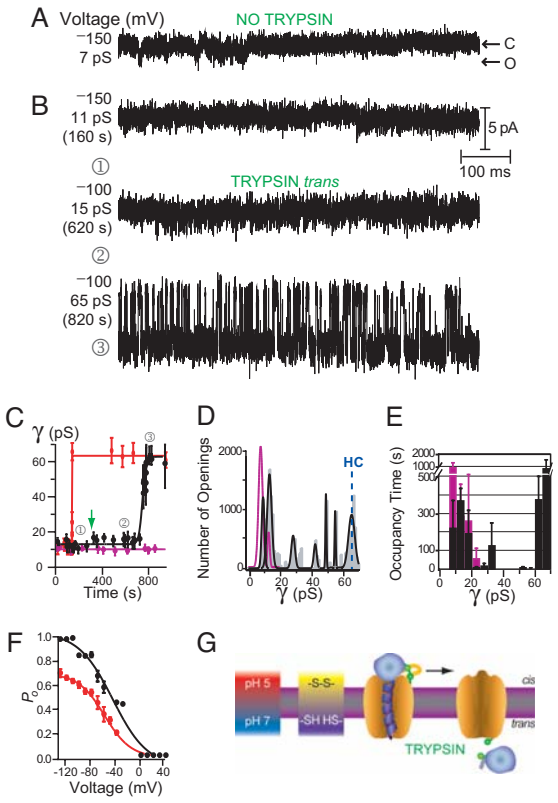

Fig. 4. The single-chain BoNT/E holotoxin requires proteolytic cleavage to complete translocation of LC. Shown are representative single-channel currents at the indicated voltages and times; consecutive voltage pulses applied to the two different patches. (*A*) Holotoxin channel activity begins 5 min (*A*) and 25 min (*B*) after GΩ seal formation. (*B*) Trypsin addition (4 mM) to the trans-side occurs at 300 s. (*C*) Time course of channel γ change of trypsin-nicked BoNT/E before exposure to the cells (red circle), single-chain holotoxin/E (pink circle), and single-chain holotoxin/E after trypsin addition to the trans-side (black circle) (green arrow) for representative experiments (average *N* per data point = 275). (*D*) γ amplitude histogram and Gaussian fit of single-chain holotoxin/E, $\gamma = 7.7 \pm 1.8$ pS and 12.7 ± 1.0 pS; Gaussian fit illustrated in pink, data not shown ($N = 10{,}840$). Holotoxin/E, after trypsin addition to the trans-side, has $\gamma = 9.3 \pm 1.3$ pS, 13.3 ± 2.0 pS, 28.4 ± 1.6 pS, 42.4 ± 1.3 pS, 49.2 ± 0.5 pS, 55.0 ± 0.5 pS, and 65.4 ± 2.8 pS; shown are raw data (gray) and Gaussian fit (black) ($N = 19{,}431$). (*E*) Average occupancy time of conductance states for trypsin-nicked holotoxin/E (black) and single-chain holotoxin/E (pink) ($n = 4$ for each experimental condition, average *N* per data point: single-chain holotoxin/E = 460, trans-trypsin nicked holotoxin/E = 1,470). (*F*) P_o as a function of voltage for holotoxin/E (black circle) and holotoxin/A (red circle); $V_{½}$ for holotoxin/E is -45.0 ± 5.4 mV ($3 \leq n \leq 11$ per data point; average *N* per data point = 2,275). (*G*) Schematic of single-chain holotoxin BoNT/E occluded channels, the subsequent cleavage of the LC from the HC by trypsin, and the consequent LC release into the neutral pH compartment.

change is illustrated in Fig. 4*C*; the green arrow indicates addition of the membrane impermeable trypsin to the trans-side and the results are depicted in black. By contrast to the sharp increment in conductance produced by trypsin addition, no increase in γ is detected for BoNT/E if trypsin is not added to the trans compartment (Fig. 4*C*): BoNT/E holotoxin channels remain in the low γ states for the entire duration of the experiments, consistent with the persistent occlusion of HC channel by the LC. Furthermore, trypsin-nicking of BoNT/E before exposure to the cells, equivalent to trypsin addition to the cis-side, evokes a pattern of channel activity indistinguishable to that produced by di-chain BoNT/A (Figs. 1 and 2 and SI Fig. 7); the results are shown in Fig. 4*C* (red) and SI Fig. 8.

Analysis of four separate experiments for single-chain BoNT/E demonstrates that, within minutes of trypsin addition to the trans-compartment, the BoNT/E channel displays a succession of discrete transient intermediate γ states associated to channel block by the LC at $\gamma \cong 9$ pS, 13 pS, 28 pS, 42 pS, 49 pS, and 55 pS before entering the unoccluded state of 65 pS, inferred to be that characteristic of the HC after completion of LC translocation (Fig. 4*D*). The timing appears slower than for BoNT/A holotoxin translocation; this apparent delay arises because trypsin was not added until 300 s after the onset of channel activity to confirm that translocation completion requires trypsin addition. These γ values approximate most of the intermediate states displayed by holotoxin/A during translocation (Fig. 2); the intermediate states at $\gamma \cong 28$ pS and 42 pS may be the result of translocating the uncleaved loop of BoNT/E through the channel. In contrast, the residency time in each intermediate state differs from BoNT/A: the occluded channel conductance intermediates with $\gamma \cong 9$ pS, 13 pS, and 28 pS are more permissive (Fig. 4*E*). This result is consistent with the view that these low conductance states are stabilized by the LC trapped within the HC. BoNT/E channels recorded after addition of trypsin to the trans-side feature a finite $\gamma \cong 65$ pS: these channels are indistinguishable to BoNT/A HC channels (Figs. 1*B* and 2 *B* and *D*) displaying similar γ and voltage dependence, consistent with the attainment of the unoccluded HC state by BoNT/E (Fig. 4*F*). Holotoxin/E exhibits a higher propensity to reside in the open state compared with holotoxin/A (Fig. 4*B Bottom*), and the $V_{½}$ is right shifted by ≈ 15 mV to −45 ± 5 mV with respect to holotoxin/A (Fig. 4*F*).

The findings with single-chain BoNT/E holotoxin demonstrate that LC translocation can be observed as a succession of discrete transient intermediate conductances associated with channel block. Release of this block only occurs after the LC completes translocation from the cis- to the trans-compartment and is physically separated from the HC channel by both reduction of the disulfide bridge and cleavage of the siscile bond (Fig. 4*G*).

Discussion

Are LC Unfolding and Translocation Coupled? It is remarkable that low γ intermediates were identified for all of the conditions in which holotoxins were examined. We infer that these intermediates, observed as occluded states, correspond to permissible chaperone-cargo conformations populated during translocation (Fig. 1). This view is in line with the time course of occurrence of the γ intermediates. Previous work demonstrated a tight correlation between the decrease in α-helical content of the LC at pH 5.0 with the occurrence of channel and protease activities of holotoxin; this finding necessarily constrains the LC-cargo to be either extended or α-helical segments to fit into a channel of ≈15 Å in diameter, as calculated from the γ of BoNT/A (25). We postulate that the residence time at each intermediate reflects the conformational changes of cargo within the chaperone pore and that these determine the efficiency and outcome of translocation. Within the occluded state, the frequency of occurrence of the lowest conductance intermediates ($\gamma \cong 12$ pS and 20 pS) is higher, as determined by their individual occupancy times (Fig. 2*C*): the low conductance states exhibit the longest occupancy time, consistent with an energetic barrier associated with the initiation of LC unfolding, presumably into a molten globule state (29), at the onset of translocation, an entry event (Fig. 5, step 2). That γ values for unmodified holotoxin/A (Fig. 2) and holotoxin/A bound to the LC-specific Fab (Fig. 3) practically overlap, and for the Fab-arrested condition the pore occupancy for such intermediates predominates, argues in favor of this

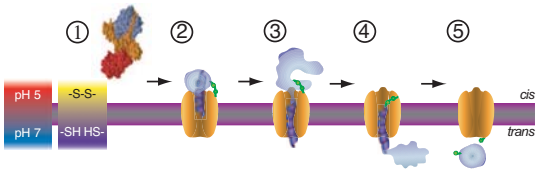

Fig. 5. Sequence of events underlying BoNT LC translocation through the HC channel. Step 1, Crystal structure of BoNT/A holotoxin (10) before insertion in the membrane. Then is shown a schematic representation of the membrane inserted BoNT/A during an entry event (step 2), a series of transfer steps (steps 3 and 4), and an exit event (step 5), under conditions that recapitulate those across endosomes.

notion and is consistent with the arrest of translocation at the entry step in the process. However, Fab binding terminates the growing γ progress by trapping the LC and the HC channel in a translocating conformation that is irreversibly arrested (Fig. 3). By contrast, intermediates with γ values between 25 and 50 pS have shorter lifetimes, presumably a result of overcoming the activation energy (Fig. 5, step 3). This sequence of transfer steps leads to a transition into the final γ intermediate measured at $\gamma \cong 55$ pS (Fig. 5, step 4). This last intermediate in the sequence (Fig. 2) is relatively long-lived at $\approx$75 s, plausibly limited by the refolding of the LC at the channel exit interface in the trans compartment and reduction of the disulfide bridge before final release from the HC channel, an exit event (Fig. 5, step 5). Thus, a single LC translocation involves an entry event, a series of transfer steps, and an exit event. The requirement for acid-induced unfolding and the timing correspond well with those reported for the translocation of the 263-residue N-terminal domain of anthrax lethal factor, the cargo, through the transmembrane pore formed by the protective antigen heptameric pore (30–32). Evidence for the importance of unfolding for efficient translocation and a propensity toward α-helical structure translocation was elegantly obtained for BoNT/D by Bade *et al*. (33) by using an entirely different experimental approach. Currently, there is no information about unfolding and refolding pathways; what can be said is that there is a trend to preserve partially unfolded, yet mobile, native-like regions.

Release of Cargo from Chaperone Is Necessary for Productive Translocation. The results obtained for BoNT/E provide compelling evidence for the requirement of cargo dissociation from chaperone as one of the final steps in the progress of translocation. The transformation of an occluded state characterized by low γ intermediates with prolonged pore occupancy into an unoccluded channel with $\gamma \approx 65$ pS (Fig. 4) is unambiguous and leads to the conclusion that the chaperone-cargo anchor must be severed to complete productive translocation.

As demonstrated previously, the disulfide bridge linkage must also be severed to release the LC cargo after completion of translocation (25). Unreduced holotoxin/A (25) and holotoxin/E (Fig. 4) do not exhibit channel activity. Further, addition of TCEP only to the cis-compartment after acidification fails to evoke channel activity (25). This observation is indicative of disulfide shielding arising from the onset of the LC translocation through the HC channel. Thus, proteolytic cleavage of LC from HC and disulfide reduction during the exit event are both required for translocation.

Alternative Models to Protein Translocation. The translocation model embodies the notion that the succession of discrete intermediate conductances reflects permissive stages during LC translocation. Alternatively, it is conceivable that the channel is a conductive oligomer resulting from the self-assembly of monomers with the intermediate conductances as reporters of the oligomerization process. Whereas the occurrence of oligomers was surmised from early images of BoNT/A incorporated into liposomes (34), the fact that the isolated HC displays a constant γ implies that this molecular entity is assembled immediately after membrane insertion. Together with evidence that growing conductance events in holotoxin (Figs. 2 and 4) lead to an end-point stable entity with characteristics equivalent to isolated HC argue against an oligomer. The single-chain BoNT/E data are inconsistent with HC oligomerization because the LC is protease protected until translocated across to the trans-side. The view that γ intermediates are only reporters of the refolding process is incompatible with both the BoNT/E and BoNT/A-Fab result. The regularity and discreteness of γ is opposite to the erratic fluctuations typical of bilayer dielectric core disturbances produced by surfactants, thus excluding unspecific perturbations.

The HC Channel in the Endosome After LC Translocation. A feature of the BoNT channel, both for BoNT/A (Fig. 2*D*) and BoNT/E (Fig. 4*F*), is that it is closed at positive voltages under conditions in which the orientation and the magnitude of the pH gradient, as well as the polarity and magnitude of the membrane potential recapitulate those across endosomes: pH 5.3 and positive potential on the compartment containing the BoNT and pH 7.0 and negative potential on the opposite compartment. This attribute suggests that the BoNT HC channel would be closed in the endosome until it is gated by the LC to initiate its translocation across the membrane into the cytosol (Figs. 2*D* and 4*F*). After completion of LC translocation, the channel would be closed, precluding the passive dissipation of the electrochemical ionic gradients across endosomes. This notion is consistent with the fact that currents evoked by short pulses of negative potential were required to monitor channel activity; however, the voltage-dependence of translocation has yet to be explored. That channel activity has been documented for BoNT/A (22, 24–26), BoNT/E (this work and ref. 24), BoNT/B (23), BoNT/C (21) and tetanus neurotoxin (TeNT) (23, 35, 36), and protein translocation activity has been shown for BoNT/A (this work and ref. 25), BoNT/E (this work) and BoNT/D (33) points to the general validity of the proposed mechanism.

The HC Channel as a Chaperone for the LC Protease. The interaction between an unfolded or partially folded LC embedded within the HC resembles the maintenance of partially folded polypeptides by chaperones. It is fitting to consider plausible similarities to these chaperones. The structures of protein-conducting channels of the *Escherichia coli* SecYEG bound to a translating ribosome (37), and the archaeon *Methanococcus jannaschii* SecYEβ (38) define blueprints for protein-conducting channels for which the underlying protein fold is a compact transmembrane α-helical bundle. Both structures suggest a resemblance to the occluded BoNT channel. These two structures outline the intricacies of the initial stages of protein translocation and are consistent with the occurrence of discrete transient intermediates involving extensive interactions between the chaperone and the cargo in a dynamic succession dictating the progress and directionality of translocation. Protein import in mitochondria and chloroplasts involves unfolded proteins (for review, see refs. 39–41). The inner mitochondrial membrane TIM23 translocase (42), the outer (Toc75) (43) and inner (Tic110) (44) chloroplast membrane translocases display pore diameters of $\approx$13 Å, $\approx$14 Å and $\approx$15 Å, respectively constraining the secondary structure of the precursor polypeptide cargos to be either extended or α-helical segments. An analogous requirement for unfolded cargo is required by β-barrel translocases: the protective antigen PA_{63} pore of anthrax toxin exhibits a central pore with a cross-section of $\approx$15 Å (32). Similar models have emerged from single channel measurements on the interactions between helical cargo pep-

tides and the transmembrane β-barrel of the α-hemolysin protein pore (45). Compared with the molecular complexity of these protein translocases the BoNT protein highlights the simplicity of its modular design to achieve its exquisite activity. The analogy that emerges from the findings reported here for BoNT, a modular nanomachine in which one of its modules (the HC channel) operates as a specific protein translocating transmembrane chaperone for another of its modules (the LC protease) is more than coincidental and points to a fundamental common principle of molecular design.

Materials and Methods

Materials. Unless otherwise specified, all chemicals were purchased from Sigma–Aldrich (St. Louis, MO). Purified native BoNT isoform A and E holotoxins and isoform A HC were from Metabiologics (Madison, WI) and the ING2 BoNT/A LC specific monoclonal antibody was kindly provided by J. Marks (University of California, San Francisco, CA). Di-chain BoNT/E holotoxin was generated by cleavage with trypsin (see *SI Text* for details).

Cell Culture and Patch Clamp Recordings. Excised patches from Neuro 2A cells in the inside-out configuration were used as described in *SI Text*. Currents were recorded under voltage-clamp conditions by the application of consecutive voltage steps 800 ms in duration from +50 mV to −150 mV. All experiments were conducted at 22°C ± 2°C.

Solutions. To emulate endosomal conditions, the trans-side (bath) solution contained 200 mM NaCl, 5 mM NaMOPS [3-(*N*-morpholino) propanesulfonic acid] (pH 7.0 with HCl), 0.25 mM TCEP, and 1 mM $ZnCl_2$; the cis-side (pipet) solution contained 200 mM NaCl and 5 mM NaMES [2-(*N*-morpholino) ethanesulfonic acid] (pH 5.3 with HCl). See *SI Text* for details.

Data Analysis. Analysis performed on single bursts of each experimental record. A single burst is defined as a set of openings and closings lasting ≥50 ms bounded by quiescent periods of ≥50 ms before and after. Only single bursts were analyzed because of the random duration of quiescent periods. See *SI Text* for details.

Protease Activity of BoNT/A and BoNT/E Holotoxins. Recombinant SNAP-25 (46, 47) was incubated with 60 ng of BoNT holotoxin in 13.2 mM Hepes (pH 7.4), 20 mM DTT, and 1 μM $Zn(CH_{3C}OOH)_2$ for 30 min at 37°C. SDS/PAGE (12%) was used to visualize cleavage of SNAP-25 by BoNT/A and BoNT/E holotoxins (48).

Fab Generation. See *SI Text* for details.

We thank M. Goodnough for his invaluable help; J. Marks and M. C. Gonzalez (University of California, San Francisco) for antibodies; J. Santos, M. Oblatt-Montal, L. Koriazova, and members of the M.M. lab for perceptive comments; and R. Hampton, S. Emr, D. Fischer, and J. Young for helpful suggestions. This work was supported by U.S. Army Medical Research and Materiel Command Grant DAMD17-02-C-0106 and National Institutes of Health Training Grant T32 GM08326.

1. Shapiro RL, Hatheway C, Swerdlow DL (1998) *Ann Intern Med* 129:221–228.
2. Arnon SS, Schechter R, Inglesby TV, Henderson DA, Bartlett JG, Ascher MS, Eitzen E, Fine AD, Hauer J, Layton M, *et al.* (2001) *J Am Med Assoc* 285:1059–1070.
3. Weber T, Zemelman BV, McNew JA, Westermann B, Gmachl M, Parlati F, Söllner TH, Rothman JE (1998) *Cell* 92:759–772.
4. Sutton RB, Fasshauer D, Jahn R, Brunger AT (1998) *Nature* 395:347–353.
5. Jahn R, Lang T, Sudhof TC (2003) *Cell* 112:519–533.
6. Schiavo G, Matteoli M, Montecucco C (2000) *Physiol Rev* 80:717–766.
7. Schiavo G, Benfenati F, Poulain B, Rossetto O, Polverino de Laureto P, DasGupta BR, Montecucco C (1992) *Nature* 359:832–835.
8. Blasi J, Chapman ER, Link E, Binz T, Yamasaki S, De Camilli P, Sudhof TC, Niemann H, Jahn R (1993) *Nature* 365:160–163.
9. Jackson MB, Chapman ER (2006) *Annu Rev Biophys Biomol Struct* 35:135–160.
10. Lacy DB, Tepp W, Cohen AC, DasGupta BR, Stevens RC (1998) *Nat Struct Biol* 5:898–902.
11. Lacy DB, Stevens RC (1999) *J Mol Biol* 291:1091–1104.
12. Swaminathan S, Eswaramoorthy S (2000) *Nat Struct Biol* 7:693–699.
13. Simpson LL (2004) *Annu Rev Pharmacol Toxicol* 44:167–193.
14. Simpson LL (1983) *J Pharmacol Exp Ther* 225:546–552.
15. Dong M, Yeh F, Tepp WH, Dean C, Johnson EA, Janz R, Chapman ER (2006) *Science* 312:592–596.
16. Mahrhold S, Rummel A, Bigalke H, Davletov B, Binz T (2006) *FEBS Lett* 580:2011–2014.
17. Rummel A, Karnath T, Henke T, Bigalke H, Binz T (2004) *J Biol Chem* 279:30865–30870.
18. Nishiki T, Tokuyama Y, Kamata Y, Nemoto Y, Yoshida A, Sekiguchi M, Takahashi M, Kozaki S (1996) *Neurosci Lett* 208:105–108.
19. Lawrence G, Wang J, Chion CK, Aoki KR, Dolly JO (2007) *J Pharmacol Exp Ther* 320:410–418.
20. Montecucco C, Schiavo G, Dasgupta BR (1989) *Biochem J* 259:47–53.
21. Donovan JJ, Middlebrook JL (1986) *Biochemistry* 25:2872–2876.
22. Blaustein RO, Germann WJ, Finkelstein A, DasGupta BR (1987) *FEBS Lett* 226:115–120.
23. Hoch DH, Romero-Mira M, Ehrlich BE, Finkelstein A, DasGupta BR, Simpson LL (1985) *Proc Natl Acad Sci USA* 82:1692–1696.
24. Sheridan RE (1998) *Toxicon* 36:703–717.
25. Koriazova LK, Montal M (2003) *Nat Struct Biol* 10:13–18.
26. Fischer A, Montal M (2006) *Neurotox Res* 9:93–100.
27. Sathyamoorthy V, DasGupta BR (1985) *J Biol Chem* 260:10461–10466.
28. Schiavo G, Rossetto O, Catsicas S, Polverino de Laureto P, DasGupta BR, Benfenati F, Montecucco C (1993) *J Biol Chem* 268:23784–23787.
29. Cai S, Kukreja R, Shoesmith S, Chang TW, Singh BR (2006) *Protein J* 25:455–462.
30. Krantz BA, Finkelstein A, Collier RJ (2006) *J Mol Biol* 355:968–979.
31. Krantz BA, Trivedi AD, Cunningham K, Christensen KA, Collier RJ (2004) *J Mol Biol* 344:739–756.
32. Zhang S, Udho E, Wu Z, Collier RJ, Finkelstein A (2004) *Biophys J* 87:3842–3849.
33. Bade S, Rummel A, Reisinger C, Karnath T, Ahnert-Hilger G, Bigalke H, Binz T (2004) *J Neurochem* 91:1461–1472.
34. Schmid MF, Robinson JP, DasGupta BR (1993) *Nature* 364:827–830.
35. Gambale F, Montal M (1988) *Biophys J* 53:771–783.
36. Borochov-Neori H, Yavin E, Montal M (1984) *Biophys J* 45:83–85.
37. Mitra K, Schaffitzel C, Shaikh T, Tama F, Jenni S, Brooks CL, III, Ban N, Frank J (2005) *Nature* 438:318–324.
38. Van den Berg B, Clemons WM, Jr, Collinson I, Modis Y, Hartmann E, Harrison SC, Rapoport TA (2004) *Nature* 427:36–44.
39. Mokranjac D, Neupert W (2005) *Biochem Soc Trans* 33:1019–1023.
40. Rehling P, Brandner K, Pfanner N (2004) *Nat Rev Mol Cell Biol* 5:519–530.
41. Schnell DJ, Hebert DN (2003) *Cell* 112:491–505.
42. Truscott KN, Kovermann P, Geissler A, Merlin A, Meijer M, Driessen AJ, Rassow J, Pfanner N, Wagner R (2001) *Nat Struct Biol* 8:1074–1082.
43. Hinnah SC, Wagner R, Sveshnikova N, Harrer R, Soll J (2002) *Biophys J* 83:899–911.
44. Heins L, Mehrle A, Hemmler R, Wagner R, Kuchler M, Hormann F, Sveshnikov D, Soll J (2002) *EMBO J* 21:2616–2625.
45. Movileanu L, Schmittschmitt JP, Scholtz JM, Bayley H (2005) *Biophys J* 89:1030–1045.
46. Blanes-Mira C, Ibanez C, Fernandez-Ballester G, Planells-Cases R, Perez-Paya E, Ferrer-Montiel A (2001) *Biochemistry* 40:2234–2242.
47. Oyler GA, Higgins GA, Hart RA, Battenberg E, Billingsley M, Bloom FE, Wilson MC (1989) *J Cell Biol* 109:3039–3052.
48. Ferrer-Montiel AV, Canaves JM, DasGupta BR, Wilson MC, Montal M (1996) *J Biol Chem* 271:18322–18325.

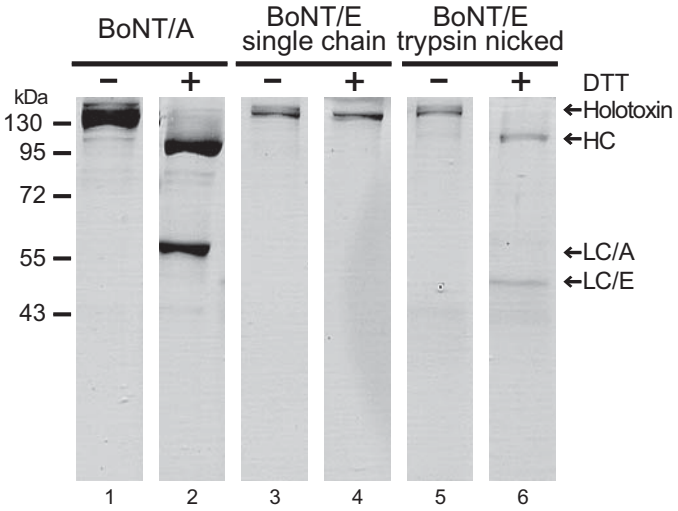

Supplementary Fig. 1. SDS-PAGE analysis of BoNT/A and BoNT/E holotoxins. Coomassie blue stained SDS-PAGE (12%) gels in the absence (-) and presence (+) of the reductant dithiothreitol (DTT). Numbers represent M_r standards. Di-chain BoNT/A (lanes 1 and 2) and BoNT/E (trypsin-nicked) (lanes 5 and 6) dissociate into LC (M_r ~50 kDa) and HC (M_r ~100 kDa) in the presence of reductant. In contrast, single-chain BoNT/E (lanes 3 and 4) migrates as a single prominent band with an apparent M_r ~150 kDa characteristic of holotoxin, irrespective of DTT.

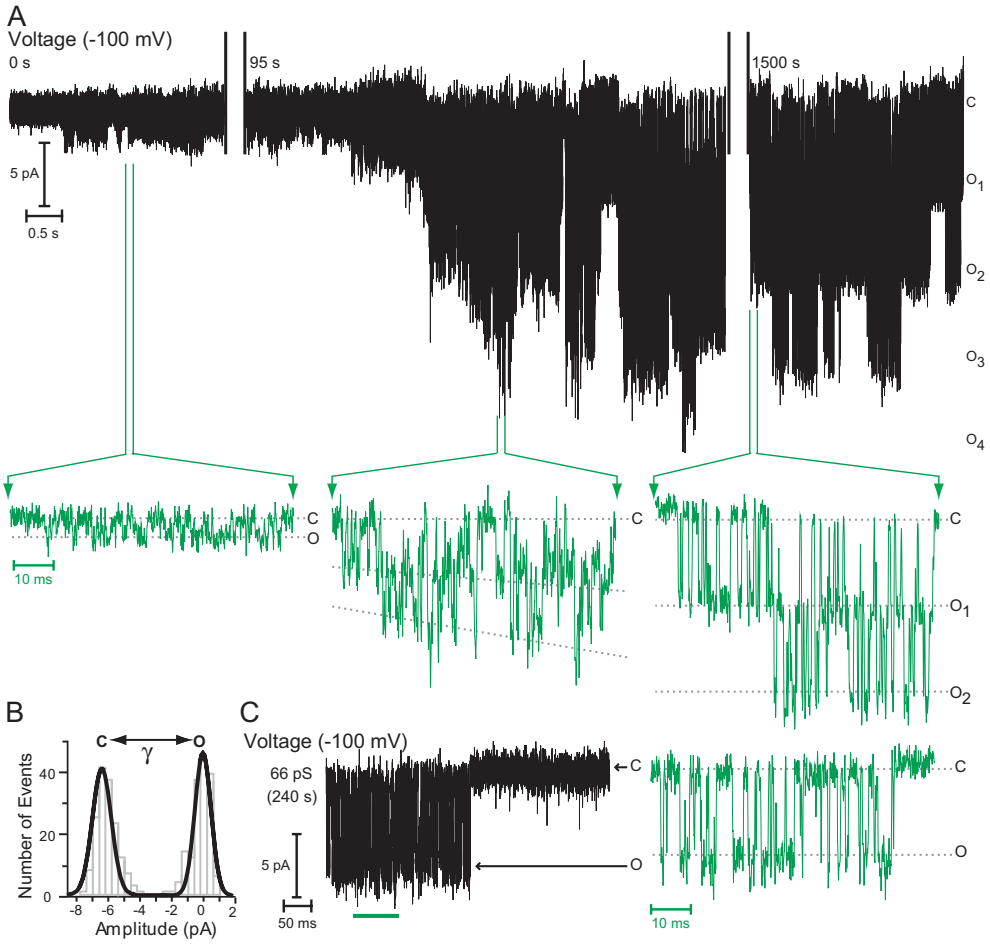

Supplementary Fig. 2. Time course of conductance change upon exposure of Neuro 2A cells to BoNT/A holotoxin. Currents were recorded at V= −100 mV under conditions identical to those described in Fig. 1 and its legend. (*A*) BoNT/A holotoxin single channel currents displayed at low time resolution to highlight the progress of conductance change during a 1 hour long experiment. The sections of the record delimited by the green arrows are shown in the green records at a 56-fold higher time resolution (note the change in time calibration). The vertical lines indicate gaps to accommodate the full recording in the limited space. The expanded green display on the left corresponds to the occurrence of the low conductance intermediate with γ values ~ 13 ± 2.0 pS. In this particular experiment, three holotoxin channels were inserted into the membrane, as shown in the middle expanded display. Note that the γ values for each of the three intermediate conductances fluctuate around 24 ± 4 pS yet they clearly exhibit a trend towards higher γ values with time, as depicted by the dotted lines. The expanded panel on the right displays two channels with an invariant γ = 67.1 ± 2.0 pS, interpreted to correspond to that of unoccluded channels attained after completion of translocation. This is based on the equivalent γ = 66.4 ± 2.4 pS featured by the isolated HC, as shown in panel *C*. (*B*) Current amplitude histogram and Gaussian fit of record shown in (*C*) of BoNT/A HC is used to outline the method to calculate the single channel conductance (γ) from Gaussian fits to current amplitude histograms, as reported previously (25, 26, 35). (*C*) High-gain and fast-time resolution of BoNT/A HC single channel currents recorded at –100 mV corresponding to the bottom trace in Figure 1*B*. Green line designates the section of the record displayed in green at a higher time resolution. Note that the signals shown in all the green displays are the prototypical discrete square events which are characteristic of unitary channel currents.

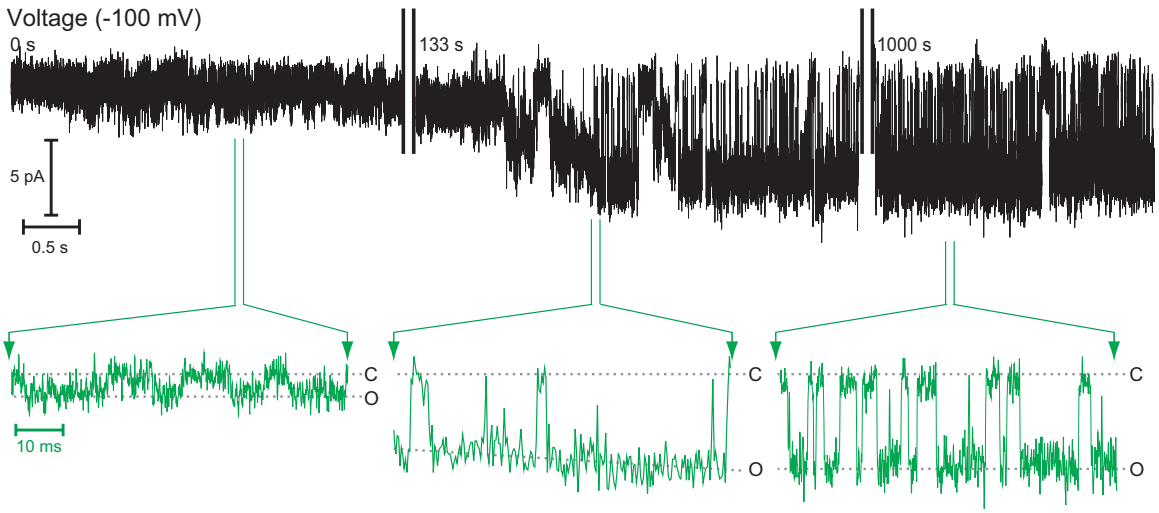

Supplementary Fig. 3. Time course of conductance change upon exposure of Neuro 2A cells to di-chain BoNT/E holotoxin. Single channel currents recorded at V= −100 mV are displayed at low time resolution to highlight the progress of conductance change. The sections of the record delimited by the green arrows are shown in the green records at a 42-fold higher time resolution. Vertical lines indicate gaps to accommodate the full record in the limited space. The expanded green display on the left corresponds to the occurrence of the low conductance intemediate with γ values ~ 10 ± 3 pS. The middle panel shows the progress of transition from γ values of 50 ± 6 pS up to 65 ± 4 pS, as depicted by the dotted lines. The acquisition rate for this segment of the record was 3.2 kHz, instead of 20 kHz used for all others. The panel on the right displays the stable state with an invariant $\gamma \cong 65 \pm 4$ pS, interpreted to correspond to that of unoccluded channels attained after completion of translocation. Other conditions identical to those described in Fig. 4 and its legend; other conventions as for Supplementary Fig. 2.

Supplementary Table 1. Summary of single channel conductance values (γ) of unoccluded BoNT/A holotoxin channel for Na^+ reported in this work, and for Na^+, K^+ and Cs^+ reported previously (24-26).

Conductive Ion	Concentration (mM)	γ (pS)
Na^+	200	67 ± 2
K^+	100	50 ± 12
	200	74 ± 12
	500	110 ± 12
Cs^+	200	105 ± 5

Supplementary Materials and Methods

Materials. BoNT/E holotoxin (0.5 mg/mL) was incubated with with 0.15 mg/mL trypsin in 20mM HEPES, pH 7.0 for 30 min at 37°C. Thereafter, trypsin was inactivated with 0.25 mg/mL trypsin soybean inhibitor for 15 min at 20°C. Trypsin and trypsin inhibitor were removed by centrifugal filtration on Millipore filters (M_r cutoff 50 kDa).

Cell Culture. Neuro 2A neuroblastoma cells, derived from a spontaneous tumor of a Strain A albino mouse, were obtained from the American Type Culture Collection and passaged in DMEM (BioWhittaker, Rockland, ME) supplemented with penicillin 10mM/streptomycin 10μg/mL/glutamine 2mM (Invitrogen Carlsbad, CA), and 5% newborn bovine serum (Invitrogen, Carlsbad, CA). Neuro 2A cells were plated onto Matrigel (BD Biosciences, San Jose, CA) coated glass coverslips at 500 cells/coverslip, and cultured at 37°C, 5% CO_2 for 1–3 days prior to patch clamp recordings.

Patch clamp Recordings. Capillaries of borosilicate glass from Hilgenberg (Germany) were polished and used at 3.5-7.0 MΩ resistance when immersed in recording solution. Excised patches in the inside-out configuration were used (1). After gigaohm (GΩ) seal formation, the patch is excised from the cell and current recordings are obtained under voltage clamp conditions. Records were acquired and analyzed using the patch clamp amplifier system (List EPC-9, HEKA Electronik, Germany) fitted with an ITC-16 interface (Instrutech, Port Washington, NY) and the Pulse/PulseFit acquisition and analysis software (HEKA, Germany).

Data were acquired at a sampling frequency 20 kHz, unless otherwise indicated, and not filtered. Data were analyzed using Clampfit v.9.2 software (Axon Instruments, Sunnyvale, CA), Microsoft Excel and IGOR Pro (Wavemetrics, Portland, OR). All experiments were conducted at 22 ± 2 °C.

Solutions. BoNT reconstitution and channel insertion was achieved by supplementing 5 μg/mL BoNT holotoxin or HC to the pipet solution, which was set to an endosomal pH of 5.3. To optimize the formation of GΩ seals, the pipet tip was first dipped in the pipet solution in the absence of BoNT, and then back-filled with solution containing BoNT. $ZnCl_2$ was used to block endogenous channel activity specific to Neuro 2A cells (2, 3). The osmolarity of pipet and bath solutions was determined to be ~390 mOsm.

Data analysis. The single channel conductance γ was calculated from Gaussian fits to current amplitude histograms. The total number of opening events analyzed was 120,022, and the intermediate conductance states were defined by a minimum of 500 events. Time course of channel conductance change for each experiment was calculated from γ of each record, where t = 0 s corresponds to onset of channel activity, and average time course was constructed from the set of individual experiments for a single condition. Average occupancy time of occluded intermediate and unoccluded channel conductance states was calculated from the total time the channel resides at a given conductance value averaged over the set of individual experiments. The voltage-dependence of channel opening was calculated from measurements of the P_O as a function of

voltage by integration of conductance histograms where γ is 64 pS ≤ γ ≤ 68 pS. Statistical values represent means ± SEM, unless otherwise indicated. n and N denote number of experiments and number of opening events.

Fab generation. The Pierce ImmunoPure Fab Preparation Kit (44885) was used to generate Fabs. BoNT/A LC Fabs were quality checked using SDS-PAGE prior to the single molecule assays.

References for Supplementary Materials and Methods

1. Hamill OP, Marty A, Neher E, Sakmann B, Sigworth FJ (1981) *Pflugers Arch* 391**:** 85-100.

2. Carpaneto A, Accardi A, Pisciotta M, Gambale F (1999) *Exp Brain Res* 124**:** 193-199.

3. Lascola CD, Nelson DJ, Kraig RP (1998) *J Neurosci* 18**:** 1679-1692.

Acknowledgements

Chapter 2, in full, is a reprint of the material as it appears in the Proceedings of the National Academy of Sciences. Fischer, Audrey and Montal, Maurice, Proceedings of the National Academy of Sciences of the United States of America, 2007. The dissertation author was the primary investigator and an author of this paper.

Chapter 3

Crucial role of the disulfide bridge between botulinum neurotoxin light and heavy chains in protease translocation across membranes

THE JOURNAL OF BIOLOGICAL CHEMISTRY VOL. 282, NO. 40, pp. 29604–29611, October 5, 2007

Crucial Role of the Disulfide Bridge between Botulinum Neurotoxin Light and Heavy Chains in Protease Translocation across Membranes*

Received for publication, May 1, 2007, and in revised form, July 30, 2007 Published, JBC Papers in Press, July 31, 2007, DOI 10.1074/jbc.M703619200

Audrey Fischer and Mauricio Montal[1]

From the Section of Neurobiology, Division of Biological Sciences, University of California, San Diego, La Jolla, California 92093-0366

Clostridial botulinum **neurotoxins (BoNTs) exert their neuroparalytic action by arresting synaptic exocytosis. Intoxication requires the disulfide-linked, di-chain protein to undergo conformational changes in response to pH and redox gradients across the endosomal membrane with consequent formation of a protein-conducting channel by the heavy chain (HC) that translocates the light chain (LC) protease into the cytosol. Here, we investigate the role of the disulfide bridge in the dynamics of protein translocation. We utilize a single channel/single molecule assay to characterize in real time the BoNT channel and chaperone activities in Neuro 2A cells under conditions that emulate those prevalent across endosomes. We show that the disulfide bridge must remain intact throughout LC translocation; premature reduction of the disulfide bridge after channel formation arrests translocation. The disulfide bridge must be on the *trans* compartment to achieve productive translocation of LC; disulfide disruption on the *cis* compartment or within the bilayer during translocation aborts it. We demonstrate that a peptide linkage between LC and HC in place of a disulfide bridge is insufficient for productive LC translocation. The disulfide linkage, therefore, dictates the outcome of translocation: productive passage of cargo or abortive channel occlusion by cargo. Based on these and previous findings we suggest a sequence of events for BoNT LC translocation to be HC insertion, coupled LC unfolding, and protein conduction through the HC channel in an N to C terminus orientation and ultimate release of the LC from the HC by reduction of the disulfide bridge concomitant with LC refolding in the cytosol.**

Clostridium botulinum neurotoxins (BoNTs)[2] inhibit synaptic exocytosis in peripheral cholinergic synapses, thereby causing flaccid paralysis (1). BoNTs are synthesized as a single polypeptide chain with a molecular mass of ~150 kDa. The BoNT polypeptide is then proteolytically cleaved by bacterial or host proteases into the activated di-chain form: an ~50-kDa light chain (LC) and an ~100-kDa heavy chain (HC). The LC and HC are cross-linked by a disulfide bond between the two chains. Structurally, BoNTs consist of three modules (1–4): The N-terminal LC is the catalytic domain, and the HC comprises the translocation domain (the N-terminal half) and the receptor-binding domain (the C-terminal half). The LCs of six of the seven isoforms of BoNT, designated A–G, have been crystallized and all share structural similarity to the Zn^{2+}-metalloprotease thermolysin (2, 4–11). BoNT LCs are sequence-specific endopeptidases that cleave unique components of the SNARE (soluble *N*-ethylmaleimide-sensitive factor attachment protein receptor) complex, the synaptic vesicle fusion complex required for membrane fusion (12–14).

BoNTs enter cells by receptor-mediated endocytosis (1, 15). It has been widely recognized that, with the exception of BoNT/D, BoNT entry into neuronal cells requires surface receptors involving a specific ganglioside, namely GT1b (16–19), together with other protein components that determine the BoNT neurotropism. Recently, the identity of the neuronal protein receptors for BoNT/A (20, 21) and BoNT/B and BoNT/G (22) were uncovered as SV2 and synaptotagmins I and II, respectively. The crystal structure of BoNT/B in complex with a peptide from the luminal domain of synaptotagmin II has defined the surface determinants that account for the high specificity of binding of the toxin to neurons (23, 24).

A key step in the intoxication process is the translocation of endocytosed toxin across intracellular membranes to reach its cytosolic targets (1, 15). It was postulated that the acid pH of endocytic vesicles induces a conformational change that promotes insertion of the HC into acidic endosomal membranes, where the HC assembles into a protein-conducting channel with the LC as cargo translocated into the cytosol (1, 25, 26). Previously, we demonstrated that the HC of BoNT/A acts as both a channel and a transmembrane chaperone for the LC to ensure a translocation-competent conformation during its transit from the acidic endosome into the cytosol, thereby recovering the endopeptidase activity of BoNT LC (27).

Here, we probed the role of the disulfide bridge in LC translocation, focusing on the interactions between the HC channel/chaperone and its LC cargo under conditions that closely

* This work was supported by the U.S. Army Medical Research and Materiel Command (DAMD17-02-C-0106), National Institutes of Health Training Grant T32 GM08326, and Pacific Southwest Regional Center of Excellence Grant AI-65359. The costs of publication of this article were defrayed in part by the payment of page charges. This article must therefore be hereby marked "*advertisement*" in accordance with 18 U.S.C. Section 1734 solely to indicate this fact.

[1] To whom correspondence should be addressed: Section of Neurobiology, Division of Biological Sciences, University of California, San Diego, 9500 Gilman Dr., La Jolla, CA 92093-0366. Tel.: 858-534-0931; Fax: 858-822-3763; E-mail: mmontal@ucsd.edu.

[2] The abbreviations used are: BoNT, botulinum neurotoxin; βME, β-mercaptoethanol; γ, single channel conductance; LC, light chain; HC, heavy chain; P_o, channel open probability; TCEP, tris-(2-carboxyethyl) phosphine; $V_{1/2}$, the voltage at which $P_o = 0.5$.

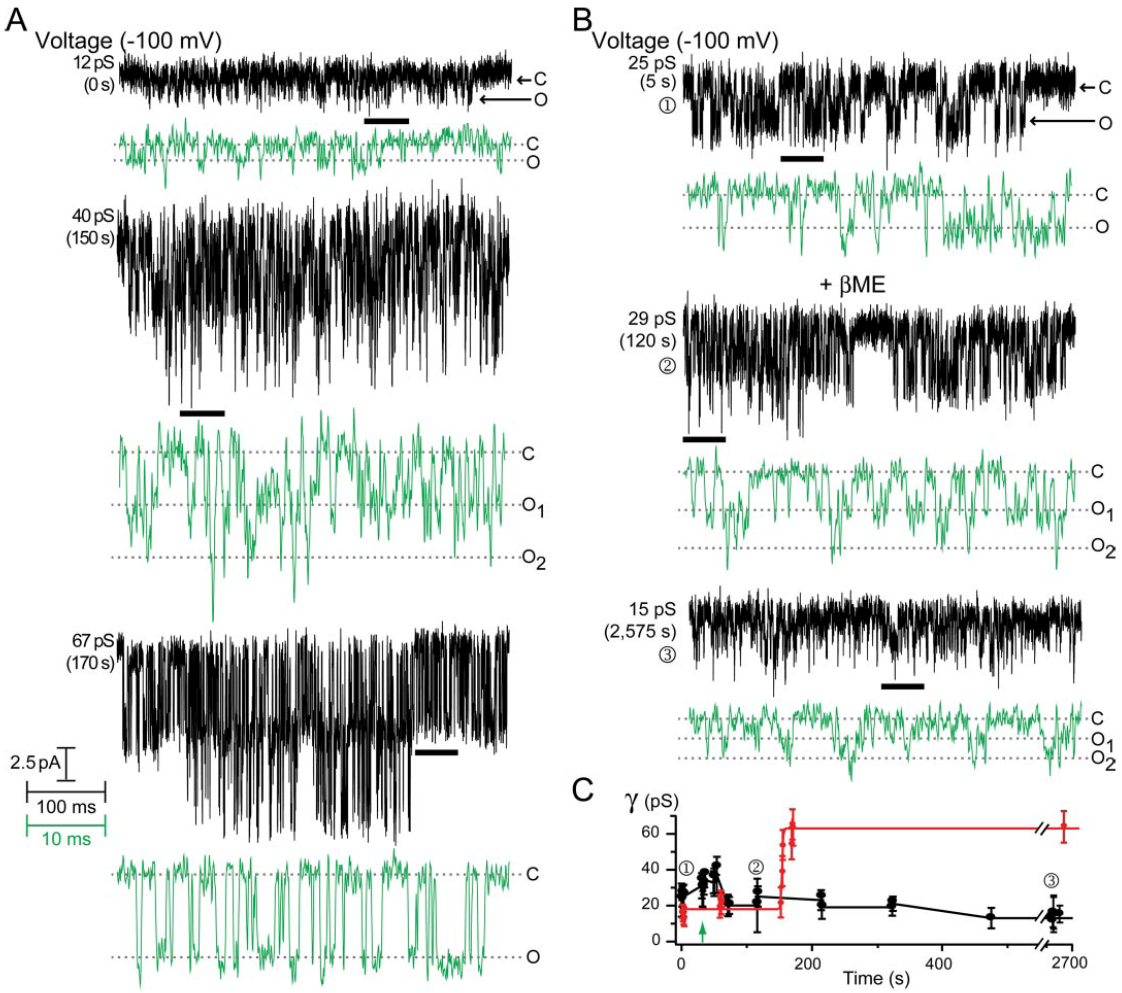

FIGURE 1. **Interruption of LC/A translocation by premature reduction of the disulfide link to the HC during early stages of translocation.** Representative single-channel currents recorded at −100 mV and at the indicated times; consecutive voltage pulses applied to the same patch. *Black line* designates the expanded region of the record displayed below the compressed record at a faster time scale, denoted by the *green scale bar*. *A*, BoNT/A holotoxin channels in excised patches of Neuro 2A cells. Channel activity begins 20 min after GΩ seal formation. Channel opening is indicated by a *downward deflection*. *C* and *O*, *closed* and *open* states. *B*, holotoxin channels with addition of βME after the onset of channel activity. Channel activity begins 5 min after GΩ seal formation. Thirty seconds later, 1 mM βME is added to the *trans* compartment. Multiple channel insertions occur with time in *panels A* and *B*. *C*, time course of channel γ change illustrated in *panel B* (average *N*/data point = 340 events). Addition of βME designated by the *arrow*. *Thin red line* represents results for holotoxin without βME addition (average *N*/data point = 686). γ values associated with raw data from *panel B* are indicated.

emulate those prevalent at the endosome. We utilized a previously developed assay in Neuro 2A cells to monitor interactions between the HC and the LC during translocation with single molecule sensitivity (28). This assay led to the identification of intermediate channel conductances that reflect permissive stages during LC translocation for both BoNT/A and BoNT/E (28). Further, we showed that productive translocation requires proteolytic cleavage of LC cargo from the HC channel (28). In this work we use the assay to examine the consequences of disulfide linkage disruption by chemical reductants accessible to different sides of the membrane. The disulfide linkage emerges as a crucial determinant required for chaperone function and LC translocation and release. These and previous findings indicate that BoNT translocation involves an acid pH-induced membrane insertion step coupled to LC unfolding and entry into the HC chaperone/channel, LC protein conduction through the HC channel in an N- to C-terminal orientation, and subsequent release of the LC cargo from chaperone by reduction of the disulfide bridge concomitant with LC refolding at the cytosol.

EXPERIMENTAL PROCEDURES

Unless otherwise specified, all chemicals were purchased from Sigma-Aldrich. Purified native BoNT/A holotoxin and

HC and BoNT/E holotoxin were from Metabiologics. The ING2 BoNT/A LC-specific monoclonal antibody was kindly provided by Dr. James Marks (University of California, San Francisco).

Cell Culture—Neuro 2A neuroblastoma cells were obtained from the American Type Culture Collection. Cells were passaged in Dulbecco's modified Eagle's medium (BioWhittaker) supplemented with penicillin 10 mM/streptomycin 10 μg/ml/glutamine 2 mM (Invitrogen), and 5% newborn bovine serum (Invitrogen). Cells were plated onto Matrigel (BD Biosciences)-coated glass coverslips at a density of ~500 cells/coverslip and cultured at 37 °C, 5% CO_2 for 1–3 days prior to patch clamp recordings.

Patch Clamp Recordings—Patch pipettes were pulled from borosilicate glass (Hilgenberg, Lambrecht, Germany), fire-polished, and used at 3.5–7.0 MΩ resistance when immersed in recording solution. Excised patches in the inside-out configuration were used (29). After gigaohm (GΩ) seal formation, the patch was excised from the cell, removed, and reimmersed through the air-water interface to achieve an inside-out configuration. Current recordings were obtained under voltage clamp conditions by the application of consecutive voltage steps 800 ms in duration from +50 mV to −150 mV at a sampling frequency 20 kHz. Records were acquired and analyzed using the patch clamp amplifier system (List EPC-9; HEKA Electronik) fitted with an ITC-16 interface (Instrutech, Port Washington, NY) and the Pulse/PulseFit acquisition and analysis software (HEKA). Data were further analyzed using Clampfit v.9.2 software (Molecular Devices, Sunnyvale, CA), Microsoft Excel, and IGOR Pro (Wavemetrics, Portland, OR). All experiments were conducted at 22 ± 2 °C.

Solutions—To emulate endosomal conditions the *trans* compartment (bath) solution contained (in mM) NaCl 200, NaMOPS [3-(*N*-morpholino) propanesulfonic acid] 5, (pH 7.0 with HCl), tris-(2-carboxyethyl) phosphine (TCEP) 0.25, $ZnCl_2$ 1, and the *cis* compartment (pipette) solution contained (in mM) NaCl 200, NaMES [2-(*N*-morpholino) ethanesulfonic acid] 5, (pH 5.3 with HCl). The osmolarity of both solutions was determined to be 390 mosM. $ZnCl_2$ was used to block endogenous channel activity specific to Neuro 2A cells (30, 31). BoNT reconstitution and channel insertion was achieved by supplementing 5 μg/ml BoNT holotoxin or HC to the pipette solution, which was set to an endosomal pH of 5.3. BoNT/E experiments were performed with 40 μM trypsin in the *trans* compartment. GΩ seal formation was optimized as follows: The pipette tip was first dipped in the pipette solution in the absence of BoNT and then back-filled with solution containing BoNT.

Data Analysis—Analysis was performed on single bursts of each experimental record; a single burst is defined as a set of openings and closings lasting ≥50 ms bounded by quiescent periods of ≥50 ms before and after. BoNT channel activity occurs in bursts, and only single bursts were analyzed due to the random duration of quiescent periods between these bursts (32). The single channel conductance (γ) was calculated from Gaussian fits to current amplitude histograms. The total number of opening events analyzed was 184,923; the intermediate γ states were defined by a minimum of 500 events. For each experiment, the time course of channel γ change was calculated from γ of each record, where $t = 0$ s corresponds to onset of channel activity and average time course was constructed from the set of individual experiments for a single condition. Average occupancy time of occluded intermediate and unoccluded channel γ states was calculated from the total time the channel resides at a given γ value averaged over the set of individual experiments. The voltage dependence of channel opening was calculated from measurements of the fraction of time that the channel is open (P_o) as a function of voltage by integration of γ histograms where γ is 64 pS ≤ γ ≤ 68 pS. Statistical values represent means ± S.E. unless otherwise indicated. n and N denote number of experiments and number of opening events.

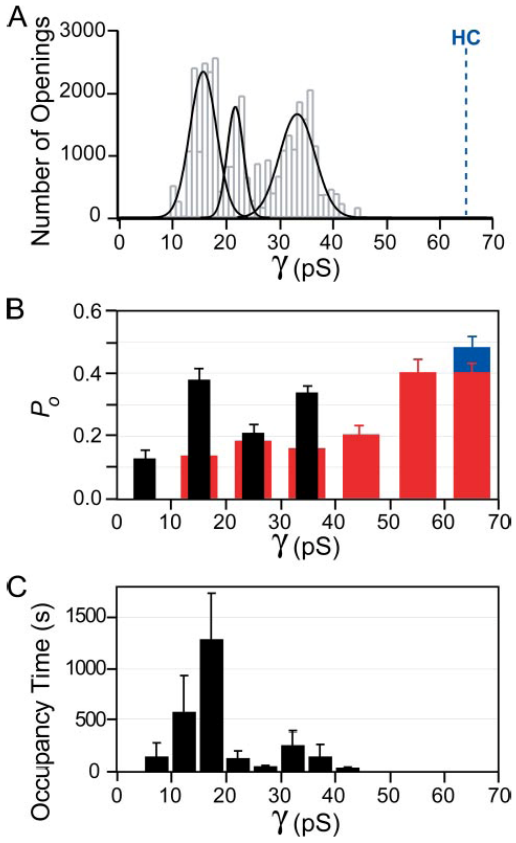

FIGURE 2. **Analysis of LC translocation arrested by premature reduction of the disulfide link to HC.** *A*, γ amplitude histogram and Gaussian fit with γ = 15.3 ± 3.6, 21.4 ± 2.2, and 33.2 ± 4.8 pS (N = 34,988 events). *HC* indicates the unoccluded HC conductance. *B*, P_o as a function of γ for premature reduction of holotoxin (*black*), holotoxin without βME addition (*red*), and unoccluded HC (*blue*) (n = 5; the average N/data point = 8,750 events). *C*, average occupancy time of conductance states for premature reduction of BoNT/A holotoxin (n = 5; average N/data point = 5,130 events).

Fab Generation—The Pierce ImmunoPure Fab Preparation kit (44885) was used to generate Fabs from BoNT/A LC antibody ING2. In short, 3 mg/ml ING2 was incubated in the equiv-

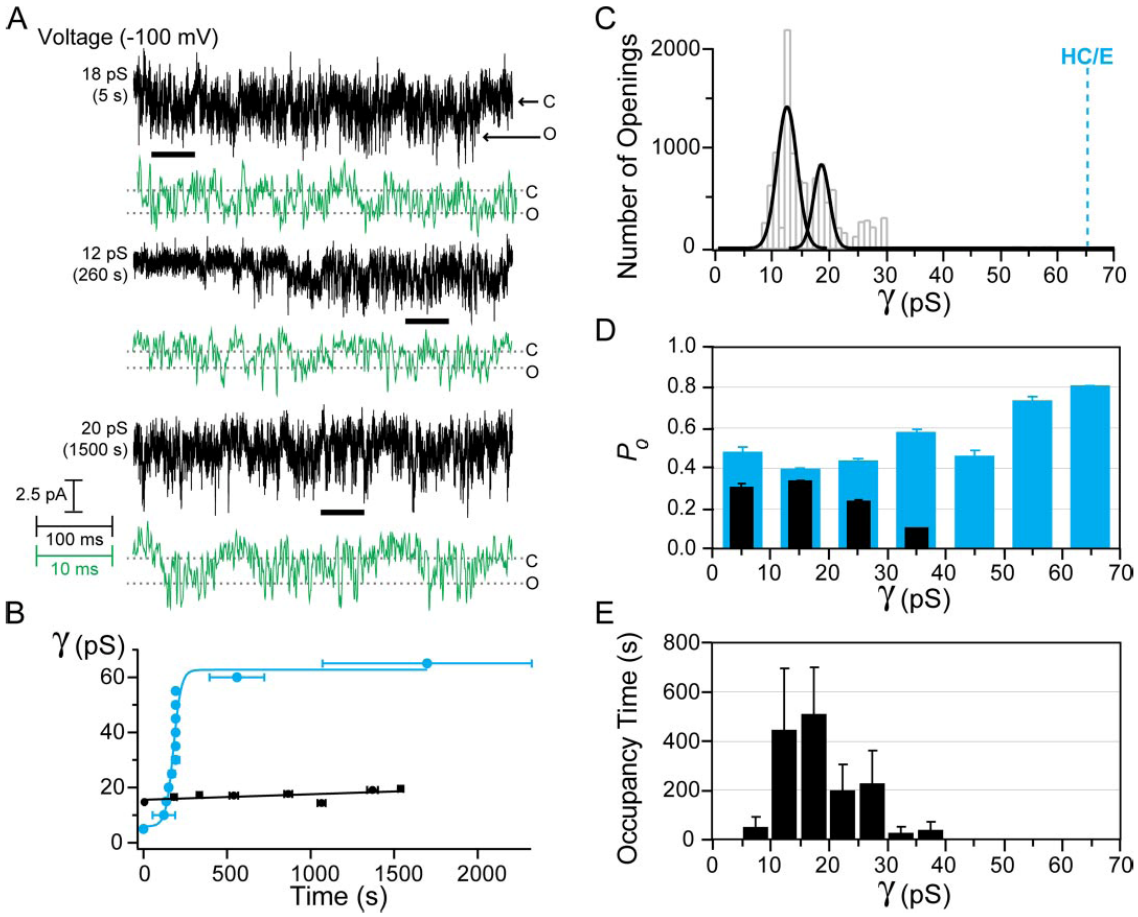

FIGURE 3. **Aborted LC/E translocation by premature reduction of the disulfide link to the HC before channel insertion.** *A*, representative single-channel currents recorded at −100 mV and at the indicated times; consecutive voltage pulses applied to the same patch. *Black line* designates the expanded region of the record displayed below the compressed record at a faster time scale, denoted by the *green scale bar*. Single-chain BoNT/E preincubated with 10 mM TCEP at room temperature for 30 min prior to the experiment; channel activity begins 25 min after GΩ seal formation. Prereduced BoNT/E does form channels; however, they do not reach the unoccluded BoNT/E γ = 65 pS resulting from disulfide bridge reduction in the *trans* compartment. *B*, average time course of channel γ change for prereduced BoNT/E (*black*) ($n = 4$) and disulfide bridge intact BoNT/E (*cyan*) ($n = 3$) (average *N*/data point for prereduced = 1,374 events and disulfide bridge intact = 890 events). *C*, γ amplitude histogram and Gaussian fit of prereduced BoNT/E with γ = 12.2 ± 2.5 and 25.8 ± 2.0 pS ($N = 11{,}065$ events). *HC/E* indicates the unoccluded BoNT/E conductance. *D*, P_o as a function of γ for prereduced BoNT/E ($n = 4$; average *N*/data point = 2,196 events, *black*), and disulfide bridge intact BoNT/E ($n = 3$; average *N*/data point = 2,821 events, *cyan*). *E*, average occupancy time of conductance states ($n = 4$; average *N*/data point = 890 events).

alent volume of immobilized papain at 37 °C for 5 h. The digested ING2 was transferred to a Protein A column to separate the Fabs from the Fc and undigested ING2: the Fabs flow through the column whereas the Fc and undigested IgG are retained and elute later. BoNT/A LC Fabs were quality-checked using SDS-PAGE prior to the single molecule assays. Purified Fabs were concentrated to 1 mg/ml in patching bath solutions prior to incubation with BoNT/A holotoxin.

RESULTS AND DISCUSSION

Single Molecule Translocation Assay—Translocation of BoNT/A LC by the BoNT/A HC channel can be monitored in real time and at the single molecule level in excised membrane patches from Neuro 2A cells (28). Translocation requires pH 5.3 on the *cis* compartment, defined as the compartment containing BoNT/A, and pH 7.0 on the *trans* compartment, which is supplemented with the membrane-nonpermeable reductant TCEP, conditions that emulate those prevalent across endosomes. Translocation is then observed as a time-dependent increase in Na^+ conductance through the HC channel, as illustrated by the control experiment shown in Fig. 1*A*. The time course of change of the single channel conductance γ after insertion of BoNT/A holotoxin into the membrane displays multiple discrete transient intermediate conductances before achieving a γ of 67.1 ± 2.0 pS (Fig. 1*C*, *red trace*). The *top panel* of Fig. 1*A* shows that at the onset of translocation small, discrete events with a γ ~ 12 pS are clearly discerned, as indicated by the segment of the record designated with a *black bar* that is dis-

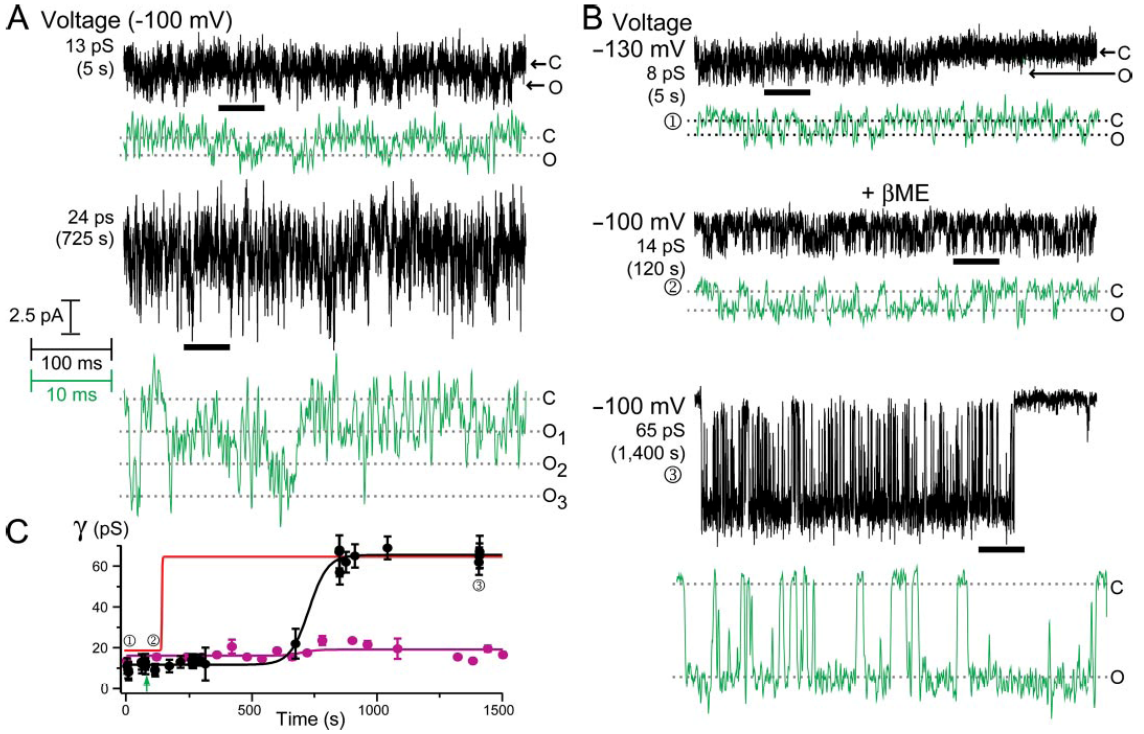

FIGURE 4. **LC/A translocation arrest by an LC/A-specific Fab and relief from arrest by reduction of the LC-HC disulfide bridge.** Representative single-channel currents recorded at the indicated times and voltages; consecutive voltage pulses applied to the same patch. *Black line* designates the expanded region of the record displayed below the compressed record at a faster time scale, denoted by the *green scale bar*. *A*, BoNT/A holotoxin preincubated with a 5-fold molar excess of Fab on ice at pH 7 for 1 h prior to the experiment; channel activity begins 5 min after GΩ seal formation. Multiple channel insertions occur with time; however, in contrast to unmodified holotoxin, the conductance never reaches the unoccluded HC γ = 66 pS. *B*, holotoxin preincubated with Fab; channel activity begins 10 min after GΩ seal formation. Low conductance intermediate states persist until the addition of βME. Eighty seconds after onset of channel activity, 1 mM βME is added to the *trans* compartment. Within minutes γ increases to the larger intermediate conductance states and ultimately achieves the unoccluded HC channel γ = 66 pS. *C*, time course of channel γ change illustrated in Fig. 4*B* (*black*) and average time course of channel γ change for holotoxin preincubated with Fab (average *N*/data point for Fab preincubated with BoNT/A without addition of βME = 1,003 events and with addition of βME = 180 events; *n* = 5 for each condition, *magenta*). Addition of βME designated by the *green arrow*. *Thin red line* represents results for holotoxin without βME addition; γ values associated with raw data from *panel B* are indicated.

played at higher time resolution under the trace. Progressively, γ increases and, as shown in the *middle panel* of Fig. 1*A*, reaches a value of ~40 pS; note the insertion of two channels into the membrane, designated O_1 and O_2, which even during the short segment displayed undergo a continuous increase in conductance, ultimately reaching a stable value of 67 pS (*bottom panel*), a conductance at which they remain for the duration of the experiment (Fig. 1*C*, *red trace*). A γ of 67.1 ± 2.0 pS is also the characteristic conductance of isolated HC recorded under identical conditions; therefore it represents the conductance of the unoccluded HC in holotoxin experiments after translocation is complete. We interpret these different conductance events as reporters of discrete intermediate stages during the translocation of the LC across the membrane. During protease translocation, the protein-conducting channel progressively conducts more Na^+ around the polypeptide chain before entering an exclusively ion-conductive state. This typical pattern of channel activity for holotoxin proceeds under conditions that mimic those across endosomes and lead to LC translocation and retrieval of protease activity after completion of translocation (27). Thus, we have used this assay to examine the role of the interchain disulfide linkage on the translocation process.

Premature Reduction of the Disulfide Bridge after Channel Formation Arrests LC Translocation—Previous work has demonstrated the important role of the disulfide bridge in the translocation process (27). We used the differential accessibility of the disulfide linkage between the HC and the LC to TCEP to identify requirements for translocation and showed that LC translocation requires both a pH gradient and a redox gradient, acidic and oxidizing on the *cis* compartment and neutral and reducing on the *trans* compartment. Significantly, addition of TCEP only to the *cis* compartment after acidification fails to evoke channel activity. This is indicative of disulfide shielding arising from the onset of the LC translocation through the HC channel. Here, we pursue this strategy to determine how the disulfide bridge affects the progress of LC translocation. β-mercaptoethanol (βME) is a powerful tool for this task. First, βME does not modify HC channel activity, and preincubation of BoNT/A

with reductants results in HC channel activity (data not shown). Additions to the *cis* compartment cannot be directly made after seal formation; therefore membrane-permeable reagents that equilibrate across both compartments are required. In contrast to TCEP (33), βME can traverse the lipid bilayer and reduce the disulfide bridge from either side of the membrane. If the disulfide bridge were translocated first across the membrane and were confined to the TCEP-containing *trans* compartment during the early steps of translocation, then addition of βME should have no effect on channel activity and growing conductance would end invariably in an unoccluded channel with $\gamma \sim 67$ pS. The conductance growth of holotoxin channels is interrupted by addition of βME immediately after its onset, as shown in Fig. 1*B*. The *top panel* shows a single BoNT/A channel undergoing a progressive increase in conductance, comparable with the entry events characteristically displayed by holotoxin (Fig. 1*A*). Addition of βME, however, precludes entry into the higher γ intermediates, as evidenced in the *middle* and *bottom panels* of Fig. 1*B* in which two channels that inserted into the membrane prior to βME addition remain in one of the low conductance states for the remainder of the experiment (Fig. 1*C*, *black trace*). The current transitions are faster and shorter-lived than those typical of unmodified, unoccluded holotoxin, giving the appearance of flickering between low and high conductance states, a characteristic feature of channel block (27, 34). Analysis of the results of five experiments of this type (Fig. 2) shows that LC translocation is arrested by reduction of the disulfide linkage after the initiation of translocation. Under these conditions, the holotoxin channel preferentially resides in one of the following conductance states (Fig. 2*A*): 10, 17, or 31 pS. The lowest two states detected correspond to the entry event identified for holotoxin if translocation is unperturbed (28); however, the 31-pS intermediate may correspond to a non-productive, dead-end state for the LC and HC. The increased P_o of the low conductance states ($\gamma \sim 10$ and 30 pS, Fig. 2*B*) and the preponderant occupancy of these occluded intermediate states (Fig. 2*C*) further demonstrate that intermediate steps in the growing conductance of the holotoxin channel are stabilized, thereby precluding completion of LC translocation: the HC channel is occluded by the LC and translocation is arrested.

Premature Reduction of the Disulfide Bridge of Single-chain BoNT/E before Channel Formation Arrests LC Translocation—The finding that interruption of BoNT/A LC translocation results from premature reduction of the disulfide bridge leads to the hypothesis that the LC must be anchored to the HC during translocation. Is any linkage between the LC and HC sufficient to promote LC translocation or is the intact disulfide bridge specifically required? Whereas BoNT/A is cleaved to the mature di-chain within the *Clostridium* bacteria, BoNT/E is not cleaved before secretion. We previously demonstrated that, for the single-chain BoNT/E, completion of LC translocation proceeds only after proteolytic cleavage by trypsin and disulfide reduction in the *trans* compartment (28). Single-chain BoNT/E holotoxin is, therefore, an appropriate system to explore the linkage requirements for LC translocation. Accordingly,

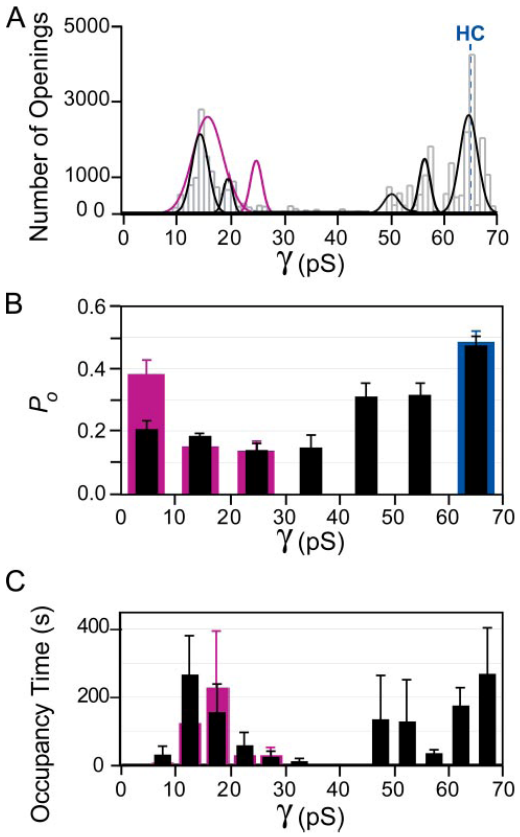

FIGURE 5. **Analysis of Fab-mediated BoNT/A holotoxin channel block released by reduction of the LC-HC disulfide bridge.** *A*, γ amplitude histogram (*gray*) and Gaussian fit (*black*) of Fab preincubated with BoNT/A and then reduced with βME after the onset of channel activity with intermediate γ = 13.4 ± 2.2, 18.7 ± 1.1, 50.1 ± 2.1, 56.5 ± 1.5, and 65.0 ± 2.4 pS (*N* = 31,202 events). BoNT/A preincubated with Fab without βME addition Gaussian fit illustrated in *pink*, data not shown (*N* = 22,113 events). *B*, P_o as a function of γ for Fab BoNT/A complex (*pink*) (*n* = 5; the average *N*/data point = 7,350 events), Fab BoNT/A complex with βME addition (*black*) (*n* = 5; the average *N*/data point = 8,750 events), and unoccluded HC (*blue*) (*n* = 1; the average *N*/data point = 1,024 events). *C*, average occupancy time of conductance states for BoNT/A-Fab complex with (*black*) and without (*pink*) addition of βME after onset of channel activity (with βME, *n* = 4, average *N*/data point = 2,840 events; without βME, *n* = 5, average *N*/data point = 5,170 events).

BoNT/E was incubated with 10 mM TCEP for 30 min at room temperature before the translocation assay. Prereduced BoNT/E displays channel activity as illustrated in Fig. 3*A*. Channel openings exhibit a γ similar to that of the early intermediates detected for unmodified BoNT/E (28); however, these low γ events do not undergo a transition to the higher γ intermediates or to unoccluded states (Fig. 3*A*). Despite the fact that trypsin is present in the *trans* compartment, the channel remains in low γ states for the lifetime of the experiment.

Analysis of four separate experiments under these conditions demonstrates that the channel activity of prereduced single-chain BoNT/E is different from that of the intact, disulfide cross-linked BoNT/E, never reaching the unoccluded channel state $\gamma \sim 65$ pS. BoNT/E with an intact disulfide bridge transi-

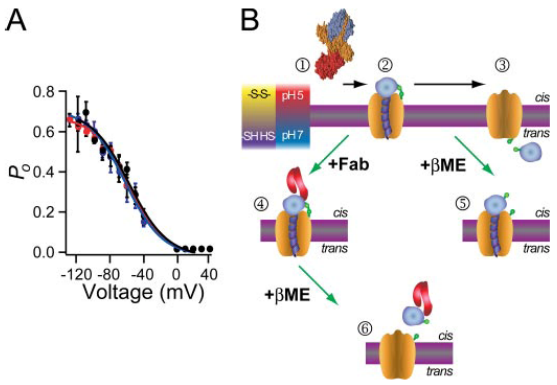

FIGURE 6. **Summary of BoNT/A channel characteristics and dependence upon LC translocation.** *A*, P_o as a function of voltage for holotoxin bound to Fab with βME addition (*black*), unmodified holotoxin (*red*), and unoccluded HC (*blue*). $V_{1/2}$ for holotoxin bound to Fab + βME is −59.0 ± 4.5 mV, for unmodified holotoxin is −58.3 ± 1.7 mV, and for HC is −63.4 ± 2.4 mV ($3 \leq n \leq 11$/data point; average *N*/data point = 2,260 events). *B*, structure of BoNT/A holotoxin (2): LC, *purple*, translocation domain, *orange*, and receptor-binding domain, *red*, prior to insertion in the membrane (*gray bar with magenta boundaries*) ①; then schematic representation of BoNT/A inserted during translocation of the LC through the HC channel (*orange*) with intact disulfide bridge (*green*) while located in the *cis*-compartment ② and the unoccluded HC channel in the membrane after LC dissociation③. Occluded HC channels can be trapped in low conductance states under two experimental conditions: ④ LC translocation arrested by Fab and ⑤ LC translocation arrested by premature reduction of the LC-HC disulfide bridge. Channels formed by holotoxin bound to an LC/A-specific Fab can be unoccluded by the subsequent βME-induced release of the LC-Fab complex into the acid pH compartment ⑥.

tions from occluded to unoccluded channel activity within 300 s (Fig. 3*B*, *cyan*); reduction of the disulfide prior to channel insertion results in a permanently occluded channel with intermediate conductance states at γ ~ 12 and 26 pS (Fig. 3*B*, *black*, and 3*C*). The conductance intermediate at 26 pS is similar to the prematurely reduced BoNT/A intermediate at 31 pS and may correspond to a dead-end intermediate state. The persistent occupancy of these low γ states and decreased P_o with respect to unmodified BoNT/E further demonstrate the requirement for an intact disulfide bridge before channel insertion and throughout LC translocation (Fig. 3, *D* and *E*). The peptidic linkage between the LC and HC is insufficient to promote productive LC translocation. The disulfide bond may serve to maintain a translocation-competent conformation of the LC and its close proximity to the HC channel; reduction of the disulfide cross-link may dissociate such dynamic interaction.

These results indicate that the disulfide bridge must be on the *trans* (cytosolic) compartment to achieve productive translocation of the LC; disulfide disruption on the *cis* compartment or within the bilayer during translocation aborts it. Disulfide disruption at different intermediate γ states resulted in arrested LC translocation; therefore, we infer that completion of LC translocation occurs as the disulfide bridge, C terminus of the LC, enters the cytosolic compartment. This analysis supports a model of N- to C-terminal orientation of cargo during translocation with the C terminus as the last portion to be translocated and exit the channel. We propose that an intact disulfide bridge is a necessary condition for translocation but not for channel insertion, as demonstrated by the facts that the isolated HC channel is unperturbed by chemical reductants (27) and that prematurely reduced single-chain BoNT/E exhibits low conductance channel activity. The tight coupling of translocation completion with disulfide reduction strongly argues in favor of the view that LC refolding precludes retrotranslocation. From this viewpoint, refolding in cytosol may be interpreted as a trap that prevents retrotranslocation and dictates the unidirectional nature of the translocation process. The disulfide linkage is, therefore, a crucial aspect of the BoNT toxicity and is required for chaperone function, acting as a principal determinant for cargo translocation and release.

An LC-specific Antibody Arrests LC Translocation—To selectively restrict the location of the disulfide linkage to the entry site into the HC and to probe its accessibility to βME, we exploited an LC-specific monoclonal antibody previously documented to block LC translocation (28). For this type of experiment Fab fragments are preincubated with BoNT/A for 1 h at pH 7 before the translocation assay. Under these conditions, low conductance channels are detected within a few minutes after patch excision (Fig. 4*A*, *top panel*). The initial conductances are comparable with those characteristic of the early events in unmodified LC translocation; however, the channels remain in the low conductance states throughout the experiment (Fig. 4*A*, *bottom panel*). We interpret these intermediates as early steps in translocation in which the HC has formed a channel that is partially occluded by the LC. Fab binding to the LC allows channel formation and early translocation, presumably stabilizing intermediate protein-protein interactions. However, it locks the channel and the LC in a translocating conformation that is irreversibly incomplete.

Reduction of the Disulfide Bridge Releases the Fab-induced HC Channel Block by LC—Reduction of the disulfide bridge between the LC and the HC may facilitate release of the Fab-LC complex, thereby unoccluding the HC channel. The disulfide on the Fab will be concurrently reduced; accordingly, only if the complex remains intact under reducing conditions will release of HC channel block ensue. This model was tested by preincubating the Fab with the BoNT/A, followed by supplementing βME to the *trans* compartment after the onset of the channel activity. Within minutes of βME addition the low conductance channel does enter the unoccluded channel state (Fig. 4*B*, *bottom panel*, and 4*C*, *black*) in sharp contrast to the Fab-induced block of channel activity (Fig. 4*C*, *pink*). The latency period for release of the HC channel from block by the LC estimated from these measurements is ~730 s (Fig. 4*C*, *black*) as compared with ~150 s for unabated LC translocation in unmodified holotoxin (Fig. 4*C*, *red*). Holotoxin channels under these conditions exhibit discrete transient intermediate conductances at $\gamma \cong 13$, 19, 50, and 57 pS before entering the unoccluded state at $\gamma \cong 65$ pS, as evidenced from analysis of four separate experiments (Fig. 5, *A* and *B*). These γ and P_o (Fig. 5*C*, *pink*) values approximate the low conductance intermediate states of holotoxin during productive LC translocation (Fig. 5*C*, *black*). However, the occupancy time in each conductance intermediate is longer as compared with unperturbed holotoxin (Fig. 5*C*) (28). The low γ intermediate states are stabilized by the Fab (Fig. 5*A*); however, the prolonged residency in the larger γ intermedi-

ates (Fig. 5*B*) is a unique aspect of this experimental condition. These findings indicate that although the LC is released from the HC channel, the kinetics are different from that of unabated translocation. The release of channel block is consistent with the strong binding affinity of the Fab for the LC: even though the disulfide bridge holding the two Fab subunits has been reduced the binding affinity is sufficient to facilitate dissociation of the LC from the HC channel. In the presence of Fab, therefore, translocation is aborted and disulfide reduction releases the LC to the *cis* compartment, thereby unblocking the HC channel.

Importantly, the unoccluded HC channels that result from this experimental strategy (Fig. 6*A*, *black*) are indistinguishable from channels produced by isolated HC/A (Fig. 6*A*, *blue*) and by holotoxin/A after productive translocation of LC (Fig. 6*A*, *red*). These three experimental conditions lead to a channel entity that exhibits comparable voltage dependence: the $V_{½}$ is ~−60 mV (Fig. 6*A*). In the presence of Fab translocation is aborted (Fig. 6*B*, *pathway* ④) and disulfide reduction releases the LC on the *cis* compartment, thereby unblocking the HC channel (Fig. 6*B*, *pathway* ⑥).

Concluding Remarks—The new findings here described and our interpretation are summarized in the scheme shown in Fig. 6*B*. The initial condition ①, illustrated with a surface representation of the crystal structure of BoNT/A (2), depicts the holotoxin as an aqueous soluble protein at neutral pH. Exposure to a pH gradient and a redox gradient comparable with those across endosomal membranes leads to a conformational change of the holotoxin with the consequent insertion of the HC into the membrane and the onset of LC translocation, manifested as occluded channels with a characteristic small γ (Fig. 6*B*, *pathway* ②). Productive translocation leads to the release of the LC in the *trans* compartment, with the ultimate refolding of the LC and retrieval of its protease activity, and the consequent unblocking of the HC (Fig. 6*B*, *pathway* ③). Two experimental conditions arrest LC translocation and yield occluded HC channels. Preincubation of holotoxin with an LC-specific Fab allows HC channel formation yet it aborts LC translocation (Fig. 6*B*, *pathway* ④). Premature reduction of the disulfide linkage of BoNT/A holotoxin after channel formation terminates LC translocation (Fig. 6*B*, *pathway* ⑤); in accordance, premature reduction of single-chain BoNT/E holotoxin before channel formation allows channel insertion yet aborts LC translocation. Pathway ⑥ highlights the result that reduction of the disulfide bridge on the *cis* compartment releases the Fab-induced HC channel block by LC with the ensued dissociation of the LC-Fab complex into the *cis* compartment, thereby unblocking the HC channel. The unoccluded HC channel entity that results from the productive translocation of the LC (pathway ① → ② → ③) (32) or from the disulfide reduction-mediated relief of the Fab-induced HC channel block (pathway ① → ④ → ⑥) is indistinguishable from that produced by the isolated HC (27) in terms of single channel conductance, selectivity, and voltage-dependence features.

Acknowledgments—We thank M. Goodnough for invaluable help, J. Marks and M. C. Gonzalez for antibodies, J. Santos, M. Oblatt-Montal, L. Koriazova, and members of the Montal laboratory for perceptive comments, and R. Hampton, S. Emr, and J. Young for helpful suggestions.

REFERENCES

1. Schiavo, G., Matteoli, M., and Montecucco, C. (2000) *Physiol. Rev.* **80,** 717–766
2. Lacy, D. B., Tepp, W., Cohen, A. C., DasGupta, B. R., and Stevens, R. C. (1998) *Nat. Struct. Biol.* **5,** 898–902
3. Lacy, D. B., and Stevens, R. C. (1999) *J. Mol. Biol.* **291,** 1091–1104
4. Swaminathan, S., and Eswaramoorthy, S. (2000) *Nat. Struct. Biol.* **7,** 693–699
5. Agarwal, R., Binz, T., and Swaminathan, S. (2005) *Biochemistry* **44,** 11758–11765
6. Agarwal, R., Eswaramoorthy, S., Kumaran, D., Binz, T., and Swaminathan, S. (2004) *Biochemistry* **43,** 6637–6644
7. Arndt, J. W., Chai, Q., Christian, T., and Stevens, R. C. (2006) *Biochemistry* **45,** 3255–3262
8. Arndt, J. W., Yu, W., Bi, F., and Stevens, R. C. (2005) *Biochemistry* **44,** 9574–9580
9. Breidenbach, M. A., and Brunger, A. T. (2004) *Nature* **432,** 925–929
10. Hanson, M. A., and Stevens, R. C. (2000) *Nat. Struct. Biol.* **7,** 687–692
11. Segelke, B., Knapp, M., Kadkhodayan, S., Balhorn, R., and Rupp, B. (2004) *Proc. Natl. Acad. Sci. U. S. A.* **101,** 6888–6893
12. Jahn, R., Lang, T., and Sudhof, T. C. (2003) *Cell* **112,** 519–533
13. Sutton, R. B., Fasshauer, D., Jahn, R., and Brunger, A. T. (1998) *Nature* **395,** 347–353
14. Weber, T., Zemelman, B. V., McNew, J. A., Westermann, B., Gmachl, M., Parlati, F., Söllner, T. H., and Rothman, J. E. (1998) *Cell* **92,** 759–772
15. Simpson, L. L. (2004) *Annu. Rev. Pharmacol. Toxicol.* **44,** 167–193
16. Ginalski, K., Venclovas, C., Lesyng, B., and Fidelis, K. (2000) *FEBS Lett.* **482,** 119–124
17. Nishiki, T., Tokuyama, Y., Kamata, Y., Nemoto, Y., Yoshida, A., Sekiguchi, M., Takahashi, M., and Kozaki, S. (1996) *Neurosci. Lett.* **208,** 105–108
18. Tsukamoto, K., Kohda, T., Mukamoto, M., Takeuchi, K., Ihara, H., Saito, M., and Kozaki, S. (2005) *J. Biol. Chem.* **280,** 35164–35171
19. Yowler, B. C., Kensinger, R. D., and Schengrund, C. L. (2002) *J. Biol. Chem.* **277,** 32815–32819
20. Dong, M., Yeh, F., Tepp, W. H., Dean, C., Johnson, E. A., Janz, R., and Chapman, E. R. (2006) *Science* **312,** 592–596
21. Mahrhold, S., Rummel, A., Bigalke, H., Davletov, B., and Binz, T. (2006) *FEBS Lett.* **580,** 2011–2014
22. Rummel, A., Karnath, T., Henke, T., Bigalke, H., and Binz, T. (2004) *J. Biol. Chem.* **279,** 30865–30870
23. Chai, Q., Arndt, J. W., Dong, M., Tepp, W. H., Johnson, E. A., Chapman, E. R., and Stevens, R. C. (2006) *Nature* **444,** 1096–1100
24. Jin, R., Rummel, A., Binz, T., and Brunger, A. T. (2006) *Nature* **444,** 1092–1095
25. Finkelstein, A. (1990) *J. Physiol.* **84,** 188–190
26. Gambale, F., and Montal, M. (1988) *Biophys. J.* **53,** 771–783
27. Koriazova, L. K., and Montal, M. (2003) *Nat. Struct. Biol.* **10,** 13–18
28. Fischer, A., and Montal, M. (2007) *Proc. Natl. Acad. Sci. U. S. A.* **104,** 10447–10452
29. Hamill, O. P., Marty, A., Neher, E., Sakmann, B., and Sigworth, F. J. (1981) *Pflugers Arch. Eur. J. Physiol.* **391,** 85–100
30. Carpaneto, A., Accardi, A., Pisciotta, M., and Gambale, F. (1999) *Exp. Brain Res.* **124,** 193–199
31. Lascola, C. D., Nelson, D. J., and Kraig, R. P. (1998) *J. Neurosci.* **18,** 1679–1692
32. Fischer, A., and Montal, M. (2006) *Neurotox. Res.* **9,** 93–100
33. Getz, E. B., Xiao, M., Chakrabarty, T., Cooke, R., and Selvin, P. R. (1999) *Anal. Biochem.* **273,** 73–80
34. Hille, B. (2001) *Ion Channels of Excitable Cells*, 3rd Ed., Sinauer, Sunderland, MA

Acknowledgements:

Chapter 3, in full, is a reprint of the material as it appears in the Journal of Biological Chemistry. Fischer, Audrey and Montal, Maurice, American Society for Biochemistry and Molecular Biology, 2007. The dissertation author was the primary investigator and an author of this paper.

Chapter 4

Molecular architecture of Botulinum neurotoxin E revealed by single particle electron microscopy

MOLECULAR ARCHITECTURE OF BOTULINUM NEUROTOXIN E REVEALED BY SINGLE PARTICLE ELECTRON MICROSCOPY

Audrey Fischer[1], Consuelo Garcia-Rodriguez[2], Isin Geren[2], Jianlong Lou[2], James D. Marks[2], Terunaga Nakagawa[3, 4]*, and Mauricio Montal[1, 4]*

From the Section of Neurobiology, Division of Biological Sciences, University of California San Diego, La Jolla, CA 92093-0366[1], the Departments of Anesthesia and Pharmaceutical Chemistry, University of California San Francisco, San Francisco, CA 94143[2] and the Department of Chemistry and Biochemistry, University of California San Diego, La Jolla, CA 92093[3]

[4]Both authors contributed equally as senior authors

Running title: 3D structure of BoNT/E

*Address correspondence to: Mauricio Montal and Terunaga Nakagawa, 9500 Gilman Dr., La Jolla, CA 92093.Fax: 858-822-3763; Email: mmontal@ucsd.edu. Fax: 858-534-7042; Email: nakagawa@ucsd.edu

Abstract

Clostridial botulinum neurotoxin (BoNT) causes a neuroparalytic condition recognized as botulism by arresting synaptic vesicle exocytosis. While the crystal structures of full-length BoNT/A and BoNT/B holotoxins are known, the molecular architecture of the five other serotypes remains elusive. Here, we present the structures of BoNT/A and BoNT/E using single-particle electron microscopy

(EM). Labeling of the particles with three different monoclonal antibodies raised against BoNT/E revealed the positions of their epitopes in the EM structure, thereby identifying the three hallmark domains of BoNT (protease, translocation and receptor binding). Correspondingly, these antibodies selectively inhibit BoNT translocation activity as detected using a single-molecule assay. The global structure of BoNT/E is strikingly different from that of BoNT/A despite strong sequence similarity. We postulate that the unique architecture of functionally conserved modules underlies the distinguishing attributes of BoNT/E and contributes to differences with BoNT/A.

Introduction

Botulinum neurotoxin (BoNT), considered the most potent toxin known, causes botulism (1) by selectively inhibiting synaptic vesicle exocytosis (2). This conspicuously specific activity has transformed BoNT into the first bacterial toxin approved by the FDA for treatment of a number diseases characterized by abnormal muscle contraction, a blockbuster cosmeceutical, and a most feared bioweapon (1,3). *Clostridium botulinum* cells produce seven BoNT isoforms designated serotypes A to G (2). All BoNT serotypes are synthesized as a single polypeptide chain with M_r ~150 kDa. This precursor protein is cleaved by a clostridial protease into two polypeptides which remain linked by a disulfide bridge. The mature di-chain toxin consists of a 50 kDa light chain (LC) Zn^{2+}-metalloprotease and a 100 kDa heavy chain (HC). The HC encompasses the translocation domain (TD) (the N-terminal half) and the receptor-binding domain (RBD) (the C-terminal half). BoNT/E is atypical in that it is not activated by proteolytic cleavage in the clostridial cells, thereby requiring unidentified proteases in the host cells to cleave the LC from the HC to achieve full toxicity (4,5).

BoNTs exert their neuroparalytic effect by a multistep mechanism (2,6). RBD-mediated binding to protein and lipid receptors on the cell surface of peripheral nerve endings (7-11) triggers receptor-mediated endocytosis and traffic to the endosomes. The acidic pH of endosomes induces a conformational change of the toxin; the HC inserts into the lipid bilayer and forms a protein-

conducting channel (12,13). The HC channel then translocates the protease domain into the cytoplasm (13) colocalizing with its substrate SNARE (soluble NSF attachment protein receptor) (14-16). Because the SNARE core complex is essential for synaptic vesicle fusion with the presynaptic membrane (14-16), BoNTs efficiently block synaptic vesicle exocytosis.

In contrast to BoNT/A (17), little is known about the molecular architecture of BoNT/E, making it a novel target for structural analysis. Here we report the three-dimensional (3D) structure of BoNT/E holotoxin at ~30 Å resolution as determined by single-particle electron microscopy (EM). Domains of BoNT/E were assigned to the globular features observed in the structure by labeling the toxin with functionally relevant monoclonal antibodies (mAbs). While the individual domains of BoNT/E are similar to those of BoNT/A, their spatial arrangement within the global fold is unique. Analysis of the BoNT/E structure and structure-function correlation studies with mAbs bound to BoNT/A and BoNT/E define previously unrecognized biophysical characteristics that differ between these two BoNT isoforms.

Experimental Procedures

Materials - Unless otherwise specified, all chemicals were purchased from Sigma-Aldrich. Purified native BoNT serotypes A and E holotoxins were from Metabiologics. Di-chain BoNT/E holotoxin was generated by cleavage with trypsin: BoNT/E holotoxin (0.5 mg/mL) was incubated with 0.15 mg/mL trypsin in

20mM HEPES, pH 7.0 for 30 min at 37^{o}C. Thereafter, trypsin was inactivated with 0.25 mg/mL trypsin soybean inhibitor for 15 min at 20^{o}C. Trypsin and trypsin inhibitor were removed by centrifugal filtration on Millipore filters (M_r cutoff 50 kDa).

Cell culture and patch clamp recordings - Excised patches from Neuro 2A cells in the inside-out configuration were used as described (18). Current recordings were obtained under voltage clamp conditions. All experiments were conducted at 22 $\pm$ 2 °C.

Data Analysis - Analysis performed on single bursts of each experimental record. Single channel conductance (γ was calculated from Gaussian fits to current amplitude histograms (18). The total number of opening events (N) analyzed was 84,443. Time course of single channel conductance change for each experiment was calculated from γ of each record, where t = 0 s corresponds to onset of channel activity, and average time course was constructed from the set of individual experiments for a single condition. n denotes the number of different experiments.

Monoclonal Antibody Generation and K_D measurements - Human IgG1/kappa mAbs were isolated from a single chain Fv library generated from a human volunteer immunized with pentavalent BoNT toxoid and displayed on yeast (19) (manuscript in preparation). IgG expression cassettes were constructed from the immunoglobulin heavy and light chain variable region genes of the scFv and used to generate stable CHO cell lines from which the IgG were expressed and purified, exactly as previously described (20). Binding K_Ds were

determined using flow fluorimetry in a KinExA (19). The epitopes of each mAb were determined using yeast displayed BoNT/A or BoNT/E domains as previously described for BoNT/A mAbs. The epitopes and binding K_Ds of these mAbs are summarized in Table 1.

Fab generation - The Pierce ImmunoPure Fab Preparation Kit (44885) was used to generate Fabs. BoNT/A LC Fabs were quality checked using SDS-polyacrylamide gel electrophoresis (SDS-PAGE) prior to the single molecule assays.

Protein Analysis - SDS-PAGE gels (12%) were used to visualize BoNT/A and BoNT/E holotoxins (21). If indicated, loading buffer was supplemented with 100 mM dithiothreitol (DTT) prior to sample addition.

Specimen preparation and electron microscopy - BoNT/A and BoNT/E holotoxin in 0.05% (w/v) dodecylphosphocholine (DPC) and 20 mM HEPES, pH 7.0 were negatively stained with 0.75% (w/v) uranyl formate as described (22). DPC was used to increase the propensity to generate uniform populations of single-particles; in the EM samples, its final concentration is $>10^3$ lower than the cmc, and at best <5% of the BoNT molecule is decorated with DPC molecules (13). BoNT-Fab complexes were prepared by incubating Fab fragments with BoNT holotoxin (2:1 molar ratio) in 0.05% DPC and 20 mM HEPES, pH 7.0 for 24 hr at 4 ^oC prior to negative stain. Images were recorded using a FEI Sphera electron microscope equipped with a LaB_6 filament; operated at an acceleration voltage of 200 KeV. Images were taken at a magnification of 50,000 X; defocus value = -1.5 μm to -1.8 □m. Specimens were imaged at 0° and 60° tilt for 3D

reconstruction; the defocus value for 0° = -1.5 ~ -1.8 μm and 60° tilt = -2.0 ~ -2.2 μm. All images were recorded using SO-163 film with a Kodak D-19 developer at full strength for 12 min at 20 °C.

Image processing - Electron micrographs were digitized with a CoolScan 9000 (Nikon) using a step size 6.35 μm and 3 x 3 pixels were binned so the specimen level pixel size used was 3.75 Å. Projection averages were calculated from windowed small images of 74 x 74 pixels over 10 cycles of K-means classification and multi-reference alignment specifying 50 or 100 classes (two-dimensional only). For 3D reconstructions of BoNT/E, a total of 7,090 particle pairs were interactively selected using WEB display program for SPIDER (23), windowed, and averaged into 50 classes as before. Images of the tilted specimens for each class were used to calculate initial 3D reconstructions of individual classes by back-projection, back-projection refinement, and angular refinement. The final volume obtained by angular refinement with SPIDER was used as the input model for FREALIGN (24); this was used for refinement of orientation parameters of individual particles and for individual image contrast transfer function correction based upon the defocus value. The defocus of each particle was deduced from its position on the micrograph and tilt angles and defocus values determined with CTFTILT (25). Particles selected from tilted and untilted specimens were used for FREALIGN refinement. The final 3D reconstruction was in good agreement with the raw data as the particle images were compared with reprojections from the reconstruction. UCSF Chimera was

used to render BoNT structures (http://www.rbvi.ucsf.edu/chimera/) using PDB accession codes 3BTA (17) and 1T3A (26) for BoNT/A holotoxin and BoNT/E LC.

Results

Modular organization of BoNT/A and BoNT/E holotoxins - BoNT/A and BoNT/E exhibit high sequence similarity at each of their functional domains, with more conservation at the RBD and TD as compared to the LC (Fig. 1A) (27). Because an endogenous clostridial protease cleaves BoNT/A holotoxin between the LC and the HC purified BoNT/A appears as two bands in SDS-PAGE after reduction with DTT (Figs. 1A, 1B). In contrast, purified BoNT/E migrates in SDS-PAGE as a single band even after chemical reduction, consistent with an uncleaved full-length single-chain protein (Figs. 1A, 1B). Highly purified preparations (≥95%) of both BoNT/A and BoNT/E holotoxin proteins were used to conduct further experiments.

Different molecular shapes of BoNT/A and BoNT/E holotoxin - The molecular weight of BoNT is ~150 kDa, a size relatively small to conduct single particle analyses. Therefore, we first examined if BoNT/A, whose crystal structure is known (17), could be visualized by EM after negative staining. BoNT/A particles were monodispersed and homogeneous in size and shape (Fig. 2A). These particle images were subjected to image classification and alignment using multivariate statistics and multireference alignment. Representative class averages shows a butterfly-like particle with dimensions 130 Å x 120 Å. The

particle displays a central elongated domain (30 Å x 120 Å) bounded by a globular domain on either side (Fig. 2B): a double-lobed domain with dimensions 40 Å x 80 Å, and a spherical domain with dimensions of 60 Å x 60 Å. Under our imaging conditions, BoNT/A adopted a single conformation similar to the known crystal structure (17) determined at pH 7.0 (Fig. 2C). The density of TD, consisting of a packed bundle of four α-helices (17,28), emerged as a conspicuous feature in the class averages appearing as the central elongated domain. The overlay of the projection structure obtained by EM (Fig. 2C -left; scale bar = 5 nm) and the known crystal structure (Fig. 2C -middle) provides an unambiguous correspondence of the overall structure (Fig. 2C -right): the elongated TD flanked by the double-lobed RBD and the globular LC. Collectively, these results validate that molecular features of BoNT can be studied by single-particle EM.

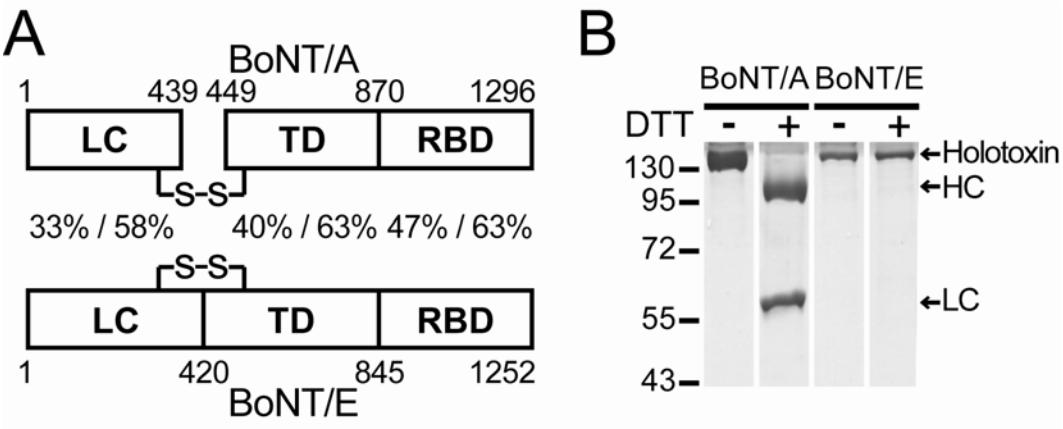

Fig. 1. Modular organization of BoNT/A and BoNT/E holotoxins. *A*. Schematic representation of BoNT/A and /E holotoxins showing domain organization; percent numbers indicate relative identity/similarity. Disulfide bonds in the mature toxins are indicated by –S-S-. *B*. Coomassie blue stained SDS-PAGE analysis; numbers denote M_r standards; DTT (+) (-) indicate presence or absence of dithiothreitol.

Negative stained BoNT/E molecules reveal monomeric particles with shapes distinct from BoNT/A (Fig. 2D). BoNT/E particles appear monodispersed and uniform in size. The particles, however, exhibit a heterogeneous population as demonstrated in the representative class averages obtained from 6,370 particles (Fig. 2E). All class average represents a global bi-lobed structure of BoNT/E with small variation, which we classify into three categories. Type 1 (top panel) is the most prevalent shape (35%), as compared to type 2 (middle-24%), and type 3 (bottom-21%). The relative angle of the two global lobes is different between type 1 and type 2. The small lobe of the type 3 particle is smaller than the small lobes in types 1 and 2 particles. The similarities in structural details between the class averages reveal the overall BoNT/E structure to consist of two lobes of different sizes connected together (Figs. 2D, 2E).

Identification and biophysical characterization of BoNT domain-specific monoclonal antibodies- To gain molecular insights into the EM structure of BoNTs, we explored functionally relevant molecular probes that can be used to label the individual domains. We identified four antibodies that bind with high affinity to individual modules of BoNT/A or BoNT/E (Table 1). First, we tested if Fab fragments derived from these antibodies have any functional effect on the toxins, specifically, on the translocation activity of BoNTs across neuronal membranes. Previous work led to the development of a single-molecule assay that electrophysiologically monitors translocation of BoNT LC by the BoNT HC channel in excised membrane patches from Neuro 2A neuroblastoma cells (18)

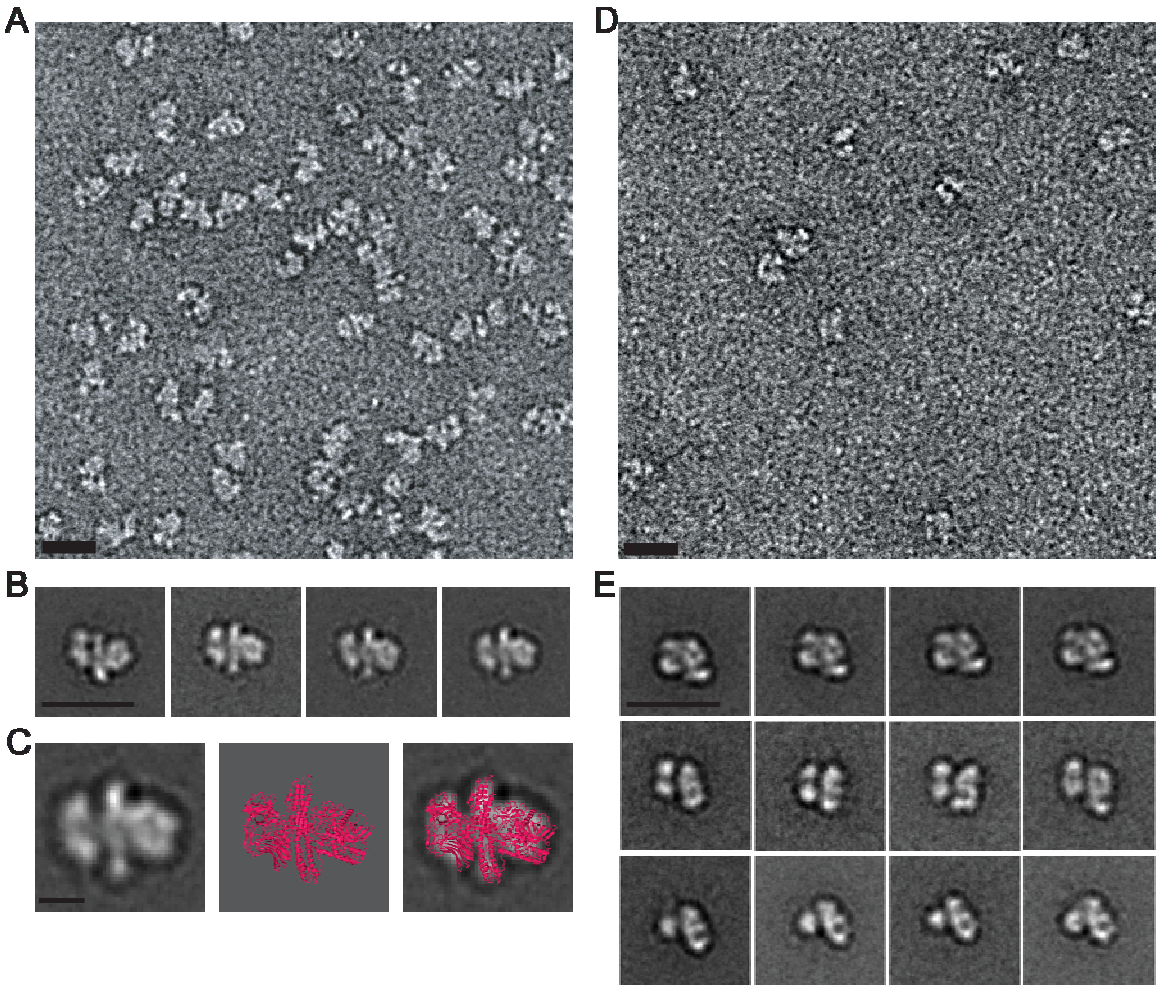

Fig. 2. Single-particle electron microscopy of BoNT/A and BoNT/E holotoxins. *A* and *B.* Image area of BoNT/A negatively stained with uranyl formate (A) and representative class averages (B) corresponding to 93% of all particle images (N=7,058) (bottom). Scale bar = 20 nm. *C.* Left, representative class average. Middle, BoNT/A crystal structure (17); ribbon representation of the Cα backbone (PDB accession code 3BTA). Right, manually docked superposition of crystal structure (17) over the class average. Scale bar = 5 nm. *D* and *E.* Image area of negatively stained BoNT/E (D) and representative class averages of particle images (E). Type 1 (top), 2 (middle) and 3 (bottom) represent different particle classes visualized on the grid from a total number of particles (N=6,370). Brackets on right panels illustrate the interpretation of the small lobe (*) and large lobe (**). Scale bar = 20 nm.

(Fig. 3). BoNT LC translocation requires conditions that emulate the pH and redox gradient across endosomes (18). Initially, the protein-conducting channel is occupied by the partially unfolded LC and by Na^+ present in the solutions bathing the membrane. The LC partially occludes the permeation pathway for the measured conductive species (Na^+), detected as a low γ. After translocation is complete the channel is unoccluded attaining a higher, constant $\tilde{\gamma}$ The entire process is recorded in the control experiments; representative single channel currents of BoNT/A and BoNT/E obtained at the beginning (10 s) and the end (1000s) of LC translocation are displayed in the top two panels of Fig. 3A. The characteristic fast transitions between the closed and open states are clearly discernible. The amplitude of γ is determined from the fluctuations between the closed and open states. The average time course of change of γ for nine experiments is shown in Fig 3B. BoNT channel activity is initially measured at γ = 12 pS (Figs. 3A, 3B). The HC channel is occluded by the LC during transit, diminishing its conductance (13,18); the reduced γ and flickery transitions between the open and closed state are characteristic of blocked channels. γ increases over time to a stable endpoint γ of 66 pS (Figs. 3A right panel, 3B), characteristic of both BoNT/A and BoNT/E unoccluded HC channels (18) (Fig. 3B).

We analyzed the effects of mAbs by pre-incubating BoNTs with Fabs for 1 h at pH 7 prior to the translocation assay. As illustrated in a representative

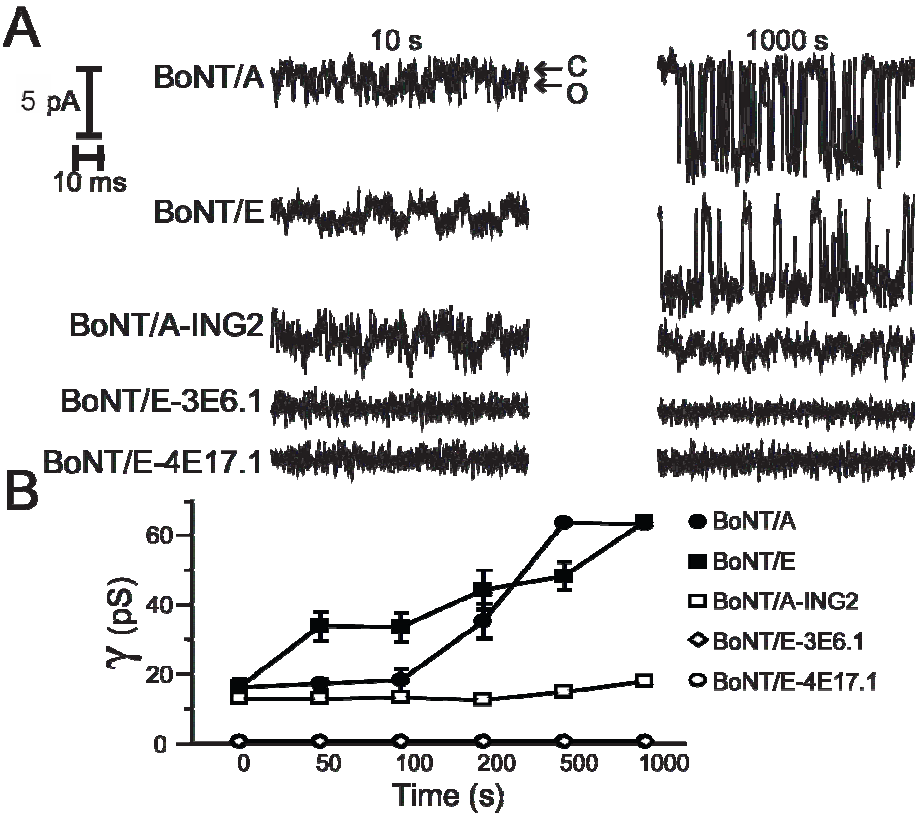

Fig. 3. BoNT LC translocation arrest by domain-specific Fab fragments. *A.* High-gain and fast-time resolution of BoNT single channel currents recorded at -100 mV and the indicated times on Neuro 2A cells. C and O denote the closed and open states. Segments of representative current recordings are displayed for each experimental condition. Unmodified BoNT/A holotoxin, unmodified BoNT/E holotoxin, and BoNT/A-ING2 complex channel activity begins 20 min, 9 min and 7 min after GΩ seal formation, respectively; t = 0 s corresponds to onset of channel activity. BoNT/E-3E6.1 complex and BoNT/E-4E17.1 complex do not exhibit channel activity; t = 0 s corresponds to start of experiment. *B.* Average time course of γ change for BoNT/A holotoxin (n=6), BoNT/E holotoxin (n=3), BoNT/A-ING2 complex (n=5), BoNT/E-3E6.1 complex (n=24), and BoNT/E-4E17.1 complex (n=24) (average N per data point = 4,690 for each experimental set for which channel activity was monitored).

experiment, a Fab specific for BoNT/A LC (ING2, Table 1) induces persistent block of the HC channel (Fig. 3A). Analysis of five experiments shows that the Fab ING2 allows channel formation, detected within minutes of patch formation at γ = 21 pS (Figs. 3A, 3B). Thus, ING2 arrests translocation after initiation of LC entry into the HC channel (18).

Next, we asked if mAb 3E6.1 or mAb 4E17.1, selective for BoNT/E TD (Table 1) affect the translocation step. The epitope of 3E6.1 is located in the region demarcated by residues 573-579 which, by sequence similarity to BoNT/A, maps to an extended region parallel to the helical bundle of the TD (17). In contrast, the epitope of 4E17.1 has been mapped to the loop region at one end of the BoNT/E TD encompassing residues 752-759. Preincubation of BoNT/E with 3E6.1 or 4E17.1 results in no channel activity monitored over the minimum experimental time of 30 min (n=24 experiments for each condition) (Figs. 3A, 3B). Thus, these Fab fragments bind to the BoNT/E TD with sub nM affinity (Table 1), precluding its insertion into the membrane and selectively disrupting the BoNT translocation activity.

BoNT domain labeling by monoclonal antibodies - A complex formed of BoNT/A holotoxin and ING2 Fab was imaged by negative stain EM and further analyzed by image classification and averaging. Representative class averages of the BoNT/A-ING2 complex are shown in Fig. 4A. By comparing the structure of the complex (Fig. 4A -middle panels) with BoNT/A alone (Fig. 4A -left panel), we infer that the extra density appearing on the BoNT/A-Fab complex structure corresponds to the bound Fab. A schematic diagram is shown in the right panel

Table 1. Specificity of mAbs against BoNT/A or BoNT/E

Antibody	BoNT	Epitope (Residue Number)	K_D (pM)
ING2	A	LC	9.6
4E16.1	E	LC (around 142)	3.4
4E17.1	E	TD (752-759)	240
3E6.1	E	TD (573-579)	40

of Fig. 4A which depicts the profile of BoNT/A in white (designated by *) and the Fab outline in grey (indicated with an arrow). At the resolution of our imaging, the binding of the Fab to BoNT/A shows minimal distortion of the native conformation of the toxin. The recognizable silhouette of the Fab fragment in the complex allows us to unambiguously assign the location of the LC in the holotoxin structure.

Next, we labeled BoNT/E with the Fabs derived from anti BoNT/E antibodies (Table 1). The epitope of mAb 4E16.1 is centered on the surface exposed residue 142 in the LC of BoNT/E (Table 1). When compared with the structure of BoNT/E alone, the particles of BoNT/E-4E16.1 Fab complex (Fig. 4B -middle panels) exhibit an extra density attached to the intermediate protrusion of the large lobe of BoNT/E (Fig. 4B -left panel, also see scheme in right panel). Similar to ING2 Fab, 4E16.1 Fab binds to the particle without creating any distortion to the overall structure, thus unambiguously assigning the location of the LC epitope (residue 142) in BoNT/E structure.

Unique identification of individual domains of the BoNT/E holotoxin molecule was further ensured by using TD specific mAbs. In the structure of the BoNT/E-Fab 4E17.1 complex (Fig. 4C)**,** the BoNT/E and the Fab are easily discerned. The extra density attached to the tip of the large lobe on the BoNT/E-Fab complex structure corresponds to the bound Fab, as shown in the schematic of Fig. 4C. Although 4E17.1 Fab blocks the translocation activity of the toxin, the overall structure of BoNT/E was not affected by its binding. The particles of the BoNT/E-Fab 3E6.1 complex display a drastically different profile from that of

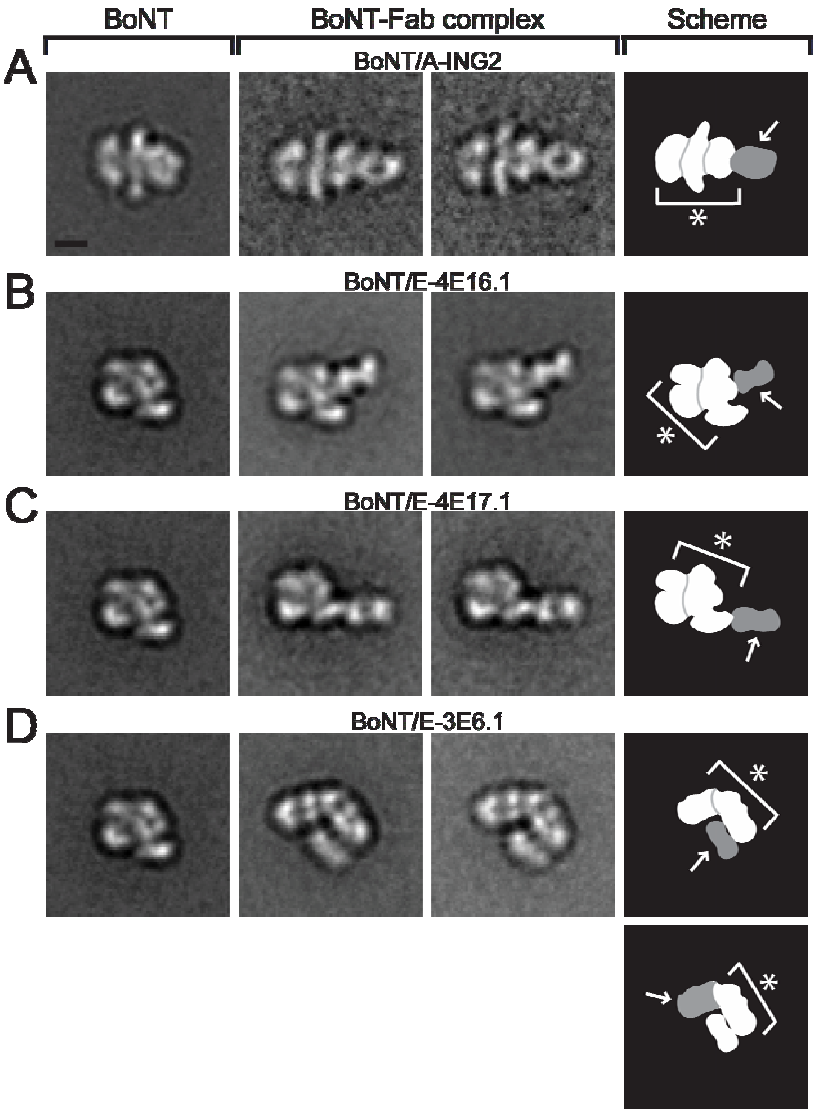

Fig. 4. BoNT domain identification by Fabs. *A.* Left, representative class average of BoNT/A holotoxin. Scale bar = 5 nm. Middle, representative class averages of the BoNT/A-ING-2 complex (N=4,567). Right, schematic diagram of protein complex; BoNT/A is designated by * and the Fab is indicated with an arrow. *B.* Left, representative class averages of BoNT/E. Middle, representative class averages of the BoNT/E-4E16.1 complex (N=5,807). Right, schematic diagram of protein complex. *C.* Left, representative class averages of BoNT/E. Middle, representative class averages of the BoNT/E-4E17.1 complex (N=3,388). Right, schematic diagram of protein complex. *D.* Left, representative class averages of BoNT/E. Middle, representative class averages of the BoNT/E-3E6.1 complex (N=2,951). Right, schematic diagram of protein complex with alternative interpretation depicted in bottom panel.

BoNT/E (Fig. 4D -left panel), as reflected in the representative particle averages shown in Fig. 4D -middle panels. Given the size and shape of the smaller density appearing in the center of the BoNT/E-Fab complex structure, we infer it corresponds to the bound Fab with the L-shaped particle representing BoNT/E, as depicted on the right panel of Fig. 4D. The result also suggests that upon binding to its epitope in the TD of BoNT/E, 3E6.1 Fab fragment blocks translocation activity of the toxin by severely distorting the structure of BoNT/E (Figs. 3A, 3B, 4D). It is conceivable that BoNT/E is minimally distorted by the 3E6.1 Fab. This alternative notion does not alter our interpretation about the position of the epitope of 3E6.1 as part of the large lobe. This model is illustrated in the bottom panel of Fig. 4D, in which the arrow indicates the Fab and the asterisk the large lobe. Note that the white profile depicting the alternative interpretation for BoNT/E resembles a mirror image of the Type 2 particle in Figure 2. Collectively, these Fab labeling experiments unambiguously assign the location of the TD and LC and suggest that the large lobe consists of TD and LC. The remaining small lobe, therefore, consists of the RBD.

3D structure of BoNT/E holotoxin - The three dimensional structure of BoNT/E particle was calculated by random conical tilt reconstruction. For this purpose, negative stained particle images of BoNT/E were taken as tilt pairs (0^o and 60^o). Untilted particle images were subjected to multivariate statistical analysis, multi-reference alignment and classification into 50 classes. A well defined class average from type 1 particles was chosen to further calculate the 3D structure using the corresponding tilted particle images. The 3D structure of

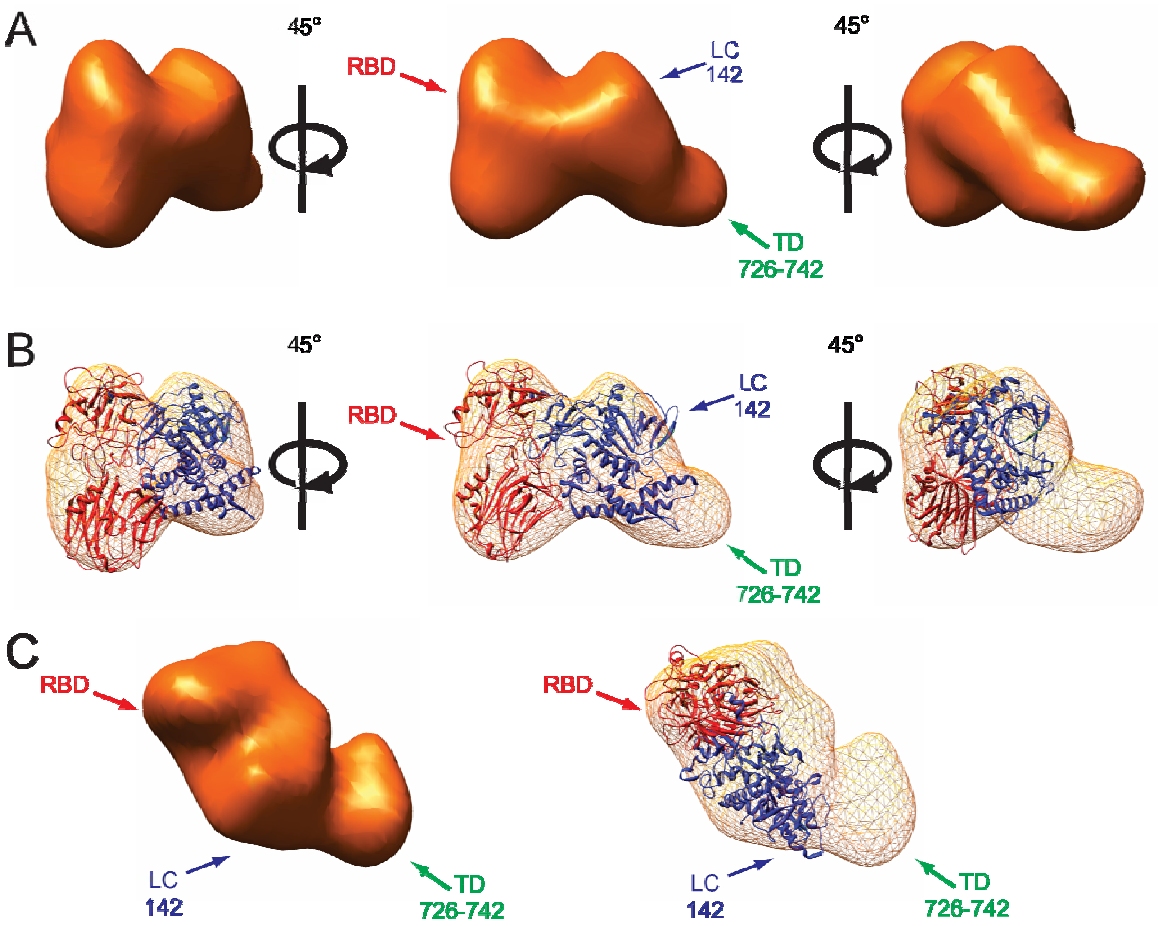

Fig. 5. 3D reconstruction of single-chain BoNT/E holotoxin and placement of crystal structure into the density map. *A.* 3D map of BoNT/E holotoxin is shown from three different angles. RBD is the small lobe; large lobe consists of LC and TD. Positions of the epitopes of the monoclonal antibodies used for labeling experiments are indicated by arrows. The precise residues of the epitopes are indicated as numbers (Table 1). *B.* Placement of known crystal structures into the EM density map. The PDB accession codes for the crystal structures used are: RBD of BoNT/A (3BTA; red) and LC of BoNT/E (1T3A; blue). *C.* View from a different angle.

BoNT/E after FREALIGN refinement is shown in Fig. 5A. The structure of BoNT/E holotoxin was strikingly different from that of BoNT/A. The small lobe and the large lobe are mostly separated except at the junction point. Within the 3D structure of BoNT/E, the central elongated domain representing the unique feature of TD in the BoNT/A, was less defined. Thus, in BoNT/E the TD is closely associated to either the LC or the RBD.

The 3D reconstruction of different class averages (type 1 - 3) produced similar 3D structures (data not shown). We conjecture that the subtle conformational variability represented in the class averages reflects the conformational flexibility of the BoNT/E; this interpretation is consistent with the widely recognized difficulty to generate quality crystals of BoNT/E. A more interesting inference is that it reflects the conformational plasticity BoNT/E exposing different conformational states related to its function. Based upon the Fourier shell correlation (FSC), the resolution of the final density map was estimated to be 24 Å with the FSC = 0.143 criterion and 30 Å with the more conservative FSC = 0.5 criterion (29).

The domain assignment derived from the analysis of BoNT/E in complex with domain-specific mAbs allows further interpretation of the 3D structure. The crystal structures of the LC of BoNT/E (26) and of the RBD of BoNT/A (17) were placed into the EM density map of BoNT/E (Figs. 5B, 5C). The large lobe consists of LC and TD; within the large lobe, the location of LC is restricted to the proximity of the binding site of 4E16.1 Fab. The crystal structure of LC (blue) was

therefore placed such that the epitope of 4E16.1 aligns with the region on the density map corresponding to the Fab binding site. Because the 4E17.1 Fab recognizes the TD and binds to the tip of the large lobe, we inferred that the small lobe represents the RBD and placed the crystal structure of RBD of BoNT/A, accordingly. The size and shape of the crystal structure of the RBD (red) is consistent with the density of the small lobe and reveals that the RBD for BoNT/E is well defined as a separate module in the tri-modular arrangement of the holotoxin. A large unaccounted density was identified which includes the tip of the large lobe where the 4E17.1 Fab binds. We interpret that this unaccounted density corresponds to the TD, apparently bent at its central region where it presumably accommodates the LC.

Discussion

Our data highlight for the first time the global structure of BoNT/E. The 3D reconstruction and the manual docking of the crystal structures of the isolated LC and RBD domains outline the novel architecture of BoNT/E, and the different arrangement of domains within the tri-modular holotoxin with respect to BoNT/A (17) and BoNT/B (28). These structural features imply an intricate association of the LC and the TD thereby constraining the global fold. The LC cargo appears closely apposed to the TD channel, consistent with the continuity of the polypeptide in the single-chain BoNT/E. Furthermore, the distance between LC and RBD in BoNT/E is shorter (Fig. 5C) compared to BoNT/A (17) (Fig. 2) or

BoNT/B (28). The structure of BoNT/E is also different from that of the closely related *Clostridial* tetanus toxin (TeNT) (27) obtained by electron crystallography (30).

The structures of the seven BoNT LCs have been solved at atomic resolution (17,26,28,31-37). They share a similar 3D structure irrespective of the distinct SNARE substrate specificity, and are structurally similar to the Zn^{2+}-metalloprotease thermolysin. High resolution structures for the RBD of BoNT/A (17), BoNT/B (38,39), and TeNT (40,41) are available; these structures have provided insights into the detailed binding of their respective neuronal protein receptor and ganglioside co-receptor, particularly for BoNT/B (38,39). Overall, the RBD and the protease domain behave as independently folded units. In contrast, this assertion cannot be extended to the TD given that no crystal structure is available for the isolated TD of any of the *Clostridial* neurotoxins. Remarkably, it is the TD of BoNT/E the module that exhibits the strongest disparity (Fig. 5). To the extent that our analysis is restricted to intermediate resolution, we suggest that the distinctively different global architectures of BoNT/A and BoNT/E (Figs. 2, 4, 5) imply that the holotoxins within cells are subjected to different processing which, ultimately, determine the fate of the proteases (21,42,43) and the duration of their proteolytic consequences on their SNARE substrates (44-46).

Interesting inferences about the functional disparities between BoNT/A and BoNT/E can be drawn from our analysis. Intriguingly, cleavage of the same substrate by BoNT/A and BoNT/E produces the longest (several months) and the

shortest (few days) duration of neurotransmitter blockade. Several factors contribute to this discrepant effect. The two serotypes cleave the SNARE component SNAP-25 (synaptosome-associated protein of 25 kDa) at different sites near the C-terminus (47) producing SNAP-25 fragments of different size which inhibit exocytosis by competing for SNARE complex assembly (44-46). In addition, the sub-cellular distribution of the two toxins is known to be different. BoNT/A LC co-localizes with the truncated SNAP-25 product at the plasma membrane, whereas BoNT/E appears to be diffusely distributed in the cytoplasm (48). Differences in the intricacies of BoNTs intracellular trafficking, modification and degradation have been reported (42,43), which may be accounted for in part by the fact that individual modules in BoNT/A are more segregated rather than bundled as resolved in BoNT/E. These functional and structural differences between BoNT/A and BoNT/E highlight the elegance of BoNT molecular design, which appears to exploit the host cellular systems for its own function at each step of the intoxication process.

The BoNT/E and BoNT/A structures provide insights into the translocation function of the toxin. The channel activity of BoNT/E and BoNT/A is very similar (Fig. 3) (18), suggesting that the channel entity acts as a universal transporter of proteins (49). The strong sequence similarity within the TD between the two serotypes contrasted with the ambiguous structural alignment highlight the inherent flexibility of the TD domain. Notable is the tight correlation between the mAbs used to identify domains on the structure (Fig. 4) and their selective disruption of BoNT translocation activity in the electrophysiological assay (Fig. 3).

The mAbs which recognize unique regions of the TD preclude the insertion of the TD into the membrane and the ensued formation of channels. ING2, a LC/A specific antibody, does not inhibit HC channel insertion; however, it arrests translocation after initiation of LC entry into the HC channel. The ING2 Fab locks the channel and the LC in a translocating conformation that is irreversibly incomplete (18). Beyond their application for domain assignment on the EM structure of BoNT/E (Fig. 4), these Fab fragments emerge as powerful tools to gain insights into the mechanism of LC translocation. It will be interesting to visualize structural changes of the interacting HC channel with the LC cargo under conditions that imitate those across endosomes by pursuing the strategy outlined here in combination with a set of serotype-specific (BoNT/A or BoNT/E) and domain-specific (LC or TD) (Figs. 2, 4) antibodies.

Acknowledgements

We thank H. Viadiu, J. Santos, M. Oblatt-Montal, L. Koriazova and members of the Montal lab for perceptive comments. This work was supported by the Pacific Southwest Regional Center of Excellence (NIH AI065359 to M.M), NIAID/NIH U01 AI056493 (J.D.M.), and Defense Threat Reduction Agency contract HDTRA1-07-C-0030 (J.D.M.). We acknowledge the UCSD Cryo-Electron Microscopy Facility which is supported by NIH grants 1S10RR20016 and GM033050 to Timothy S. Baker and a gift from the Agouron Institute to UCSD. Structural analysis software was provided through SBgrid.

Chapter 4, in full, is a reprint of the material as it will appear in the Journal of Biological Chemistry. Fischer, Audrey; Garcia-Rodriguez, Consuelo; Geren, Isin; Lou, Jianlong; Marks, James D; Nakagawa, Terunaga and Montal, Maurice, American Society for Biochemistry and Molecular Biology , 2007. The dissertation author was the primary investigator and an author of this paper.

References

1. Arnon, S. S., et al. (2001) *JAMA* **285**(8), 1059-1070

2. Schiavo, G., Matteoli, M., and Montecucco, C. (2000) *Physiol Rev* **80**(2), 717-766

3. Davletov, B., Bajohrs, M., and Binz, T. (2005) *Trends Neurosci* **28**(8), 446-452

4. Sathyamoorthy, V., and DasGupta, B. R. (1985) *J Biol Chem* **260**(19), 10461-10466

5. Schiavo, G., Rossetto, O., Catsicas, S., Polverino de Laureto, P., DasGupta, B. R., Benfenati, F., and Montecucco, C. (1993) *J Biol Chem* **268**(32), 23784-23787

6. Simpson, L. L. (2004) *Annu Rev Pharmacol Toxicol* **44**, 167-193

7. Dong, M., Richards, D. A., Goodnough, M. C., Tepp, W. H., Johnson, E. A., and Chapman, E. R. (2003) *J Cell Biol* **162**(7), 1293-1303

8. Dong, M., Yeh, F., Tepp, W. H., Dean, C., Johnson, E. A., Janz, R., and Chapman, E. R. (2006) *Science* **312**(5773), 592-596

9. Mahrhold, S., Rummel, A., Bigalke, H., Davletov, B., and Binz, T. (2006) *FEBS Lett* **580**(8), 2011-2014

10. Nishiki, T., Tokuyama, Y., Kamata, Y., Nemoto, Y., Yoshida, A., Sekiguchi, M., Takahashi, M., and Kozaki, S. (1996) *Neurosci Lett* **208**(2), 105-108

11. Rummel, A., Karnath, T., Henke, T., Bigalke, H., and Binz, T. (2004) *J Biol Chem* **279**(29), 30865-30870

12. Hoch, D. H., Romero-Mira, M., Ehrlich, B. E., Finkelstein, A., DasGupta, B. R., and Simpson, L. L. (1985) *Proc Natl Acad Sci U S A* **82**(6), 1692-1696.

13. Koriazova, L. K., and Montal, M. (2003) *Nat Struct Biol* **10**(1), 13-18

14. Jahn, R., and Scheller, R. H. (2006) *Nat Rev Mol Cell Biol* **7**(9), 631-643

15. Sutton, R. B., Fasshauer, D., Jahn, R., and Brunger, A. T. (1998) *Nature* **395**(6700), 347-353

16. Weber, T., Zemelman, B. V., McNew, J. A., Westermann, B., Gmachl, M., Parlati, F., Söllner, T. H., and Rothman, J. E. (1998) *Cell* **92**(6), 759-772

17. Lacy, D. B., Tepp, W., Cohen, A. C., DasGupta, B. R., and Stevens, R. C. (1998) *Nat Struct Biol* **5**(10), 898-902.

18. Fischer, A., and Montal, M. (2007) *Proc Natl Acad Sci U S A* **104**(25), 10447-10452

19. Levy, R., Forsyth, C. M., LaPorte, S. L., Geren, I. N., Smith, L. A., and Marks, J. D. (2007) *J Mol Biol* **365**(1), 196-210

20. Nowakowski, A., et al. (2002) *Proc Natl Acad Sci U S A* **99**(17), 11346-11350
21. Ferrer-Montiel, A. V., Canaves, J. M., DasGupta, B. R., Wilson, M. C., and Montal, M. (1996) *J Biol Chem* **271**(31), 18322-18325

22. Ohi, M., Li, Y., Cheng, Y., and Walz, T. (2004) *Biol Proced Online* **6**, 23-34

23. Frank, J., Radermacher, M., Penczek, P., Zhu, J., Li, Y., Ladjadj, M., and Leith, A. (1996) *J Struct Biol* **116**(1), 190-199

24. Stewart, A., and Grigorieff, N. (2004) *Ultramicroscopy* **102**(1), 67-84

25. Mindell, J. A., and Grigorieff, N. (2003) *J Struct Biol* **142**(3), 334-347

26. Agarwal, R., Eswaramoorthy, S., Kumaran, D., Binz, T., and Swaminathan, S. (2004) *Biochemistry* **43**(21), 6637-6644

27. Lacy, D. B., and Stevens, R. C. (1999) *J Mol Biol* **291**(5), 1091-1104.

28. Swaminathan, S., and Eswaramoorthy, S. (2000) *Nat Struct Biol* **7**(8), 693-699.

29. Rosenthal, P. B., and Henderson, R. (2003) *J Mol Biol* **333**(4), 721-745

30. Robinson, J. P., Schmid, M. F., Morgan, D. G., and Chiu, W. (1988) *J Mol Biol* **200**(2), 367-375

31. Agarwal, R., Binz, T., and Swaminathan, S. (2005) *Biochemistry* **44**(35), 11758-11765

32. Arndt, J. W., Chai, Q., Christian, T., and Stevens, R. C. (2006) *Biochemistry* **45**(10), 3255-3262

33. Arndt, J. W., Yu, W., Bi, F., and Stevens, R. C. (2005) *Biochemistry* **44**(28), 9574-9580

34. Breidenbach, M. A., and Brunger, A. T. (2005) *Biochemistry* **44**(20), 7450-7457

35. Breidenbach, M. A., and Brunger, A. T. (2004) *Nature* **432**(7019), 925-929

36. Rao, K. N., Kumaran, D., Binz, T., and Swaminathan, S. (2005) *Toxicon* **45**(7), 929-939

37. Jin, R., Sikorra, S., Stegmann, C. M., Pich, A., Binz, T., and Brunger, A. T. (2007) *Biochemistry*

38. Jin, R., Rummel, A., Binz, T., and Brunger, A. T. (2006) *Nature* **444**(7122), 1092-1095

39. Chai, Q., Arndt, J. W., Dong, M., Tepp, W. H., Johnson, E. A., Chapman, E. R., and Stevens, R. C. (2006) *Nature* **444**(7122), 1096-1100

40. Jayaraman, S., Eswaramoorthy, S., Kumaran, D., and Swaminathan, S. (2005) *Proteins* **61**(2), 288-295

41. Fotinou, C., Emsley, P., Black, I., Ando, H., Ishida, H., Kiso, M., Sinha, K. A., Fairweather, N. F., and Isaacs, N. W. (2001) *J Biol Chem* **276**(34), 32274-32281

42. Rickman, C., Meunier, F. A., Binz, T., and Davletov, B. (2004) *J Biol Chem* **279**(1), 644-651

43. Verderio, C., et al. (2007) *Traffic* **8**(2), 142-153

44. Ferrer-Montiel, A. V., Gutiérrez, L. M., Apland, J. P., Canaves, J. M., Gil, A., Viniegra, S., Biser, J. A., Adler, M., and Montal, M. (1998) *FEBS Lett* **435**(1), 84-88

45. Bajohrs, M., Rickman, C., Binz, T., and Davletov, B. (2004) *EMBO Rep* **5**(11), 1090-1095

46. Keller, J. E., and Neale, E. A. (2001) *J Biol Chem* **276**(16), 13476-13482

47. Vaidyanathan, V. V., Yoshino, K., Jahnz, M., Dorries, C., Bade, S., Nauenburg, S., Niemann, H., and Binz, T. (1999) *J Neurochem* **72**(1), 327-337.

48. Fernandez-Salas, E., et al. (2004) *Proc Natl Acad Sci U S A* **101**(9), 3208-3213

49. Bade, S., Rummel, A., Reisinger, C., Karnath, T., Ahnert-Hilger, G., Bigalke, H., and Binz, T. (2004) *J Neurochem* **91**(6), 1461-1472

Footnotes

The abbreviations used are: 3D, three-dimensional; γ, single channel conductance; BoNT, botulinum neurotoxin; DTT, dithiothreitol; EM, electron microscopy; LC, light chain; HC, heavy chain; mAb, monoclonal antibody; RBD, receptor binding domain; SNAP-25, synaptosome-associated protein of 25 kDa; SDS-PAGE, SDS-polyacrylamide gel electrophoresis; SNARE, soluble NSF attachment protein receptor; TD, translocation domain.

Chapter 5

Botulinum Neurotoxin Heavy Chain Belt as an Intramolecular Chaperone for the Light Chain

OPEN ACCESS Freely available online

PLoS PATHOGENS

Opinion

Botulinum Neurotoxin Heavy Chain Belt as an Intramolecular Chaperone for the Light Chain

Axel T. Brunger*, Mark A. Breidenbach, Rongsheng Jin, Audrey Fischer, Jose S. Santos, Mauricio Montal*

Background

Botulism is a neuroparalytic illness caused by botulinum neurotoxin (BoNT). Seven BoNT serotypes (designated as A to G) are produced by *Clostridium botulinum*, a spore-forming, obligate anaerobic bacterium. BoNT, widely considered the most potent toxin known and a major bioweapon [1], is a potent blocker of synaptic transmission in peripheral cholinergic nervous system synapses, thereby causing paralysis. Based on its exquisitely powerful neuroparalytic activity, BoNT has gained tremendous popularity in the past few years since becoming the first biological toxin (BoNT serotype A) to receive US Food and Drug Administration approval for the treatment of human disease [2].

Biochemically, BoNTs are synthesized as single polypeptide chains and then cleaved by bacterial proteases into a di-chain molecule linked by a disulfide bond: an ~50-kDa light chain (LC) and an ~100-kDa heavy chain (HC). Structurally, BoNTs encompass three modules [3–6]: the N-terminal LC is a metalloprotease, whereas the HC comprises the translocation domain (the N-terminal segment) and the receptor-binding domain (the C-terminal segment). The modular architecture of the neurotoxin is clearly visible in the crystal structures of BoNT/A [4] (Figure 1A) and BoNT/B [6]. All seven BoNT serotypes exhibit significant amino acid sequence conservation [5], although all are antigenically distinct.

It is generally agreed that BoNTs exert their neurotoxic effect by a four-step mechanism [3,7] that involves (1) binding to high-affinity receptors on peripheral nerve endings, (2) receptor-mediated endocytosis, (3) LC translocation across endosomal membranes into the cytosol upon exposure to endosomal pH, and (4) proteolytic degradation of target. The BoNT LCs are sequence-specific endopeptidases that cleave SNARE (soluble N-ethylmaleimide-sensitive factor attachment protein receptor) proteins. SNAREs form a complex that mediates synaptic vesicle fusion [8–10]. Accordingly, SNARE proteolysis destabilizes or prevents full assembly of the SNARE core complex, abrogating fusion of synaptic vesicles with the plasma membrane, thereby aborting neurotransmitter release [3,11]. BoNT serotypes A, E, and C all cleave the plasma membrane–associated protein SNAP-25 (synaptosome-associated protein of 25 kDa), and serotype C also cleaves the plasma membrane–associated SNARE syntaxin. In contrast, BoNT/B, D, F, and G all proteolyze synaptobrevin, a synaptic vesicle–associated membrane protein, also known as VAMP, at unique sites [3]. The active site region of the BoNT LCs shares structural similarity to the Zn^{2+}-metalloprotease thermolysin [4,6,12–17]. In contrast to other Zn^{2+}-proteases, the BoNTs require an extended enzyme-substrate interface for optimal catalytic efficiency [18–20]. Indeed, the X-ray structure of BoNT/A-LC in complex with sn2 [16]—the C-terminal residues 141–204 of BoNT/A substrate SNAP-25—revealed an extensive array of substrate binding sites distant from the active site (exosites) that orient the substrate onto the vicinity of the active site and determine the target specificity [16,21].

A key step for intoxication is the translocation of endocytosed toxin across intracellular membranes to reach its cytosolic targets [3]. The HC likely acts as both a channel and a transmembrane chaperone for the LC protease to ensure a translocation-competent conformation during transit from acidic endosomes into the cytosol [22–24]. The details of the translocation process are largely unknown. However, available crystal structures of BoNT/A [4] and BoNT/B [6] holotoxins and of BoNT/A-LC in complex with sn2 [16] provide illuminating clues about possible mechanisms, which we consider next.

The so-called translocation domain belt is a most intriguing structural feature in the crystal structures of both BoNT/A [4] and BoNT/B [6]: It is a loop in a mostly extended conformation (consisting of residues 492–545 for BoNT/A, and 481–532 for BoNT/B) that wraps around the catalytic domain in the structures solved at pH 7.0 and 6.0, respectively. The active site of the LC is buried ~20 Å deep in the protein and is accessible through a negatively charged crevice, which may be partially occluded by the belt in the unreduced holotoxin. The belt is highlighted in magenta on

Editor: Marianne Manchester, The Scripps Research Institute, United States of America

Citation: Brunger AT, Breidenbach MA, Jin R, Fischer A, Santos JS, et al. (2007) Botulinum neurotoxin heavy chain belt as an intramolecular chaperone for the light chain. PLoS Pathog 3(9): e113. doi:10.1371/journal.ppat.0020113

Abbreviations: α-LP, α-lytic protease; BoNT, botulinum neurotoxin; HC, heavy chain; IUP, intrinsically unstructured protein; LC, light chain; SNAP, synaptosome-associated protein; SNARE, soluble N-ethylmaleimide-sensitive factor attachment protein receptor

Axel T. Brunger, Mark A. Breidenbach, and Rongsheng Jin are with the Departments of Molecular and Cellular Physiology, Neurology and Neurological Science, Structural Biology, and Stanford Synchrotron Radiation Laboratory, Stanford University, Stanford, California, United States of America, and the Howard Hughes Medical Institute, Stanford, California, United States of America. Mark A. Breidenbach is currently with the Department of Chemistry, University of California, Berkeley, California, United States of America. Audrey Fischer, Jose S. Santos, and Mauricio Montal are with the Section of Neurobiology, University of California San Diego, La Jolla, California, United States of America.

* To whom correspondence should be addressed. E-mail: brunger@stanford.edu (ATB), mmontal@ucsd.edu (MM)

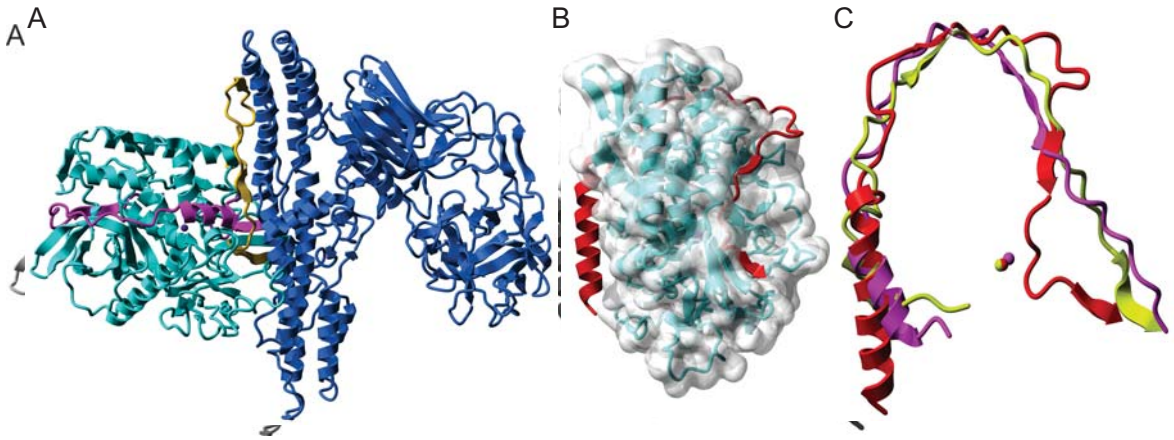

doi:10.1371/journal.ppat.0020113.g001

Figure 1. Structures of BoNT/A Holotoxin, BoNT/A LC-sn2 Complex, and Overlay of sn2 Segment with Belt Regions of BoNT/A and BoNT/B

(A) Structure of BoNT/A. The Cα backbone of the LC (left) is represented as cyan ribbons; the purple sphere highlights the catalytic Zn^{2+} at the protease active site. The HC belt segment encompassing residues 492–545 is displayed in magenta and the 449–491 region in gold. The HC is depicted in blue, in which the helical module (middle) is the translocation domain, and the two sub-domains consisting primarily of β-strands constitute the receptor-binding domain (right).

(B) Structure of BoNT/A-LC in complex with the sn2 segment of SNAP-25 [16]. The Cα backbone of the LC is represented as cyan ribbons and its molecular surface in transparent grey. The sn2 segment is depicted in red and the catalytic Zn^{2+} at the active site as a purple sphere.

(C) Superposition of the structures of the sn2 segment in complex with the LC/A, the HC belt of BoNT/A, and the HC belt of BoNT/B. LC removed for display. For the superposition, the backbone atoms of the LCs were used for the best fit between the structures. sn2 segment depicted in red; overlay of the Cα backbone of BoNT/A [4] and BoNT/B [6] belts represented as magenta and lime ribbons. Spheres represent the catalytic Zn^{2+} at the active site of BoNT/A (red and magenta) and BoNT/B (lime). All images were rendered with YASARA [40].

the structure of the holotoxin/A [4] displayed in Figure 1A. In addition, there is a second unstructured loop encompassing residues 449–491 for BoNT/A; this segment, depicted in gold, is partially apposed to the LC, perpendicular to the belt, and is parallel to the long helices of the translocation domain. The structure of the BoNT/A-LC complex with the sn2 segment [16] is shown in Figure 1B. Figure 1C displays a superposition of the Cα positions of the structures of the BoNT/A-LC complex with the sn2 segment (red), the HC belt of BoNT/A (magenta), and the HC belt of BoNT/B (lime). The belt of BoNT/A is more distant to the catalytic Zn^{2+} (distance between M^{530} and Zn^{2+} is ~15 Å) than the cognate substrate (distance between Q^{197} and Zn^{2+} is ~7 Å). Note the remarkable structural similarity between sn2 and the belt in the absence of stringent sequence similarity [5,6]. This is relevant given the low sequence similarity (24%) of the belts among the seven BoNT serotypes and the related clostridial toxin, tetanus [5,25].

What is the role of this belt?

Hypothesis

We propose that the belt region of the BoNT HC is a surrogate pseudosubstrate inhibitor of the LC protease and acts as a chaperone during translocation across the endosomal membrane into the cytosol. The key points are: (1) The intrinsically unstructured sn2 fragment of SNAP-25 [16,26] adopts partial secondary structural elements upon binding to the LC in the binary complex crystal structure [16] and occupies a similar position as the belt in the holotoxin crystal structures of both BoNT/A [4] and BoNT/B [6]. (2) In analogy to other "intrinsically unstructured proteins" (IUPs) [27,28], the belt undergoes binding to its LC partner, thereby functioning as a chaperone [24]. (3) The belt occupies the exosites, the extensive enzyme surface allocated for substrate binding, yet it does not contain the scissile bond, thus potentially inhibiting the LC protease.

Mechanism

A number of plausible mechanisms can be envisioned. One, protein-assisted unfolding and pseudosubstrate-assisted refolding of the protease could be an attribute of chaperone action. There is precedence for protease inhibitors acting as intramolecular chaperones [29,30]. A case in point is subtilisin, for which propeptides, located between the signal peptide and the mature segments of the protease, function as protease inhibitors by lodging into the substrate binding pocket [30]. These peptides are effectively IUPs [26] because they lack 3-D structure in isolation, yet adopt secondary structure upon forming a complex with the cognate protease [29–31]. They are involved in the last steps of protein folding of the enzyme. The crystal structure at 2.0 Å resolution of the propeptide–subtilisin complex shows that the prosegment C-terminus (Figure 2, magenta) binds in the enzyme active site (Figure 2, cyan) in a product-like manner with Y^{77} (tip of the β-strand) in the P1 binding pocket [32,33]. POIA1 (*Pleurotus ostreatus* proteinase A inhibitor 1, PDB accession code 1ITP [34]), a mushroom peptide that acts as an intramolecular chaperone and inhibitor to subtilisin yet has only 18% sequence similarity to the cognate propeptide, has a similar tertiary structure to that of the propeptide of subtilisin. Similar mechanisms have been found for other bacterial proteases, including metalloproteases [29]. The analogy that emerges from the considerations described here for BoNT is remarkable and may be the crucial event underlying the

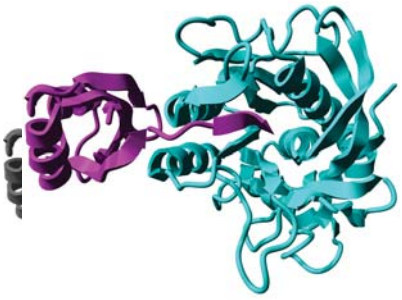

doi:10.1371/journal.ppat.0020113.g002

Figure 2. Structure of the Subtilisin–Pro-Domain Complex

The Cα backbone of subtilisin is represented as cyan ribbons and that of the pro-domain in magenta. Note that the C-terminus of the pro-domain is lodged in a crevice at the protease active site; the tip of the β-strand highlights Y^{77} at the active site. Image rendered using subtilisin BPN′ prosegment complexed with a mutant subtilisin BPN′ [31,32] with YASARA [40].

activity of the BoNT HC belt as both an inhibitor and chaperone. However, the belt does not actually protrude into the BoNT active site. The putative inhibitory activity of the belt would therefore be restricted to the remote substrate binding interfaces of the exosites.

Two, the belt as a continuous segment, residues 449–545 for BoNT/A, may undergo a concerted structural transition at endosomal pH with profound consequences for the translocation process [24]. It is conceivable that a pH-induced transition of this segment may trigger the insertion of the translocation domain into the membrane. Since the belt embraces the LC, the belt may be a structural entity that facilitates or coordinates the concerted partial unfolding of the LC at the endosomal acidic pH and directs the beginning of its translocation through the membrane.

Three, a surrogate pseudosubstrate role is plausible. There is weak sequence similarity between the HC belt and sn2, which extends up to residue D^{195} of SNAP-25 and E^{528} of the HC belt [16,21,35]. Furthermore, the LC undergoes autocatalytic proteolytic fragmentation [17,36], which is prevented in the presence of a competitive inhibitory peptide with a sequence of CRATKML [19]; this peptide closely emulates the sequence of the SNAP-25 C-terminal fragment released by proteolysis of SNAP-25 (residues 197–203 with sequence QRATKML [20], in which the scissile bond is between Q^{197} and R^{198}). However, this non-specific autocatalytic activity is known to occur only at high enzyme concentrations, such as in the context of crystallization trials, so a physiological role is questionable.

It is conceivable that combinations of these three mechanisms act in concert to enhance translocation efficiency. A relevant example is the extensively studied bacterial α-lytic protease (α-LP) [37,38]. The native state of α-LP is unstable and, if unfolded, exhibits a large barrier to refold. Folding of α-LP requires the chaperone activity of its N-terminal pro-domain, which confers strong inhibition on the protease. α-LP initiates degradation of the pro-domain by proteolytic cleavage of an intervening loop at the C-end of the pro-domain, thereby releasing the α-LP from the pro-domain and allowing folding. Cleavage of α-LP pro-domain, therefore, enables efficient folding by lowering the free energy of the folded state and lowering the transition state barrier between unfolded and folded states. Upon release of the pro-domain, the kinetic barriers for unfolding dramatically increase and the α-LP becomes highly protease resistant. Concurrently, the folded state becomes destabilized yet remains kinetically trapped in its native state by a large transition state barrier. We speculate that the belt could enable efficient folding and/or unfolding akin to the α-LP pro-domain. Once it is released inside the neuron, the protease is kinetically trapped and resistant to degradation by cellular proteases or autoproteolysis, thereby implying a convergence of chaperone and surrogate substrate mechanisms. Combined with the exquisite neurotropism of BoNT conferred by its receptor-binding domain, and the target specificity and optimal catalytic efficiency endowed on its protease domain, the holotoxin emerges as a marvel of protein design.

Concluding Remarks and Perspective

These hypotheses naturally lead to testable questions: Is a beltless holotoxin toxic in vivo, e.g., in the context of a mouse toxicity bio-assay [39]? Is the belt required for channel formation? Is it required for LC translocation? Is the belt the trigger for translocation or a modulator? Are there conformational transitions upon entering the acidic environment of the endosome? The implication is that the belt region of BoNT/A HC must be subjected to a rigorous structural and functional analysis to evaluate its possible role in the translocation process, in particular with regards to a pH-induced conformational change. Accordingly, beltless variants of the HC, in which the belt region is eliminated or systematically truncated, could be recombinantly expressed, and their channel and translocation activities examined after reconstitution in lipid bilayers [24] and in neuronal cells [22,23] as described for the intact BoNT/A.

A surrogate pseudosubstrate role of the belt could be probed by using synthetic peptides that mimic the amino acid sequence of the belt, yet incorporate SNAP-25 residues present at the toxin cleavage site as potential toxin substrates. Conversely, one could design a synthetic holotoxin in which the HC belt is replaced by the sn2 segment of SNAP-25 (Figure 1B), comprising a non-cleavable bond instead of the native scissile bond. Would this chimera exhibit translocation features comparable to those of the native holotoxin?

Are the belt regions truly IUPs, and do they contribute to the thermodynamic stability of the LCs? To assess whether belt peptides are true IUPs, their solution structures could be assessed with circular dichroism and nuclear magnetic resonance spectroscopies. To investigate the chaperone activity of the belt, the unfolding and refolding kinetics of LC protease could be studied in the absence and presence of peptides that imitate the belt (Figure 1C) and compared to those of a complex of LC/A and sn2 (Figure 1B). Answers to these questions could substantially improve our understanding of the most enigmatic step in the molecular mechanism of BoNT intoxication. ■

Supporting Information

Accession Numbers

The Protein Data Bank (PDB, http://www.rcsb.org/pdb/) accession codes for the proteins discussed in this paper are BoNT/A (3BTA [4]), BoNT/A-LC in complex with the sn2 segment of SNAP-25 (1XTG [16]), BoNT/B (1EPW [6]), and subtilisin BPN′ prosegment complexed with a mutant subtilisin BPN′ (1SPB [32,33]).

Acknowledgments

We thank Demet Arak, Shilpa Sambashivan, Lilia Koriazova, and Myrta Oblatt-Montal for critical reading and discussions.

Author contributions. ATB and MM conceived the hypotheses. ATB, MAB, RJ, AF, JSS, and MM wrote the paper.

Funding. This work was supported by the Department of Defense and Defense Threat Reduction Agency proposal number 3.10024__06__RD__B (to ATB) and by the US Army Medical Research and Materiel Command (DAMD17–02-C-0106 to MM), and by the Pacific Southwest Regional Center of Excellence (AI065359 to MM).

Competing interests. The authors have declared that no competing interests exist.

References

1. Arnon SS, Schechter R, Inglesby TV, Henderson DA, Bartlett JG, et al. (2001) Botulinum toxin as a biological weapon: Medical and public health management. JAMA 285: 1059–1070.
2. Jankovic J (2004) Botulinum toxin in clinical practice. J Neurol Neurosurg Psychiatry 75: 951–957.
3. Schiavo G, Matteoli M, Montecucco C (2000) Neurotoxins affecting neuroexocytosis. Physiol Rev 80: 717–766.
4. Lacy DB, Tepp W, Cohen AC, DasGupta BR, Stevens RC (1998) Crystal structure of botulinum neurotoxin type A and implications for toxicity. Nat Struct Biol 5: 898–902.
5. Lacy DB, Stevens RC (1999) Sequence homology and structural analysis of the clostridial neurotoxins. J Mol Biol 291: 1091–1104.
6. Swaminathan S, Eswaramoorthy S (2000) Structural analysis of the catalytic and binding sites of *Clostridium botulinum* neurotoxin B. Nat Struct Biol 7: 693–699.
7. Simpson LL (2004) Identification of the major steps in botulinum toxin action. Annu Rev Pharmacol Toxicol 44: 167–193.
8. Jahn R, Scheller RH (2006) SNAREs–Engines for membrane fusion. Nat Rev Mol Cell Biol 7: 631–643.
9. Sutton RB, Fasshauer D, Jahn R, Brunger AT (1998) Crystal structure of a SNARE complex involved in synaptic exocytosis at 2.4 A resolution. Nature 395: 347–353.
10. Weber T, Zemelman BV, McNew JA, Westermann B, Gmachl M, et al. (1998) SNAREpins: Minimal machinery for membrane fusion. Cell 92: 759–772.
11. Jahn R, Lang T, Sudhof TC (2003) Membrane fusion. Cell 112: 519–533.
12. Agarwal R, Binz T, Swaminathan S (2005) Structural analysis of botulinum neurotoxin serotype F light chain: Implications on substrate binding and inhibitor design. Biochemistry 44: 11758–11765.
13. Agarwal R, Eswaramoorthy S, Kumaran D, Binz T, Swaminathan S (2004) Structural analysis of botulinum neurotoxin type E catalytic domain and its mutant Glu212–>Gln reveals the pivotal role of the Glu212 carboxylate in the catalytic pathway. Biochemistry 43: 6637–6644.
14. Arndt JW, Chai Q, Christian T, Stevens RC (2006) Structure of botulinum neurotoxin type D light chain at 1.65 A resolution: Repercussions for VAMP-2 substrate specificity. Biochemistry 45: 3255–3262.
15. Arndt JW, Yu W, Bi F, Stevens RC (2005) Crystal structure of botulinum neurotoxin type G light chain: Serotype divergence in substrate recognition. Biochemistry 44: 9574–9580.
16. Breidenbach MA, Brunger AT (2004) Substrate recognition strategy for botulinum neurotoxin serotype A. Nature 432: 925–929.
17. Segelke B, Knapp M, Kadkhodayan S, Balhorn R, Rupp B (2004) Crystal structure of *Clostridium botulinum* neurotoxin protease in a product-bound state: Evidence for noncanonical zinc protease activity. Proc Natl Acad Sci U S A 101: 6888–6893.
18. Rossetto O, Schiavo G, Montecucco C, Poulain B, Deloye F, et al. (1994) SNARE motif and neurotoxins. Nature 372: 415–416.
19. Schmidt JJ, Stafford RG, Bostian KA (1998) Type A botulinum neurotoxin proteolytic activity: Development of competitive inhibitors and implications for substrate specificity at the S1' binding subsite. FEBS Lett 435: 61–64.
20. Vaidyanathan VV, Yoshino K, Jahnz M, Dorries C, Bade S, et al. (1999) Proteolysis of SNAP-25 isoforms by botulinum neurotoxin types A, C, and E: Domains and amino acid residues controlling the formation of enzyme-substrate complexes and cleavage. J Neurochem 72: 327–337.
21. Breidenbach MA, Brunger AT (2005) New insights into clostridial neurotoxin-SNARE interactions. Trends Mol Med 11: 377–381.
22. Fischer A, Montal M (2006) Characterization of *Clostridial botulinum* neurotoxin channels in neuroblastoma cells. Neurotox Res 9: 93–100.
23. Fischer A, Montal M (2007) Single molecule detection of intermediates during Botulinum neurotoxin translocation across membranes. Proc Natl Acad Sci U S A 104: 10447–10452.
24. Koriazova LK, Montal M (2003) Translocation of botulinum neurotoxin light chain protease through the heavy chain channel. Nat Struct Biol 10: 13–18.
25. Drummond AJ, Ashton B, Heled J, Kearse M, Moir R, et al. (2006) Geneious version 2.5.4. Available: http://www.geneious.com/. Accessed 25 August 2007.
26. Fasshauer D, Bruns D, Shen B, Jahn R, Brunger AT (1997) A structural change occurs upon binding of syntaxin to SNAP-25. J Biol Chem 272: 4582–4590.
27. Dyson HJ, Wright PE (2005) Intrinsically unstructured proteins and their functions. Nat Rev Mol Cell Biol 6: 197–208.
28. Tompa P (2005) The interplay between structure and function in intrinsically unstructured proteins. FEBS Lett 579: 3346–3354.
29. Shinde U, Fu X, Inouye M (1999) A pathway for conformational diversity in proteins mediated by intramolecular chaperones. J Biol Chem 274: 15615–15621.
30. Shinde UP, Liu JJ, Inouye M (1997) Protein memory through altered folding mediated by intramolecular chaperones. Nature 389: 520–522.
31. Kojima S, Iwahara A, Yanai H (2005) Inhibitor-assisted refolding of protease: A protease inhibitor as an intramolecular chaperone. FEBS Lett 579: 4430–4436.
32. Bryan P, Wang L, Hoskins J, Ruvinov S, Strausberg S, et al. (1995) Catalysis of a protein folding reaction: Mechanistic implications of the 2.0 A structure of the subtilisin-prodomain complex. Biochemistry 34: 10310–10318.
33. Gallagher T, Gilliland G, Wang L, Bryan P (1995) The prosegment-subtilisin BPN' complex: Crystal structure of a specific 'foldase'. Structure 3: 907–914.
34. Sasakawa H, Yoshinaga S, Kojima S, Tamura A (2002) Structure of POIA1, a homologous protein to the propeptide of subtilisin: Implication for protein foldability and the function as an intramolecular chaperone. J Mol Biol 317: 159–167.
35. Chen S, Kim JJ, Barbieri JT (2007) Mechanism of substrate recognition by botulinum neurotoxin serotype A. J Biol Chem 282: 9621–9627.
36. Ahmed SA, Byrne MP, Jensen M, Hines HB, Brueggemann E, et al. (2001) Enzymatic autocatalysis of botulinum A neurotoxin light chain. J Protein Chem 20: 221–231.
37. Cunningham EL, Agard DA (2004) Disabling the folding catalyst is the last critical step in alpha-lytic protease folding. Protein Sci 13: 325–331.
38. Jaswal SS, Sohl JL, Davis JH, Agard DA (2002) Energetic landscape of alpha-lytic protease optimizes longevity through kinetic stability. Nature 415: 343–346.
39. Eubanks LM, Hixon MS, Jin W, Hong S, Clancy CM, et al. (2007) An in vitro and in vivo disconnect uncovered through high-throughput identification of botulinum neurotoxin A antagonists. Proc Natl Acad Sci U S A 104: 2602–2607.
40. YASARA Biosciences (2007) YASARA: Yet another scientific artificial reality application. Available: http://www.yasara.org/. Accessed 25 August 2007.

Acknowledgements:

Chapter 5, in full, is a reprint of the material as it appears in the Public Library of Science, Pathogens. Brunger, Axel T.; Breidenbach, Mark A; Jin, Rongsheng; Fischer, Audrey; Santos, Jose S. and Montal, Maurice, Public Library of Science, 2007. The dissertation author was an investigator and author of this paper.

Chapter 6

Molecular Dissection of Botulinum Neurotoxin Reveals Interdomain Chaperone Function

Abstract

Clostridial botulinum neurotoxins (BoNTs) are Zn^{2+}-endoproteases that block synaptic exocytosis by cleaving SNARE proteins. Intoxication requires the multi-domain protein to undergo conformational changes in response to pH and redox gradients across the endosomal membrane leading to the formation of a protein-conducting channel by the ~100 kD heavy chain (HC) that translocates the ~50 kD light chain (LC) protease into the cytosol, colocalizing it with the substrate SNARE proteins. The HC can be further subdivided into two halves: the N-terminal translocation domain (TD) and the C-terminal Receptor Binding Domain (RBD). Here, we investigate the minimal requirements for channel activity and LC translocation. We utilize a cellular protection assay and a single channel/single molecule LC translocation assay to characterize in real time the channel and chaperone activities of BoNT/A truncation constructs in Neuro 2A cells. The unstructured, elongated belt region of the TD is demonstrated to be unnecessary for channel activity, although may be required for productive LC translocation. We show that the RBD is not necessary for channel activity or LC translocation, however it dictates the pH threshold of channel insertion into the membrane. These findings indicate that each domain functions as a chaperone for the others in addition to their individual functions, working in concert to achieve productive intoxication.

Introduction

Botulinum neurotoxin (BoNT) inhibits synaptic exocytosis in peripheral cholinergic synapses causing botulism, a disease characterized by descending flaccid paralysis. *Clostridium botulinum* cells secrete seven BoNTs isoforms known as BoNT/A to G[1]. All BoNT isoforms are synthesized as a single polypeptide chain with a molecular mass of ~150 kDa. The precursor protein is cleaved either by clostridial or host cell proteases into two polypeptide chains linked by a disulfide bridge[2]. The mature di-chain toxin consists of a 50 kDa light chain (LC) protease and a 100 kDa heavy chain (HC). The HC consists of the translocation domain (TD) (the N-terminal half), a long 4 α-helix bundle, and the receptor-binding domain (RBD) (the C-terminal half), consisting of a single β-barrel and a single β-trefoil motif[1, 3-5].

BoNT enter neurons by receptor-mediated endocytosis, initiated by the interactions between the BoNT RBD and a specific ganglioside, GT_{1B}[6-9], and protein co-receptor, SV2 for BoNT/A[10, 11] and synaptotagmins I and II for BoNT/B and BoNT/G[12]. Exposure of the BoNT-receptor complex to the acidic environment of endosomes induces a conformational change whereby the HC inserts into the endosomal bilayer membrane[1, 13, 14]. Previously, we demonstrated that the HC forms a protein-conducting channel under endosomal conditions[15], and translocates the LC protease into the cytosol[16, 17], colocalizing it with its substrate SNARE (soluble NSF attachment protein receptor) protein[1, 18, 19].

The LC and the C-terminal half of the RBD crystals have been solved for multiple serotypes and their functions clearly defined[20-28]; however the central motifs of the protein are less well understood. The recent crystal structures of the BoNT/B RBD C-terminal half interacting with its ganglioside and protein co receptors raises queries regarding the purpose of the N-terminal half of the RBD[25, 26]. Potentially the N-terminal motif of the RBD could serve a function in priming the TD to an insertion competent orientation with respect to the membrane, or function as part of the protein-conducting channel itself. The elongated, unstructured belt region of the TD is another domain with an elusive function; potentially acting as a pseudo-substrate/chaperone for the LC during the majority of the intoxication process[29].

In this work, we isolated the TD with and without the belt region and the TD disulfide linked to the catalytic LC. We assayed the resulting channel activity with single molecule resolution on excised patches of neuronal cells[16]. The system allowed us to determine the minimal domain required for BoNT channel activity and productive LC translocation as well as the threshold of acidic pH necessary for each of these functions. We utilized a cell based neurotoxicity assay to further quantitate the single molecule studies. RBD was determined to be unnecessary for both channel activity and LC translocation under weakly acidic conditions. In contrast, the RBD restricted the TD insertion into the membrane until localized to an acidic endosomal compartment where low pH induces channel insertion concurrent with partial unfolding of the LC cargo,

thereby promoting productive LC translocation and release into the cytosolic compartment.

Experimental Procedures

Materials – Unless otherwise specified, all chemicals were purchased from Sigma-Aldrich. Purified native BoNT/A holotoxin and HC were from Metabiologics.

Bacterial strains – E. coli strain DH5α cells were used in the cloning procedures and E. coli strain BL21.DE3.pLysS was used for protein over expression.

Construction of pET-23a BoNT/A translocation domain, pET-23a BoNT/A beltless translocation domain and BoNT/A light chain-translocation domain – Plasmid DNA used for cloning and sequencing was prepared with QIAGEN mini prep kit. DNA encoding the BoNT/A translocation domain (TD), amino acids 449-870, and the BoNT/A beltless translocation domain (BTD), amino acids 546-870, were isolated from the previously described BoNT/A Heavy chain clone [30] by PCR. Oligonucleotides were designed against the N-terminus and C-terminus of the TD and BTD to include two unique restriction sites and a C-terminal His Tag. PCR products were gel purified and extracted using the QIAGEN gel extraction kit. Following resuspension in water, the DNA was ligated into the pET-23a vector (Novagen).

Construction of BoNT/A light chain-translocation domain – DNA corresponding to the BoNT/A catalytic and translocation domains was obtained from two separate starting vectors: BoNT/A LC (DBL, unpublished results; a wild-type BoNT/A catalytic domain sequence) and HC_N-SDmut (DBL, [31]; a wild-type translocation domain amino acid sequence with silent mutations to disrupt an internal Shine Dalgarno site). The catalytic domain was amplified with primers that introduced a 5' NdeI site (GGAATTCCATATGCCATTTGTTAATAAAC) and 3' Sac1 site (GGCGAGCTCGCTTATTGTATCCTTTATCTAATG) and ligated into a TOPO vector (Invitrogen). An internal SacI site was then removed by QUIK-Change mutagenesis using the primer CTCTGGCACACGAACTGATCCACGCTGGTC and its reverse complement.

The translocation domain was amplified with primers that introduced a 5' SacI site (GCCGAGCTCTGAACGATCTGTGTATCAAAGTTAATAATTGGG) and 3' XhoI site (CCGCTCGAGGTTCTTAATATATTCAGTAAATGTAG) and ligated into a TOPO vector. The catalytic and translocation domains were excised from the TOPO vectors using NdeI/SacI and SacI/XhoI, respectively and ligated into a pET24b vector that had been digested with NdeI/XhoI. The use of the engineered SacI site results in the insertion of an Arg between K447 (cat) and A448 (trans), a feature that was included in the design to improve the efficiency of trypsin activation. This work was performed by Dr. Borden Lacy.

Expression and purification of the TD, BTD and LC-TD – Expression and purification of the TD and LC-TD was performed by Dr. Borden Lacy and Darren

Mushrush at Vanderbilt University; expression and purification of the BTD was performed by Shilpa Sambashivan at Dr. Axel Brunger's lab in Standford. Expression and purification of all constructs was performed as previously described [31] with the following modifications. BoNT/A TD and LC-TD were eluted from the Ni-affinity column in the presence of 0.2% DDM and then concentrated to 0.375 mg/mL in 0.2%DDM, 20mM Tris, 150mM NaCl, pH 8.0. Di-chain BoNT/A LC-TD was generated by cleavage with trypsin in purification buffer: BoNT/A LC-TD (0.5 mg/mL) was incubated with 1 μg/mL trypsin overnight at room temperature. Thereafter, trypsin was inactivated with 0.25 mg/mL trypsin soybean inhibitor for 15 min at room temperature. BoNT/A BTD was eluted from the Ni-affinity column in the presence of 1% Tween-20 and 1% Triton X-100 or and then buffered exchanged and concentrated to 0.6 mg/mL in 0.2% dodecyl maltoside (DDM), 150 mM NaCl, 50 mM Tris, pH 8.0. BoNT/A BTD was also purified in the presence of either 0.2% DDM or 1% octyl glucoside (OG) without additional detergents.

Protein Analysis – Purity of BoNT truncation mutant proteins was determined qualitatively with SDS Page analysis, as shown in figure 1. SDS-PAGE gels (12%) were used to visualize BoNT/A constructs. If indicated, loading buffer was supplemented with 100 mM dithiothreitol (DTT) prior to sample addition.

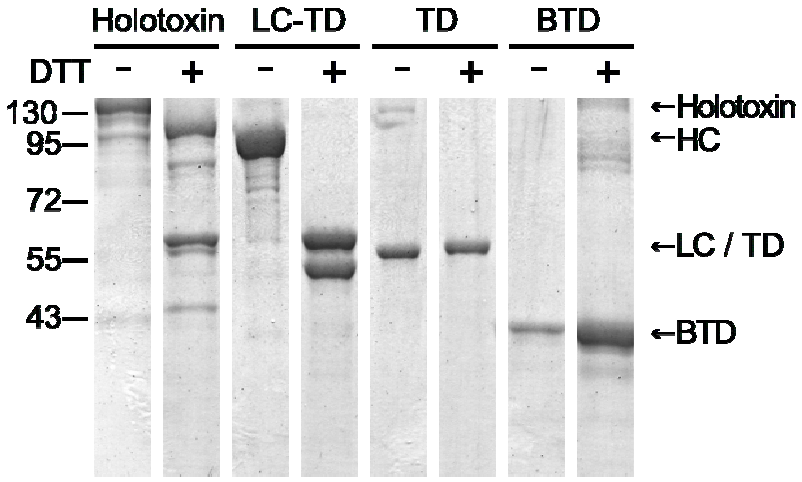

Fig. 1. Coomassie blue stained SDS-PAGE analysis of BoNT/A holotoxin, LC-TD, TD and BTD. Numbers denote M_r standards; DTT (+) (-) indicate presence or absence of dithiothreitol.

Protease Activity of BoNT/A and BoNT/E Holotoxins – Recombinant SNAP-25 [32, 33] was incubated with 60 ng of BoNT holotoxin 13.2 mM Hepes (pH 7.4), 20 mM DTT, and 1 μM $Zn(CH_3COOH)_2$ for 30 min at 37°C. SDS/PAGE (12%) was used to visualize cleavage of SNAP-25 by BoNT/A and BoNT/E holotoxins[34].

Cell culture and patch clamp recordings – Excised patches from Neuro 2A cells in the inside-out configuration were used as described[35]. Current recordings were obtained under voltage clamp conditions. Records were acquired at a sampling frequency 20 kHz and where mentioned filtered online to 2 kHz with Gaussian filter. All experiments were conducted at 22 ± 2 °C.

Solutions – To emulate endosomal conditions the *trans* compartment (bath) solution contained (in mM) NaCl 200, NaMOPS [3-(N-morpholino) propanesulfonic acid] 5, (pH 7.0 with HCl), tris-(2-carboxyethyl) phosphine (TCEP) 0.25, $ZnCl_2$ 1, and the *cis* compartment (pipet) solution contained (in mM) NaCl 200, NaMES [2-(N-morpholino) ethanesulfonic acid] 5, (pH 5.3 or pH 6.0 with HCl). When *cis* compartment was filled with pH 7 buffer *trans* compartment solution set to pH 7.0 was used. The osmolarity of both solutions was determined to be ~390 mOsm. $ZnCl_2$ was used to block endogenous channel activity specific to Neuro 2A cells[36, 37]. BoNT reconstitution and channel insertion was achieved by supplementing 5-2.5 μg/mL BoNT holotoxin, HC, LC-TD, TD, BTD to the pipet solution, which was set to an endosomal pH of 5.3, pH 6.0 or pH 7.0.

Data Analysis – Analysis performed on single bursts of each experimental record. Single channel conductance (γ) was calculated from Gaussian fits to current amplitude histograms. The total number of opening events (*N*) analyzed was 207,139. Time course of single channel conductance change for each experiment was calculated from γ of each record, where t = 0 s corresponds to onset of channel activity, and average time course was constructed from the set of individual experiments for a single condition. The voltage-dependence of channel opening was calculated from measurements of the fraction of time that the channel is open (P_o) as a function of voltage by integration of γ histograms where γ is $60 \leq \gamma \geq 75$ pS. Statistical values represent means ± SEM, unless otherwise indicated. *n* denotes the number of different experiments.

Cell based intoxication assay – Cellular protection against BoNT/A with selected compounds was investigated by using Neuro 2A cells as previously described[34]. Neuro-2a cells were seeded at a density of ~ 120,000 cells per well in a 12-well tissue culture plate in DMEM culture medium. After incubation for 24 h, the media were removed and replaced serum-free media containing 5.0 μg of BoNT/A holotoxin, LC-TD or TD. After incubation for ~ 48 h, the cells were harvested by removing the media, adding 160 μL of 1× NuPAGE LDS sample buffer (Invitrogen, Carlsbad, CA), and boiling for 10 min.

Western Blot Analysis – Proteins within the whole-cell extract samples were separated by SDS/PAGE on a 12% Bis-Tris NuPAGE gel in Mops/SDS running buffer (Invitrogen) before transfer to a 0.2 μm nitrocellulose membrane for 120 min at 30 V[34]. After blocking in 2% skim milk/H_2O for 20 min at room temperature, the membrane was washed three times for 5 min at room temperature with TBST [25 mM Tris (pH 7.4), 137 mM NaCl, 2.7 mM KCl, and 0.1% Tween 20]. Primary antibody, anti-SNAP-25 mouse monoclonal IgG_1 (200 μg/ml; Santa Cruz Biotechnology, Santa Cruz, CA) diluted 1:1,000 into 2% skim milk/H_2O, was added, and the blot was incubated for 20 min at room temperature followed by four 5-min washes with TBST at room temperature. Next, secondary antibody, goat anti-mouse HRP-conjugated (10 μg/ml; Pierce, Rockford, IL) diluted 1:500 into 2% skim milk/H_2O, was added, and the blot was incubated for 1 h at room temperature followed by washing for 120 min at room temperature. Bands were visualized with 4 ml of SuperSignal West Dura Chemiluminescent Substrate (Pierce) and analyzed with an X-OMAT 2000A processor (Kodak). Quantization of the Western blot analysis was conducted with the use of Image J software (NIH).

Results

BoNT/A translocation domain exhibits channel activity

Several truncation mutants of BoNT/A holotoxin were examined for potential channel activity: HC, N-terminal half of the HC called the translocation

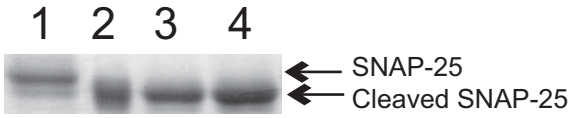

Fig. 2. Coomassie blue stained SDS-PAGE analysis of *in vitro* SNAP-25 cleavage of BoNT/A holotoxin and LC-TD. Lane 1 contains 20 mM HEPES incubated negative control, lane 2 contains 21 kDa molecular weight standard protein, lane 3 contains SNAP-25 cleaved with BoNT/A holotoxin, and lane 4 contains SNAP-25 cleaved with BoNT/A LC-TD. 100% of SNAP-25 was cleaved by both BoNT/A holotoxin and LC-TD as compared to uncleaved control presented in lane 1.

Fig. 3. BoNT/A HC, TD, LC-TD and BTD channel activity measured on excised patches of Neuro 2A cells. Representative single-channel currents at the indicated voltages; consecutive voltage pulses applied to the same patch for each experimental condition. Channel opening is indicated by a downward deflection; C and O respectively denote the closed and open states. The single channel conductance for HC (*A*) = 65.3 ± 0.4 pS, TD (*B*) = 64.4 ± 0.4 pS, LC-TD (*C*) = 69.2 ± 0.9 pS, and BTD (*D*) = 66.6 ± 0.6 pS.

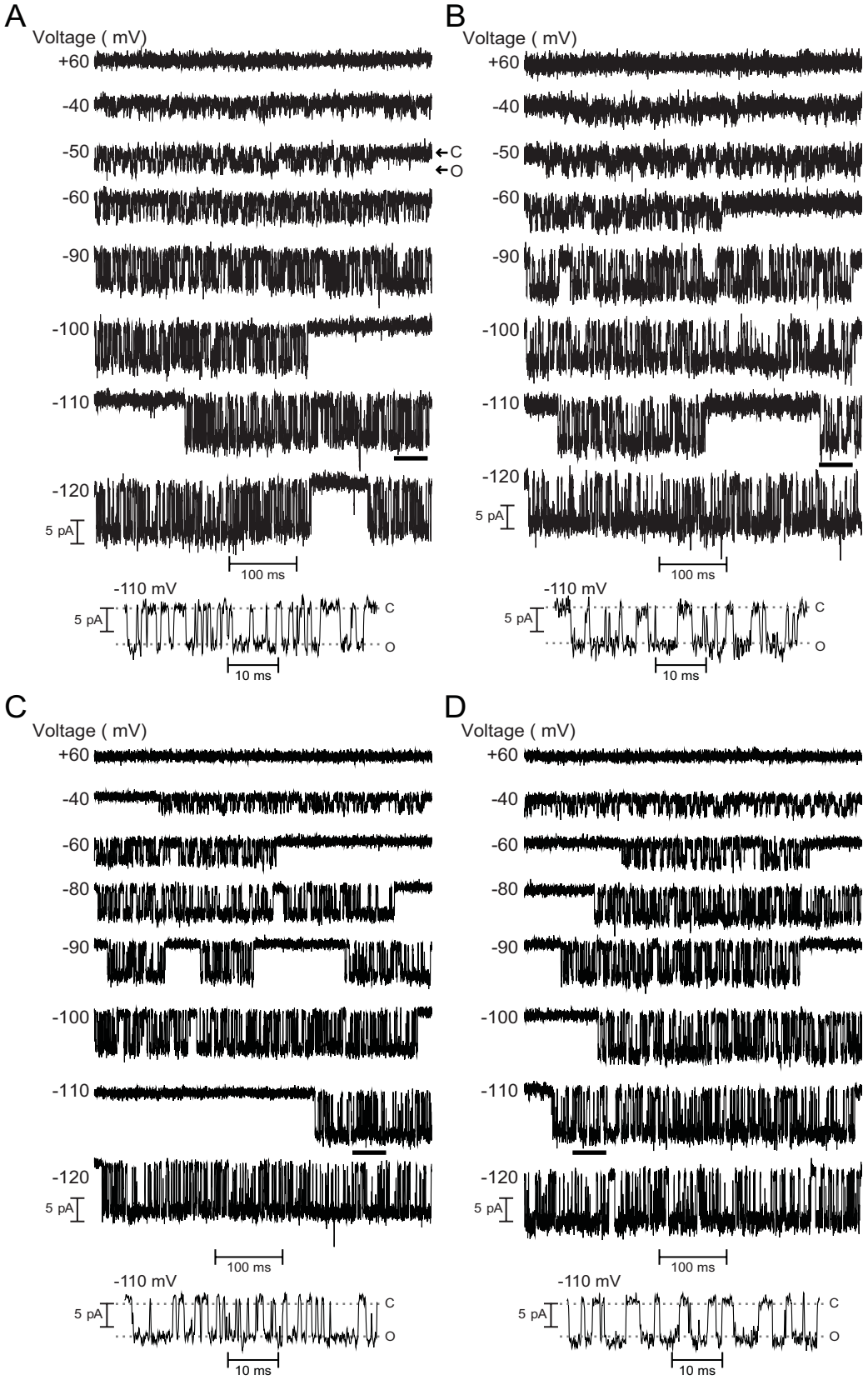
A
Voltage (mV)
+60
-40
-50
C
O
-60
-90
-100
-110
-120
5 pA
100 ms
-110 mV
5 pA
C
O
10 ms
B
Voltage (mV)
+60
-40
-50
-60
-90
-100
-110
-120
5 pA
100 ms
-110 mV
5 pA
C
O
10 ms
C
Voltage (mV)
+60
-40
-60
-80
-90
-100
-110
-120
5 pA
100 ms
-110 mV
5 pA
C
O
10 ms
D
Voltage (mV)
+60
-40
-60
-80
-90
-100
-110
-120
5 pA
100 ms
-110 mV
5 pA
C
O
10 ms

domain (TD), the Light chain and the translocation domain linked by a disulfide bridge (LC-TD), and the TD without the N-terminal 100 amino acids known as the belt region (BTD). The LC-TD is generated as a single polypeptide chain of ~100 kDa with a disulfide bridge; the functionally relevant di-chain protein was generated with trypsin cleavage of the loop region between the disulfide bridge cysteine residues. Trypsin nicking does not disrupt the disulfide bridge as demonstrated by SDS Page analysis (Fig. 1) or abolish the enzymatic activity of the LC (Fig. 2). Protein insertion and channel formation was monitored on excised membrane patches from Neuro 2A cells under conditions which recapitulate those across endosomal membranes: the *cis* compartment, defined as the compartment containing BoNT/A protein, was held at pH 5.3 and the *trans* compartment was maintained at pH 7.0 and supplemented with the membrane nonpermeable reductant TCEP. Channel activity was monitored for all four of the proteins tested; representative records over a range of applied voltage potentials are shown in Figure 3. Channel activity of the truncation mutants, LC-TD, TD, and BTD, exhibit similar characteristics to HC. Single channel conductance (γ) was determined to be ~ 65 pS as measured from the transition from the closed (C) to open (O) states; channel activity occurs in bursts interspersed between periods of no channel activity. The presence of the subconductance state (S), define at the onset of a burst when the channel enters the ~ 10 pS subconductance state and then undergoes quick transitions between the intermediate state and the open state, is clearly visible over the more negative

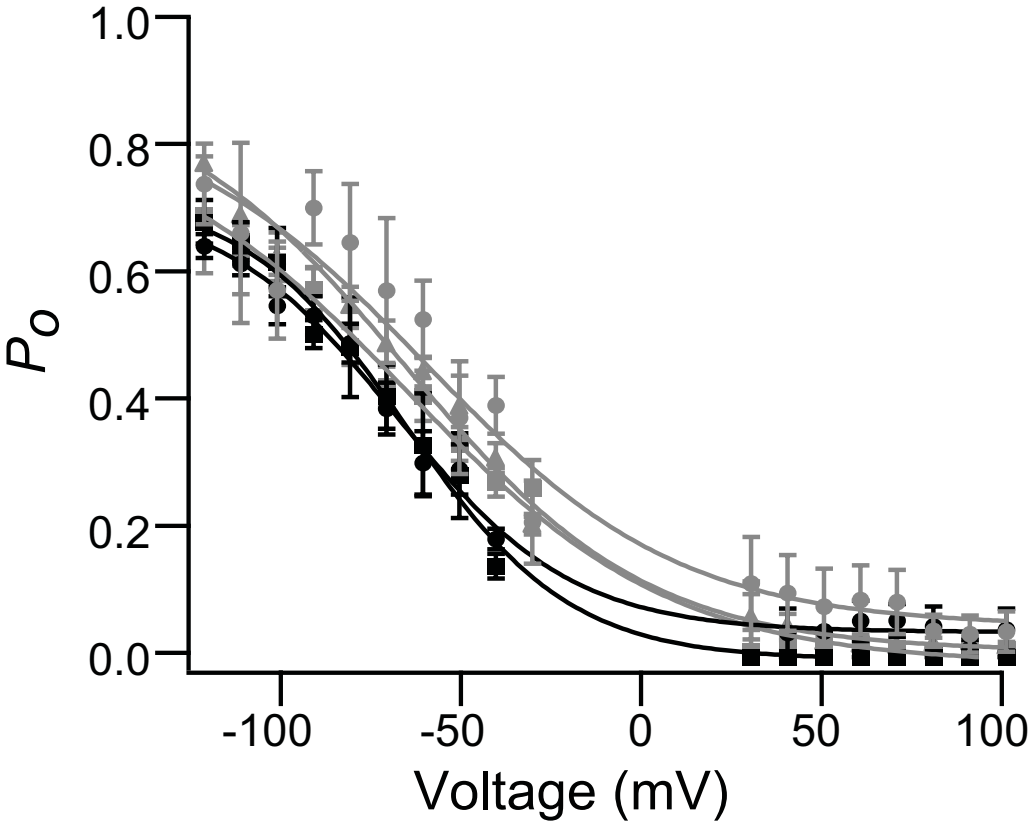

Fig. 4. Analysis of unoccluded BoNT/A channels in Neuro 2A cells under endosomal conditions. P_o as a function of voltage for BoNT/A holotoxin (●) ($V_{½}$ = –67.2 ± 2.9 mV), HC (■) ($V_{½}$ = –64.6 ± 2.2 mV), LC-TD (●) ($V_{½}$ = –59.0 ± 9.1 mV), TD (■) ($V_{½}$ = –64.0 ± 4.2 mV), BTD (▲) ($V_{½}$ = –64.9 ± 2.2 mV); ($3 \leq n \leq 6$ per data point; average N per data point = 1,428).

voltage potential current records (Fig. 3).The probability to reside in the open state (P_o), measured from the ms timescale transitions between the open and closed states, of each protein were all indistinguishable from that of BoNT/A HC as illustrated by the time expansion of current records shown in Figure 3. The LC-TD, TD and BTD have similar voltage dependence to unoccluded BoNT/A channel activity (Fig. 4); $V_{1/2}$, the voltage at which P_o = 0.5, ~ –67 mV for holotoxin, ~ –59 mV for LC-TD, ~ –64 mV for TD, and ~ –65 mV for BTD.

Channel insertion is pH independent in the absence of the RBD

The pH threshold for membrane insertion was investigated by varying *cis* compartment pH conditions within the single molecule electrophysiology assay for each of the truncation mutants. While BoNT/A holotoxin and HC statistically resulted in channel activity every third experiment when the *cis* compartment was set to pH 5.3, channel activity was not monitored over the minimum individual experimental time of 30 min when the *cis* compartment was maintained at pH 6 or pH 7 over 8 separate experiments for each condition (Fig. 4*B*). These results correspond well with circular dichroism studies of the HC, maintaining ~ 35% helicity over the range pH 7 to pH 4.5[17]. Preliminary circular dichroism studies with the TD, LC-TD and BTD indicate that these proteins are much more unfolded over the neutral to acidic pH range (data not shown) and potentially insert into the membrane under more neutral *cis* compartment conditions.

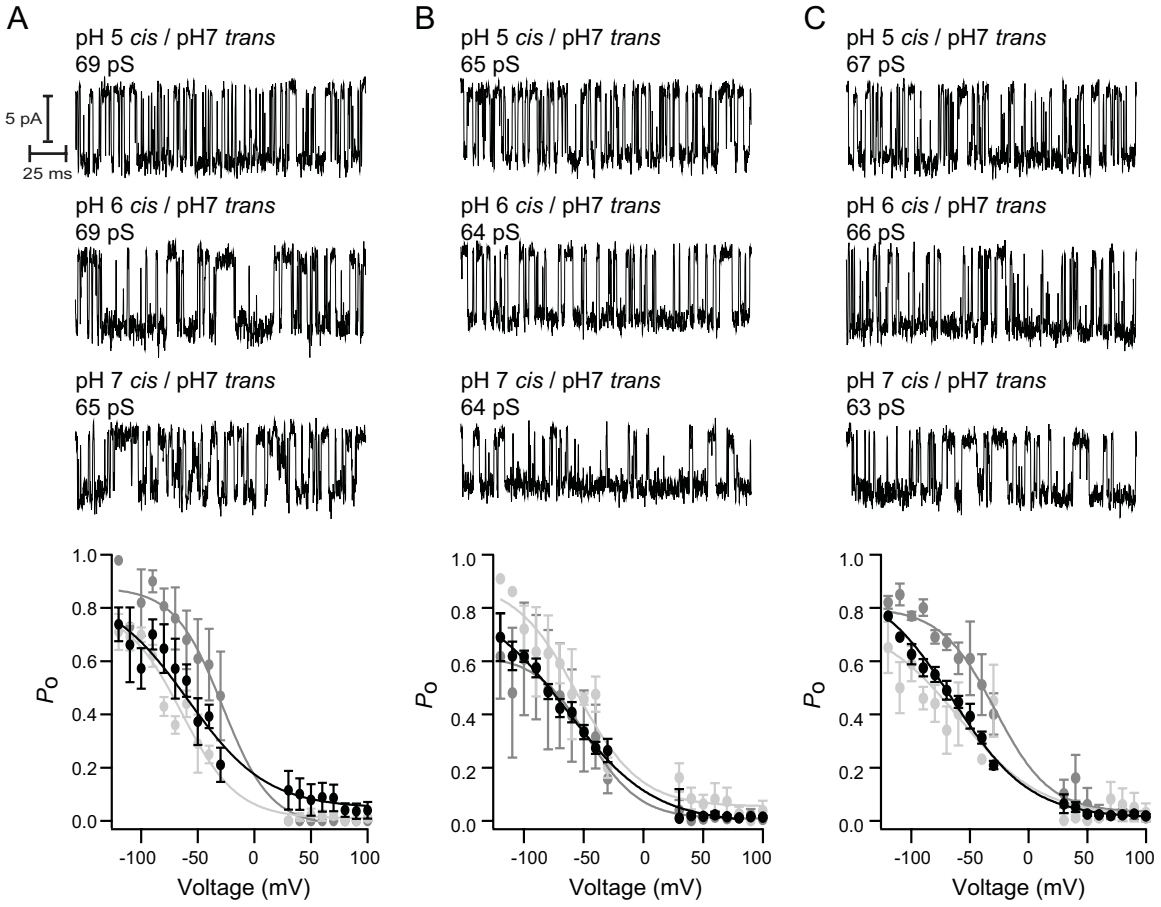

Fig. 5. BoNT/A LC-TD, TD, and BTD channel activity is independent of pH gradient across membrane. *A*, *B*, and *C*, top panel of channel activity illustrates channel activity monitored with pH 5 *cis* / pH 7 *trans*, middle panel shows pH 6 *cis* / pH 7 *trans* and bottom panel shows pH 7 *cis* / pH 7 *trans*; records were Gaussian filtered at 2 kHz. *A*, BoNT/A LC-TD channel activity begins 10 min after GΩ seal formation at pH 5 *cis* / pH 7 *trans*, 13 min after GΩ seal formation at pH 6 *cis* / pH 7 *trans*, and 50 min after GΩ seal formation at pH 7 *cis* / pH 7 *trans.* For conditions with pH 5 and pH6 in the *cis* compartment stable unoccluded channel activity is monitored following completion of LC translocation; however low conductance intermediates were not visualized for experiments with pH 7 in the *cis* compartment. *Bottom*, Analysis of unoccluded channel activity for BoNT/A LC-TD for pH 5 *cis* / pH 7 *trans* (●), pH 6 *cis* / pH 7 *trans* (●) ($V_{½}$ = –28.1 ± 4.5 mV), pH 7 *cis* / pH 7 *trans* (●) ($V_{½}$ = –64.1 ± 2.9 mV). *B*, BoNT/A TD channel activity begins 30 min after GΩ seal formation at pH 5 *cis* / pH 7 *trans*, 14 min after GΩ seal formation at pH 6 *cis* / pH 7 *trans*, and 30 min after GΩ seal formation at pH 7 *cis* / pH 7 *trans.* Low conductance intermediates were not visualized. *Bottom*, Analysis of unoccluded channel activity for BoNT/A TD for pH 5 *cis* / pH 7 *trans* (●), pH 6 *cis* / pH 7 *trans* (●) ($V_{½}$ = –46.8 ± 3.1 mV), pH 7 *cis* / pH 7 *trans* (●) ($V_{½}$ = –55.3 ± 3.8 mV). *C*, BoNT/A BTD channel activity begins 13 min after GΩ seal formation at pH 5 *cis* / pH 7 *trans*, 23 min after GΩ seal formation at pH 6 *cis* / pH 7 *trans*, and 60 min after GΩ seal formation at pH 7 *cis* / pH 7 *trans.* Low conductance intermediates were not visualized. *Bottom*, Analysis of unoccluded channel activity for BoNT/A BTD for pH 5 *cis* / pH 7 *trans* (●), pH 6 *cis* / pH 7 *trans* (●) ($V_{½}$ = –29.4 ± 4.2 mV), pH 7 *cis* / pH 7 *trans* (●) ($V_{½}$ = –58.9 ± 9.0 mV).

Channel activity was monitored for all TD, LC-TD and BTD when the cis compartment solution was adjusted to pH 6 and pH 7; representative records over a range of applied voltage potentials are shown in Figure 3. Channel activity of the truncation mutants, LC-TD, TD, and BTD, exhibit similar characteristics. Single channel conductance (γ) was determined to be pH gradient independent, remaining constant at ~ 65 pS (Fig. 5). Bursting channel activity with transitions between the closed, subconductance and open states were unaffected by varying the pH of the *cis* compartment. The voltage dependence of the P_o was modulated by the more neutral pH gradient as shown in the lower panel graphs of Figure 5. The $V_{1/2}$ of all three proteins was right shifted when the *cis* compartment was maintained at pH 6.0: ~ –28 mV for LC-TD, ~ –47 mV for TD, and ~ –29 mV for BTD. However symmetric pH conditions resulted values closer resembling those for pH 5 *cis* / pH 7 *trans*: ~ –64 mV for LC-TD, ~ –55 mV for TD, and ~ –59 mV for BTD. The TD interaction with the RBD therefore alters the pH threshold for membrane insertion; in the absence of the RBD the less folded LC-TD, TD and BTD readily form channels at neutral pH.

BoNT/A LC-TD translocates LC in a pH dependent manner

Translocation of BoNT/A LC by the BoNT/A channel can be monitored in real time and at the single molecule level in excised membrane patches from Neuro 2A cells[16]. LC Translocation through the HC channel requires conditions which emulate those prevalent across endosomes. Translocation is then

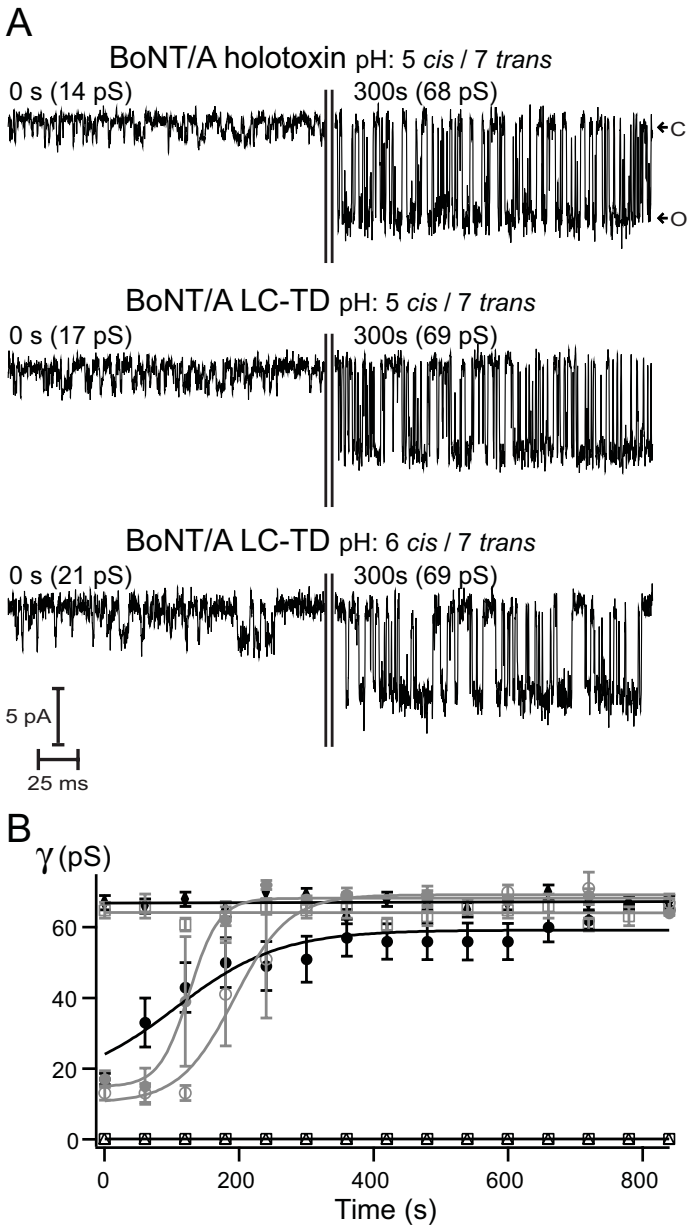

Fig. 6. BoNT/A channel activity in excised patches of Neuro 2A cells over range of pH values in the *cis* compartment. Records were Gaussian filtered at 2 kHz. *A*, BoNT/A holotoxin channel activity begins 10 min after GΩ seal formation, t=0 s, and transitions from low conductance intermediate state to the unoccluded state after completion of LC translocation. BoNT/A LC-TD channel activity begins 10 min after GΩ seal formation for pH 5 *cis* / pH 7 *trans* and 12 min after seal formation for pH 6 *cis* / pH 7 *trans*. Under all above mentioned experimental conditions channel activity transitions from low conductance intermediate state to the unoccluded state within 300s of onset of channel activity. Channel opening is indicated by a downward deflection. *B*, Average time course of conductance BoNT/A holotoxin pH 5 *cis* / pH 7 *trans* (●), HC pH 5 *cis* / pH 7 *trans* (♦), LC-TD pH 5 *cis* / pH 7 *trans* (■), LC-TD pH 6 *cis* / pH 7 *trans* (○), and LC-TD pH 7 *cis* / pH 7 *trans* (□), ($3 \leq n \leq 6$ per data point; average *N* per data point =829 events). No channel activity was monitored for BoNT/A holotoxin under the following experimental conditions: pH 6 *cis* / pH 7 *trans* (□) (*n*=8) and pH 7 *cis* / pH 7 *trans* (△) (*n*=8).

observed as a time-dependent increase in Na+ conductance through the HC channel, as illustrated by the control experiment shown in the top panel of Fig. 6*A*. The top, left panel of Fig. 6*A* shows that at the onset of channel activity, small, discrete events with a γ ~ 14 pS are clearly discerned. Progressively, γ undergoes a continuous increase until reaching a stable value of 68 pS (top, right panel), a conductance at which they remain for the duration of the experiment (Fig. 6*B*, black opaque circle).

The average time course of change of the single channel conductance γ after insertion of BoNT/A holotoxin into the membrane displays multiple discrete transient intermediate conductances before achieving the γ of 67.1 ± 2.0 pS (Fig. 4*A*, top, right panel). The half-time for completion of such event, estimated fromthe transition to high conductance is ~150 s (Fig. 4*B*). The steady-state γ is also the characteristic conductance of isolated HC recorded under identical conditions; therefore it represents the conductance of the unoccluded HC in holotoxin experiments after translocation is complete. We interpret the intermediate conductance states as reporters of discrete transient steps during the translocation of the LC across the membrane. During protease translocation, the protein-conducting channel progressively conducts more Na+ around the polypeptide chain before entering an exclusively ion-conductive state. This typical pattern of channel activity for holotoxin proceeds under conditions which mimic those across endosomes and lead to LC translocation and retrieval of protease activity after completion of translocation.

To investigate the potential role of the receptor binding domain in LC translocation we analyzed the LC-TD channel at early time points of channel activity. Under endosomal conditions, LC-TD channel activity was similar to holotoxin; low conductance intermediate states were visualized before the unoccluded state. The middle, left panel of Fig. 6*A* illustrates that at the onset of channel activity, small, discrete events with a γ ~ 17 pS are clearly discerned. Progressively, γ undergoes a continuous increase until reaching a stable value of 69 pS (Figs. 6*A*, middle, right panel and 6*B*, black opaque circle). The average time course of change of γ after insertion of BoNT/A LC-TD into the membrane occurs with a $T_{1/2} \approx 130$ s and displays multiple discrete transient intermediate conductances before achieving the γ of 69.2 ± 0.9 pS (Fig. 6*B*). LC-TD forms channels that exhibit a growing conductance event before stabilization to ~ 69 pS under pH6 *cis* / pH 7 *trans* (Fig. 6*A*, lower panel). The $T_{1/2}$, measured from the average time course of change of γ after insertion, is increased from that of pH 5 *cis* conditions to 190 ± 10 s (Fig. 6*B*, gray opaque circle). The longer time required to complete LC translocation may be due the level of fold the LC maintains at pH 6. Previous work by Simpson has shown that bafilomycin a proton pump inhibitor which neutralizes endosomal compartments effectively inhibits BoNT intoxication[38]. The LC may require more time to overcome the energy barrier associated with transitioning from the entry in the HC channel translocating as a single chain or α helix. Interestingly, when the excised patches of neuronal cells are bathed in symmetric neutral pH solutions, the LC-TD forms

HC like channels (Fig. 6*B*, gray open circle). No low conductance intermediate states are monitored. Circular dichroism analysis of the LC at pH 7 indicates a strongly α helical protein that would remained folded rather than adopt a translocation competent conformation[17]. We interpret that LC does not unfold at pH 7 and therefore cannot be translocated through the ~15 Å pore of the TD channel[39, 40].

Affect of LC-TD on Neuro 2A cells

The prediction that emerges from these findings is that while BoNT/A holotoxin readily enters neuronal cells, the LC-TD would be trapped at the plasma membrane unable to cleave the substrate SNARE proteins. To test this theory, we utilized a cell based assay that monitors the amount of intact versus cleaved SNAP-25 protein within Neuro-2a cells[41]. In the absence of BoNT/A holotoxin or in the presence of isolated TD, SNAP-25 remains fully intact (Fig. 7, lane 1 and 4), and in the presence of toxin, a lower-molecular-weight proteolysis product of ~24 KDa is observed (Fig. 7, lane 2). In contrast to our prediction incubation of Neuro 2A cells with LC-TD results in cleavage of SNAP-25 as demonstrated on lane 3 of a representative western shown in Figure 7. These results indicate that BoNT/A LC-TD can enter neurons without the aid of the RBD when given 48 hr exposure, and potentially enter other cell types with equivalent efficiency.

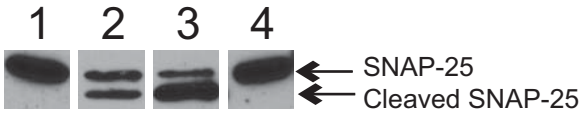

Fig. 7. Western blot analysis of BoNT/A cleavage of SNAP-25 within Neuro 2A cells. Lane 1 contains 20 mM HEPES incubated negative control, lane 2 contains endogenous SNAP-25 cleaved with BoNT/A holotoxin, lane 3 contains endogenous SNAP-25 cleaved with BoNT/A LC-TD, and lane 4 contains endogenous SNAP-25 unaffected by incubation of Neuro 2A cells with BoNT/A TD.

Discussion

Minimal protein necessary for BoNT channel activity and LC translocation

Previous studies have shown that BoNT forms pH dependent and voltage dependent channels in lipid bilayers [39, 42, 43] and neuronal cells [16, 44]. Similar channel activity has been demonstrated for the closely related tetanus toxin [14, 39, 45]and diphtheria toxin[14, 39, 46, 47]. BoNT channel activity was determined to be limited to the N-terminal half of the HC [43] (Figs. 3*B*, 3*C* and 4). The present study further delineated the channel forming domain to be the protein coding to amino acids 546-870 of the HC (Figs. 3*D* and 4), termed the beltless translocation domain as the two unstructured loops running perpendicular and parallel to the LC substrate recognition exosites were truncated out. Removal of the RBD released the pH dependence of channel formation, as demonstrated by channel activity of the TD and BTD under symmetric neutral pH conditions (Fig. 5).

BoNT intoxication requires that channel formation occurs concomitant with protein translocation; therefore we investigated the minimal domains required for productive LC translocation. The C-terminal half of the HC responsible for cell binding and internalization was determined to be unnecessary for BoNT/A LC translocation (Fig. 6). Although the belt region is not required for reconstitution of channel activity it may facilitate productive LC unfolding to a translocation competent conformation within the acidic compartment of the endosome.

Role of the Receptor binding domain in BoNT neurotoxicity

The receptor binding domain of BoNT insures efficient intoxication by three unique mechanisms. Initially, BoNT requires the RBD to reach the peripheral nervous system. BoNT holotoxin RBD binds receptors on the mucosal surface of gut epithelial cells; this process occurs independent of associated BoNT complex proteins. The holotoxin then undergoes receptor mediated endocytosis and transcytosis with subsequent delivery to the basolateral side of the epithelial cell [48-50]. Once released to the circulation BoNT holotoxin reaches cholinergic nerve cells and a second round of cell entry occurs. BoNTs enter sensitive neurons *via* receptor-mediated endocytosis [1, 51, 52]. The BoNT receptor-binding domain establishes the cellular specificity mediated by its high affinity interaction with a surface protein receptor and a ganglioside (GT_{1B}) co-receptor[8, 10-12]. The protein receptors involved in transcytosis through gut epithial cells have yet to be determined; the protein receptors mediating neuronal cell receptor mediated endocytosis have been determined for three of the seven serotypes: synaptic vesicle protein SV2 for BoNT/A, and synaptotagmins I and II for BoNT/B and BoNT/G. During cell binding and internalization the RBD restricts the TD from membrane insertion until residence within the acidic environment of the endosome. Without the RBD present the TD readily inserts into the plasma membrane of neuronal cells (Fig. 5*B*). The LC remains folded in the neutral pH environment outside the cell, incapable of translocating through the ~15 Å pore of the TD channel and remains a globular protein tethered to its carrier on the cell

surface by the disulfide linkage. In this manner the RBD serves to chaperone the LC and TD, insuring that partial unfolding of the LC is concurrent with TD channel formation thereby promoting productive LC translocation.

BoNT as a modular tool

The findings presented here illustrate the modular nature of BoNT, a protein in which each component functions individually yet the tight interplay governs that each domain serves as a chaperone for the others. The RBD insures TD channel formation occurs concurrently with LC unfolding to a translocation competent conformation (Figs. 5 and 6). The LC gates the TD channel within the positive potential membrane of the endosomal compartment in order to initiate LC translocation[16]. The TD belt protects the LC from premature cleavage of non-specific substrates until localization within the cytosol[29]. The TD itself protects the LC within the acidic environment of the endosome, chaperones the LC to the cytosol, and releases the LC in an enzymatically active conformation to the substrate SNARE proteins[17]. This modular function makes BoNT and similar modular toxins a tool for biomolecule delivery to predetermined target tissues[53-58]. Proteins of choices have been tethered to enzymatically inactive BoNT and demonstrated to translocate and function within the neuronal cell[58]. These studies have limited themselves to inactivation or removal of the enzymatic domain and addition of a new protein; however the replacement of the neuronal targeting receptor binding domain with one that recognizes a unique

cellular surface protein could make BoNT a putative delivery system for almost any cargo protein to the scientist's target tissue of choice.

Paradox of LC-TD channel activity vs. cellular specificity

Upon initial inspection the results of the single molecule electrophysiology seem to be disparate from the cell based neurotoxicity assay. In order to unravel the paradox we will consider the properties of the individual BoNT domains in the context of neuronal cells. Multiple studies have demonstrated that the LC partially unfolds, potentially to a molten globule state, upon residence within an acidic pH environment and remains folded and enzymatically active at neutral pH[17, 59, 60]. Therefore the LC must presumably enter an acidic environment in order to translocate to the cytosol. As demonstrated by the electrophysiology assay TD inserts into the membrane of Neuro 2A cells and transitions between the open and closed state under potentials prevalent at the plasma membrane (Fig. 7*B*). The TD channel would dissipate the electrochemical ionic gradient across the plasma membrane, potentially disrupting normal cellular function. The aberrant channel activity exhibited by the TD may stimulate endocytosis of that patch of membrane in an effort to resume normal cellular function. The folded LC tethered to the TD channel upon entering the endosomal compartment would translocate and the disulfide bridge be reduced to release the LC to the cytosol. In order to substantiate this theory one could assay the ability of extra cellular LC and single chain LC-TD to cleave endogenous SNAP 25 within Neuro 2A cells. Irrespective

of the paradox the result that BoNT/A LC-TD intoxicates neuronal cells in the absence of the cell targeting RBD demonstrates that LC-TD may be an even more effective therapy for muscle contraction disorders and a more dangerous bioweapon.

Acknowledgements

We thank J. Santos, M. Oblatt-Montal, L. Koriazova for perceptive comments. This work was supported by the Pacific Southwest Regional Center of Excellence NIH AI065359.

Chapter 6, in part, will be submitted for publication of the material as it may appear. I, Audrey Fischer, will be a contributing author of this paper.

References

1. Schiavo, G., M. Matteoli, and C. Montecucco, *Neurotoxins affecting neuroexocytosis.* Physiol Rev, 2000. **80**(2): p. 717-66.

2. Sathyamoorthy, V. and B.R. DasGupta, *Separation, purification, partial characterization and comparison of the heavy and light chains of botulinum neurotoxin types A, B, and E.* J Biol Chem, 1985. **260**(19): p. 10461-6.

3. Swaminathan, S., and Eswaramoorthy, S., *Structural analysis of the catalytic and binding sites of Clostridium botulinum neurotoxin B.* Nat Struct Biol, 2000. **7**: p. 693-699.

4. Lacy, D.B. and R.C. Stevens, *Sequence homology and structural analysis of the clostridial neurotoxins.* J Mol Biol, 1999. **291**(5): p. 1091-104.

5. Lacy, D.B., W. Tepp, A.C. Cohen, B.R. DasGupta, and R.C. Stevens, *Crystal structure of botulinum neurotoxin type A and implications for toxicity.* Nat Struct Biol, 1998. **5**(10): p. 898-902.

6. Yowler, B.C., R.D. Kensinger, and C.L. Schengrund, *Botulinum neurotoxin A activity is dependent upon the presence of specific gangliosides in neuroblastoma cells expressing synaptotagmin I.* J Biol Chem, 2002. **277**(36): p. 32815-9.

7. Tsukamoto, K., T. Kohda, M. Mukamoto, K. Takeuchi, H. Ihara, M. Saito, and S. Kozaki, *Binding of Clostridium botulinum type C and D neurotoxins to ganglioside and phospholipid. Novel insights into the receptor for clostridial neurotoxins.* J Biol Chem, 2005. **280**(42): p. 35164-71.

8. Nishiki, T., Y. Tokuyama, Y. Kamata, Y. Nemoto, A. Yoshida, K. Sato, M. Sekiguchi, M. Takahashi, and S. Kozaki, *The high-affinity binding of Clostridium botulinum type B neurotoxin to synaptotagmin II associated with gangliosides GT1b/GD1a.* FEBS Lett, 1996. **378**(3): p. 253-7.

9. Ginalski, K., C. Venclovas, B. Lesyng, and K. Fidelis, *Structure-based sequence alignment for the beta-trefoil subdomain of the clostridial neurotoxin family provides residue level information about the putative ganglioside binding site.* FEBS Lett, 2000. **482**(1-2): p. 119-24.

10. Dong, M., F. Yeh, W.H. Tepp, C. Dean, E.A. Johnson, R. Janz, and E.R. Chapman, *SV2 is the protein receptor for botulinum neurotoxin A.* Science, 2006. **312**(5773): p. 592-6.

11. Mahrhold, S., A. Rummel, H. Bigalke, B. Davletov, and T. Binz, *The synaptic vesicle protein 2C mediates the uptake of botulinum neurotoxin A into phrenic nerves.* FEBS Lett, 2006. **580**(8): p. 2011-4.

12. Rummel, A., T. Karnath, T. Henke, H. Bigalke, and T. Binz, *Synaptotagmins I and II act as nerve cell receptors for botulinum neurotoxin G.* J Biol Chem, 2004. **279**(29): p. 30865-70.

13. Gambale, F. and M. Montal, *Characterization of the channel properties of tetanus toxin in planar lipid bilayers.* Biophys J, 1988. **53**(5): p. 771-83.

14. Finkelstein, A., *Channels formed in phospholipid bilayer membranes by diphtheria, tetanus, botulinum and anthrax toxin.* J Physiol (Paris), 1990. **84**(2): p. 188-90.

15. Fischer, A. and M. Montal, *Characterization of Clostridial botulinum neurotoxin channels in neuroblastoma cells.* Neurotox Res, 2006. **9**(2-3): p. 93-100.

16. Fischer, A. and M. Montal, *Single molecule detection of intermediates during botulinum neurotoxin translocation across membranes.* Proc Natl Acad Sci U S A, 2007. **104**(25): p. 10447-52.

17. Koriazova, L.K. and M. Montal, *Translocation of botulinum neurotoxin light chain protease through the heavy chain channel.* Nat Struct Biol, 2003. **10**(1): p. 13-8.

18. Blasi, J., E.R. Chapman, E. Link, T. Binz, S. Yamasaki, P. De Camilli, T.C. Sudhof, H. Niemann, and R. Jahn, *Botulinum neurotoxin A selectively cleaves the synaptic protein SNAP-25.* Nature, 1993. **365**(6442): p. 160-3.

19. Schiavo, G., F. Benfenati, B. Poulain, O. Rossetto, P. Polverino de Laureto, B.R. DasGupta, and C. Montecucco, *Tetanus and botulinum-B neurotoxins block neurotransmitter release by proteolytic cleavage of synaptobrevin.* Nature, 1992. **359**(6398): p. 832-5.

20. Breidenbach, M.A. and A.T. Brunger, *Substrate recognition strategy for botulinum neurotoxin serotype A.* Nature, 2004. **432**(7019): p. 925-9.

21. Arndt, J.W., Q. Chai, T. Christian, and R.C. Stevens, *Structure of botulinum neurotoxin type D light chain at 1.65 A resolution: repercussions for VAMP-2 substrate specificity.* Biochemistry, 2006. **45**(10): p. 3255-62.

22. Arndt, J.W., W. Yu, F. Bi, and R.C. Stevens, *Crystal structure of botulinum neurotoxin type G light chain: serotype divergence in substrate recognition.* Biochemistry, 2005. **44**(28): p. 9574-80.

23. Agarwal, R., S. Eswaramoorthy, D. Kumaran, T. Binz, and S. Swaminathan, *Structural analysis of botulinum neurotoxin type E catalytic domain and its mutant Glu212-->Gln reveals the pivotal role of the Glu212 carboxylate in the catalytic pathway.* Biochemistry, 2004. **43**(21): p. 6637-44.

24. Agarwal, R., T. Binz, and S. Swaminathan, *Structural analysis of botulinum neurotoxin serotype F light chain: implications on substrate binding and inhibitor design.* Biochemistry, 2005. **44**(35): p. 11758-65.

25. Chai, Q., J.W. Arndt, M. Dong, W.H. Tepp, E.A. Johnson, E.R. Chapman, and R.C. Stevens, *Structural basis of cell surface receptor recognition by botulinum neurotoxin B.* Nature, 2006. **444**(7122): p. 1096-100.

26. Jin, R., A. Rummel, T. Binz, and A.T. Brunger, *Botulinum neurotoxin B recognizes its protein receptor with high affinity and specificity.* Nature, 2006. **444**(7122): p. 1092-5.

27. Segelke, B., M. Knapp, S. Kadkhodayan, R. Balhorn, and B. Rupp, *Crystal structure of Clostridium botulinum neurotoxin protease in a product-bound state: Evidence for noncanonical zinc protease activity.* Proc Natl Acad Sci U S A, 2004. **101**(18): p. 6888-93.

28. Hanson, M.A. and R.C. Stevens, *Cocrystal structure of synaptobrevin-II bound to botulinum neurotoxin type B at 2.0 A resolution.* Nat Struct Biol, 2000. **7**(8): p. 687-92.

29. Brunger, A.T., M.A. Breidenbach, R. Jin, A. Fischer, J.S. Santos, and M. Montal, *Botulinum neurotoxin heavy chain belt as an intramolecular chaperone for the light chain.* PLoS Pathog, 2007. **3**(9): p. 1191-4.

30. Binz, T., H. Kurazono, M. Wille, J. Frevert, K. Wernars, and H. Niemann, *The complete sequence of botulinum neurotoxin type A and comparison with other clostridial neurotoxins.* J Biol Chem, 1990. **265**(16): p. 9153-8.

31. Lacy, D.B. and R.C. Stevens, *Recombinant expression and purification of the botulinum neurotoxin type A translocation domain.* Protein Expr Purif, 1997. **11**(2): p. 195-200.

32. Blanes-Mira, C., C. Ibanez, G. Fernandez-Ballester, R. Planells-Cases, E. Perez-Paya, and A. Ferrer-Montiel, *Thermal stabilization of the catalytic domain of botulinum neurotoxin E by phosphorylation of a single tyrosine residue.* Biochemistry, 2001. **40**(7): p. 2234-42.

33. Oyler, G.A., G.A. Higgins, R.A. Hart, E. Battenberg, M. Billingsley, F.E. Bloom, and M.C. Wilson, *The identification of a novel synaptosomal-associated protein, SNAP-25, differentially expressed by neuronal subpopulations.* J Cell Biol, 1989. **109**(6 Pt 1): p. 3039-52.

34. Ferrer-Montiel, A.V., L.M. Gutierrez, J.P. Apland, J.M. Canaves, A. Gil, S. Viniegra, J.A. Biser, M. Adler, and M. Montal, *The 26-mer peptide released from SNAP-25 cleavage by botulinum neurotoxin E inhibits vesicle docking.* FEBS Lett, 1998. **435**(1): p. 84-8.

35. Fischer, A. and M. Montal, *Crucial role of the disulfide bridge between botulinum neurotoxin light and heavy chains in protease translocation across membranes.* J Biol Chem, 2007.

36. Carpaneto, A., A. Accardi, M. Pisciotta, and F. Gambale, *Chloride channels activated by hypotonicity in N2A neuroblastoma cell line.* Exp Brain Res, 1999. **124**(2): p. 193-9.

37. Lascola, C.D., D.J. Nelson, and R.P. Kraig, *Cytoskeletal actin gates a Cl- channel in neocortical astrocytes.* J Neurosci, 1998. **18**(5): p. 1679-92.

38. Simpson, L.L., *The interaction between aminoquinolines and presynaptically acting neurotoxins.* J Pharmacol Exp Ther, 1982. **222**(1): p. 43-8.

39. Hoch, D.H., M. Romero-Mira, B.E. Ehrlich, A. Finkelstein, B.R. DasGupta, and L.L. Simpson, *Channels formed by botulinum, tetanus, and diphtheria toxins in planar lipid bilayers: relevance to translocation of proteins across membranes.* Proc Natl Acad Sci U S A, 1985. **82**(6): p. 1692-6.

40. Smart, O.S., J. Breed, G.R. Smith, and M.S. Sansom, *A novel method for structure-based prediction of ion channel conductance properties.* Biophys J, 1997. **72**(3): p. 1109-26.

41. Eubanks, L.M., M.S. Hixon, W. Jin, S. Hong, C.M. Clancy, W.H. Tepp, M.R. Baldwin, C.J. Malizio, M.C. Goodnough, J.T. Barbieri, E.A. Johnson, D.L. Boger, T.J. Dickerson, and K.D. Janda, *An in vitro and in vivo disconnect uncovered through high-throughput identification of botulinum neurotoxin A antagonists.* Proc Natl Acad Sci U S A, 2007. **104**(8): p. 2602-7.

42. Donovan, J.J. and J.L. Middlebrook, *Ion-conducting channels produced by botulinum toxin in planar lipid membranes.* Biochemistry, 1986. **25**(10): p. 2872-6.

43. Blaustein, R.O., W.J. Germann, A. Finkelstein, and B.R. DasGupta, *The N-terminal half of the heavy chain of botulinum type A neurotoxin forms channels in planar phospholipid bilayers.* FEBS Lett, 1987. **226**(1): p. 115-20.

44. Sheridan, R.E., *Gating and permeability of ion channels produced by botulinum toxin types A and E in PC12 cell membranes.* Toxicon, 1998. **36**(5): p. 703-17.

45. Boquet, P. and E. Duflot, *Tetanus toxin fragment forms channels in lipid vesicles at low pH.* Proc Natl Acad Sci U S A, 1982. **79**(24): p. 7614-8.

46. Donovan, J.J., M.I. Simon, R.K. Draper, and M. Montal, *Diphtheria toxin forms transmembrane channels in planar lipid bilayers.* Proc Natl Acad Sci U S A, 1981. **78**(1): p. 172-6.

47. Silverman, J.A., J.A. Mindell, H. Zhan, A. Finkelstein, and R.J. Collier, *Structure-function relationships in diphtheria toxin channels: I. Determining a minimal channel-forming domain.* J Membr Biol, 1994. **137**(1): p. 17-28.

48. Maksymowych, A.B., M. Reinhard, C.J. Malizio, M.C. Goodnough, E.A. Johnson, and L.L. Simpson, *Pure botulinum neurotoxin is absorbed from the stomach and small intestine and produces peripheral neuromuscular blockade.* Infect Immun, 1999. **67**(9): p. 4708-12.

49. Maksymowych, A.B. and L.L. Simpson, *Binding and transcytosis of botulinum neurotoxin by polarized human colon carcinoma cells.* J Biol Chem, 1998. **273**(34): p. 21950-7.

50. Maksymowych, A.B. and L.L. Simpson, *Structural features of the botulinum neurotoxin molecule that govern binding and transcytosis across polarized human intestinal epithelial cells.* J Pharmacol Exp Ther, 2004. **310**(2): p. 633-41.

51. Simpson, L.L., *Ammonium chloride and methylamine hydrochloride antagonize clostridial neurotoxins.* J Pharmacol Exp Ther, 1983. **225**: p. 546-552.

52. Simpson, L.L., *Identification of the major steps in botulinum toxin action.* Annu Rev Pharmacol Toxicol, 2004. **44**: p. 167-193.

53. Dobrenis, K., A. Joseph, and M.C. Rattazzi, *Neuronal lysosomal enzyme replacement using fragment C of tetanus toxin.* Proc Natl Acad Sci U S A, 1992. **89**(6): p. 2297-301.

54. Francis, J.W., B.A. Hosler, R.H. Brown, Jr., and P.S. Fishman, *CuZn superoxide dismutase (SOD-1):tetanus toxin fragment C hybrid protein for targeted delivery of SOD-1 to neuronal cells.* J Biol Chem, 1995. **270**(25): p. 15434-42.

55. Liu, X.H., J.C. Castelli, and R.J. Youle, *Receptor-mediated uptake of an extracellular Bcl-x(L) fusion protein inhibits apoptosis.* Proc Natl Acad Sci U S A, 1999. **96**(17): p. 9563-7.

56. Ichinose, M., X.H. Liu, N. Hagihara, and R.J. Youle, *Extracellular Bad fused to toxin transport domains induces apoptosis.* Cancer Res, 2002. **62**(5): p. 1433-8.

57. Duggan, M.J., C.P. Quinn, J.A. Chaddock, J.R. Purkiss, F.C. Alexander, S. Doward, S.J. Fooks, L.M. Friis, Y.H. Hall, E.R. Kirby, N. Leeds, H.J. Moulsdale, A. Dickenson, G.M. Green, W. Rahman, R. Suzuki, C.C. Shone, and K.A. Foster, *Inhibition of release of neurotransmitters from rat dorsal root ganglia by a novel conjugate of a Clostridium botulinum toxin A endopeptidase fragment and Erythrina cristagalli lectin.* J Biol Chem, 2002. **277**(38): p. 34846-52.

58. Bade, S., A. Rummel, C. Reisinger, T. Karnath, G. Ahnert-Hilger, H. Bigalke, and T. Binz, *Botulinum neurotoxin type D enables cytosolic delivery of enzymatically active cargo proteins to neurones via unfolded translocation intermediates.* J Neurochem, 2004. **91**(6): p. 1461-72.

59. Cai, S., R. Kukreja, S. Shoesmith, T.W. Chang, and B.R. Singh, *Botulinum neurotoxin light chain refolds at endosomal pH for its translocation.* Protein J, 2006. **25**(7-8): p. 455-62.

60. Li, L. and B.R. Singh, *Spectroscopic analysis of pH-induced changes in the molecular features of type A botulinum neurotoxin light chain.* Biochemistry, 2000. **39**(21): p. 6466-74.

Chapter 7

Toosendanin Functions as a Translocation Dependent Inhibitor of Botulinum Neurotoxin

Abstract

Clostridial botulinum neurotoxin (BoNT) causes descending flaccid paralysis by blocking synaptic exocytosis. BoNT intoxication requires the di-chain protein to undergo conformational changes in response to pH and redox gradients across the endosomal membrane with consequent formation of a protein-conducting channel by the heavy chain (HC) that translocates the light chain (LC) protease into the cytosol. Here, we investigate the mechanism by which Toosendanin (TSDN), a triterpenoid derivative extracted from a Chinese traditional medicine, inhibits BoNT intoxication. We utilize a single molecule assay that monitors in real time the BoNT LC translocation through the HC channel in Neuro 2A cells under conditions which closely emulate those prevalent across endosomes. We show that TSDN arrests LC translocation with an IC_{50} ~ 4 nM. Interestingly, TSDN does not inhibit HC channel activity, instead increasing the channel propensity to reside within the open state. Toosendanin acts as a translocation dependent inhibitor of BoNT intoxication, highlighting the requirements for the tight interactions between the LC-cargo and the HC-chaperone during the entire progress of LC translocation across endosomal membranes.

Introduction

Botulinum neurotoxin (BoNT) is considered the most potent toxin known to humankind; inhibiting synaptic exocytosis in peripheral cholinergic synapses. Block of the neurotransmitter acetylcholine results in flaccid paralysis and death by respiratory failure. BoNT is utilized as a therapy for a number diseases characterized by abnormal muscle contraction; however, BoNT also poses as threat as a most feared bioweapon[1]. *Clostridium botulinum* cells secrete seven BoNTs isoforms known as BoNT/A to G. All isoforms are Zn^{2+}-endoproteases that block synaptic exocytosis by cleaving SNARE (soluble NSF attachment protein receptor) proteins[2-7]; their assembly into the SNARE core complex is considered a key step in fusion of the synaptic vesicle membrane with the neuronal plasma membrane[3, 5, 8]. Accordingly, there is a significant interest in developing effective anti-botulismic drugs that do not preclude the use of BoNT as a therapy or cosmeceutical.

All BoNT isoforms are synthesized as a single polypeptide chain with a molecular mass of ~150 kDa. Prior to secretion the precursor protein is cleaved into two polypeptides which remain linked by a disulfide bridge. The mature di-chain toxin consists of a 50 kDa light chain (LC) protease and a 100 kDa heavy chain (HC). The HC contains the translocation domain (TD) (the N-terminal half) and the receptor-binding domain (RBD) (the C-terminal half)[5, 9-11]. BoNT enter neurons by receptor-mediated endocytosis, initiated by the interactions between a specific ganglioside and protein co-receptor on the cell surface with the BoNT

RBD[5, 12]. Exposure of the BoNT-receptor complex to the acidic environment of endosomes induces a conformational change inserting the HC into the endosomal bilayer membrane[12-15]. Previously, we demonstrated that the HC forms a protein-conducting channel under endosomal conditions, translocating the LC protease into the cytosol and colocalizing it with its substrate SNARE protein[16, 17].

Toosendanin (TSDN) has been shown to have anti-botulismic effects, effectively protecting monkeys and mice from intoxication with BoNT/A[18, 19]; however the specific mechanism of action has yet to be elucidated. While TSDN has been shown to have no inhibition of BoNT/A LC protease[20], delay of the onset of HC channel activity has been shown in PC12 membranes[21]. These results indicated that TSDN acts at the step of LC translocation rather than receptor binding or SNARE cleavage. Here, we probed the effects of TSDN on each step of LC translocation through the HC channel/chaperone under conditions which closely emulate the endosomal compartment. We utilized a previously developed assay in Neuro 2A cells to monitor interactions between the HC and the LC during translocation with single molecule sensitivity. The assay allows us to determine in real time how TSDN inhibits BoNT intoxication. TSDN addition during early steps of LC translocation arrests LC translocation. TSDN addition after completion of LC translocation modulates HC channel activity, increasing the time the channel remains open rather than closed. These and previous findings indicate that TSDN interacts with the LC and the HC during the LC translocation step stabilizing an intermediate state, precluding completion of

translocation without directly inhibiting HC channel activity or LC proteolytic activity.

Experimental Procedures

Materials - Unless otherwise specified, all chemicals were purchased from Sigma-Aldrich. Purified native BoNT/A holotoxin was from Metabiologics. Toosendanin was a gift from Dr. Kim Janda, Scripps Research Institute.

Cell culture and patch clamp recordings - Excised patches from Neuro 2A cells in the inside-out configuration were used as described[22]. Current recordings were obtained under voltage clamp conditions. Records were acquired at a sampling frequency 20 kHz and filtered online to 2 kHz with Gaussian filter. All experiments were conducted at 22 $\pm$ 2 °C.

Solutions - To emulate endosomal conditions the *trans* compartment (bath) solution contained (in mM) NaCl 200, NaMOPS [3-(N-morpholino) propanesulfonic acid] 5, (pH 7.0 with HCl), tris-(2-carboxyethyl) phosphine (TCEP) 0.25, $ZnCl_2$ 1, and the *cis* compartment (pipet) solution contained (in mM) NaCl 200, NaMES [2-(N-morpholino) ethanesulfonic acid] 5, (pH 5.3 with HCl). The osmolarity of both solutions was determined to be ~390 mOsm. $ZnCl_2$ was used to block endogenous channel activity specific to Neuro 2A cells[23, 24]. BoNT reconstitution and channel insertion was achieved by supplementing 5 μg/mL BoNT holotoxin to the pipet solution, which was set to an endosomal pH of 5.3.

Data Analysis – Analysis performed on single bursts of each experimental record. Single channel conductance (γ) was calculated from Gaussian fits to current amplitude histograms. The total number of opening events (*N*) analyzed was 167,427. Time course of single channel conductance change for each experiment was calculated from γ of each record, where t = 0 s corresponds to onset of channel activity, and average time course was constructed from the set of individual experiments for a single condition. The voltage-dependence of channel opening was calculated from measurements of the fraction of time that the channel is open (P_o) as a function of voltage by integration of γ histograms where γ is $60 \leq \gamma \geq 75$ pS. Statistical values represent means ± SEM, unless otherwise indicated. *n* denotes the number of different experiments.

Results

Single molecule translocation assay

Translocation of BoNT/A LC by the BoNT/A HC channel can be monitored in real time and at the single molecule level in excised membrane patches from Neuro 2A cells[16]. Translocation requires pH 5.3 on the *cis* compartment, defined as the compartment containing BoNT/A, and pH 7.0 on the *trans* compartment which is supplemented with the membrane nonpermeable reductant TCEP, conditions which emulate those prevalent across endosomes. Translocation is then observed as a time-dependent increase in Na+ conductance through the HC channel, as illustrated by the control experiment

shown in Fig. 1*A*. Characteristic BoNT channel activity occurs in bursts and has ms transitions between the open (O) and closed (C) states[25]. The time course of change of the single channel conductance, γ, after insertion of BoNT/A holotoxin into the membrane displays multiple discrete transient intermediate conductances before achieving a γ of 67.1 ± 2.0 pS (Fig. 1*A*, right panel)[16]. This steady-state γ is also the characteristic conductance of isolated HC recorded under identical conditions; therefore it represents the conductance of the unoccupied HC in holotoxin experiments after LC translocation is complete. This pattern of channel activity allows us to operationally define two states of BoNT channel activity. An “occluded state” with the partially unfolded LC trapped within the channel during the translocation process. This is identified as a set of intermediate conductances corresponding to transitions between the closed state and several blocked open states. Upon completion of translocation and release of the LC an “unoccluded state” is visible associated to transitions between the closed state and the fully open state. We interpret the intermediate conductance states as reporters of discrete transient steps during the translocation of the LC across the membrane. During protease translocation, the protein-conducting channel progressively conducts more Na+ around the polypeptide chain before entering an exclusively ion-conductive state. This typical pattern of channel activity for holotoxin proceeds under conditions which mimic those across endosomes and lead to LC translocation and retrieval of protease activity after completion of translocation[17]. Thus, we have used this assay to examine the potential inhibition of the translocation process by Toosendanin.

Toosendanin modulates occluded and unoccluded BoNT/A channel activity

Previous studies have demonstrated that Toosendanin (TSDN) confers resistance against botulism by inhibiting entry of BoNT/A into cells[18, 19, 21]. To investigate if a step of the translocation process is inhibited by TSDN we utilized the translocation assay with time dependent additions of TSDN. BoNT/A holotoxin channels were allowed to form in the absence of TSDN; after onset of low conductance channel activity TSDN was added to the *trans* compartment at varying concentrations. 0.4 nM TSDN has no affect on channel activity; the time course of LC translocation is unaffected and always results in unoccluded channel activity. However, 4 nM TSDN arrests channel activity at an intermediate γ (Fig. 1*B*). This arrest of LC translocation persists for the remainder of the experiment. Addition of 40μM TSDN during the low conductance intermediates blocks any further channel activity as shown in the bottom panel of Figure 1*B*.

Addition of TSDN to the *trans* compartment to the unoccluded HC channel, $\gamma \approx 66$ pS, after completion of LC translocation results in altered channel kinetics. While γ remains constant, the probability of the channel to reside in the open state (P_o) is increased (Figure 1*C*). Addition of TSDN to the *trans* compartment at a concentration of 0.4 μM TSDN increases the P_o, promoting prolonged residence within the open state in a dose dependent manner as illustrated in the representative records shown in Figure 1*C*.

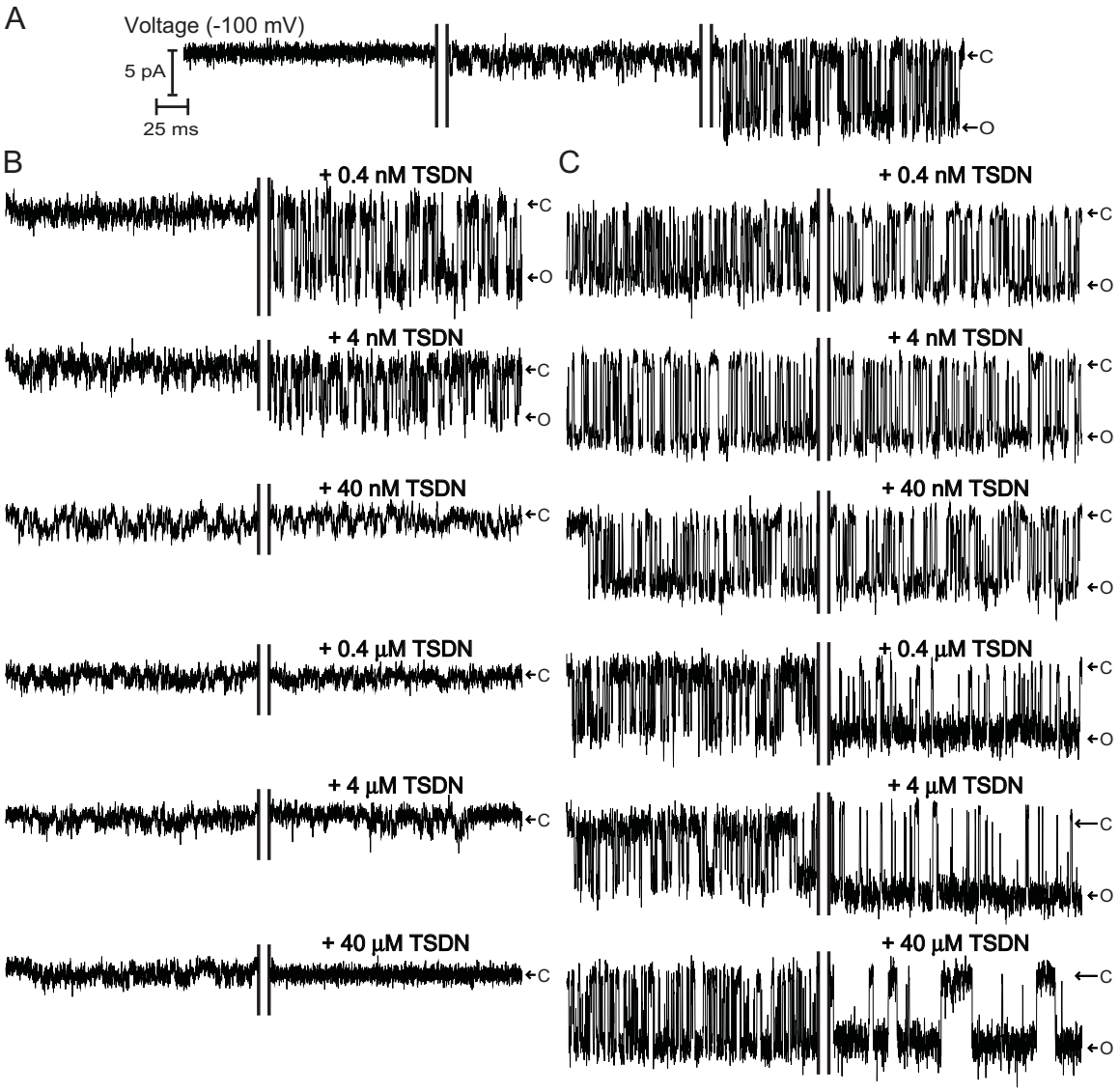

Fig. 1. BoNT holotoxin channels are modulated by Toosendanin added to the *trans* compartment. *A*, BoNT/A holotoxin channels in excised patches of Neuro 2A cells; patches start with no ion channel activity as shown in first record. BoNT channel activity begins 20 min after GΩ seal formation transitioning from low conductance intermediate state to the unoccluded state after completion of LC translocation. Channel opening is indicated by a downward deflection; C and O respectively denote the closed and open states. *B*, After BoNT/A channel insertion and during low conductance intermediates (left panel) TSDN addition inhibits growing conductance event monitored in *A* (right panel). 40 μM TSDN completely blocks BoNT channel activity, 0.4 μM TSDN arrests the channel in low conductance intermediate state for the lifetime of the patch, 0.4 nM TSDN has no affect on LC translocation. *C*, After completion of BoNT/A LC translocation TSDN addition modulates unoccluded BoNT channel activity. While 40 nM TSDN has no affect on channel kinetics, 0.4 μM TSDN increases BoNT channel $P_{o.}$

Toosendanin arrests LC translocation without inhibition of unoccluded HC channel activity

Analysis of the channel kinetics for BoNT/A with TSDN addition before and after completion of LC translocation resolves a unique binding pattern between TSDN and HC channel. A single growing conductance event associated with channel insertion and LC translocation and release has an average half-time for completion ($T_{½}$), estimated from the transition to high conductance is 150 ± 25 s (Fig. 2*A*). TSDN inhibits this process by decreasing the P_o of the channel and arresting LC translocation. Addition of 0.4 nM TSDN delays the completion of LC translocation as determined from the average $T_{½}$ = 220 ± 10 s (Fig 2*A*). Addition of 4 nM TSDN results in an incomplete time course, the steady state γ ~ 35 pS (Fig 2*A*). The $T_{½}$ increases from 150 s up to 350 s; nearly double the time and still never achieving the unoccluded HC channel $\gamma \cong$ 66 pS (ref) (Fig 2*A*). TSDN concentrations above 4 nM irreversibly arrest the BoNT/A channel in a low conductance state. Analysis of the steady state conductance of the TSDN treated channel activity determined that TSDN arrests LC translocation with an IC_{50} value of 4.0 ± 1.8 nM (Fig. 2*A*, 2*B*). In contrast, TSDN addition to the unoccluded HC channel after completion of LC translocation does not inhibit channel activity; rather it results in channel activity with an increased P_o. In addition, the channel activity is shifted from only being active at negative membrane potentials towards activity at concomitantly increased positive membrane potentials with the concentration of TSDN (Fig. 2*C*). The voltage at which P_o = 0.5, $V_{1/2}$, for unmodified, unoccluded HC channels is ~ –67 mV (ref, Fig. 2*C*). Nanomolar

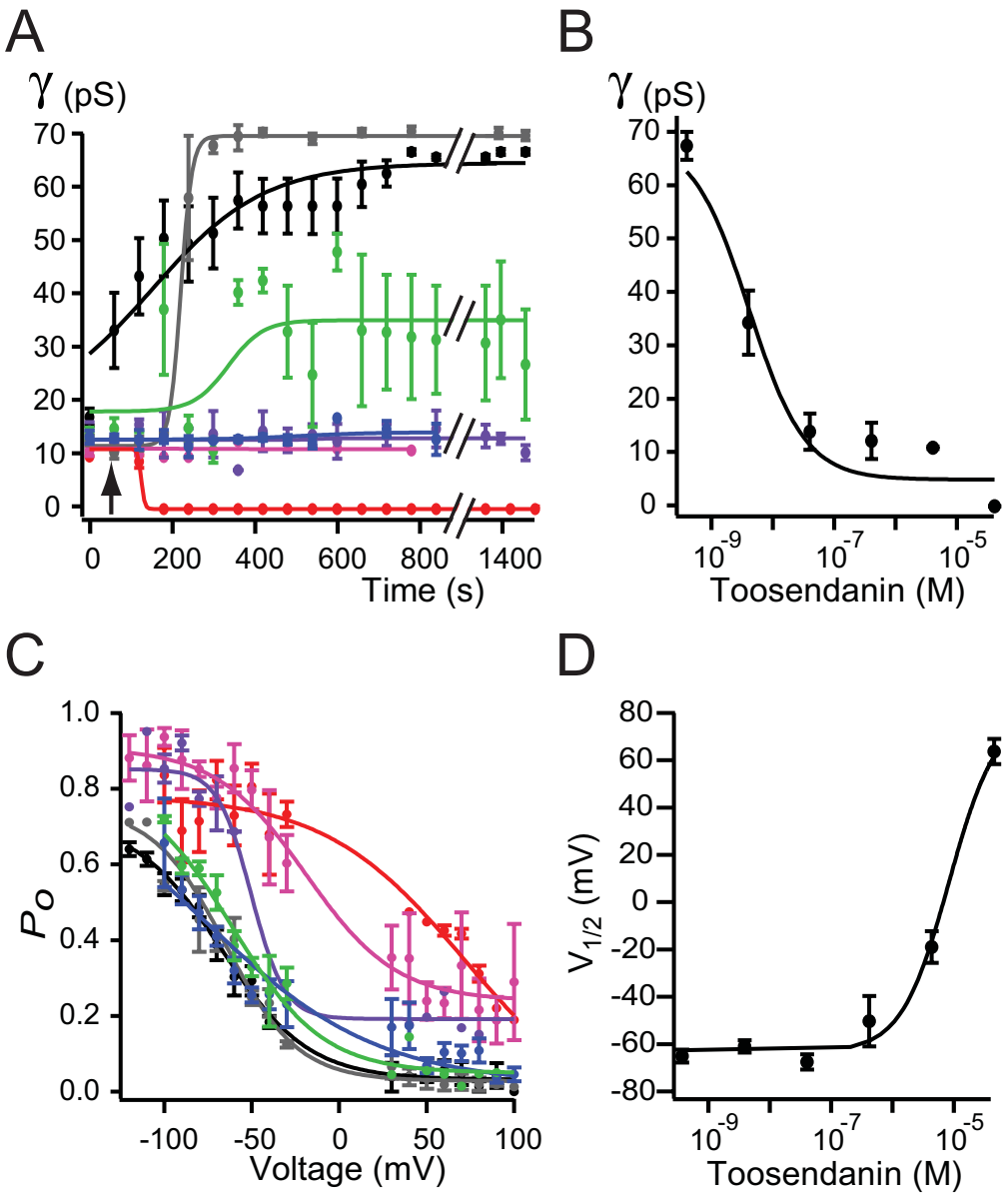

Fig. 2. Analysis of TSDN modulation of BoNT/A channel activity before (*A* and *B*) and after (*C* and *D*) completion of LC translocation. *A*, Average time course of growing conductance intermediates states of LC translocation for BoNT/A –TSDN (●) (*n*=6), 0.4 nM TSDN (●) (*n*=2), 4 nM TSDN (●) (*n*=3), 40 nM TSDN (●) (*n*=3), 0.4 μM TSDN (●) (*n*=2), 4 μM TSDN (●) (*n*=1), and 40 μM TSDN (●) (*n*=1) (average *N* per data point = 2,744 events). Arrow indicates time point at which TSDN was added to the *trans* compartment. *B*, Steady state single channel conductance as a function of Toosendanin concentration for data in *A*; IC_{50} = 3.8 ± 2.0 nM. *C*, P_o as a function of voltage for unoccluded BoNT/A –TSDN (●) (*n*=6), 0.4 nM TSDN (●) (*n*=2), 4 nM TSDN (●) (*n*=1), 40 nM TSDN (●) (*n*=3), 0.4 μM TSDN (●) (*n*=2), 4 μM TSDN (●) (*n*=3), and 40 μM TSDN (●) (*n*=2) (average *N* per data point = 784 events). *D*, $V_{1/2}$ as a function of Toosendanin concentration for data in *C*; IC_{50} = 8.9 ± 1.8 μM.

Table 1. Unoccluded BoNT/A channel characteristics are altered by addition of TSDN to *trans* compartment

Condition	$V_{1/2}$ (mV)	P_o max
- TSDN	-67.1 ± 3.2	0.67 ± 0.05
0.4nM TSDN	-69.6 ± 3.0	0.80 ± 0.02
4 nM TSDN	-62.5 ± 5.5	0.84 ± 0.06
40nM TSDN	-65.3 ± 5.2	0.65 ± 0.05
0.4 μM TSDN	-50.3 ± 10.6	0.85 ± 0.03
4 μM TSDN	-19.0 ± 7.2	0.95 ± 0.05
40 μM TSDN	+63.7 ± 5.4	0.85 ± 0.10

concentrations of TSDN do not affect the unoccluded BoNT/A channel kinetics; however, addition of 0.4 μM TSDN shifts the P_o vs. voltage curve to the right, with a $V_{1/2} \cong -50$ mV. Further, channel activity is now clearly distinguishable at + 60 mV (Fig. 2*C*). Addition of 40 μM TSDN drastically alters unoccluded BoNT/A channel activity; $V_{1/2} = +63.7 \pm 5.4$ mV and transitions to the open state persist at and above a membrane potential of +100 mV (Figs. 2*C* and 2*D*). TSDN's affect on unoccluded BoNT/A channel activity was quantified from measurements of the $V_{1/2}$ as a function of TSDN concentration. The $IC_{50} = 8.9 \pm 1.8$ μM, a concentration ~2000 fold above that necessary to arrest LC translocation (Fig. 2*D*).

Discussion

BoNT HC Channel as a Target for Intervention

The HC channel may represent the most effective target for inhibition of BoNT neurotoxicity, although most studies consider the LC a technically less challenging target for intervention. The endopeptidase activity of the LC is similar to other Zn metalloproteases like thermolysin making small molecule interaction modeling a powerful tool[26]. The crystal structures of six of the seven LC serotypes have been solved, some with small molecules coordinated in the active site[10, 11, 27-33]. Drug sensitivity can be improved by coordination with the Zn ion. Unfortunately, these drugs all have a high degree of cross reactivity to cellular proteases as the active site is highly conserved and not involved in high

specificity substrate recognition. The extended enzyme substrate interface required for optimal substrate recognition, involves an array of substrate binding sites distant from the active site[31, 34]. These exosites may be a more effective target for LC neutralization; however each serotype has a different substrate, requiring design of seven unique peptides. Studies focused on inhibition at the early stages of intoxication have aimed to develop blockers of RBD interaction with known receptors[35, 36]. This approach is limited to developing therapies for those serotypes that the protein co-receptor has been determined, namely BoNT/A which recognizes SV2 and BoNT/B and G which recognize Synaptotagmin II[37-39]. These studies have shown that while peptides can be developed to high sensitivity, blockers are difficult to improve to the extent that the molecules can compete with neuronal cells for binding[35, 36]. The RBD and LC serotype specificity arises from interactions with host cellular proteins whereas the TD functions to chaperone the LC cargo in response to the targeting of the RBD. The TD may function as a universal carrier; small molecules that inhibit BoNT/A channel activity exhibit similar effects on the other serotypes (data not shown) thereby eliminating the necessity to develop multiple therapies. Small molecule drugs that serve as efficient blockers of voltage dependent channels are subject to combinatorial based chemistry optimization to improve both binding affinity and cross reactivity with host channel proteins[40-42]. Even though the HC has no crystal structure as a membrane inserted protein and the mechanism of small molecule binding has not been structurally determined, the

functional study presented here, inhibition of BoNT/A single channels (Fig. 1*B*), has been supported by animal models that demonstrate efficient protection[18].

TSDN affect on the HC within the endosome after LC translocation

The BoNT channel is closed within the environment of the endosomal membrane, namely pH 5.3 and positive voltage potentials within the *cis* compartment and pH 7.0 and negative potentials on the opposite compartment[16, 25]. After LC translocation the closed HC channel conformation precludes the passive dissipation of the electrochemical ionic gradients across endosome. Micro molar concentrations of TSDN shift the voltage dependence of the HC channel (Fig. 2*D*); consequently the unoccluded HC channel would transition to the open state within endosomal membranes. The resulting dissipation in electrochemical gradient could disrupt endosomal function and potentially harming host cellular processes. Interestingly, the modulation of HC channel activity by TSDN occurs at a concentration 2000 fold above the concentration at which LC translocation is efficiently arrested. The dual mode modulation of BoNT channel activity is sufficiently disparate in concentration as to promote TSDN use as a prophylactic.

Mechanism of LC translocation arrest by TSDN

We propose that TSDN arrest of LC translocation is dependent upon the protein-protein interactions between the HC and LC during this process.

Preliminary studies have shown no inhibition of the enzymatic activity of the LC by TSDN; however, TSDN may still interact with the LC. The enzymatically active folded LC presents different residues and an accordingly unique surface area environment from that of the partially unfolded LC exposed to endosomal pH and within the pore of the HC channel[17, 43]. TSDN does not function as an open channel blocker of the HC (Fig. 1*C*); characterized as attenuating the single channel conductance, shortening the open channel lifetime and reducing the channel open probability. While an open channel blocker may inhibit voltage dependent channel openings, the LC induced gating of the channel during translocation may reverse that block. At micomolar concentrations TSDN delays but does not effectively inhibit channel formation as demonstrated in studies with BoNT/A in PC12 cells by Li and Shi[21]. In contrast, TSDN arrests LC translocation through preformed HC channels with nanomolar sensitivity. TSDN inhibition may arise from the coordination of the elongated LC with the HC channel as the LC traverses from the endosomal to cytosolic compartments by stabilizing intermediate conformations of the channel-cargo complex during LC translocation. TSDN coupling of the LC to the HC locks the complex in a translocating conformer that is irreversibly incomplete.

Acknowledgements

We thank J. Santos, M. Oblatt-Montal, L. Koriazova for perceptive comments. This work was supported by the Pacific Southwest Regional Center of Excellence NIH AI065359.

Chapter 7, in part, will be submitted for publication of the material as it may appear. I, Audrey Fischer, will be the primary author of this paper.

References

1. Arnon, S.S., R. Schechter, T.V. Inglesby, D.A. Henderson, J.G. Bartlett, M.S. Ascher, E. Eitzen, A.D. Fine, J. Hauer, M. Layton, S. Lillibridge, M.T. Osterholm, T. O'Toole, G. Parker, T.M. Perl, P.K. Russell, D.L. Swerdlow, and K. Tonat, *Botulinum toxin as a biological weapon: medical and public health management.* Jama, 2001. **285**(8): p. 1059-70.

2. Blasi, J., E.R. Chapman, E. Link, T. Binz, S. Yamasaki, P. De Camilli, T.C. Sudhof, H. Niemann, and R. Jahn, *Botulinum neurotoxin A selectively cleaves the synaptic protein SNAP-25.* Nature, 1993. **365**(6442): p. 160-3.

3. Jahn, R., T. Lang, and T.C. Sudhof, *Membrane fusion.* Cell, 2003. **112**(4): p. 519-33.

4. Schiavo, G., O. Rossetto, A. Santucci, B.R. DasGupta, and C. Montecucco, *Botulinum neurotoxins are zinc proteins.* J Biol Chem, 1992. **267**(33): p. 23479-83.

5. Schiavo, G., M. Matteoli, and C. Montecucco, *Neurotoxins affecting neuroexocytosis.* Physiol Rev, 2000. **80**(2): p. 717-66.

6. Sutton, R.B., Fasshauer, D., Jahn, R., and Brunger, A. T., *Crystal structure of a SNARE complex involved in synaptic exocytosis at 2.4 A resolution.* Nature, 1998. **395**: p. 347-353.

7. Weber, T., Zemelman, B. V., McNew, J. A., Westermann, B., Gmachl, M., Parlati, F., Söllner, T. H., and Rothman, J. E., *SNAREpins: minimal machinery for membrane fusion.* Cell, 1998. **92**(759-772).

8. Jackson, M.B. and E.R. Chapman, *Fusion pores and fusion machines in Ca2+-triggered exocytosis.* Annu Rev Biophys Biomol Struct, 2006. **35**: p. 135-60.

9. Lacy, D.B. and R.C. Stevens, *Sequence homology and structural analysis of the clostridial neurotoxins.* J Mol Biol, 1999. **291**(5): p. 1091-104.

10. Lacy, D.B., W. Tepp, A.C. Cohen, B.R. DasGupta, and R.C. Stevens, *Crystal structure of botulinum neurotoxin type A and implications for toxicity.* Nat Struct Biol, 1998. **5**(10): p. 898-902.

11. Swaminathan, S., and Eswaramoorthy, S., *Structural analysis of the catalytic and binding sites of Clostridium botulinum neurotoxin B.* Nat Struct Biol, 2000. **7**: p. 693-699.

12. Simpson, L.L., *Identification of the major steps in botulinum toxin action.* Annu Rev Pharmacol Toxicol, 2004. **44**: p. 167-193.

13. Simpson, L.L., *Ammonium chloride and methylamine hydrochloride antagonize clostridial neurotoxins.* J Pharmacol Exp Ther, 1983. **225**: p. 546-552.

14. Montecucco, C., G. Schiavo, and B.R. Dasgupta, *Effect of pH on the interaction of botulinum neurotoxins A, B and E with liposomes.* Biochem J, 1989. **259**(1): p. 47-53.

15. Lawrence, G., J. Wang, C.K. Chion, K.R. Aoki, and J.O. Dolly, *Two protein trafficking processes at motor nerve endings unveiled by botulinum neurotoxin E.* J Pharmacol Exp Ther, 2007. **320**(1): p. 410-8.

16. Fischer, A. and M. Montal, *Single molecule detection of intermediates during botulinum neurotoxin translocation across membranes.* Proc Natl Acad Sci U S A, 2007. **104**(25): p. 10447-52.

17. Koriazova, L.K. and M. Montal, *Translocation of botulinum neurotoxin light chain protease through the heavy chain channel.* Nat Struct Biol, 2003. **10**(1): p. 13-8.

18. Shi, Y.L. and Z.F. Wang, *Cure of experimental botulism and antibotulismic effect of toosendanin.* Acta Pharmacol Sin, 2004. **25**(6): p. 839-48.

19. Shih, Y.L. and K. Hsu, *Anti-botulismic effect of toosendanin and its facilitatory action on miniature end-plate potentials.* Jpn J Physiol, 1983. **33**(4): p. 677-80.

20. Zhou, J.Y., Z.F. Wang, X.M. Ren, M.Z. Tang, and Y.L. Shi, *Antagonism of botulinum toxin type A-induced cleavage of SNAP-25 in rat cerebral synaptosome by toosendanin.* FEBS Lett, 2003. **555**(2): p. 375-9.

21. Li, M.F. and Y.L. Shi, *Toosendanin interferes with pore formation of botulinum toxin type A in PC12 cell membrane.* Acta Pharmacol Sin, 2006. **27**(1): p. 66-70.

22. Fischer, A. and M. Montal, *Crucial role of the disulfide bridge between botulinum neurotoxin light and heavy chains in protease translocation across membranes.* J Biol Chem, 2007.

23. Carpaneto, A., A. Accardi, M. Pisciotta, and F. Gambale, *Chloride channels activated by hypotonicity in N2A neuroblastoma cell line.* Exp Brain Res, 1999. **124**(2): p. 193-9.

24. Lascola, C.D., D.J. Nelson, and R.P. Kraig, *Cytoskeletal actin gates a Cl- channel in neocortical astrocytes.* J Neurosci, 1998. **18**(5): p. 1679-92.

25. Fischer, A. and M. Montal, *Characterization of Clostridial botulinum neurotoxin channels in neuroblastoma cells.* Neurotox Res, 2006. **9**(2-3): p. 93-100.

26. Cai, S. and B.R. Singh, *Strategies to design inhibitors of Clostridium botulinum neurotoxins.* Infect Disord Drug Targets, 2007. **7**(1): p. 47-57.

27. Agarwal, R., T. Binz, and S. Swaminathan, *Structural analysis of botulinum neurotoxin serotype F light chain: implications on substrate binding and inhibitor design.* Biochemistry, 2005. **44**(35): p. 11758-65.

28. Agarwal, R., S. Eswaramoorthy, D. Kumaran, T. Binz, and S. Swaminathan, *Structural analysis of botulinum neurotoxin type E catalytic domain and its mutant Glu212-->Gln reveals the pivotal role of the Glu212 carboxylate in the catalytic pathway.* Biochemistry, 2004. **43**(21): p. 6637-44.

29. Arndt, J.W., Q. Chai, T. Christian, and R.C. Stevens, *Structure of botulinum neurotoxin type D light chain at 1.65 A resolution: repercussions for VAMP-2 substrate specificity.* Biochemistry, 2006. **45**(10): p. 3255-62.

30. Arndt, J.W., W. Yu, F. Bi, and R.C. Stevens, *Crystal structure of botulinum neurotoxin type G light chain: serotype divergence in substrate recognition.* Biochemistry, 2005. **44**(28): p. 9574-80.

31. Breidenbach, M.A. and A.T. Brunger, *Substrate recognition strategy for botulinum neurotoxin serotype A.* Nature, 2004. **432**(7019): p. 925-9.

32. Segelke, B., M. Knapp, S. Kadkhodayan, R. Balhorn, and B. Rupp, *Crystal structure of Clostridium botulinum neurotoxin protease in a product-bound state: Evidence for noncanonical zinc protease activity.* Proc Natl Acad Sci U S A, 2004. **101**(18): p. 6888-93.

33. Silvaggi, N.R., G.E. Boldt, M.S. Hixon, J.P. Kennedy, S. Tzipori, K.D. Janda, and K.N. Allen, *Structures of Clostridium botulinum Neurotoxin Serotype A Light Chain complexed with small-molecule inhibitors highlight active-site flexibility.* Chem Biol, 2007. **14**(5): p. 533-42.

34. Chen, S. and J.T. Barbieri, *Multiple pocket recognition of SNAP25 by botulinum neurotoxin serotype E.* J Biol Chem, 2007. **282**(35): p. 25540-7.

35. Eswaramoorthy, S., D. Kumaran, and S. Swaminathan, *Crystallographic evidence for doxorubicin binding to the receptor-binding site in Clostridium botulinum neurotoxin B.* Acta Crystallogr D Biol Crystallogr, 2001. **57**(Pt 11): p. 1743-6.

36. Arkin, M.R., Wells, J. A., *Small-molecule inhibitors of protein-protein interactions: progressing towards the dream.* Nat Rev Drug Dis., 2004. **3**: p. 301-317.

37. Dong, M., F. Yeh, W.H. Tepp, C. Dean, E.A. Johnson, R. Janz, and E.R. Chapman, *SV2 is the protein receptor for botulinum neurotoxin A.* Science, 2006. **312**(5773): p. 592-6.

38. Mahrhold, S., A. Rummel, H. Bigalke, B. Davletov, and T. Binz, *The synaptic vesicle protein 2C mediates the uptake of botulinum neurotoxin A into phrenic nerves.* FEBS Lett, 2006. **580**(8): p. 2011-4.

39. Rummel, A., T. Karnath, T. Henke, H. Bigalke, and T. Binz, *Synaptotagmins I and II act as nerve cell receptors for botulinum neurotoxin G.* J Biol Chem, 2004. **279**(29): p. 30865-70.

40. Lacinova, L., *Voltage-dependent calcium channels.* Gen Physiol Biophys, 2005. **24 Suppl 1**: p. 1-78.

41. Lipton, S.A., *Failures and successes of NMDA receptor antagonists: molecular basis for the use of open-channel blockers like memantine in the treatment of acute and chronic neurologic insults.* NeuroRx, 2004. **1**(1): p. 101-10.

42. Hirsh, A.J., B.F. Molino, J. Zhang, N. Astakhova, W.B. Geiss, B.J. Sargent, B.D. Swenson, A. Usyatinsky, M.J. Wyle, R.C. Boucher, R.T. Smith, A. Zamurs, and M.R. Johnson, *Design, synthesis, and structure-activity relationships of novel 2-substituted pyrazinoylguanidine epithelial sodium channel blockers: drugs for cystic fibrosis and chronic bronchitis.* J Med Chem, 2006. **49**(14): p. 4098-115.

43. Cai, S., R. Kukreja, S. Shoesmith, T.W. Chang, and B.R. Singh, *Botulinum neurotoxin light chain refolds at endosomal pH for its translocation.* Protein J, 2006. **25**(7-8): p. 455-62.

Chapter 8

Conclusions and Looking Forward

Introduction

"The dose makes the poison". This statement, attributed to Paracelsus, the father of toxicology (1493-1541), is embodied by Botulinum neurotoxins (BoNT). On one hand BoNT is the most poisonous toxin known and the causative agent of botulism; on the other, it is a wonderful drug. Based on its exquisitely powerful neuroparalytic activity, BoNT has gained tremendous popularity in the past few years as it became the first biological toxin (BoNT serotype A) to receive FDA approval for the treatment of human disease, most notably for dystonias, blepharospasm, cervical torticollis, and strabismus, though it has been elevated to the practical rank of "panacea" for a rapidly growing list of conditions involving muscle spasm, not the least its cosmeceutical blockbuster role. Notably, BoNT is a most feared bioweapon still without an antidote[1].

Clostridium botulinum cells produce seven BoNT isoforms designated serotypes A to G[2]. All BoNT serotypes are synthesized as a single polypeptide chain with M_r ~150 kDa. This precursor protein is cleaved by a clostridial protease into two polypeptides which remain linked by a disulfide bridge[3]. The mature di-chain toxin consists of a 50 kDa light chain (LC) Zn^{2+}-metalloprotease and a 100 kDa heavy chain (HC). The HC encompasses the translocation domain (TD) and the receptor-binding domain (RBD)[2, 4-6]. It is generally agreed that BoNTs exert their neurotoxic effect by a multi-step mechanism[1, 2, 7]: binding, internalization, translocation across endosomal membranes (Fig. 1), and proteolytic degradation of target. The LCs act as sequence-specific endoproteases that cleave unique components of the SNARE (soluble NSF

attachment protein receptor) complex − a protein assembly known to mediate synaptic vesicle fusion[2, 8-10]. Accordingly, SNARE proteolysis destabilizes or prevents full assembly of the SNARE core complex, abrogating fusion of synaptic vesicles with the plasma membrane and aborts neurotransmitter release.

From the fundamental viewpoint, BoNT is a modular nanomachine and a marvel of protein design. The BoNT protein highlights the simplicity of its modular design to attain its exquisite activity. The challenge is to understand how this protein machine has evolved to such level of sophistication; how this modular nanomachine is designed to accomplish the exquisite and selective transport of one of its modules - an enzyme, by another module - a protein-conducting channel (Fig. 1). Our previous endeavor has established the notion that BoNT exploits its modular design to achieve its potent toxicity which relies on the transmembrane chaperone activity of one of its modules (the heavy chain –HC– protein-conducting channel, depicted in orange in Fig. 1) to protect the conformation of another module, its light chain (LC) cargo during transit and ensure its proper refolding at the completion of translocation. The LC is illustrated in purple (Fig. 1) to highlight the unfolding/refolding dynamics of cargo during transit and the associated transient interactions between cargo and channel.

BoNT Channel Activity Under Conditions Prevalent at Endosomes

Figure 1 depicts a model of the sequence of events underlying BoNT LC translocation through the HC channel which is consistent with the findings collected thus far[11-14] and reviewed in this Chapter. Step 1 shows the crystal

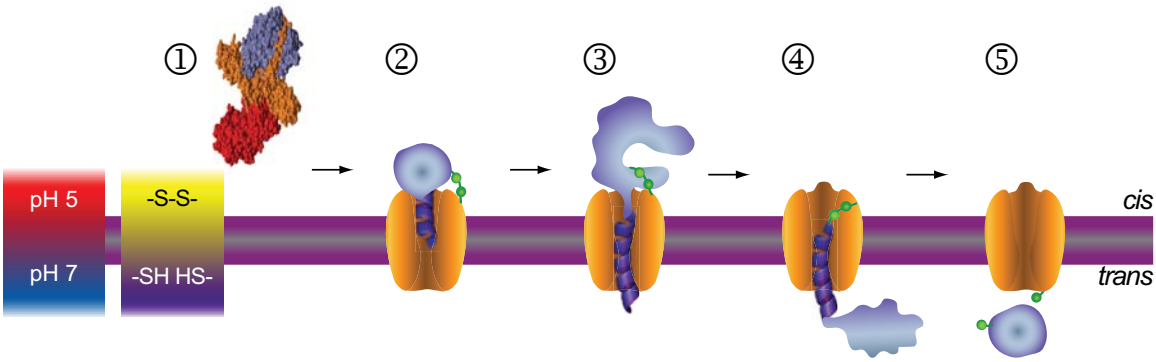

Fig. 1. Sequence of events underlying BoNT LC translocation through the HC channel. ① BoNT/A holotoxin prior to insertion in the membrane (grey bar with magenta boundaries); BoNT/A is represented by the crystal structure rendered on YASARA (www.YASARA.org) using Protein Data Bank accession code 3BTA [6]. Then, schematic representation of the membrane inserted BoNT/A during an entry event②, a series of transfer steps (③,④) and an exit event⑤, under conditions that recapitulate those across endosomes. Reproduced with permission from reference [14]. Copyright (2007), National Academy of Sciences, U.S.A.

structure BoNT/A prior to insertion into the membrane[5]: LC is purple, TD is orange, and RBD is red. Then is shown a schematic representation of the membrane inserted BoNT/A at the onset of translocation (step 2) with a partially unfolded LC (purple) trapped within the HC channel (orange), a series of transfer steps (steps 3 and 4), and an exit event at the completion of translocation (step 5). Translocation proceeds under conditions that recapitulate those across endosomes: the interchain disulfide bridge (green) is intact in the low pH, oxidizing environment of the *cis* compartment, corresponding to the endosome interior. The presence of reductant and neutral pH in the *trans* compartment, corresponding to the cytosol, promotes refolding of LC and release from HC after completion of translocation.

What is the evidence for the model? First, we probed the role of the disulfide bridge in the translocation process[12]. We exploited the differential accessibility of the disulfide cross-link between the HC and the LC to a membrane-impermeant reductant (tris-(2-carboxyethyl) phosphine-TCEP) to identify requirements for translocation across membranes. We showed that channel formation and LC translocation across membranes require both a pH gradient and a redox gradient, acidic and oxidizing on the *cis* compartment in which BoNT/A is present and neutral and reducing on the *trans* compartment in which the substrate SNAP-25 is present. These conditions emulate the pH and redox gradients across endosomes [12-14]and allow the formation of transmembrane channels by BoNT/A and BoNT/E. The initial results were obtained from planar lipid bilayer membranes devoid of any additional cellular

components[12]. The equivalent pattern of activity is recorded from membrane patches isolated from neuroblastoma cells[13-15]. In contrast, unreduced di-chain BoNT/A does not form channels under otherwise equivalent conditions and disulfide bridge reduced and peptide linked BoNT/E forms persistently occluded channels. Given that pre-reduced BoNT/A forms channels with properties equivalent to those of the isolated HC[12-14], and that the HC is a channel irrespective of the redox state[12-14], the inescapable conclusion is that the anchored LC cargo occludes the HC channel.

Release of Cargo from Chaperone is Necessary for Productive Translocation.

For BoNT/A, the disulfide crosslink between LC and HC must be on the *trans* (cytosolic) compartment to achieve productive translocation of the LC cargo (Fig. 1, Step 5)[12, 14, 15]. Disulfide reduction on the *cis* compartment dissociates the LC cargo from the HC prior to translocation and therefore generates a HC channel devoid of translocation activity[12, 13]. Disulfide disruption within the bilayer during translocation aborts it[15]. We infer that completion of LC translocation occurs as the disulfide bridge, C-terminus of the LC, enters the cytosolic compartment. This analysis supports a model of N- to C-terminal orientation of cargo during translocation with the C-terminus as the last portion to be translocated and exit the channel (Fig. 1, Step 5). We propose that an intact disulfide bridge is a necessary condition for translocation but not for channel insertion, as demonstrated by the fact that the isolated HC channel is

unperturbed by chemical reductants[12]. The tight coupling of translocation completion with disulfide reduction strongly argues in favor of the view that LC refolding precludes retrotranslocation. From this viewpoint, refolding in cytosol may be interpreted as a trap that prevents retrotranslocation and dictates the unidirectional nature of the translocation process. The disulfide linkage is, therefore, a crucial aspect of the BoNT toxicity and is required for chaperone function, acting as a principal determinant for cargo translocation and release.

Is the intact disulfide bridge specifically required for LC translocation? While BoNT/A is cleaved to the mature di-chain within the *Clostridium* bacteria, BoNT/E is not cleaved before secretion[3]. Therefore, the single-chain BoNT/E holotoxin provides a path to explore the linkage requirements for LC translocation. For BoNT/E, completion of LC translocation occurs only after proteolytic cleavage by trypsin and disulfide reduction in the *trans* compartment, implying that release of cargo from chaperone is necessary for productive translocation (Fig. 1, Step 5)[14]. In the absence of trypsin in the *trans* compartment channel insertion and onset of translocation proceed to a steady state characterized by unrelieved occlusion of the HC channel by the LC. In contrast, presence of trypsin in the *trans* compartment leads to the appearance of channels with single channel properties equivalent to those of isolated HC, a hallmark of unoccluded channels. Furthermore, single-chain BoNT/E, reduced prior to the translocation assay, displays persistently occluded channel activity despite the fact that trypsin is present in the *trans* compartment. Proteolytic cleavage of LC from HC and disulfide reduction during the exit event are

therefore required for productive translocation (Fig. 1, Step 5). These findings also imply that the transformation of an occluded state characterized by low γ intermediates with prolonged pore occupancy into an unoccluded channel with γ ~ 65 pS only occurs after the LC completes translocation from the *cis* to the *trans* compartment and is physically separated from the HC channel by both reduction of the disulfide bridge and cleavage of the scissile bond. Thus, the chaperone-cargo anchor must be severed to complete productive translocation[14].

Discrete Intermediates during BoNT Translocation Reveal the Conformational Dynamics of Cargo-Channel Interactions

The beginning and the end of the translocation step are known (Fig. 1); the intricacies of the translocation process were elucidated when we developed an assay that monitors the translocation of BoNT LC by the BoNT HC channel in real time and at the single-molecule level in excised membrane patches[16] from BoNT-sensitive Neuro 2A neuroblastoma cells[14, 15]. The assay allows us to probe Steps 2, 3, 4 and 5 of Fig. 1, namely, the conformational transitions of both HC and LC linked to translocation across membranes, and the requirements for LC refolding and release at the endosome surface after translocation.

A key feature of the single-molecule translocation assay is sensitivity, which led us to discover a succession of discrete transient intermediate channel conductances which reflect permissive stages during LC translocation for both BoNT/A and BoNT/E. This is illustrated in Figure 2 for BoNT/A; the top panel shows the absence of channel currents prior to BoNT/A insertion into the

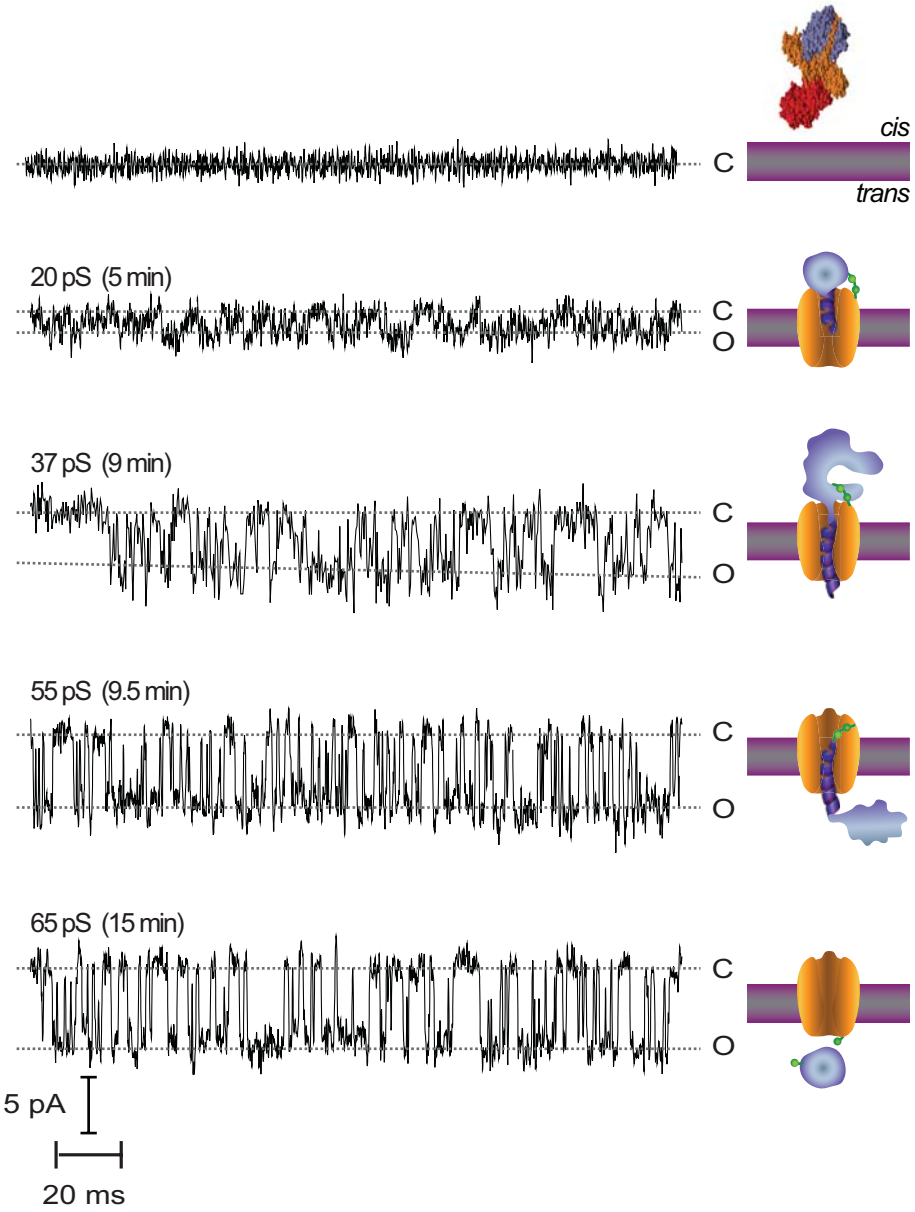

Fig. 2. Single-molecule detection of discrete intermediates during BoNT translocation. High-gain and fast-time resolution of BoNT/A single channel currents recorded at –100 mV in excised patches of Neuro 2A cells, with schematic representation (right). Top panel shows absence of channel currents prior to exposure to BoNT/A. Subsequent panels represent the time course of change of channel conductance. Each segment indicates the representative γ at the recorded time; the dotted lines are traced on the average current for the closed and open states. All other conditions were identical to those previously described [14, 15]and other conventions as in Fig. 1.

membrane. The time course of channel conductance change after exposure to BoNT/A (defined as zero time), is shown in the next four panels which display representative consecutive segments recorded at the indicated times during a single, one hour long experiment. Intermediate conductances were discerned at $\gamma \cong 20$ pS (after 5 min), $\cong 37$ pS (after 9 min), and $\cong 55$ pS (after 5.5 min) before entering the stable γ of 65 pS. Note that the γ values for each of the intermediate conductances fluctuate, yet they clearly exhibit a trend towards higher γ values with time, as depicted by the dotted lines. This pattern of channel activity characteristic of holotoxin (Fig. 2) allows us to operationally define three states of the BoNT channel. First, a closed state, and second, an “occluded state” with the partially unfolded LC trapped within the channel during the translocation process (Fig. 1, Steps 2, 3 and 4). This occluded state is identified as a set of intermediate conductances corresponding to transitions between the closed state and several blocked open states. Third, an “unoccluded state” visible upon completion of translocation and release of the LC associated to transitions between the closed state and the fully open state (Fig. 1, Step 5). The terminal and stable γ for holotoxin channels ($\cong$ 67 pS,) and the distinctive γ of HC channels ($\cong$ 66 pS) exhibit similar characteristics, thereby supporting the view of the HC channel as an endpoint achieved after completion of LC translocation through the HC channel, as observed in holotoxin/A and holotoxin/E channels (Fig. 1, Step 5)[12-14]. We interpret the progressive, stepwise increase in channel conductance with time as the progress of LC translocation during which

the protein-conducting HC channel conducts Na^+ and partially unfolded LC (illustrated as a helix in Fig. 1, Step 2) detected as channel block. After translocation is complete the channel is unoccluded (Fig. 1, Step 5). In other words, during translocation the HC channel conducts gradually more Na^+ around the unfolded LC polypeptide chain before entering an exclusively ion-conductive state.

What is the significance of the newly identified intermediate states? We conjecture that the residence time at each intermediate reflects the conformational changes of cargo within the chaperone pore and that these determine the efficiency and outcome of translocation. Within the occluded state, the low conductance intermediates (Fig. 2, $\gamma \cong 20$ pS) exhibit the longest occupancy time, consistent with an energetic barrier associated with the initiation of LC unfolding, presumably into a molten globule state, at the onset of translocation – an entry event (Fig. 1, Step 2). By contrast, intermediates with γ values $\gamma \cong 40$ pS (Fig. 2) have shorter lifetimes, presumably a result of overcoming the activation energy (Fig. 1, Step 3). This sequence of transfer steps leads to a transition into the final γ intermediate with $\gamma \cong 55$ pS (Fig. 1, Step 4). This last intermediate in the sequence (Fig. 2) is relatively long-lived, plausibly limited by the refolding of the LC at the channel exit interface in the *trans* compartment and reduction of the disulfide bridge before final release from the HC channel, an exit event (Fig. 1, Step 5; Fig. 2). Thus, the main consequence of this analysis is the resolution of LC translocation into an entry event, a series of transfer steps, and an exit event.

The key unanswered questions are now centered on an understanding of the precise conformational state at each one of the identified intermediates; what we can say is that the trend is to preserve partially unfolded conformers, (evidenced by the occluded intermediates) (Fig. 1, Steps 2-4; Fig. 2) [14]and native-like conformers (evidenced by the recovery of LC protease activity at the end of translocation) (Fig. 1, Step 5)[12]. We have shown that molecular tools like high specificity binding Fab fragments isolated from monoclonal antibodies raised against unique regions of BoNT LC arrest LC translocation during the intermediate steps[14, 15]. These Fab arrested cargo-carrier protein complexes could be probed with fluorescent markers to establish the conformational state of both the HC channel and the LC cargo. Fluorescence resonance energy transfer (FRET) between two dyes at defined sites within a protein within the Ribosome have been demonstrated to determine the folded state of the nascent chain[17, 18]. Use of this technique on the LC, HC or on the LC and HC can be utilized to determine the molecular architecture of the LC cargo and HC channel during different Fab binding stabilized stages of LC translocation.

Toosendanin (TSDN) may serve in a similar capacity as LC specific Fab fragments to enable further understanding of the translocation conformers of LC and HC. TSDN, a derivative found in Chinese herbal medicine, has been shown to have anti-botulismic effects, effectively protecting monkeys and mice from intoxication with BoNT/A [19, 20]; however our work elucidated the specific mechanism of action (Chapter 7). TSDN does not function as a channel blocker; however it does inhibit LC translocation with nM sensitivity (Chapter 7). TSDN

inhibition may arise from the coordination of the elongated LC with the HC channel as the LC traverses from the endosomal to cytosolic compartments by stabilizing intermediate conformations of the channel-cargo complex during LC translocation. TSDN coupling of the LC to the HC locks the complex in a translocating conformer that is irreversibly incomplete and readily studied with fluorescently labeled sites within the LC and HC.

The BoNT Channel as a Chaperone for the LC Protease

At the root of the BoNT translocation process is the interaction between an unfolded LC cargo embedded within the HC protein-conducting channel (Fig. 1, Steps 2-4). An analogous scheme has been invoked for the translocation of the catalytic domain (A chain) by the transmembrane (T) domain of diphtheria toxin[21-23], and for the translocation of the anthrax toxin lethal factor by the protective antigen pore[24, 25]. That channel activity has been documented for BoNT/A[12, 13, 26, 27], BoNT/E[27], BoNT/B[28], BoNT/C[29] and tetanus neurotoxin[28, 30, 31], and protein translocation activity has been shown for BoNT/A[12, 14], BoNT/E [14, 15]and BoNT/D[32] points to the general validity of the idea. This notion is reminiscent of the maintenance of an unfolded or partially folded state of polypeptides by chaperones. Compared to the molecular complexity of the mitochondrial and chloroplast protein translocases, and the translocons in eukarya, bacteria and archae the BoNT protein highlights the simplicity of its modular design to achieve its exquisite activity. A fundamental common principle of molecular design emerges from the studies with BoNT and

the translocases, all of which clearly catalyze the concerted and intertwined unfolding, translocation and refolding of cargo proteins. It will be interesting to compare protein translocation dynamics in the more complex mitochondrial and chloroplast protein translocases, and the translocons in eukarya, bacteria and archae by utilizing the real time single molecule protein translocation assay developed for BoNT.

Structural Analysis of BoNT holotoxin

BoNT/E is among the smallest proteins for which the structure has been determined by single-particle EM[4, 5, 33, 34]. The number of structures determined at intermediate resolution by single-particle EM is rapidly increasing thereby supporting the validity of this strategy, in particular for molecules which resist crystallization and molecules such as BoNTs which become membrane proteins during their intraneuronal traffic after exposure to the acidic endosomal pH. An additional advantage is the opportunity to visualize structural changes of the holotoxin while retaining the critical interactions that occur between the HC channel and the LC cargo under conditions that imitate those prevalent during translocation across endosomal membranes. It will be interesting to follow the repositioning of domains upon exposure to acidic pHs, potentially determining the oligomeric state of the HC channel in addition to the unfolded state of the LC cargo, by pursuing the strategy outlined here in combination with a set of serotype-specific (BoNT/A or BoNT/E) and domain-specific (LC or TD) antibodies[34].

Minimal protein necessary for BoNT channel activity and LC translocation

Previous studies have shown that BoNT forms pH dependent and voltage dependent channels in lipid bilayers [26, 28, 29]and neuronal cells[14, 27]. Similar channel activity has been demonstrated for the closely related tetanus toxin [28, 35, 36]and diphtheria toxin[28, 31, 35, 37, 38]. BoNT channel activity was shown to be limited to the N-terminal half of the HC[26], specifically, the protein coding to amino acids 546-870 of the HC (Chapter 6). This section of BoNT was termed the beltless translocation domain (BTD) as the two unstructured loops running perpendicular and parallel to the LC substrate recognition exosites were truncated out. Removal of the RBD released the pH dependence of channel formation, as demonstrated by channel activity of the TD and BTD under symmetric neutral pH conditions. BoNT intoxication requires that channel formation occurs concomitant with protein translocation; therefore we investigated the minimal domains required for productive LC translocation. The C-terminal half of the HC responsible for cell binding and internalization was determined to be unnecessary for BoNT/A LC translocation. The minimal domain required to form BoNT channel activity is restricted to a protein of ~ 38 kDa, a size more amenable to NMR and X-Ray crystallization studies. This minimal protein may pave the way to resolution of a structure of the BoNT channel inserted into the membrane.

Although the belt region is not required for reconstitution of channel activity it may facilitate protein-assisted unfolding and pseudosubstrate-assisted

refolding of the protease[39]. A similar inter-chaperone protease protein is subtilisin for which propeptides, located between the signal peptide and the mature segments of the protease, function as protease inhibitors by lodging into the substrate binding pocket[40]. These peptides are effectively IUPs[41] since they lack 3-D structure in isolation yet adopt secondary structure upon forming a complex with the cognate protease[40, 42, 43]. Since the belt embraces the LC, the belt may be a structural entity that facilitates or coordinates the concerted partial unfolding of the LC at the endosomal acidic pH and directs the beginning of its translocation through the membrane. This could be determined by generating BoNT LC-TD protein with different length linkers replacing the belt region and assaying these new truncation mutants on the single molecule LC translocation assay. The amino acids around the LC exosite binding regions could also be mutated to determine if BoNT intoxication is affected by a compromised pseudo-substrate belt region. Answers to these issues will bring us closer to understanding the elusive role of the belt in the action of this family of potent toxins.

BoNT as a modular tool

The findings presented here illustrate the modular nature of BoNT, a protein in which each component functions individually yet the tight interplay governs that each domain serves as a chaperone for the others. The RBD insures TD channel formation occurs concurrently with LC unfolding to a translocation competent conformation (Chapter 6). The LC gates the TD channel

within the positive potential membrane of the endosomal compartment in order to initiate LC translocation. The TD belt protects the LC from premature cleavage of non-specific substrates until localization within the cytosol[39]. The TD itself protects the LC within the acidic environment of the endosome, chaperones the LC to the cytosol, and releases the LC in an enzymatically active conformation to the substrate SNARE proteins[12]. This modular function makes BoNT and similar modular toxins a tool for biomolecule delivery to predetermined target tissues[32, 44-48]. Proteins of choices have been tethered to enzymatically inactive BoNT and demonstrated to translocate and function within the neuronal cell[32]. These studies have limited themselves to inactivation or removal of the enzymatic domain and addition of a new protein; however the replacement of the neuronal targeting receptor binding domain with one that recognizes a unique cellular surface protein could make BoNT a putative delivery system for almost any cargo protein to the scientist's target tissue of choice.

BoNT Channel as a Target for Intervention

The TD channel may represent the most effective target for inhibition of BoNT neurotoxicity; although most studies consider the LC a technically less challenging target for intervention. The endopeptidase activity of the LC is similar to other Zn metalloproteases like thermolysin making small molecule interaction modeling a powerful tool[49]. Drug sensitivity can be improved by coordination with the Zn ion. Unfortunately, these drugs all have a high degree of cross reactivity to cellular proteases as the active site is highly conserved and not

involved in high specificity substrate recognition. The extended enzyme substrate interface required for optimal substrate recognition, involves an array of substrate binding sites distant from the active site[50, 51]. These exosites may be a more effective target for LC neutralization; however each serotype has a different substrate, requiring design of seven unique peptides. Studies focused on inhibition at the early stages of intoxication have aimed to develop blockers of RBD interaction with known receptors[52, 53]; these are similarly limited by the few serotypes for which the protein receptor is known. The RBD and LC serotype specificity arises from interactions with host cellular proteins whereas the TD functions to chaperone the LC cargo in response to the targeting of the RBD. The TD may function as a universal carrier; small molecules that inhibit BoNT/A channel activity exhibit similar effects on the other serotypes thereby eliminating the necessity to develop multiple therapies (data not shown). Small molecule drugs that serve as efficient blockers of voltage dependent channels are subject to combinatorial based chemistry optimization to improve both binding affinity and cross reactivity with host channel proteins[54-56]. Even though the HC has no crystal structure as a membrane inserted protein and the mechanism of small molecule binding has not been structurally determined, inhibition of BoNT/A single channels has been supported by animal models that demonstrate efficient protection[19]. Given that the translocation process is essential for BoNT neurotoxicity, the BoNT protein-conducting channel emerges as a potential target for antidote design and discovery.

Concluding Remarks

This endeavor has demonstrated that the BoNT protein-conducting channel acts as a chaperone and requires acidification in *cis* and reduction in *trans.* Under these conditions, the RBD mediates entry into the acidic endosomal compartment thereby promoting concerted TD domain insertion into the endosomal membrane and partial unfolding of the LC protease. LC protease activity is retrieved in the *trans* compartment, consistent with the translocation of the cargo protease through the channel. Identification of translocation intermediates allowed us to define that LC translocation by the TD protein-conducting channel involves an entry event, a series of transfer steps, and an exit event. The collective findings represent a significant advance in our understanding of BoNT translocation; yet they also raise a new set of questions needing further study, particularly regarding the precise conformational states of the cargo within the channel/chaperone at each one of the identified intermediate states (Fig. 2, Steps 2-4)[12, 14]. Overall, the findings imply that within the cell, the LC protease unfolds inside acidic oxidizing endosomes, goes through the TD protein-conducting channel, refolds at the interface and dissociates from the channel in the cytosolic reducing milieu where it cleaves its substrate SNARE, SNAP-25. Given that the translocation process is essential for BoNT neurotoxicity, the BoNT protein-conducting channel emerges as a potential target for antidote design and discovery.

References

1. Arnon, S.S., R. Schechter, T.V. Inglesby, D.A. Henderson, J.G. Bartlett, M.S. Ascher, E. Eitzen, A.D. Fine, J. Hauer, M. Layton, S. Lillibridge, M.T. Osterholm, T. O'Toole, G. Parker, T.M. Perl, P.K. Russell, D.L. Swerdlow, and K. Tonat, *Botulinum toxin as a biological weapon: medical and public health management.* Jama, 2001. **285**(8): p. 1059-70.

2. Schiavo, G., M. Matteoli, and C. Montecucco, *Neurotoxins affecting neuroexocytosis.* Physiol Rev, 2000. **80**(2): p. 717-66.

3. Sathyamoorthy, V. and B.R. DasGupta, *Separation, purification, partial characterization and comparison of the heavy and light chains of botulinum neurotoxin types A, B, and E.* J Biol Chem, 1985. **260**(19): p. 10461-6.

4. Swaminathan, S., and Eswaramoorthy, S., *Structural analysis of the catalytic and binding sites of Clostridium botulinum neurotoxin B.* Nat Struct Biol, 2000. **7**: p. 693-699.

5. Lacy, D.B. and R.C. Stevens, *Sequence homology and structural analysis of the clostridial neurotoxins.* J Mol Biol, 1999. **291**(5): p. 1091-104.

6. Lacy, D.B., W. Tepp, A.C. Cohen, B.R. DasGupta, and R.C. Stevens, *Crystal structure of botulinum neurotoxin type A and implications for toxicity.* Nat Struct Biol, 1998. **5**(10): p. 898-902.

7. Davletov, B., M. Bajohrs, and T. Binz, *Beyond BOTOX: advantages and limitations of individual botulinum neurotoxins.* Trends Neurosci, 2005. **28**(8): p. 446-52.

8. Schiavo, G., F. Benfenati, B. Poulain, O. Rossetto, P. Polverino de Laureto, B.R. DasGupta, and C. Montecucco, *Tetanus and botulinum-B neurotoxins block neurotransmitter release by proteolytic cleavage of synaptobrevin.* Nature, 1992. **359**(6398): p. 832-5.

9. Schiavo, G., O. Rossetto, A. Santucci, B.R. DasGupta, and C. Montecucco, *Botulinum neurotoxins are zinc proteins.* J Biol Chem, 1992. **267**(33): p. 23479-83.

10. Blasi, J., E.R. Chapman, E. Link, T. Binz, S. Yamasaki, P. De Camilli, T.C. Sudhof, H. Niemann, and R. Jahn, *Botulinum neurotoxin A selectively cleaves the synaptic protein SNAP-25.* Nature, 1993. **365**(6442): p. 160-3.

11. Oblatt-Montal, M., M. Yamazaki, R. Nelson, and M. Montal, *Formation of ion channels in lipid bilayers by a peptide with the predicted*

transmembrane sequence of botulinum neurotoxin A. Protein Sci, 1995. **4**(8): p. 1490-7.

12. Koriazova, L.K. and M. Montal, *Translocation of botulinum neurotoxin light chain protease through the heavy chain channel.* Nat Struct Biol, 2003. **10**(1): p. 13-8.

13. Fischer, A. and M. Montal, *Characterization of Clostridial botulinum neurotoxin channels in neuroblastoma cells.* Neurotox Res, 2006. **9**(2-3): p. 93-100.

14. Fischer, A. and M. Montal, *Single molecule detection of intermediates during botulinum neurotoxin translocation across membranes.* Proc Natl Acad Sci U S A, 2007. **104**(25): p. 10447-52.

15. Fischer, A. and M. Montal, *Crucial role of the disulfide bridge between botulinum neurotoxin light and heavy chains in protease translocation across membranes.* J Biol Chem, 2007.

16. Hamill, O.P., A. Marty, E. Neher, B. Sakmann, and F.J. Sigworth, *Improved patch-clamp techniques for high-resolution current recording from cells and cell-free membrane patches.* Pflugers Arch, 1981. **391**(2): p. 85-100.

17. Woolhead, C.A., P.J. McCormick, and A.E. Johnson, *Nascent membrane and secretory proteins differ in FRET-detected folding far inside the ribosome and in their exposure to ribosomal proteins.* Cell, 2004. **116**(5): p. 725-36.

18. Johnson, A.E., *The co-translational folding and interactions of nascent protein chains: a new approach using fluorescence resonance energy transfer.* FEBS Lett, 2005. **579**(4): p. 916-20.

19. Shi, Y.L. and Z.F. Wang, *Cure of experimental botulism and antibotulismic effect of toosendanin.* Acta Pharmacol Sin, 2004. **25**(6): p. 839-48.

20. Shih, Y.L. and K. Hsu, *Anti-botulismic effect of toosendanin and its facilitatory action on miniature end-plate potentials.* Jpn J Physiol, 1983. **33**(4): p. 677-80.

21. Collier, R.J., *Understanding the mode of action of diphtheria toxin: a perspective on progress during the 20th century.* Toxicon, 2001. **39**(11): p. 1793-803.

22. Ren, J., K. Kachel, H. Kim, S.E. Malenbaum, R.J. Collier, and E. London, *Interaction of diphtheria toxin T domain with molten globule-like proteins and its implications for translocation.* Science, 1999. **284**(5416): p. 955-7.

23. Oh, K.J., L. Senzel, R.J. Collier, and A. Finkelstein, *Translocation of the catalytic domain of diphtheria toxin across planar phospholipid bilayers by its own T domain.* Proc Natl Acad Sci U S A, 1999. **96**(15): p. 8467-70.

24. Zhang, S., E. Udho, Z. Wu, R.J. Collier, and A. Finkelstein, *Protein translocation through anthrax toxin channels formed in planar lipid bilayers.* Biophys J, 2004. **87**(6): p. 3842-9.

25. Krantz, B.A., A. Finkelstein, and R.J. Collier, *Protein translocation through the anthrax toxin transmembrane pore is driven by a proton gradient.* J Mol Biol, 2006. **355**(5): p. 968-79.

26. Blaustein, R.O., W.J. Germann, A. Finkelstein, and B.R. DasGupta, *The N-terminal half of the heavy chain of botulinum type A neurotoxin forms channels in planar phospholipid bilayers.* FEBS Lett, 1987. **226**(1): p. 115-20.

27. Sheridan, R.E., *Gating and permeability of ion channels produced by botulinum toxin types A and E in PC12 cell membranes.* Toxicon, 1998. **36**(5): p. 703-17.

28. Hoch, D.H., M. Romero-Mira, B.E. Ehrlich, A. Finkelstein, B.R. DasGupta, and L.L. Simpson, *Channels formed by botulinum, tetanus, and diphtheria toxins in planar lipid bilayers: relevance to translocation of proteins across membranes.* Proc Natl Acad Sci U S A, 1985. **82**(6): p. 1692-6.

29. Donovan, J.J. and J.L. Middlebrook, *Ion-conducting channels produced by botulinum toxin in planar lipid membranes.* Biochemistry, 1986. **25**(10): p. 2872-6.

30. Gambale, F. and M. Montal, *Characterization of the channel properties of tetanus toxin in planar lipid bilayers.* Biophys J, 1988. **53**(5): p. 771-83.

31. Borochov-Neori, H., Yavin, E. and Montal, M., *Tetanus Toxin Forms Channels in Planar Lipid Bilayers Containing Gangliosides.* Biophys J, 1984. **45**: p. 83-85.

32. Bade, S., A. Rummel, C. Reisinger, T. Karnath, G. Ahnert-Hilger, H. Bigalke, and T. Binz, *Botulinum neurotoxin type D enables cytosolic delivery of enzymatically active cargo proteins to neurones via unfolded translocation intermediates.* J Neurochem, 2004. **91**(6): p. 1461-72.

33. Agarwal, R., S. Eswaramoorthy, D. Kumaran, T. Binz, and S. Swaminathan, *Structural analysis of botulinum neurotoxin type E catalytic domain and its mutant Glu212-->Gln reveals the pivotal role of the Glu212*

carboxylate in the catalytic pathway. Biochemistry, 2004. **43**(21): p. 6637-44.

34. Fischer, A., C. Garcia-Rodriguez, I. Geren, J. Lou, J.D. Marks, T. Nakagawa, and M. Montal, *Molecular architecture of Botulinum neurotoxin E revealed by single particle electron microscopy.* J Biol Chem, 2007.

35. Finkelstein, A., *Channels formed in phospholipid bilayer membranes by diphtheria, tetanus, botulinum and anthrax toxin.* J Physiol (Paris), 1990. **84**(2): p. 188-90.

36. Boquet, P. and E. Duflot, *Tetanus toxin fragment forms channels in lipid vesicles at low pH.* Proc Natl Acad Sci U S A, 1982. **79**(24): p. 7614-8.

37. Donovan, J.J., M.I. Simon, R.K. Draper, and M. Montal, *Diphtheria toxin forms transmembrane channels in planar lipid bilayers.* Proc Natl Acad Sci U S A, 1981. **78**(1): p. 172-6.

38. Silverman, J.A., J.A. Mindell, H. Zhan, A. Finkelstein, and R.J. Collier, *Structure-function relationships in diphtheria toxin channels: I. Determining a minimal channel-forming domain.* J Membr Biol, 1994. **137**(1): p. 17-28.

39. Brunger, A.T., M.A. Breidenbach, R. Jin, A. Fischer, J.S. Santos, and M. Montal, *Botulinum neurotoxin heavy chain belt as an intramolecular chaperone for the light chain.* PLoS Pathog, 2007. **3**(9): p. 1191-4.

40. Kojima, S., A. Iwahara, and H. Yanai, *Inhibitor-assisted refolding of protease: a protease inhibitor as an intramolecular chaperone.* FEBS Lett, 2005. **579**(20): p. 4430-6.

41. Dyson, H.J. and P.E. Wright, *Intrinsically unstructured proteins and their functions.* Nat Rev Mol Cell Biol, 2005. **6**(3): p. 197-208.

42. Shinde, U.P., J.J. Liu, and M. Inouye, *Protein memory through altered folding mediated by intramolecular chaperones.* Nature, 1997. **389**(6650): p. 520-2.

43. Shinde, U., X. Fu, and M. Inouye, *A pathway for conformational diversity in proteins mediated by intramolecular chaperones.* J Biol Chem, 1999. **274**(22): p. 15615-21.

44. Dobrenis, K., A. Joseph, and M.C. Rattazzi, *Neuronal lysosomal enzyme replacement using fragment C of tetanus toxin.* Proc Natl Acad Sci U S A, 1992. **89**(6): p. 2297-301.

45. Francis, J.W., B.A. Hosler, R.H. Brown, Jr., and P.S. Fishman, *CuZn superoxide dismutase (SOD-1):tetanus toxin fragment C hybrid protein for*

targeted delivery of SOD-1 to neuronal cells. J Biol Chem, 1995. **270**(25): p. 15434-42.

46. Duggan, M.J., C.P. Quinn, J.A. Chaddock, J.R. Purkiss, F.C. Alexander, S. Doward, S.J. Fooks, L.M. Friis, Y.H. Hall, E.R. Kirby, N. Leeds, H.J. Moulsdale, A. Dickenson, G.M. Green, W. Rahman, R. Suzuki, C.C. Shone, and K.A. Foster, *Inhibition of release of neurotransmitters from rat dorsal root ganglia by a novel conjugate of a Clostridium botulinum toxin A endopeptidase fragment and Erythrina cristagalli lectin.* J Biol Chem, 2002. **277**(38): p. 34846-52.

47. Ichinose, M., X.H. Liu, N. Hagihara, and R.J. Youle, *Extracellular Bad fused to toxin transport domains induces apoptosis.* Cancer Res, 2002. **62**(5): p. 1433-8.

48. Liu, X.H., J.C. Castelli, and R.J. Youle, *Receptor-mediated uptake of an extracellular Bcl-x(L) fusion protein inhibits apoptosis.* Proc Natl Acad Sci U S A, 1999. **96**(17): p. 9563-7.

49. Agarwal, R., T. Binz, and S. Swaminathan, *Structural analysis of botulinum neurotoxin serotype F light chain: implications on substrate binding and inhibitor design.* Biochemistry, 2005. **44**(35): p. 11758-65.

50. Breidenbach, M.A. and A.T. Brunger, *Substrate recognition strategy for botulinum neurotoxin serotype A.* Nature, 2004. **432**(7019): p. 925-9.

51. Chen, S. and J.T. Barbieri, *Multiple pocket recognition of SNAP25 by botulinum neurotoxin serotype E.* J Biol Chem, 2007. **282**(35): p. 25540-7.

52. Arkin, M.R., Wells, J. A., *Small-molecule inhibitors of protein-protein interactions: progressing towards the dream.* Nat Rev Drug Dis., 2004. **3**: p. 301-317.

53. Eswaramoorthy, S., D. Kumaran, and S. Swaminathan, *Crystallographic evidence for doxorubicin binding to the receptor-binding site in Clostridium botulinum neurotoxin B.* Acta Crystallogr D Biol Crystallogr, 2001. **57**(Pt 11): p. 1743-6.

54. Hirsh, A.J., B.F. Molino, J. Zhang, N. Astakhova, W.B. Geiss, B.J. Sargent, B.D. Swenson, A. Usyatinsky, M.J. Wyle, R.C. Boucher, R.T. Smith, A. Zamurs, and M.R. Johnson, *Design, synthesis, and structure-activity relationships of novel 2-substituted pyrazinoylguanidine epithelial sodium channel blockers: drugs for cystic fibrosis and chronic bronchitis.* J Med Chem, 2006. **49**(14): p. 4098-115.

55. Lacinova, L., *Voltage-dependent calcium channels.* Gen Physiol Biophys, 2005. **24 Suppl 1**: p. 1-78.

56. Lipton, S.A., *Failures and successes of NMDA receptor antagonists: molecular basis for the use of open-channel blockers like memantine in the treatment of acute and chronic neurologic insults.* NeuroRx, 2004. **1**(1): p. 101-10.